2003 Atomic, Molecular and Optical Sciences

Research Meeting

Granlibakken Conference Center
Tahoe City, California
September 21-23, 2003

Sponsored by:
U.S. Department of Energy
Office of Basic Energy Sciences
Chemical Sciences, Geosciences & Biosciences Division

Foreword

This volume summarizes the scientific content of the 2003 Research Meeting of the Atomic, Molecular and Optical Sciences (AMOS) Program sponsored by the U. S. Department of Energy (DOE), Office of Basic Energy Sciences (BES). This meeting is held annually for the DOE laboratory and university principal investigators within the BES AMOS Program in order to facilitate scientific interchange among the PIs and to promote a sense of program identity. For the past five years, the meeting has included significant participation from scientists outside of the BES AMOS Program and has had a specific topical focus. The 2003 meeting continues this format with a topical focus on "Ultrafast X-Ray Science."

The study of real-time dynamics in chemical, physical and biological systems seems poised to make huge strides in the near future as ultrafast optical probes are extended on two frontiers: shorter times and higher photon energies. The Office of Basic Energy Sciences, with its strong tradition of developing, building and maintaining state-of-the-art x-ray light sources, is keenly interested in the application of new x-ray sources to ultrafast dynamics. The BES AMO Sciences Program is home to several projects using laser-based sources of EUV and x-ray photons to explore chemical and physical change on the femtosecond time scale. BES is investing more broadly in the coupling of lasers and third generation synchrotrons to enable ultrafast science in the x-ray region and in new efforts in accelerator-based x-ray sources, such as the Sub-Picosecond Photon Source experiment at SLAC. Finally, BES is funding the design for the Linac Coherent Light Source at SLAC, which will be the world's first hard x-ray free electron laser. The LCLS passed a significant project milestone this year, with a successful review and subsequent DOE approval to proceed with long-lead procurement of the undulator and photoinjector systems in FY2005 (subject, of course, to Congressional budget approval).

I have recently been "promoted" to the position of Team Leader for Fundamental Interactions and now have two other research programs, in addition to the AMOS Program, that demand my attention. While it seems that much of my time is now occupied staring at Excel spreadsheets and balancing the bottom line, I remain interested and engaged in the AMOS Program. Although my new position dictates less direct contact with many PIs (which is my loss), I am always available for questions, concerns or to hear research updates. I am delighted that Dave Ederer has joined us from Argonne National Laboratory on a temporary assignment. Dave will be handling most of the projects in the AMOS Program and I encourage all the PIs to take the opportunity to say hello to Dave at this year's meeting.

I gratefully acknowledge the contributions of this year's speakers, particularly those not supported by the BES AMOS program, for their investment of time and for their willingness to share their ideas with the meeting participants. Thanks also to the staff of the Oak Ridge Institute of Science and Education, in particular Kellye Sliger, Julie Malicoat and Rachel Smith, and the Granlibakken Conference Center for assisting with logistical aspects of the meeting.

Eric Rohlfing
Chemical Sciences, Geosciences and Biosciences Division
Office of Basic Energy Sciences
August 2003

Agenda

U. S. Department of Energy
Office of Basic Energy Sciences
2003 Meeting of the Atomic, Molecular and Optical Sciences Program

Ultrafast X-Ray Science

Sunday, September 21

2:00-5:00 pm **** Registration ****
5:00 pm **** Reception (No Host) ****
6:00 pm **** Dinner ****

7:20 pm *Introductory Remarks*
Eric Rohlfing and Dave Ederer, BES/DOE

Session I: Ultrafast X-Ray Science
Chair: **Eric Rohlfing**

7:30 pm *Update on the Linac Coherent Light Source*
John Galayda, Stanford Linear Accelerator Center
8:20 pm *Ultrafast X-Ray Probing of Molecules*
Steve Leone, Lawrence Berkeley National Laboratory
9:10 pm *Linear Accelerator Based X-Ray Sources: The Subpicoscecond Pulse Source*
Jerry Hastings, Stanford Synchrotron Radiation Laboratory

Monday, September 22

7:00 am **** Breakfast ****

Session I: Ultrafast X-ray Science (cont.)
Chair: **Dave Ederer**

8:00 am *Advances at the DESY Free Electron Lasers*
Bernd Sonntag, Universtität Hamburg
8:50 am *Table-Top X-Ray Sources and Applications to Structural Measurements of Transition Metal Coordination Complexes*
Christoph Rose-Petruck, Brown University
9:20 am *Ultrafast Atomic and Molecular Optics at Short Wavelengths*
Margaret Murnane, University of Colorado

9:50 am **** Break ****

Session II: Ultracold Atoms and Molecules
Chair: **David Schultz**

10:10 am *Experiments in Ultracold Collisions*
Phil Gould, University of Connecticut
10:40 am *Cold Rydberg Atoms, Gases and Plasmas in Strong Magnetic Fields*
G. Raithel, University of Michigan
11:10 am *Exploring Quantum Degenerate Bose-Fermi Mixtures*
Deborah Jin, University of Colorado
11:40 am *Quantum Dynamics of Ultracold Fermionic Vapors*
John E. Thomas, Duke University

12:15 pm **** Lunch ****
5:00 pm **** Reception (No Host) ****
6:00 pm **** Dinner ****

Session II: Ultracold Atoms and Molecules (continued)
Chair: **Phil Gould**

7:20 pm *Ground-State Properties of Artificial Bosonic Atoms, Bose Interaction Blockade and the Single-Atom Pipette*
Eugene B. Kolomeisky, University of Virginia
7:50 pm *MOTRIMS as a Probe of AMO Processes*
Brett DePaola, Kansas State University
8:20 pm *Chemistry with Ultracold Molecules*
Dudley Herschbach and Bretislav Friedrich, Harvard University
8:50 pm *Research with Slow Molecules and Slow Atoms*
Harvey Gould, Lawrence Berkeley National Laboratory

Tuesday, Sept. 23

7:00 am **** Breakfast ****

Session III: Ions, Atoms and Molecules
Chair: **Brett DePaola**

8:00 am *Studies of Autoionizing States Relevant to Dielectric Recombination*
Tom Gallagher, University of Virginia
8:30 am *Ion/Excited-Atom Collision Studies with a Rydberg Target and a CO_2 Laser*
Steve Lundeen, Colorado State University
9:00 am *Light Emission from Sharp Metal Tips*
Lukas Novotny, University of Rochester
9:30 am *Time-Dependent Treatment of Electron Capture in $a + H_2^+$ Collisions*
Brett Esry, Kansas State University

10:00 am *** Break ****

10:30 am *X-ray Processes in the Presence of Strong Optical Fields*
Linda Young, Argonne National Laboratory
11:00 am *Energetic Photon and Electron Interactions with Positive Ions*
Ron Phaneuf, University of Nevada-Reno
11:30 am *Physics of Correlated Systems*
Chris Greene, University of Colorado

12:00 pm **** Lunch ****

Session IV: Electron Impact and Photoionization
Chair: **Tom Gallagher**

3:00 pm *Time-Dependent, Lattice Approach for Atomic Collisions and the ORNL MIRF Upgrade*
David Schultz, Oak Ridge National Laboratory
3:30 pm *Electron-Molecular Ion Fragmentation*
M. E. Bannister, Oak Ridge National Laboratory
4:00 pm *Electron Driven Processes in Polyatomic Molecules*
Vincent McKoy, California Institute of Technology

4:30 pm *** Break ****

4:45 pm *Electron Emission From Atoms and Small Molecules*
Mike Prior, Lawrence Berkeley National Laboratory
5:15 pm *Closing Remarks*
Eric Rohlfing, BES/DOE

6:00 pm **** Reception (No Host) ****
7:00 pm **** Banquet Dinner ****

Invited Presentations

(ordered by agenda)

Update on the Linac Coherent Light Source

John Galayda
Stanford Linear Accelerator Center

The Linac Coherent Light Source will be the world's first "hard" x-ray free-electron laser. It will produce an intense, spatially coherent beam of x-rays spanning 0.8 - 8 keV by means of *self-amplified spontaneous emission*, a process by which the current of an extremely intense and bright electron beam is modulated by the beam's own synchrotron radiation. This coherent modulation enhances coherence and intensity of the synchrotron radiation over a billionfold, compared to a typical synchrotron radiation source. Project engineering design activities for the Linac Coherent Light Source began in March of 2003, and it is expected that the facility will begin operation at the end of FY 2008. The LCLS will produce x-ray pulses with over 10^{11} photons in less than 230 fs for research in atomic physics, chemical and materials dynamics, plasma physics and structural biology.

This work is supported under contract DE-AC03-76SF00515 by the US Department of Energy.

Ultrafast X-Ray Probing of Molecules

Stephen R. Leone
Departments of Chemistry and Physics
and Lawrence Berkeley National Laboratory,
University of California
Berkeley CA 94720

Soft x-ray time dynamical studies offer new opportunities to probe the electrons in various orbitals in molecules, as bonds are broken or rearranged on excited state or ground state potential surfaces. New ultrafast laser methods have been developed to produce femtosecond soft x-ray pulses and to obtain camera-like snapshots of soft x-ray photoelectron spectra of molecules during their dissociation and transformation. The method uses high order harmonic generation of a Ti:sapphire ultrafast laser. Results are presented from the investigator's laboratory on the technique, on the characterization of femtosecond soft x-ray pulses, and on the first observations of photoelectron processes of dissociating molecules. Both valence shell and inner core electrons can be probed. Results will be presented on observations of photoelectron processes of dissociating bromine molecules and excited states. New information about ionization cross sections of transient states and their photoelectron spectra are obtained. The results pave the way for a general method to probe transient states in molecules, but based on the methods of photoelectron spectroscopy that have been so successfully employed for ground state analyses. Results will also be presented using a low harmonic of the Ti:sapphire laser to form Rydberg wave packets directly in atoms for two-color time-dependent wave packet studies. These experiments will be discussed and future time-resolved photoelectron work on other molecules will be considered. In other laboratories, laser–based harmonic generation methods are pushing towards the attosecond frontier of time domain in the x-ray region. This allows for the possibility to study electron rearrangements, such as Auger processes, in real time in the future.

Concepts of user facilities based on linac accelerator technologies are also being pursued to address the growing international interest in ultrafast x-ray scientific research. A recirculating linac-based ultrafast x-ray facility called LUX has been proposed by LBNL. It is based on electron beam accelerator technology, coupled with an array of advanced tunable femtosecond lasers for pump-probe experiments. This facility would represent a near-complete union of laser and accelerator-based technologies. The facility would be capable of performing a large variety of pump-probe type experiments (or multiple beam and coherence experiments) with soft and hard x-rays, experiments that cut across all fields of science, biology, chemistry, and physics, also including highly nonlinear phenomena. Such facilities would have greatly improved brightness, peak power, coherence, and tunability, for accelerator based x-ray sources, and would provide 10-50 femtosecond pulses, with opportunities to obtain sub-1-fs pulses in the future. A brief description of the characteristics of such a source will be outlined.

L. Nugent-Glandorf, M. Scheer, M. Krishnamurthy, J.W. Odom and S. R. Leone, "Photoelectron spectroscopic determination of the energy bandwidths of high harmonics (7th-55th) produced by an ultrafast laser in neon," Phys. Rev. A 62, 023812-1(2000).

L. Nugent-Glandorf, M. Scheer, D. A. Samuels, A. M. Mulhisen, E. R. Grant, X. Yang, V. M. Bierbaum, and S. R. Leone, "Ultrafast time-resolved soft x-ray photoelectron spectroscopy of dissociating Br_2," Phys. Rev. Lett. 87, 193002/1-4 (2001).

L. Nugent-Glandorf, M. Scheer, D. A. Samuels, V. M. Bierbaum, and S. R. Leone, "A laser-based instrument for the study of ultrafast chemical dynamics by soft x-ray-probe photoelectron spectroscopy," Rev. Sci. Instrum. **73**, 1875-1886 (2002).

L. Nugent-Glandorf, M. Scheer, D. A. Samuels, V. M. Bierbaum, and S. R. Leone, "Ultrafast photodissociation of Br_2: Laser-generated high-harmonic soft x-ray probing of the transient photoelectron spectra and ionization cross sections," J. Chem. Phys. **117**, 6108 (2002).

L. Nugent-Glandorf, “Time resolved photoelectron spectroscopy with ultrafast soft x-ray light,” Ph.D. Thesis, University of Colorado, Boulder (2001).

Web site incorporating information about the proposed LUX source, http://jncorlett.lbl.gov/FsX-raySource/LUXReview2003/

Linear Accelerator Based X-Ray Sources: The Sub Picosecond Pulse Source

J. B. Hastings
SSRL
Stanford Linear Accelerator Center

Accelerator based synchrotron radiation (SR) sources are now commonplace in the world with the USA (APS), Japan (Spring-8) and Europe (ESRF) each operating storage ring sources in the hard x-ray energy range that provide unique radiation for studies in the chemical, biological and materials sciences. These sources are critical to the understanding of complex static structures and through inelastic x-ray scattering the dynamics. They have also been applied to time resolved diffraction on the scale of the photon pulse length ~100 psec. Photon beams with all the properties of SR but with pulse lengths of ~100fsec are now available from linear accelerator based sources, for example the Sub-Picosecond Pulse Source (SPPS) at the Stanford Linear accelerator Center (SLAC). A description of SPPS, its present status and early results will be presented.

Advances at the DESY Free – Electron – Lasers

B. Sonntag
Institut für Experimentalphysik, Universtität Hamburg,
Luruper Chaussee, 149, 22761 Hamburg
E-mail: Sonntag@desy.de

Advances in linear accelerators, new developments in low-emittance electron guns, and the feasibility of ultra-precise long undulators open up the exciting possibility of building single pass Free Electron Lasers (FEL) based on self-amplified spontaneous emission (SASE). These FEL's promise to provide extremely intense, polarized ultra-short pulse radiation for the VUV and x-ray regimes. In addition their high peak and average brilliance, the tunability of the photon energy and the lateral coherence of the radiation will make the FEL's unique sources.

At the Deutsches Elektronen-Synchrotron (DESY) a SASE-FEL has been successfully operated in the vacuum ultraviolet (VUV) region. Saturation has been achieved at wavelengths between 80 nm and 120 nm. The characteristic parameters of the FEL, of the photon beam and the first results obtained on free atoms and clusters will be presented (1, 2, 3). At present the FEL is upgraded in order to allow for electron energies up to 1 GeV and for photon energies up to 194 eV in the first harmonic. The start-up for this FEL is scheduled for the beginning of next year. The installation of five experimental station in the new experimental hall is under way. This includes a facility for pump-probe experiments (see e.g. 4). The first experiments are scheduled for 2004. Non linear interactions and ultra-fast processes are the focus of many studies on atoms, molecules, clusters, plasmas and surfaces proposed for this VUV-FEL. Outstanding examples will be presented to showcase the opportunities and challenges of this new area of research.

Beginning of this year the Federal Government of Germany decided to support the construction of a X-ray FEL at DESY. This FEL should be realized within an European collaboration. The X-ray FEL will be based on the same TESLA superconducting accelerator technology successfully implemented at the VUV-FEL. The planning for the X-FEL is well under way. The characteristic parameters envisaged for this X-FEL will be presented together with a road-map towards its realization (5).

References

1) V. Ayvazan et al. Phys. Rev. Lett 88, 104802 (2002)

2) V. Ayvazan et al. Eur. Phys. J. D 20, 149 (2002)

3) H. Wabnitz et al. Nature 420, 482 (2002)

4) http://www-hasylab.desy.de/facility/fel

5) TESLA X-FEL, Technical Design Report, Supplement, edited by J. Andruszkow et al., DESY 2002 – 167 and http://www-tesla.desy.de/tdr-update

Table-Top X-Ray Sources and Applications to Structural Measurements of Transition Metal Coordination Complexes

Christoph Rose-Petruck
Department of Chemistry
Brown University
Providence, RI 02912

Ultrafast high-intensity laser pulses incident upon condensed matter targets can generate high-density plasmas that emit x-ray pulses with sub-picosecond temporal structure, significant spatial coherence, and high brightness. Such a laser-driven plasma x-ray source operating at kilohertz repetition rates has been developed in our laboratory. Details of the experimental apparatus, including the x-ray optics are presented. Essential performance features are discussed along with future performance improvements. The benefits of the combined use of table-top and accelerator-based ultrafast x-ray sources are discussed.

Using this ultrafast laser driven x-ray source, the first x-ray absorption fine structure (XAFS) spectra of solvated $Fe(CO)_5$ were measured. These spectra are compared to static x-ray spectra measured with a micro-focus x-ray tube as well as a synchrotron source. Furthermore, the data are compared to theoretical XAFS spectra based on electronic structure calculations of the solvated complex. All experimental and theoretical structure data were found to be in close agreement.

The structure of $Fe(CO)_5$ and its ligand substitution dynamics depends on the interaction with surrounding solvent molecules. Furthermore, the solute's vibrational modes, measured by FTIR spectroscopy, and their structures, measured by XAFS spectroscopy, are correlated. It was found that the solvation of iron pentacarbonyl induces substantial solvent-depended structural deformations with significant predicted impact on, e.g., the ultrafast dynamics of ligand substitution processes.

Ultrafast Atomic and Molecular Optics at Short Wavelengths

P.I.s: Henry C. Kapteyn and Margaret M. Murnane
Department of Physics and JILA
University of Colorado at Boulder, Boulder, CO 80309-0440
Phone: (303) 492-8198; FAX: (303) 492-5235; E-mail: kapteyn@jila.colorado.edu

PROGRAM SCOPE

The goal of this work is to study of the interaction of atoms and molecules with intense and very short (<20 femtosecond) laser pulses, with the purpose of developing new short-wavelength light sources, particularly at short wavelengths. We are also developing novel optical pulseshaping techniques to enable this work. In the past year, we have made a number of new advances, that will increase the utility of short wavelength sources for applications in spectroscopy and imaging.

RECENT PROGRESS

1. **High harmonic generation from ions (Ref. 14):** In recent work shown in Fig. 1, we experimentally demonstrated very high order harmonic generation of up to 250eV from Argon ions for the first time. Using a hollow waveguide filled with low-pressure gas, we can guide a laser beam in a highly ionized plasma, to reduce the effect of ionization-induced laser defocusing. As a result, we can extend the highest harmonic orders observable using 800nm driving-laser radiation by a factor of 2.5 compared with previous work. This corresponds to an extension of the cutoff by 150eV or 100 harmonic orders. These are higher photon energies than have previously been observed using either Argon or Neon gas under any conditions. At the laser intensities required to generate these harmonics, no neutral atoms remain. Thus, the harmonic emission originates from ionization of Ar+.

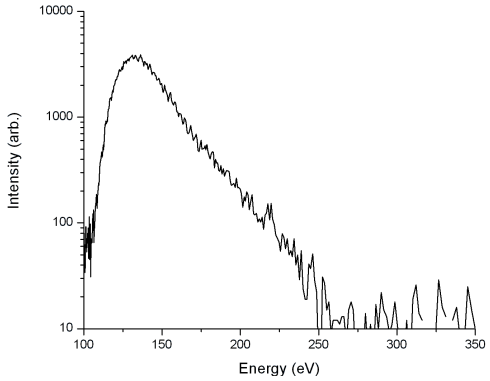

Figure 1: Harmonic emission from a 150μm diameter, 2.5cm long, fiber filled with low-pressure 7 Torr of Ar, excited by an 18fs pulse at a peak intensity of $\approx 1.3 \times 10^{15} Wcm^{-2}$.

The significance of this work is threefold. First, we have shown that high harmonic generation from ions can be used to greatly extend the coherent photon energies obtainable using HHG. Second, we demonstrated that large ions such as Argon with high nonlinear susceptibilities compared to Helium, can be used to generate high-energy harmonics. This is of potential significance for developing useful coherent EUV and soft x-ray sources for many applications in science and technology. Finally, we demonstrated that the hollow waveguide geometry can generate higher photon energies than otherwise possible using a conventional gas jet or cell geometry. This work has been submitted to Physical Review Letters.

2. **Molecular optoelectronics (Ref. 5, 8, 10):** By inducing molecules in a gas to coherently spin, the very-fast time-dependent phase modulation induced by these molecular rotational

quantum "wave packets" can spectrally-modulate and compress ultrashort light pulses. Using impulsively excited rotational wave packets in CO_2, we dramatically increased the bandwidth of a short-wavelength light pulse. This pulse was then compressed duration by an order of magnitude, simply by propagation through a fused silica window, *without the use of a pulse compressor*. This is a very general and novel technique for optical phase modulation, which can be applied to pulses in virtually any region of the spectrum from the IR to the VUV. It appears to be particularly useful for compressing light pulses in the VUV region of the spectrum, where conventional pulse compression techniques fail. In recent work, we extended work published in PRL in 2002 to generate even shorter duration light pulses, as shown in Fig. 2 below.

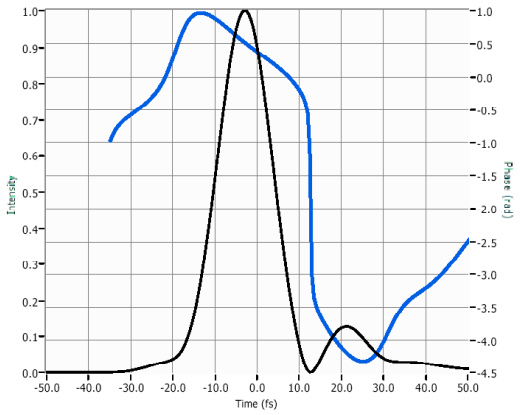

Figure 2: Intensity (black curve) and phase (blue curve) of a self-compressed pulse that compressed a 100fs transform-limited pulse to 12fs, without using prisms or gratings.

In addition, very recently, in work published in Optics Letters, we proposed a new method for phase-matched frequency conversion in a gas that we call *transient birefringent phase-matching*. In this method, an intense linearly-polarized light pulse induces the molecules in an anisotropic molecular gas to align. A gas of molecules with an anisotropic polarizability normally exhibits no anisotropy since the molecules are randomly oriented. However, a random distribution of molecules can be aligned using an intense light field to induce a torque on any molecule not oriented either parallel or perpendicular to the laser field. In the case of an alignment pulse shorter than the rotational period of the molecule (typically less than a few ps), the pulse exerts an impulsive torque on the molecules. This results in a change in the rotational angular momentum, and an excited distribution of rotational energy levels. Even after the alignment pulse has passed, this ensemble of molecules experiences a periodic realignment determined by the excited angular momentum states and the molecular rotational energy level structure. These alignments modify the macroscopic polarizability of the ensemble of molecules, creating a gas phase "quasi-crystal" and inducing time-dependent changes in the index of refraction. This birefringence created by an ensemble of aligned molecules can be used to phase match nonlinear frequency conversion. In particular, we calculated the conditions required to phase match third harmonic generation in a hollow-core fiber, and found them to be very reasonable. We also measured the induced birefringence.

3. **Using learning algorithms to study attosecond science (Refs.1, 4, 13):** In recent work in collaboration with Herschel Rabitz and Ivan Christov, we demonstrated that the data generated using a learning algorithm to optimize a quantum system is useful in helping to understand the physics behind the process being optimized. In its optimization process, the learning algorithm naturally finds a particularly interesting region of parameter space and probes it extensively. Analyzing the statistical behavior of the solutions found by the algorithm confirms our theoretical models of the process. In particular, by optimizing high harmonic emission using a learning algorithm, and then analyzing the data resulting from the optimization process, we can verify our understanding of the temporal dynamics of the process.

4. **EUV Photonics – Quasi phase matching at short wavelengths (Refs. 9, 12):** In two recent papers (one published in Nature in January 2003, and one currently under review by Science), we demonstrated that concepts from visible-wavelength photonics are useful for extending the efficient wavelength range of high harmonic generation. HHG is an excellent source of coherent EUV light, at photon energies up to ≈ 0.5keV. In HHG, a femtosecond laser is focused into a gas, and high harmonics of the fundamental laser are radiated in the forward direction. However, although HHG can generate high-energy photons, efficient HHG has been demonstrated only at photon energies of ≈ 50-100eV. Higher photon energies are generated at higher intensities, after much of the gas has ionized. This ionization prevents the laser and the EUV light from propagating at the same speed, severely limiting conversion efficiency. Thus, overcoming the detrimental effects of ionization has been a critical challenge for further development of coherent EUV light sources. In January 2003, we reported the first demonstration of quasi-phase-matched frequency conversion of laser light into the extreme-ultraviolet (EUV) region of the spectrum. Using a modulated hollow-core waveguide, with periods of 1mm – 0.5mm, to periodically vary the intensity of the light driving the conversion, we efficiently generated EUV light even in the presence of substantial ionization of ≈ 8%. Use of a modulated fiber shifts the spectrum of the high-harmonic light to significantly higher harmonic photon energies than would otherwise be possible. It may also allow for the generation of isolated attosecond pulses.

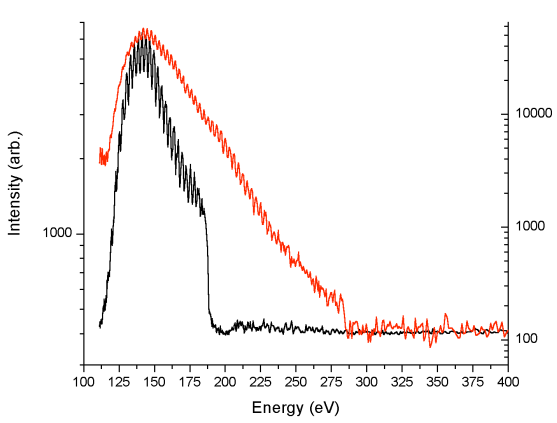

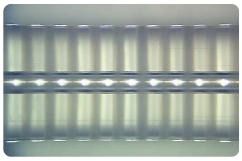

Figure 3: (left) Harmonic emission from 9 Torr of Neon in 2.5cm long, 0.25mm period, modulated fiber, through Boron (black) and Carbon (red) filters, at a laser intensity of ≈ 1.6 x 10^{15}Wcm^{-2}. An Ag filter is used to reject the laser light and absorbs at low energies. (top) Picture of a modulated hollow-core fiber.

In more recent work, we demonstrated for the first time that quasi phase matching of HHG using modulated fibers can operate in a *fully-ionized* gas. As shown in Fig. 3, we demonstrated for the first time that nonlinear-optical phase-matching technologies can be applied to the generation of light in the scientifically and technologically important region of the spectrum around the carbon K absorption edge at 284eV (4.4nm). This energy range is significant for biological and materials imaging, because water is transparent to soft x-ray radiation above 284eV, while carbon absorbs this light. This work demonstrated for the first time water window coherent light generation using Neon gas as the nonlinear medium. Previous work had succeeded in generating only very small fluxes of light in the water window using Helium gas. The effective nonlinear susceptibility in HHG depends on the recollision cross section of an ionized electron with its parent ion; this collision cross-section is smaller for He ions than for Ne.

FUTURE WORK

In future work, we will extend our coherent "molecular modulation" techniques to the generation of very short-duration, 1-10 fs, light pulses in both the deep-ultraviolet and the vacuum-ultraviolet regions of the spectrum. We plan to pursue this technology, with the goal of

developing a high-power deep-ultraviolet light source to be used to study ultrafast dynamics in chemical species, clusters, and materials. We are also investigating HHG with aligned molecules. We will also extend past work on HHG driven by two-color light to study nonlinear optical processes in the extreme-ultraviolet region of the spectrum, to attempt to understand in more detail how atoms interact with light at "ionizing" photon energies, in the extreme-ultraviolet region of the spectrum. Finally, new techniques have been developed at JILA that make it possible to control not only the intensity "envelope" of an ultrafast light pulse, but also the absolute position of the individual oscillations of the electromagnetic field of the light; i.e. the "carrier-envelope offset" or *CEO*. We plan to pursue the development of phase stabilized ultrafast laser-amplifier sources, and to use these sources to study absolute-phase sensitive nonlinear optics.

Publications (refereed) as a result of DOE support since 2001

1. R. Bartels, S. Backus, I. P. Christov, M. M. Murnane, H. C. Kapteyn, "Attosecond timescale feedback control of coherent x-ray generation", invited paper, Chemical Physics **267**, 277 (2001).
2. S. Backus, R. Bartels, S. Thompson, R. Dollinger, H. C. Kapteyn, M. M. Murnane, "High efficiency, single-stage, 7 kHz high average power ultrafast laser system", Optics Letters **26**, 465 (2001).
3. L. Misoguti, S. Backus, C. Durfee, R. Bartels, M. Murnane and H. Kapteyn, "Generation of broadband VUV light using third-order cascaded processes", Physical Review Letters **87**, 13601 (July 2, 2001).
4. I.P. Christov, M. M. Murnane and H.C. Kapteyn, "Attosecond time-scale intra-atomic phase matching of high harmonic generation", Physical Review Letters **86**, No. 24, 5458 (2001).
5. R. Bartels, T. Weinacht, N. Wagner, M. Baertschy, C. Greene, M. Murnane, H. Kapteyn , "Phase Modulation of Ultrashort Light Pulses using Molecular Rotational Wavepackets", Physical Review Letters **88**, 019303 (2002).
6. C. Durfee, L. Misoguti, S. Backus, R. Bartels, M. Murnane and H. Kapteyn, "Phase Matching in Cascaded Third-Order Processes, JOSA B **19** (4): 822-831 (2002).
7. S. Christensen, H.C. Kapteyn, M.M. Murnane, and S. Backus , "Simple, high power, compact, intracavity frequency-doubled Q-switched Nd:YAG laser," Review of Scientific Instruments **73** (5): 1994-1997 (2002).
8. R.A. Bartels, N.L. Wagner, M. Baertschy, J.Wyss, M.M. Murnane, H.C. Kapteyn, "Phase-matching conditions for nonlinear frequency conversion by use of aligned molecular gases," Optics Letters **28**, 346 (2003).
9. Ariel Paul, Randy Bartels, Ivan Christov, Henry Kapteyn, Margaret Murnane, Sterling Backus, "Multiphoton photonics: quasi phase matching in the EUV", *Nature* **421**, 51 (2003).

Publications (not refereed) as a result of DOE support since 2001

10. R. Bartels, T. Weinacht, M. Baertschy, N. Wagner, C. Greene, M. Murnane, H. Kapteyn, "Self-Compression of Ultrafast Optical Pulses using Molecular Phase Modulation", OSA Proc. Ultrafast Phenomena XIII (Springer Series in Chemical Physics), page 199.
11. S. Backus, R. Bartels, S. Thompson, S. Christensen, H Kapteyn, M. Murnane, "High average power, 10kHz, ultrafast laser system", OSA Proc. Ultrafast Phenomena XIII (Springer Series in Chemical Physics), page 128.

Publications submitted as a result of DOE support

12. Emily A. Gibson, A. Paul, N. Wagner, R. Tobey, I.P. Christov, D.T. Attwood, E. Gullikson, A. Aquila, M.M. Murnane, H.C. Kapteyn, "Generation of coherent soft x-rays in the water window using quasi phase-matched harmonic generation", submitted to Science (2003).
13. Randy A. Bartels, Margaret M. Murnane, Ivan P. Christov, Herschel Rabitz, and Henry C. Kapteyn , "Using learning algorithms to study attosecond dynamics", submitted to Phys. Rev. Lett. (2003).
14. Emily A. Gibson, A. Paul, N. Wagner, R. Tobey, I.P. Christov, M.M. Murnane, H.C. Kapteyn, "Very High Order Harmonic Generation in Highly Ionized Argon", submitted to Physical Review Letters (2003).
15. L. Misoguti, R. Bartels, I.P. Christov, S. Backus, M. Murnane, H. Kapteyn, "Nonlinear Optics in the Extreme Ultraviolet", submitted to Physical Review Rapid Communications (2003).

Experiments in Ultracold Collisions

Phillip L. Gould
Department of Physics U-3046
University of Connecticut
2152 Hillside Road
Storrs, CT 06269-3046
<gould@uconnvm.uconn.edu>

Program Scope:

Many areas of atomic, molecular, and optical (AMO) physics have benefited from advances in ultracold atoms. Examples include: Bose-Einstein condensation (BEC) and atom lasers; degenerate Fermi gases; optical lattices; quantum optics and quantum computing; ultracold Rydberg atoms and plasmas; photoassociative spectroscopy; ultracold molecule production; precision spectroscopy and improved atomic clocks; studies of photoionization, electron scattering, and ion-atom collisions; and fundamental atomic and nuclear physics experiments with radioactive isotopes. Because many of these applications of laser cooling and trapping utilize high-density samples (e.g., $n>10^{11}$ cm^{-3}) of ultracold atoms (e.g., $T<100$ μK), ultracold collisions are an important factor. For example, inelastic collisions can cause the loss of atoms from traps and/or increase their temperature. Ultracold collisions can also be beneficial. Evaporative cooling, the final stage of BEC production, relies on elastic collisions for thermalization. Also, quantum computation schemes involving cold atoms require some type of collisional interaction for communication between the qubits. In general, improved knowledge of these collisional interactions, and their possible control, will significantly benefit studies involving ultracold atoms. The main motivation of our experimental program is to improve our understanding of ultracold collisions, especially those which occur in a typical laser trap environment.

In addition to the relevance of our studies to applications of laser cooling, there is significant fundamental interest in collisions at extremely low energy (e.g., $\sim 10^{-8}$ eV). Because the colliding partners are barely moving, they are easily influenced by the long-range dipole-dipole interactions involving excited atoms. This allows the collision dynamics to be controlled with laser light – both enhancement and suppression have been demonstrated. The long-range of these interactions (e.g., R~100 nm), combined with the low collisional velocity, can result in collision times exceeding the excited-state radiative lifetime. Therefore, the atomic excitation can spontaneously decay during a slow collision, effectively terminating the collision in midcourse. Such "survival" effects are unique to the ultracold domain.

Our ultracold samples of rubidium are generated in a magneto-optical trap (MOT) utilizing diode lasers at 780 nm. The choice of rubidium is based on three factors: 1) its resonance lines are well-matched to readily available diode lasers; 2) there are two stable and abundant isotopes (^{85}Rb and ^{87}Rb), allowing isotopic collisional effects to be investigated; and 3) it has played a prominent role in BEC experiments and other ultracold applications. In our experiments, atoms are loaded into the MOT, and inelastic collisions are measured by monitoring the loss rate of atoms from the trap.

Recent Progress:

During the past year, we have made progress in two main areas. First, we have continued our work on ultracold collisions induced by frequency-chirped laser light. Second, we have

investigated ultracold collisions of atoms in the highly-excited Rb 5D level. We briefly describe each of these advances below.

The influence of laser light on ultracold collisions has been studied extensively by our group and others. However, the majority of these experiments have used fixed-frequency light which is applied continuously. A notable exception was our previous use of short (e.g., 100 ns) pulses, in a pump-probe configuration, to investigate the collision dynamics. In this work, the first pulse was tuned close to the atomic resonance, exciting the colliding atom pair at very long range. The atoms then accelerated towards each other on the attractive excited-state potential, decaying back to the ground state as they approached short range. A second pulse, detuned significantly below the atomic resonance, re-excited this enhanced collisional flux, causing an observable inelastic process at short range. We are presently extending this work by chirping the frequency of the laser light on the time scale of the atomic collisions. This may ultimately allow us to exert coherent control over various collisional processes, such as those used in ultracold molecule formation. If the excitation is adiabatic, i.e., if the laser intensity is high enough, atom pairs which are resonant at some point during the chirp will be efficiently transferred to the excited state. The direction of the chirp (red-to-blue vs. blue-to-red) will be important if the atomic motion is significant on the time scale of the chirp.

With regard to the experiment, we have recently improved our magneto-optical trap (MOT) apparatus, incorporating a double-MOT to allow more sensitive collisional measurements. A source MOT is used to load a second MOT, located in an ultrahigh vacuum region, where the trap-loss collision data is acquired. The optical set-up uses several injection-locked diode lasers for higher power, increased laser frequency stability, and improved reliability. For the chirped light, we ramp the current of external-cavity diode laser and are able to achieve chirp rates in excess of 1 GHz in 100 ns. This chirp can be transferred to an injection-locked "slave" laser, which results in a significant increase in usable output power. We can then select the desired portion (e.g., 100 ns) of the chirp with an acousto-optic modulator. We thus have control of both the frequency (or phase) and the amplitude of this light.

Ultracold collisions involving the highly-excited Rb 5D level are an interesting contrast to the extensively studied 5P collisions. The R^{-6} interaction potential for 5S+5D atoms is significantly shorter range than the R^{-3} potential for 5S+5P. Also, the radiative lifetime of the 5D level is much longer than that of the 5P: 240 ns vs. 27 ns. The combination of these factors means that, once produced, the 5D excitation should easily "survive" to short range. The experiments are performed by exciting cold atoms in a vapor-cell MOT with continuous two-photon two-color diode-laser excitation: 5S 5P 5D, and measuring the density-dependent loss rate due to collisions. In addition, the competing density-independent loss rate due to 5D photoionization (caused by both excitation lasers) must be accounted for. We previously determined this photoionization cross section by trap loss measurements.

Future Plans:

Our plans for the coming year involve two ultracold collisions experiments. First, we will continue our work with frequency-chirped collisions, building on the promising preliminary results we have obtained so far and incorporating our higher-power injection-locked chirped laser. These studies will involve characterizing the collisions as a function of the rate, range, and direction of the frequency chirp, as well as the intensity of the laser. If these results are promising, we will pursue more sophisticated schemes for coherent control of ultracold collisions, such as nonlinear chirps and multiple lasers.

In our second planned experiment, we will trap both isotopes (^{85}Rb and ^{87}Rb) and study collisions involving both species. Interactions between different species of ultracold atoms are of

interest for many reasons: sympathetic cooling of one species by another, mixed Bose-Einstein condensates and degenerate Fermi gas systems, and the formation of heteronuclear molecules which have electric dipole moments. In terms of ultracold collisions, the ground-excited potential between two atoms at long range depends on whether the atoms are identical (R^{-3}) or different (R^{-6}). Therefore, some of the trap-loss processes in mixed isotopes should be suppressed by the shorter range of the potential. The measurements will be carried out by observing how the trap-loss rate of one species is modified by the presence of the other.

Recent Publications:

"Measurement of the Rb($5D_{5/2}$) Photoionization Cross Section Using Trapped Atoms", B.C. Duncan, V. Sanchez-Villicana, P.L. Gould, and H.R. Sadeghpour, Phys. Rev. A **63**, 043411 (2001).

"A Frequency-Modulated Injection-Locked Diode Laser for Two-Frequency Generation", R. Kowalski, S. Root, S.D. Gensemer, and P.L. Gould, Rev. Sci. Instrum. **72**, 2532 (2001).

Cold Rydberg Atom Gases and Plasmas in Strong Magnetic Fields

G. Raithel, FOCUS Center, Physics Department, University of Michigan
500 East University, Ann Arbor, MI 48109-1120, *e-mail: graithel@umich.edu*

Program Scope.

Cold plasmas and gases of cold Rydberg atoms in a high-magnetic-field (high-B) environment are investigated. An extension of existing low-B cold-plasma research into the high-B domain is desirable because strong magnetic fields occur in many astrophysical, terrestrial or man-made plasmas. A strong magnetic field will increase the plasma lifetime, alter the plasma dynamics, and change the nature of any Rydberg atoms contained within the plasma. Further, due to the pinning of free charges to **B**-field lines, the addition of a strong B-field to cold plasmas is likely to suppress collisional electron heating mechanisms[1], potentially opening an avenue to the generation of a strongly coupled electron component in a cold plasma.

In a spinoff project, we investigate the stability of cold-electron gases in a combined Penning-Ioffe trap. This research relates to antihydrogen experiments[2], in which antihydrogen is formed by recombination of positrons and antiprotons confined in a nested Penning trap. The antihydrogen fallout is to be accumulated in a combined Ioffe-Penning trap, which must function both as a plasma and an atom trap. It still is to be shown whether the Ioffe-Penning trap is a stable plasma trap. Since the magnets and electrodes in our system allow us to realize Ioffe-Penning traps, we may be able to find an answer.

Methods.

The central component of our cryogenic high-B atom and plasma trap is a four-coil superconducting magnet welded into a LHe dewar. The magnet consists of a split-pair dipole coil and a pair of racetrack-shaped quadrupole coils accommodated in the bore of the dipole coils. With all four coils energized, a Ioffe-Pritchard type magnetic trap with up to 3.6T field at the trap center is obtained. The setup provides 6-way optical access to the trap center. The trap is loaded with Rb atoms using a vapor-cell pyramidal magneto-optic trap located outside the cryostat (PMOT; see Fig. 1 a). The PMOT emits a slow atomic beam that is re-captured by the cryogenic trap. An additional pusher laser beam co-aligned with the atomic beam is used to enhance the efficiency of the atom transfer.

We excite Rydberg atoms using a pulsed YAG and dye laser system. A set of Rydberg atom and plasma manipulation electrodes has been installed in the main bore of the cryogenic trap. Electrodes 2 and 3 (see Fig. 1 b) are used to apply electric fields to Rydberg atoms and plasmas. Electrodes 1 and 4 are used to shield stray electric fields and to provide well defined potentials for charged particles drifting towards the detector described below. The electrodes can also be operated in a Penning-trap mode, enabling us to study the stability of Ioffe-Penning traps and to perform certain collision experiments.

A position-sensitive detector assembly consisting of a two-stage microchannel-plate (MCP) and a phosphor screen has been installed on the axis of the main trap magnet. Electrons created at the atom trap location are guided by magnetic-field lines to the detector. The electric potential between the atom trap and the detector is controlled by drift tubes. Electrons are detected by counting MCP pulses (high temporal resolution but no spatial resolution) or by taking gated CCD images of the phosphor screen (moderate temporal resolution and high spatial resolution). Electron images of the trap center are enlarged by a linear magnification factor $\sqrt{B_0/B_{\rm det}}$, where B_0 is the magnetic field at the trap center and $B_{\rm det}$ the field at the detector location. To be able to vary the field of view of the electron detector, we have installed a water-cooled "zoom coil" around the detector head.

Results A: Cold plasmas and Rydberg atom gases in very weak magnetic fields.

Operating the superconducting trap magnet with small currents, three configurations of magneto-optic traps (MOTs) can be obtained (see Fig. 1 a). Photo-exciting atoms collected in the superconducting MOTs, we have measured the evolution of cold plasmas and Rydberg atom gases in practically zero magnetic field and black-body radiation fields of ≈ 4 Kelvin. The data in Fig. 1 c) and cuts through it show domains of l-mixing, n-mixing, and Rydberg atom formation through recombination. Also, the signatures of expanding cold plasmas can be identified. These features are known from previous experiments conducted by several

research groups in 300 K black-body radiation fields. We are studying the differences between the new results at 4 K and 300 K results. We find, for instance, that the density threshold for full-scale ionization of Rydberg gases seems higher at 4 K than it is at 300 K. At 4 K, the signature of quasi-free electrons and Rydberg states formed by recombination, marked by a white X in Fig. 1 c), is more long-lived than similar signals at 300 K. At low photo-electron energy, *i. e.* excitation closely above the photo-ionization threshold $\lambda_{\rm ion}$, we observe recombination into Rydberg levels that are much lower than at high photo-electron energy. This behavior has been predicted by Robicheaux *et al.*[3]. Atoms initially excited into high-lying (bound) Rydberg levels may evolve into surprisingly low-lying states (see signal near the question marks in Fig. 1 c). We have also observed this behavior in a 300 K radiation field, and considered Rydberg-Rydberg collisions triggered by attractive electric-dipole forces between high-l Rydberg states as an underlying mechanism.

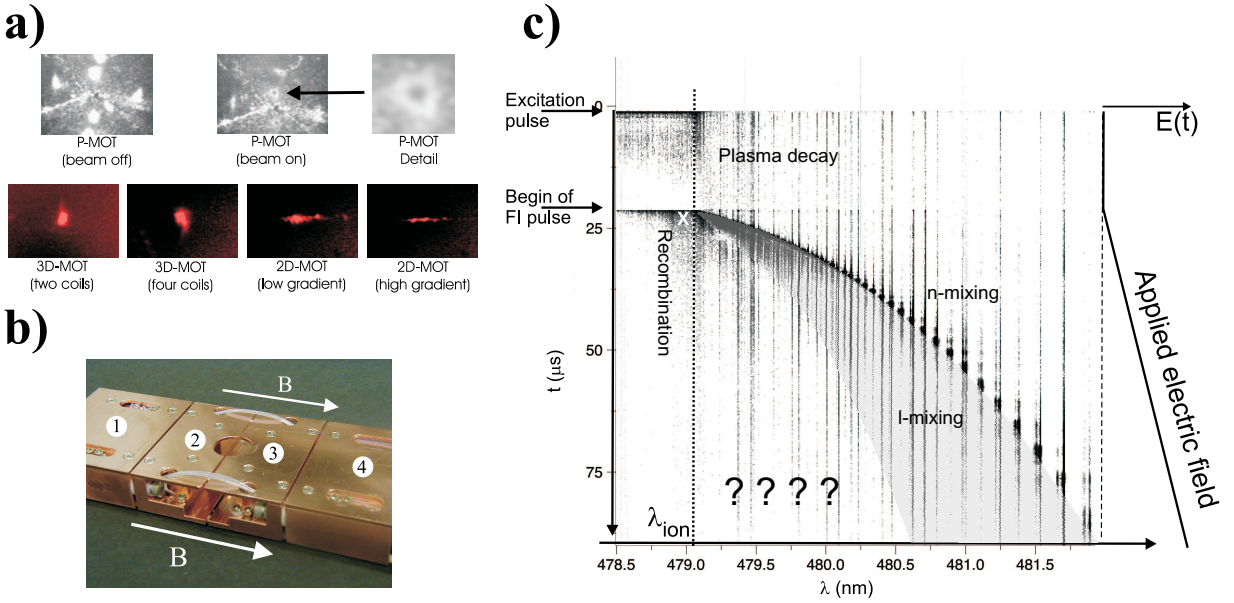

Figure 1: **a)** Top row: Primary pyramidal MOT used for atomic-beam generation. The atom cloud and multiple mirror images of it are visible. In atomic-beam mode, shown in the middle and on the right, atoms are continuously extracted from the PMOT center, leading to reduced MOT fluorescence with a characteristic doughnut-shaped outline. Bottom row: Secondary MOTs produced at the cryostat center.
b) Electrode structure inserted into the main trap magnet. The trapped-atom cloud collects at the center of the structure. The visible large openings and their hidden counterparts allow four trap laser beams to enter; two more trap beams enter through the main holes at the ends of the structure. The numbers are explained in the text.
c) Evolution of cold plasmas and Rydberg atom gases at 4 K radiation temperature in small magnetic fields. The vertical axis represents the time t (from the top down), and the horizontal axis the wavelength λ of the excitation laser. The count rate $R(t, \lambda)$ is represented using a logarithmic gray scale. The time of the excitation pulse, the onset of the electron extraction / field ionization (FI) pulse, and the photo-ionization threshold $\lambda_{\rm ion}$ are indicated. The shape of the FI pulse is sketched on the right.

Results B: Loading of the high-B molasses.

The most important recent result has been the successful loading of the high-B atom trap, which clears the way to high-B cold-plasma studies. ^{85}Rb atoms reaching the trap center in the state $|m_I = 2.5, m_S = 0.5\rangle$ are captured by a six-beam optical molasses. To date, trap loading could be demonstrated up to $B = 2.35\ T$ at the trap center, which is more than ten times higher than in previous high-B atom traps. At $B = 2.35$ T, the molasses lasers are blue-shifted from the field-free resonance by 32.9 GHz. To be able to lock and scan the molasses laser, we have constructed a temperature-stabilized Fabry-Perot-interferometer made of ULE glass. The number of atoms in the trap region is monitored via photoionization and electron counting. A typical measurement of the trap signal observed at fixed molasses laser frequency and variable trap magnetic field is shown in Fig. 2.

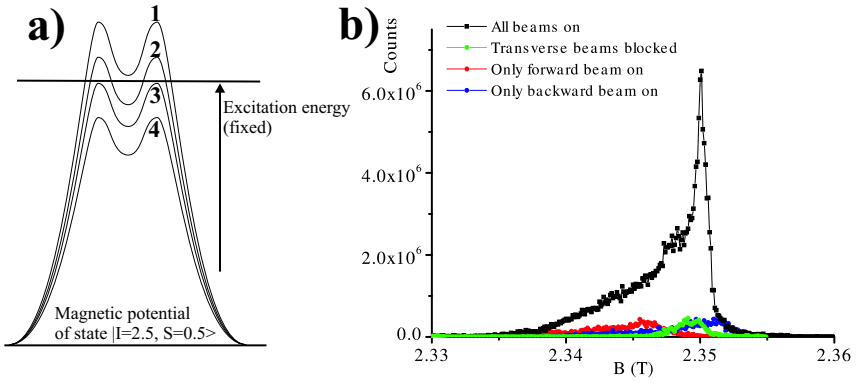

Figure 2: **a)** Magnetic potentials along the trap axis for different magnetic fields and fixed molasses laser excitation energy. The labels 1-4 indicate different heights of the trap minimum with respect to the excitation energy and correspond to the labels in panel b).
b) Trap signal measured vs. magnetic field B at the trap center. As expected, the molasses operates properly only when all six molasses beams are on and the situation labeled 1 is realized.

Results C: Electron gases in Ioffe-Penning traps.

A electron-emitting filament has been installed on the axis of the trap magnet. Applying suitable potentials to the filament and to the electrodes shown in Fig. 1 b, we can inject electrons along the magnetic-field lines into the atom trap region. These electrons serve many useful purposes. Firstly, we can trap them by switching the electrodes of Fig. 1 into an electron Penning trap configuration, allowing us to study the stability of Ioffe-Penning traps[2]. Secondly, the injected electron current can be used to operate the high-B atom trap in an "EBAT"-mode (Electron Beam Atom Trap), allowing us to study collision and recombination processes of atoms in strong B-fields as a function of a controlled electron energy. In these studies, it will be sufficient to excite a few Rydberg atoms or Rb^+-ions in the high-B molasses region.

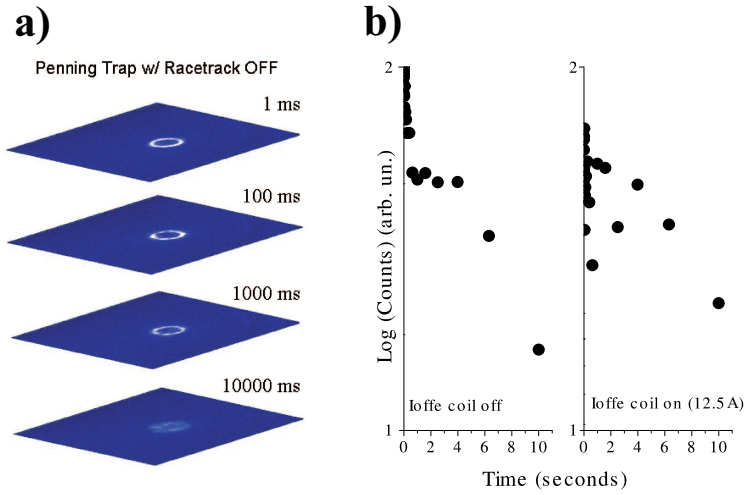

Figure 3: **a)** Images of electron clouds extracted from the high-B trap operated in a Penning trap configuration for the indicated extraction times.
b) Integral trapped-electron signal vs. extraction time in Penning (left) and Ioffe-Penning (right) configurations. The electron signal is plotted on a logarithmic scale covering a range of (only) a factor of two.

In Fig. 3, electrons have been injected into the system operated in a Penning trap mode with a center field of $B = 1$ T. The position of the loading filament has been deliberately adjusted such that the trap loading occurs off-axis, *i.e.* the injected electrons are trapped on orbits exhibiting large-diameter magnetron orbits. The electrons are extracted and imaged at variable delay times after the trap loading. The magnetron orbits appear as circles in the image plane, as seen in Fig. 3 a). The circles become washed out over time, indicating

that the magnetron radii of the trapped electrons diffuse. It is under investigation whether the diffusion is due to collisions or intrinsic instabilities of the trap. Fig. 3 b) shows the integral trapped-electron signal vs. the extraction time for the Penning (left) and the Penning-Ioffe configurations (right). So far, we could not see an influence of the Ioffe coils on the trapping time (which is good). However, our studies are just at the beginning.

Results D: Theoretical investigations.

We have supported our previous assumptions concerning the existence and the properties of long-lived high-B Rydberg states with theoretical results. We have calculated the spectra of Rydberg atoms in high B-fields using adiabatic basis sets, which reflect the different time scales of the electronic motion parallel and transverse to the magnetic field. With increasing absolute value of the azimuthal quantum number m, non-adiabatic corrections are found to become negligible, and the adiabatic basis states and their energies become exact solutions. Thereby, the statistical behavior of the spectra changes from being consistent with classically chaotic motion to being consistent with classically regular motion. We have then calculated the decay rates of both adiabatic and exact quantum states, and classified the decay modes into magnetron, z-bounce and cyclotron decays. As expected, high-$|m|$ Rydberg states were found to exhibit both long lifetimes and large densities of states.

Plans.

In the immediate future, it is planned to measure atom numbers and lifetimes of the high-B molasses. Then, the lifetimes of Rydberg atoms exited in the high-B trap will be determined as a function of excitation parameters. The effect of Rydberg-atom-electron collisions will also be studied directly using the above mentioned EBAT mode. The Penning trap studies will be continued with the goal to identify limiting conditions with regard to the operation of combined Ioffe-Penning traps.

Publications which acknowledge DoE support (2001 or later).

"High-angular-momentum Rydberg states in cold Rydberg gases," S. K. Dutta, D. Feldbaum, A. Walz-Flannigan, J. R. Guest, and G. Raithel, Phys. Rev Lett. 86, 3993 (2001).

"Spectroscopy of Rydberg Atoms is Non-neutral Cold Plasmas," D. Feldbaum, N. V. Morrow, S. K. Dutta, G. Raithel, in *Non-Neutral Plasma Physics IV*, eds. F. Anderegg, L. Schweikhard, C. F. Driscoll (AIP Conference Proceedings, Volume 606, New York 2002).

"l-Changing Collisions in Cold Rydberg Gases", A. Walz-Flannigan, D. Feldbaum, S. K. Dutta, J. R. Guest, G. Raithel, in *Photonic, Electronic and Atomic Collisions (XXII ICPEAC Proceedings)*, eds. J. Burgdörfer, J. S. Cohen, S. Datz, C. R. Vane (Rinton Press, Princeton, NJ, 2002).

"Tunneling resonances and coherence in an optical lattices," B. K. Teo, J. R. Guest, G. Raithel, Phys. Rev. Lett. **88**, 173001 (2002).

"Coulomb expansion of laser-excited ion plasmas," D. Feldbaum, N. V. Morrow, S. K. Dutta, G. Raithel, Phys. Rev. Lett. **89**, 173004 (2002).

"Decay rates of high-$|m|$ Rydberg states in strong magnetic fields," J. R. Guest, J.-H. Choi, G. Raithel, in print Phys. Rev. **A** (2003).

"High-m Rydberg states in strong magnetic fields," J. R. Guest, G. Raithel, submitted to PRA (2003).

"Time Averaging of Multi-mode Optical Fiber Output for a Magneto-Optical Trap," A. P. Povilus, J. R. Guest, S. E. Olson, R. R. Mhaskar, B. K. Teo, G. Raithel, submitted to Optics Letters (2003).

"Cold Rydberg Gas Dynamics," A. Walz-Flannigan, J. R. Guest, J.-H. Choi, and G. Raithel, submitted to PRA (2003).

References

[1] F. Robicheaux, J. D. Hanson, Phys. Rev. Lett. **88**, 55002 (2002).

[2] L. S. Brown, G. Gabrielse, Rev. Mod. Phys. **58**, 233 (1986), T. M. Squires, P. Yesley, G. Gabrielse, Phys. Rev. Lett. **86**, 5266 (2001).

[3] F. Robicheaux, J. D. Hanson, Physics of Plasmas, **10**, 2217 (2003).

Exploring Quantum Degenerate Bose-Fermi Mixtures

Deborah Jin
JILA, UCB440
University of Colorado
Boulder, CO 80309
jin@jilau1.colorado.edu

In this project we are exploring a dilute gas mixture of the bosonic ^{87}Rb atoms and fermionic ^{40}K atoms in the quantum degenerate regime. This combination of atomic species is convenient for the initial laser cooling stage, which uses a two-species vapor cell magneto-optical trap [1]. In addition, the collisional interaction between ^{87}Rb and ^{40}K atoms at ultralow temperature is relatively strong and attractive [2]. Strong interactions are favorable for the second stage of cooling. Here the gas mixture is loaded into a purely magnetic trap where the bosons are cooled via forced rf evaporation, while the Fermi gas is cooled indirectly through thermal contact with the Bose gas. The relatively strong interactions between ^{87}Rb and ^{40}K atoms will also enable us to explore interesting interaction effects in the Bose/Fermi mixture. For example, sufficiently strong mean-field interactions can cause the gas to become mechanically unstable [2].

Using a new apparatus that was constructed during the previous funding period, we typically cool $2x10^5$ Rb atoms and $2x10^4$ K atoms into the quantum degenerate regime. The cooling cycle takes roughly 1.5 minutes, after which the gas is probed using absorption imaging. We can take images of the either gas independently with the appropriate choice of probe light frequency. Absorption images can either be taken in the trap or after release from the trap followed by a period of expansion. Using time-of-flight (TOF) expansion images, we now have the capability to take images of both the Rb and K gases for a single cooling cycle.

While Bose-Einstein condensation of the Rb gas can be clearly seen in TOF images, evidence of the quantum degeneracy of the K Fermi gas is more subtle. We have recently explored the quantum degeneracy of the Fermi gas with two thermodynamic measurements. We have observed the Fermi pressure with absorption images of the trapped gas. At ultralow temperature the size of the Fermi gas becomes larger than that

of the Bose gas due their different quantum statistics. To quantitatively compare this observation with an ideal gas theory, we plot in Figure 1 the size of the trapped Fermi gas as a function of the temperature obtained from the Bose gas. This measurement shows the expected effect of Fermi pressure and demonstrates that we can reach temperatures as low as $T/T_F = 0.25$ where T_F is the Fermi temperature.

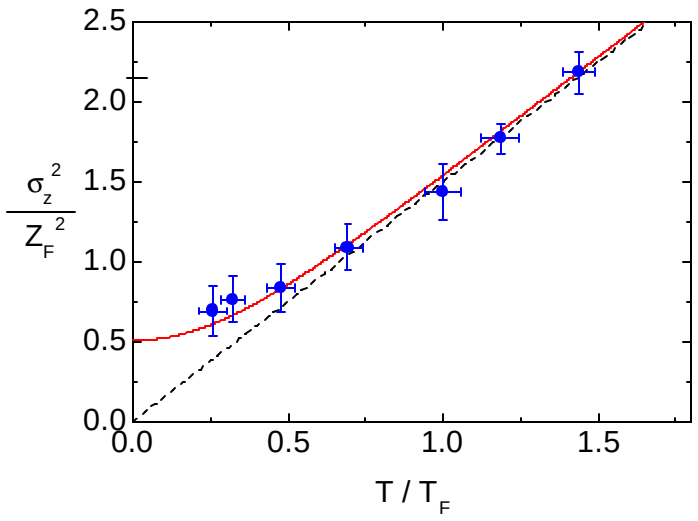

Figure 1. Measurement of Fermi pressure. The axial size σ_z of the trapped Fermi gas, obtained from a Gaussian fit to absorption images, is plotted vs. the normalized temperature T/T_F. T is determined from the Bose gas, and T_F is determined from the measured number of fermionic atoms and the harmonic trap frequencies. The cloud size has been normalized by Z_F, which is the maximum extent of the cloud at T=0. The solid line shows the expectation for an ideal Fermi gas while the dashed line is the classical expectation (no Fermi pressure).

A limitation of the measurement technique described above is that it becomes increasingly difficult to determine the gas temperature as the non-condensate fraction of the Bose gas becomes immeasurably small. This limitation can be circumvented by measuring the Fermi quantum degeneracy using only TOF images of the Fermi gas. Here we fit the absorption images to the expected Thomas-Fermi form for an ideal Fermi gas [3], with one extra fitting parameter, *z*, that describes the shape of the velocity profile. A quantum degenerate Fermi gas will have a very large z, corresponding to a strongly non-gaussian velocity distribution, while a non-degenerate gas will have *z* near 1. This

measurement is shown in Figure 2 as a function of T/T_F, where T is determined from the width of the Thomas-Fermi fit and T_F is determined from the measured atom number and harmonic trap frequency. The data shows the expected effect of the Fermi degeneracy and confirms that we can reach $T/T_F = 0.25$. Comparison with ideal gas theory (solid line) suggests that our determination of T/T_F is systematically high, corresponding for example to an underestimate of the number of atoms. Future work is needed to explore this discrepancy and to further increase the quantum degeneracy of the Fermi gas.

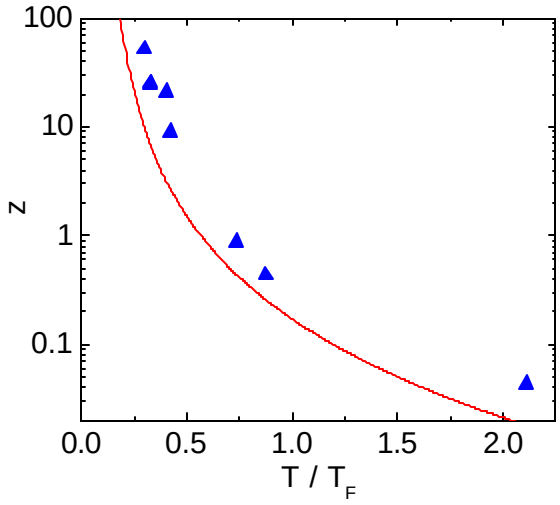

Figure 2. Measurement of Fermi degeneracy from the momentum distribution of the gas. In contrast the previous figure, here we determined T from the Fermi gas itself. Fermi quantum degeneracy gives rise to a non-gaussian momentum distribution which is measured by the Thomas-Fermi fit parameter z. The solid line shows the expectation for an ideal Fermi gas, while $z = 0$ for a classical gas.

Finally we are exploring the effect of interactions in the Bose-Fermi mixture. The importance of interactions can be enhanced by increasing the magnetic trap strength. This increases both the density of the gases and the spatial overlap (the mass difference of K and Rb can give rise to a vertical separation of the two trapped clouds due to gravity). After cooling the gas mixture into the quantum regime we have adiabatically increased the magnetic trap strength to look for interactions effects. So far dramatic effects such as collapse of the Fermi gas have not been observed.

To look more sensitively at interactions between the bosonic and fermionic atoms, we are now studying density oscillations of the trapped gas. We apply a time-dependent change in the magnetic trapping strength to drive these density oscillations. Their frequency and damping are then measured after the drive has been turned off. Recently we have observed a strong increase in the damping rate of a breathe-type excitation of the Fermi gas due to the presence of a Rb condensate. This is currently being investigated further.

Future work will concentrate on interaction effects in the quantum Bose-Fermi dilute gas mixture. After studying the magnetically trapped gas, ultimately we plan on loading the gas into a far-off-resonance optical dipole trap. Here we can explore mixtures of atoms in different spin-states and we can search for interspecies magnetic-field Feshbach resonances that would allow us to vary the interaction strength between the bosons and the fermions. The optical trap can also be used to increase the gas density (by increasing the confinement) and perhaps to perform more efficient evaporative/sympathetic cooling in the low temperature regime.

1. J. Goldwin, S. B. Papp, B. DeMarco, and D. S. Jin, "Two-species magneto-optical trap with K-40 and Rb-87," Phys. Rev. A **65**, 021402 (2002).
2. G. Modugno, G. Roati, F. Riboli, F. Ferlaino, R. J. Brecha, and M. Inguscio, "Collapse of a degenerate Fermi gas," Science **297**, 2240 (2002).
3. D. A. Butts and D. S. Rokhsar, "Trapped Fermi gases," Phys. Rev. A. **55**, 4346 (1997).

Quantum Dynamics of Ultracold Fermionic Vapors

Grant #DE-FG02-01ER15205
John E. Thomas
Physics Department, Duke University
Durham, NC 27708-0305
e-mail: jet@phy.duke.edu

1. Scope

The purpose of this program is to study collective quantum dynamics of a mechanically driven ultracold gas of ^{6}Li fermions, contained in an ultrastable CO_2 laser trap. In the vicinity of a Feshbach resonance, mixtures of the two lowest hyperfine states of ^{6}Li exhibit magnetically tunable s-wave scattering interactions ranging from zero to strongly attractive or strongly repulsive. Hence, this two-component mixture is particularly well suited for exploring fundamental interactions in Fermi gases. Pairing interactions in this system are predicted to lead to a Fermi superfluid phase at experimentally accessible temperatures, providing an atomic gas analog of a superconductor. Since the interaction strength and density can be experimentally controlled, it may be possible to study fundamental new features of spin pairing and superconductivity, such as the crossover from weak BCS pairing to Bose-Einstein condensation of strongly bound pairs.

2. Recent Progress

During the past year we have made important progress, producing a highly-degenerate Fermi gas by evaporative cooling in a CO_2 laser trap [1]. Using a high-field electromagnet, interactions are induced in the gas by tuning a bias magnetic field to the vicinity of a Feshbach resonance [2], where strong interactions are observed and very low temperatures are achieved [3]. The gas exhibits highly anisotropic expansion upon release from the optical trap, a signature of hydrodynamic behavior [3]. We have made the first study of the expansion dynamics, which may arise from collisional hydrodynamics or collisionless superfluid hydrodynamics. We have also made the first measurement of an important universal many-body parameter, the ratio of the mean field energy to the local kinetic energy [4]. These results are described briefly below.

All-Optical Production of a Highly-Degenerate, Strongly-Interacting Fermi Gas

Our experiments employ an ultrastable CO_2 laser trap which is used to confine arbitrary mixtures of the two lowest hyperfine states of ^{6}Li atoms, which are loaded from a standard magneto-optical trap (MOT) at a temperature of $\simeq 150\,\mu$K. Further cooling is accomplished by direct evaporation in the CO_2 laser trap [1]. The CO_2 laser trap has depth of 700 μK and a very low optical scattering rate of only two photons per atom per hour as as consequence of the long wavelength. The trapping laser achieves very low intensity noise, suppressing noise-induced heating. Extremely low residual heating rates of less than 5 nK/sec are measured and a lifetime of 400 seconds is achieved, comparable to the background gas limit at 10^{-11} Torr.

Rapid evaporation is achieved by applying a bias magnetic field of 910 G, near the Feshbach resonance for mixtures of the two lowest states of ^{6}Li. A 50-50 mixture is produced by rate-equation radio-frequency pumping prior to applying the bias field. High evaporation efficiency is achieved by lowering the trap depth U by a factor of $\simeq 200$ while maintaining $U/k_BT \geq 10$, where T is the temperature. The trap is then adiabatically recompressed to full trap depth. After this procedure, typically $N = 1.6 \times 10^5$ atoms remain at a temperature of $0.7\,\mu$K. The corresponding Fermi temperature is $\simeq 8\,\mu$K.

The experiments achieve the conditions predicted for the onset of resonance superfluidity in a strongly interacting Fermi gas. However, near a Feshbach resonance, the gas also exhibits unitarity-limited collisional interactions [3]. In either case, the gas is expected to expand hydrodynamically upon release from the trap [3]. This hydrodynamic behavior is observed in the experiments, and produces a highly anisotropic expansion is which the initially narrow dimension of the gas expands rapidly, while the initially long dimension hardly changes. The energy is released anisotropically because of the density gradient, which produces a much larger force in the initially narrow direction.

Mechanical Stability and Universal Behavior in a Strongly-Interacting Fermi Gas

A two-component atomic Fermi gas in the vicinity of a Feshbach resonance offers an important testing ground for exploring universal strong interactions in nature. The strong interactions of interest are characterized by a potential of short range R and a zero-energy s-wave scattering length a_S which has a magnitude large compared to the interparticle spacing L. Calculation of the many body ground state and dynamical behavior of even a simple two-component Fermi system in this regime is a difficult problem, which spans nearly thirty years and includes disciplines ranging from condensed matter to neutron stars and nuclear matter [4].

Universal behavior arises when $R << L << |a_S|$. In this limit, we have approximately $0 << L << \infty$. Hence, the only relevant length scale is the interparticle spacing L, and the only relevant energy scale is the local Fermi energy $\epsilon_F(\mathbf{x})$. Then, the mean field energy must be proportional to $\epsilon_F(\mathbf{x})$ with a universal proportionality

constant β. Predictions of β in this regime suggest that β is always negative, with a value near -0.5, independent of a_S. However, the precise value of β remains an open question. Further, the value of β is expected to differ between the normal and superfluid phases.

It is easy to show that when $|\beta| < 1$, the pressure exerted by the mean field is always smaller than the local Fermi pressure, and the gas must be mechanically stable [4]. By determining the initial radii of the trapped gas from the expansion data, we have measured β and obtain a value of -0.26 comparable to predictions.

3. Future Plans

Our immediate plans include modulating the trap depth for parametric resonance studies of the trapped gas in the strongly-interacting hydrodynamic regime. At sufficiently low temperatures, both a normal collisionless and a superfluid component should exist. Each of these components has different collective oscillation frequencies. Hence, measurement of the resonance frequencies is of great interest.

We also plan a study of the scissors mode of the trapped gas, by abruptly twisting the optical trap through a few mrad. The superfluid component of the gas is predicted to exhibit undamped oscillations in this regime which can be observed via images of the expanding gas.

Improved measurements of universal mean field interactions are also planned, to determine if the transition to a superfluid state can be measured via a change in the β parameter described above.

4. References to Publications of DOE Sponsored Research

1) S. R. Granade, M. E. Gehm, K. M. O'Hara, and J. E. Thomas, "All-Optical Production of a Degenerate Fermi Gas," Phys. Rev. Lett. **88**, 120405 (2002).

2) K. M. O'Hara, S. L. Hemmer, S. R. Granade, M. E. Gehm, and J. E .Thomas, "Measurement of the Zero Crossing in a Feshbach Resonance of Fermionic ^{6}Li," Phys. Rev. A **66**, 041401(R) (2002).

3) K. M. O'Hara, S. L. Hemmer, M. E. Gehm, S. R. Granade, and J. E. Thomas, "Observation of a Strongly Interacting Degenerate Fermi Gas of Atoms," *Science* **298**, 2179 (2003).

4) M. E. Gehm, S. L. Hemmer, S. R. Granade, K. M. O'Hara, and J. E. Thomas, "Mechanical Stability of a Strongly Interacting Fermi Gas of Atoms," Phys. Rev. A **68**, 011401(R) (2003).

- "Physics of Low-Dimensional Bose-Einstein Condensates", Grant No. DE-FG02-01ER15203

Eugene B. Kolomeisky (PI)
Department of Physics
University of Virginia
382 McCormick Road
Charlottesville, VA 22904-4714
ek6n@virginia.edu

- The project consists in investigating fundamental properties of low-dimensional superfluids (Bose-condensed alkali gases in strongly anisotropic traps, for example) and related systems within a wider scope of the DOE Nanoscale Science, Engineering, and Technology Initiative.

- **Recent Progress.** During the period of September 2002 – September 2003 we have been working on several (mostly completed projects) described below in more detail:

1. Quantum fluctuations of charge and phase transitions of a large Coulomb-blockaded quantum dot [with R. M. Konik (postdoctoral associate) and X. Qi]. This previously described work has now been published in Physical Review B. Moreover the paper has been selected for the August 15, 2002 issue of the Virtual Journal of Applications of Superconductivity, http://www.vjsuper.org and for the August 26, 2002 issue of the Virtual Journal of Nanoscale Science & Technology, http://www.vjnano.org.

2. Ground-state properties of one-dimensional matter and quantum dissociation of a Luttinger liquid [with X.Qi, and M.Timmins]. We analyzed ground-state properties of strictly one-dimensional molecular matter comprised of identical particles. An experimental example would be molecular hydrogen confined inside interstitial channels of carbon nanotube bundles. Such a class of systems can be described by an additive two-body potential whose functional form is common to all substances that only differ in the energy and range scales of the potential. The presence of a minimum in the two-body interaction potential leads to a many-body bound state which is a Luttinger liquid. As the degree of zero-point motion increases, the asymmetry of the two-body potential causes quantum expansion, softening, and eventual evaporation of the Luttinger liquid into a gas phase. Selecting the pair interaction potential in the Morse form we analytically computed the properties of the Luttinger liquid and its range of existence. As quantum fluctuations increase, the system first undergoes a discontinuous evaporation transition into a diatomic gas followed by a continuous dissociation transition into a monoatomic gas. In particular we find that spin-polarized isotopes of hydrogen and He-3 are monoatomic gases, He-4 is a diatomic gas, while molecular hydrogen and heavier substances are Luttinger liquids. We also investigated the effect of finite pressure on the properties of the liquid and monoatomic gas phases. In particular we estimate a pressure at which molecular hydrogen undergoes an inverse Peierls transition into a metallic state which is a one-dimensional analog of the transition predicted by Wigner and Huntington in 1935. This work has been published in Physical Review B.

3. The Bose molecule in one dimension (with J. P. Straley and S. C. Milne). We considered a collection of *attractive* bosons with short-range interactions in one dimension. This system which recently found an experimental realization in a ^{7}Li vapor [L. Khaykovich *et al*, Science **296**, 1290 (2002); K. E. Strecker *et al*, Nature **417**, 150 (2002)] is an example of a many-body bound state having the form of a well-localized "molecule". The properties of this molecule have been computed either exactly or using the Gross-Pitaevskii theory thus shedding some light on the range of applicability of the mean-field approach. Specifically, we have calculated the Green function, momentum distribution, two-particle correlation function, structure factor, and given an argument showing that this bosonic molecule has no excited states other than dissociation into separate pieces. This work is submitted to Journal of Statistical Physics.

DOE sponsored publications

1. Kolomeisky EB, Qi X, Timmins M, *Ground-state properties of one-dimensional matter and quantum dissociation of a Luttinger liquid*, PHYS REV B B 67(16): art. no 165407 APR 15 2003.

2. Kolomeisky EB, Konik RM, Qi X, *Quantum fluctuations of charge and phase transitions of a large Coulomb-blockaded quantum dot*, PHYS REV B 66(7): art. no. 075318 AUG 15 2002; also in the August 15, 2002 issue of the Virtual Journal of Applications of Superconductivity, http://www.vjsuper.org and in the August 26, 2002 issue of the Virtual Journal of Nanoscale Science & Technology, http://www.vjnano.org.

3. Xiaoya Qi, *Ground-state properties of one-dimensional systems and the physics of the Coulomb blockade*, PhD thesis, May 2003, University of Virginia.

- **Future plans**

Single-atom pipette and boson blockade. The manipulation and control of single particles has been a long-term goal with important applications in fundamental physics. Single-electron manipulation in quantum dots is possible because the electrons carry charge. The manipulation of neutral particles is naturally more difficult to accomplish. The goal of the project is to demonstrate feasibility of a quantum single-particle pipette using Bose-condensates of alkali vapors. The main idea parallels that of the Coulomb blockade in electronic systems. Consider a short-range atomic trap whose parameters (depth and width) can be externally controlled. Assume the trap is deep enough so that it can support at least one single-particle state. The trap can bind arbitrarily large number of *non-interacting* bosons with the system energy decreasing *linearly* with the particle number N (Bose condensation). However for *repulsive* bosons there will additionally be energy penalty roughly proportional to the number of pair interactions in the system, N(N-1)/2. As a result, the ground-state energy of the system as a function of number bound bosons, E(N), will have a minimum at some value N_c which may be called the trap capacity. The capacity depends on the trap parameters, and it becomes relevant if the trap is coupled to a reservoir of atoms. If the trap is strongly-coupled to the reservoir, then its average population will closely track N_c. In this regime if the

parameters of the trap potential change, there will be a corresponding *continuous* response of the trap population. If, on the other hand, the trap is weakly coupled to the reservoir, the discreteness of the particles becomes relevant. Generally the trap capacity N_c (which one can vary experimentally) is not an integer. As a result as N_c changes, the trap population is locked onto nearest integer until degeneracy occurs, $E(N \pm 1) = E(N)$, i.e. it becomes favorable to eject or accept a particle. At that moment the trap population will change by exactly one particle, and the dependence of the trap population N on experimentally controlled capacity N_c will have a form of *discontinuous* "boson" staircase. The trap weakly coupled to a reservoir of atoms is an example of single-atomic pipette whose operation is based on interparticle repulsion combined with their discreteness. As the parameters of the trap potential vary, the pipette can extract or release a desired number of particles one by one. This picture is oversimplified because it ignores the fact that the size of the bosonic cloud localized on the trap may depend on the particle number N. The project will address this issue; however it seems reasonable that gross physical picture will not be qualitatively affected. Another question that needs to be answered is what is the relationship between the degeneracy condition $E(N \pm 1) = E(N)$ and that of delocalization of the wave function of the system. If they coincide, then the point of degeneracy is also a critical phenomenon. Otherwise the particle extraction or addition is similar to a first-order phase transition. It is also interesting to see how the bosonic staircase evolves into the $N = N_c$ dependence as the trap is made more and more open.

•

MOTRIMS as a Probe of AMO Processes

B. D. DePaola, J. R. Macdonald Laboratory, Kansas State University
Manhattan, KS 66506 [*depaola@phys.ksu.edu; (785)532-1623*]
[Collaborators: S. R. Lundeen*, R. Brédy, M. A. Gearba, H. Nguyen, and H. Camp]

Magneto-optical trap recoil ion momentum spectroscopy (MOTRIMS) has been shown to be[1-3] a powerful tool in the study of the dynamics of ion-atom collisions. An offshoot of the proven COLTRIMS methodology, MOTRIMS has the advantages of a colder target (allowing better resolution in Q-value and scattering angle measurements) and a target which can be readily laser-excited (allowing the study of a more general class of collision systems). Critical to the study of laser-excited systems is a direct and unambiguous measurement of the fraction of atoms lying in an excited state. We will show how the MOTRIMS method can be used to *simultaneously* measure both the excited state fraction, and the relative cross sections for charge capture. These measurements are differential in scattering angle, and incoming and outgoing channels, and thus represent a "complete" measurement of the dynamics of the collision system under study. The procedures used to directly measure excited-state fractions in 2-level systems can be extended to n-level systems. For example, we will present the results of charge capture cross section measurements on the step-wise excited 3-level system: $Rb(5s) \rightarrow Rb(5p) \rightarrow Rb(4d)$.

The study of laser-excited systems can entail other complications as well. For example, in the symmetric collision system $Rb^+ + Rb$, two energetically degenerate channels dominate charge transfer: $Rb^+ + Rb(5s) \rightarrow Rb(5s) + Rb^+$, and $Rb^+ + Rb(5p) \rightarrow Rb(5p) + Rb^+$. These channels are both resonant and therefore in both cases have Q-values of identically 0. Thus, one cannot in the usual way employ the Q-value "spectrum" to isolate and compare the two channels. However, by comparing the change in populations in other non-degenerate channels while the trapping laser is chopped on and off, one can deduce the target excited-state fraction and, ultimately, the relative capture cross sections for the two degenerate channels.

The power of the MOTRIMS methodology in the measurement of excited-state fractions can be exploited in the study of other AMO processes in which ionizing collisions play no role at all.[4] Possibilities include the coherent excitation processes of STIRAP (stimulated Raman adiabatic passage) and EIT (electromagnetically induced transparency). Both of these may play important roles in quantum information technology.

In this presentation, the basics of the MOTRIMS methodology will be reviewed, and a sample of results from cross section measurements will be discussed. Finally, an update on the ongoing studies of the STIRAP process will be presented.

---

* Colorado State University, Ft. Collins, CO

1) M. van der Poel, C. V. Nielsen, M. A. Gearba, N. Andersen, Phys. Rev. Lett. **87**, 123201 (2001).
2) J. W. Turkstra, R. Hoekstra, S. Knoop, D. Meyer, R. Morgenstern, R. E. Olson, Phys. Rev. Lett. **87**, 123202 (2001).
3) X. Fléchard, H. Nguyen, E. Wells, I. Ben-Itzhak, B. D. DePaola, Phys. Rev. Lett. **87**, 123203 (2001).
4) R. Brédy, H. Nguyen, H. Camp, X. Fléchard, B. D. DePaola, Nucl. Instrum. Meth. B **205**, 191 (2003).

Chemistry with Ultracold Molecules

Dudley Herschbach and Bretislav Friedrich
Department of Chemistry and Chemical Biology,
Harvard University, Cambridge, MA 02138

This project aims to develop simpler and more versatile means of generating slow and cold molecules, and manipulating their trajectories, in order to pursue collision dynamics with "nanomatter waves" having deBroglie wavelengths of the order of 1-100 nm. During the past year, we made three chief advances, two experimental and one theoretical.

1. Cool Pulsed Molecular Micro-Beam. We have previously demonstrated a promising approach to producing intense beams of molecules with very low kinetic energy. This enhances means to influence molecular trajectories by interaction with external fields, particularly required to achieve spatial trapping. The device employs a supersonic nozzle mounted near the tip of a hollow high-speed rotor, into which a permanent gas is fed continuously. Spinning the rotor with peripheral velocities of several hundred meters/sec, contrary to the direction of gas flow from the nozzle, markedly reduces the velocity of the emerging molecular beam in the laboratory frame. For instance, we produced an O_2 beam with kinetic energy only 9 °K, corresponding to a deBroglie wavelength of 2 Å. However, the continuous gas flow has been a major limitation. It gives rise to a 360^o spray that requires drastic pumping, as slow molecules are strongly scattered by background gas. To avoid this requires a means to pulse the source, synchronously with the rotor, so that the molecular beam is emitted only in the "firing position." After much effort, we have now attained an ablation source, pulsed by a laser, which is small enough to mount on a high-speed rotor and requires minimal pumping. Moreover, we find this source is remarkably effective in cooling the ablation plume. These virtues indicate the source will prove useful in many other applications.

In a paper to appear in Rev. Sci. Inst., we describe the source and its use to produce cool, pulsed beams of CaF radicals, a candidate species for magnetic trapping. The radicals are generated by laser-ablating a solid precursor target in a small cell of volume only about 0.01 cm^3. The target is ablated through an orifice, 750 micrometers in diameter, by a pulsed Nd:YAG laser. The ablation plume supersonically expands into a vacuum chamber and cools the initially hot CaF molecules seeded in it. We enhance the supersonic character of the expansion by feeding into the ablation cell about 10 torr of He, Ar, or Xe carrier gas. The CaF molecules are probed by time-resolved laser absorption spectroscopy. With a Xe carrier, about 10^{12} molecules are found to be seeded in a single pulse and cooled down to a terminal translational temperature of about 140 °K (an order of magnitude

lower than the initial plume temperature). We expect that a wide variety of species, including highly unstable ones, will be amenable to forming such a cool intense micro-beam, to the benefit of spectroscopy, reaction dynamics, and microfabrication.

2. Silver-surface Imaging Detector. Having experienced the difficulty of determining velocity distributions of very slow molecules (bedeviled by "wrap-around" problems afflicting the usual time-of-flight methods), we decided to pursue diffraction measurements of the deBroglie wavelengths, as that is anyhow the parameter of prime interest. In order to make that feasible without constructing a very elaborate and expensive detector capable of scanning and resolving narrow diffraction structure, we decided to explore a venerable method. It is akin to that used by Otto Stern in his classic experiments 80 eighty years ago. His work with silver atom beams employed a deposition detector, and he found cigar smoke greatly enhanced the sensitivity by converting faint traces of the metal into jet black silver sulfide. After verifying this, we soon found that we could detect molecules not containing sulfur, such as hydrogen bromide, by directing a beam onto a surface coated in vacuum with a very thin layer of silver. Our aim is to record the entire diffraction pattern produced by a transmission grating and read it by means of a microscope backed by a CCD camera. We find this has yields a spatial resolution of 1 micrometer and angular resolution of about 0.3 microradians, difficult to achieve by other means. After many trials, we finally evolved a protocol that yields reproducible images of beam profiles with sensitivity corresponding to a few monolayers of HBr.

Our HBr beam is seeded in a supersonic expansion of Ar. This produces a terminal temperature of 10 °K; if the rotational temperature is also 10 °K, as expected from prior work, over 80% of the HBr molecules are in the J = 0 state. By means of an electric deflecting field, which we are now installing (while awaiting fabrication of a transmission grating), the J = 0 molecules can be efficiently steered along the field direction into a trapping region.

3. Tunneling at the Wigner Limit. If as usual a potential energy surface for a chemical reaction has an activation barrier, regime of long deBroglie wavelenths Λ tunneling becomes the dominant reaction pathway. When Λ becomes larger than the thickness of the barrier, the rate constant is governed by a threshold law derived by Wigner; to attain this limit, the relative kinetic energy of the reactants needs to be well below 1 K for a hydrogen atom reaction and about a hundredfold lower for heavier reactants like chlorine molecules. As a guide for prospective experiments and for interpreting much more elaborate theoretical studies, we have revisited the Eckart potential, a venerable one-dimensional model. For the long-wavelength limit (kinetic energy approaching 0 °K), we have obtained explicit analytical formulas for the reaction cross sections and rate constants, for

thermoneutral, exothermic, and endothermic processes. This provides a simple reduced variable plot from which tunneling can be readily estimated for a wide range of chemical systems. We have also examined specifically reactions of F, O, C, and H atoms with H_2, D_2, and hydrogen halides.

Future work: We plan now to take advantage of our ablation supersonic source, in combination with a much improved differential pumping technique (developed last year) to improve the counter-rotating nozzle apparatus and thereby obtain beams with kinetic energy below 1 K. In addition to further work with CaF radicals, particularly inviting is the possibility of generating in this way ultracold $C(^3P_j)$ atoms, well suited for magnetic trapping. Early experiments in prospect include shutting off the trap to allow the C atoms to fall in vacuum onto a cold crystal surface, with and without adsorbed reactant molecules. Another prospective experiment would aim to confine and cool haloacetylene molecules, CHCX (with X = F or Cl) in an electrostatic trap, and then let the ultracold C atoms drop into that trap (or vice-versa). These reactions are much interest in combustion and interstellar processes.

Publications: A paper titled "A Cool Pulsed Molecular Micro-Beam," by B.S. Zhao, M. Castillejo, D.S. Chung, B. Friedrich and D. Herschbach, has been accepted by Rev. Sci. Inst. Two other research papers are in preparation, describing our work with the silver-surface detector, by S. Sunil, D.S. Chung, B. Friedrich, and D. Herschbach; and the treatment of tunneling in the Wigner limit, by D. Herschbach. Also, a historical paper, which includes a description of the genesis and development of our silver-surface detector, has been accepted by Physics Today; it is titled "The Stern-Gerlach Experiment: How a Bad Cigar Helped to Reorient Atomic Physics," by B. Friedrich and D. Herschbach.

Research with Slow Molecules & Slow Atoms

Harvey Gould,
MS 71-259, Lawrence Berkeley National Laboratory, Berkeley, CA 94720 (gould@lbl.gov)

August 2003

RECENT PROGRESS

Cs Scalar Polarizability Improved to 0.14% in Slow-Atom Experiment

C_6 also determined

Jason Amini and Harvey Gould

The measurement of the static scalar dipole polarizability of cesium has been improved to 0.14% from last years preliminary uncertainty of 0.25%. This is a factor of 14 improvement over the previous published measurement and very sensitive to the 4% contribution from the core electrons: it is sufficient to test high precision calculations that include core electron contributions. A comparison between experiment and theory is shown below. A manuscript will be published in Phys. Rev. Lett. and a preprint can be found at http://arXiv.org/abs/physics/0305074

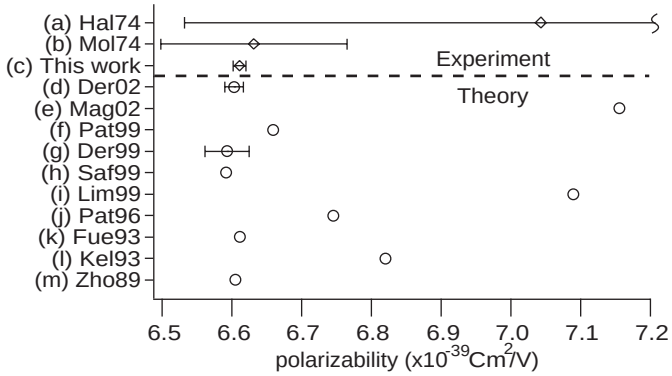

The experiment determines the scalar static polarizability by comparing the time-of-flight of a fountain of cold Cs atoms traveling through an electric field and through no electric field. This is a new technique developed by our group at LBNL.

From our polarizability result, we have derived the lifetimes of the cesium $6^2P_{1/2}$ and $6^2P_{3/2}$ states and the cesium-cesium dispersion coefficient C_6.

Supported, in its early stages, by the Division of Chemical Sciences, Geosciences & Biosciences of the U.S. DOE and currently by NASA. JA is supported by NASA and NSF.

PROGRAM SCOPE

Berkeley Molecular Decelerator Construction Begins with Dipole Moment Spectrometer

Route to slow molecule scattering expts.

H. Gould, J.G. Kalnins, G. Lambertson, & H. Nishimura

An apparatus that may ultimately measure molecule-molecule scattering at kinetic energies to below 100 mK and cross sections down 10^{-16} cm^2/molecule has had a modest beginning: it's first stage - a dipole moment spectrometer designed to separate strong-field seeking states of polar molecules is nearing completion (see accompanying article on third page). The P.I. hopes that additional stages can be constructed soon.

There is a clear need for such a machine because no scattering cross sections have been measured for molecule-molecule collisions at kinetic energies below 1 K [1]. Molecular collisions at kinetic energies below 1 K are predicted to have new and interesting quantum properties such as shape resonances and Feshbach-like resonances that cause sharp peaks in the scattering cross sections [2].

Molecule - *atom* scattering cross sections are calculated [2] to be in the range of 10^{-11} to 10^{-16} cm^2/molecule and to produce rates of over 10^{-10} cm^3/m for relaxation of high vibrational levels. Scattering cross sections between polar molecules may be even larger.

To study molecule-molecule collisions in a crossed beam geometry, two successive pulses of molecules will be decelerated. The first decelerated pulse is switched into the long arm of the crossed beam apparatus (see figure) and the second pulse of molecules is switched into the short

continued on next page

arm: the two pulses then arrive at the crossing point simultaneously. The final collision energy is varied by additional decelerating elements just before the interaction region.

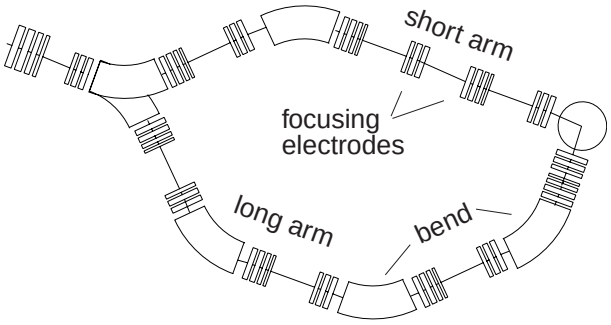

Crossed beam apparatus using a single molecular decelerator, More advanced versions would slow and collide two different molecules.

An initial set of experiments may be done in a colinear geometry by having the second pulse, slowed slightly less than a first pulse, overtake the first pulse. To study cold atom-molecule collisions, including reactive scattering, we plan to use a laser atom trap as a target. Detection can be very efficient because slow molecules stay in the detection region some 50 times longer than do thermal molecules.

The Berkeley Molecular Decelerator (see bottom figure) is designed to slow molecules in a strong-field seeking state including CH_3F, NH_3, SO_2, CH_2O, CHN, C_2H_3N, nitrobenzene, single- and di- fluoro benzene phenol, pyrimidine, pyridazine and many others. It will also work with radicals such as OH, CF, NH, methoxy, vinyloxy, and radicals of most of the molecules listed above (with lower intensities).

The decelerator design is the work of George Kalnins, Glen Lambertson, and Hiroshi Nishimura - Accelerator Physicists with many decades of experience. Papers on transporting, decelerating, and storing neutral molecules are listed in the publications section. In their design, the decelerator uses electrodes of decreasing length which provides superior bunching and focusing compared to fixed length electrodes. The initial pulse length is very long - over 150 micro s. This makes the decelerator long but is essential to achieve the very high density in the individual pulse (over 10^9 molecules cm^{-3}) necessary for the beam - beam collision experiments.

[1] There has been a single molecule-atom scattering experiment in the 0.3 - 1 K range: J. D. Weinstein, R. deCarvalho, T. Guillet, B. Friedrich & J. M. Doyle, Nature, **395**, 148 [1998].

[2] N. Balakrishnan, R.C. Forrey, and A. Dalgarno, Chem. Phys. Lett. **280** 1 (1997); R.C. Forrey, V. Kharchenko, N. Balakrishna, and A. Dalgarno, Phys. Rev. A**59**, 2146 (1999); J. Bohn, Phys. Rev. A**62**, 032701 (2000); N. Balakrishna, A. Dalgarno and R.C. Forrey, J. Chem. Phys. **113**, 621 (2000); M. Kajita, Eur. Phys. J. D**20**, 55 (2002).

JGK, GL, and H.N. are supported by LBNL Laboratory Directed Research & Development Funds

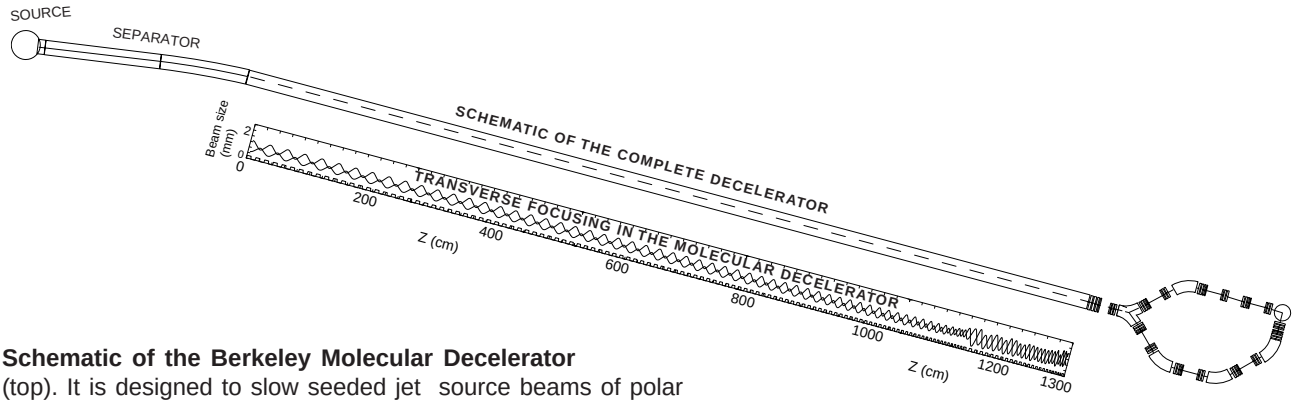

Schematic of the Berkeley Molecular Decelerator (top). It is designed to slow seeded jet source beams of polar molecules in strong-field seeking states from 310 m/s to several m/s. The calculated acceptance is 3 mm-mr in each transverse direction and the longitudinal acceptance is >1 %. The bottom figure shows the transverse optics. The decelerator includes one focusing or defocusing lens for each decelerating element. In a properly designed system the length of the decelerator does not increase the beam losses.

Dipole Moment Spectrometer to be Tested for Use with Radicals

Harvey Gould and John Bozek

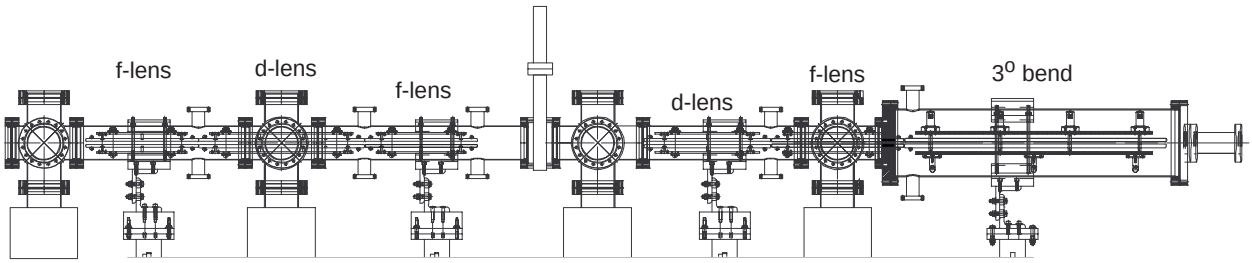

Assembly drawing of the Dipole Moment Spectrometer. Seeded jet source molecules enter from the left and are focused and transported by the long F-D-F triplet lens followed by a D-F doublet. The molecules, in a single strong-field seeking state, will focus at the end of the apparatus after the three-degree bend and acceptance match to both the Molecular Decelerator or to a photo-electron spectrometer.

Radicals, molecules with one or more unpaired electrons are important (usually) short-lived intermediate species in chemical reactions, combustion, upper atmosphere chemistry, comet and planetary atmospheric chemistry, and in other high energy environments.

Highly reactive due to their unpaired electron(s), they must usually be produced in a source closely linked to the spectroscopic experimental apparatus. They are typically produced by decomposition of a precursor resulting in a mixture of precursor with a variety of radicals. Secondary reactions of the radicals may add to the mixture.

Experiments that measure ionization potentials and vibrational and rotational energy levels (aimed at characterizing the energetics of such radical species) can selectively detect the species of interest. However this is not generally an option in synchrotron radiation and synchrotron photoelectron spectroscopy experiments. As a result, few synchrotron radiation and even fewer electron spectroscopy experiments have been carried out on these important species.

The Dipole Moment Spectrometer, whose construction is nearing completion, will be able to separate radical species by differences in their dipole moments and masses. It uses bending and electrostatic focusing elements invented by Kalnins, Lambertson, and Nishimura, and constructed at LBNL. These and its modern beam optics design give the Dipole Moment Spectrometer a high acceptance and a resolving power of ten, making it suitable for forming beams of radicals separated from the precursor.

The radical of interest would be seeded in a pulsed supersonic jet to cool the radical products in the expansion. Unlike electrostatic hexapoles, which do not focus strong-field seeking states, the Dipole Moment Spectrometer is specifically designed for molecules in a strong field seeking states and is well suited for use with polar cyclic molecules and molecules with up to eight carbon atoms as they typically have a small rotational splitting and often have substantial dipole moments.

Following commissioning and tests using a helium lamp, the Dipole Spectrometer will first be used to measure radical photo ion yields (PIY) as a function of photon energy at core edges (up to 350 eV) that are accessible on ALS beamline 10. Following this demonstration we would advance to PIY spectroscopy with a time-of-flight apparatus and finally to electron spectroscopy.

The Mechanical design was done by R. Weidenbach. JB is supported by The Division of Material Sciences, U.S. DOE.

Synchrotron Storage Ring Feasible for Strong-Field Seeking States

Calculations & Numerical Modeling used for CH_3F in J = 0 State at 30 m/s

Culmination of Laboratory Directed R & D Study

Hiroshi Nishimura, Glen Lambertson, Juris G. Kalnins, & H. Gould

Molecules, as do atoms, must be evaporatively cooled to reach quantum condensate conditions of temperature and phase space density. But only the lowest rotovibrational level is likely to survive the cooling process and this level is always strong-field seeking in the electric field needed to confine the molecules.

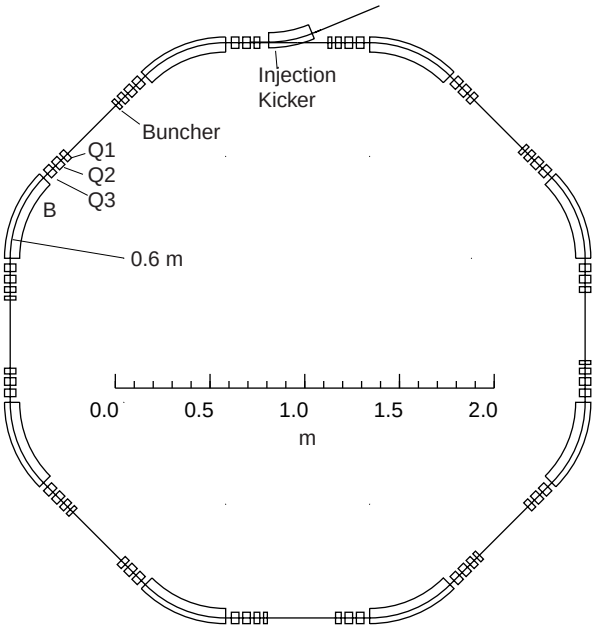

Lattice of the strong-field seeking molecular synchrotron storage ring. Each octant has of two 22.5^o bend sections, one vertically focusing and one horizontally focusing plus two triplet focusing lens sections and a buncher.

Molecules in strong field seeking states defocus in pure electric hexapole fields. They: defocus in fringe electric fields, defocus (in one or both transverse directions) when deflected, and defocus in one transverse direction when focused in the other. We have surmounted all of these obstacles and have successfully modeled a synchrotron storage ring that will store 30 m/s (2 K kinetic energy) methyl fluoride (CH_3F) in it's ground rotational (J = 0) state with the molecules surviving against storage ring losses for 30 seconds. The 8 m circumference and 30 m/s beam velocity allow the ring to hold 160 bunches of molecules.

H. N., G. L, and J.G. K. and the study were supported by LBNL Laboratory Directed Research & Development (LDRD) Funds. H.G. was partially supported by LDRD funds. .

Publications.

1. J.A. Amini and H. Gould, "High Precision Measurement of the Static Dipole Polarizability of Cesium," To be published in Phys. Rev. Lett. (E-print at http://arXiv.org/abs/physics/0305074).

2. H. Nishimura, G. Lambertson, J. G. Kalnins, and H. Gould, "Feasibility of a synchrotron storage ring for neutral polar molecules," Rev. Sci. Instr. **74**, 3271 (2003).

3. J. G. Kalnins, G. Lambertson, and H. Gould, "Improved alternating gradient transport and focusing of neutral molecules," Rev. Sci. Instr. **73**, 2557 (2002).

Acknowledgments

Except where otherwise indicated, this work is supported by the Division of Chemical Sciences, Geosciences and Biosciences; Office of Basic Energy Sciences, of the U.S. Department of Energy under Contract DE-AC03-76SF00098.

Weather Forecast

Over the next 10 billion years, expansion of the universe and inflation will lower cosmic temperatures leading to an increasing number of slow molecules.

Studies of Autoionizing States Relevant to Dielectronic Recombination

T.F. Gallagher
Department of Physics
University of Virginia
P.O. Box 400714
Charlottesville, VA 22901
tfg@virginia.edu

This program is focused on two electron phenomena in alkaline earth atoms. While the primary motivation for the research is to understand dielectronic recombination (DR) in high temperature plasmas, two electron atoms are prototype systems for the many atomic and molecular processes which occur when there are many coupled channels present. For example, the time domain manifestations of configuration interaction in atoms are analogous to intramolecular vibrational relaxation in a molecule.

In the past year most of our efforts have gone into the study of DR from a continuum of finite bandwidth.[1,2] In particular, we have finished a set of experiments on DR in combined E and B fields, carried out experiments on DR in combined static and microwave E fields, and begun work on DR using entrance channels of different ℓ.

The continuum of finite bandwidth in our case is the broad autoionizing $6p_{3/2}11d$ state converging to the $6p_{3/2}$ Ba^+ limit which straddles the $6p_{1/2}$ limit. Atoms initially excited to the $6p_{3/2}11d$ state make the interchannel transition to the degenerate $6p_{1/2}nd$ state $\left(40 < n < \infty\right)$. If they decay radiatively to the bound $6snd$ state, DR has occurred. The primary attractions of this technique are the energy resolution of ~ 0.5 cm^{-1} (< 0.1 meV) and the fact that the experiments can be done in zero field, in contrast to storage ring experiments. An additional feature, which we did not completely appreciate at the outset, is that the partial wave of the entrance channel is well defined.

In this year we completed the work on DR from the $6p_{3/2}11d$ CFB. We previously reported the enhancement of DR for $\overline{B} \perp \overline{E}$ and the absence of enhancement for $\overline{B} \parallel \overline{E}$.[3] Enhancement occurs in the former case because there is m mixing by the B field while in the latter there is not.[3,4] In the same way that E field induced ℓ mixing enhances the DR rate B field induced m mixing does.[4,5] We showed that, in the presence of an E field, as the perpendicular B field is raised from zero to 240 G the DR rate increases, whereas in the storage ring experiment of Bartsch et al., the DR rate decreased monotonically as the magnetic field was raised from 200 – 690 Gauss.[6]

After comparing all aspects of their experiment and ours we have realized that theirs is always in the weak electric field regime, in which the B field should suppress the DR rate. In contrast, ours is usually in the strong E field regime, largely because we use the $6p_{1/2}nd$ entrance channel which does not exhibit Stark mixing until the Inglis-Teller field, $E = 1/3n^5$, is reached.

We have completed an investigation of DR in combined static and microwave fields with both parallel and perpendicular polarization of the microwave field relative to the static field. There are several interesting results from this work. At low static fields we observe the $\Delta n = 1$ resonance with either polarization of the microwave field.[7] At higher static fields there is minimal effect from a parallel polarized microwave field, but a large effect due to a microwave field polarized perpendicular to the static field. In this case the microwave field drives $\Delta m = 1$ transitions between Stark states. These transitions occur at the frequency $\omega = 3n\mathrm{E}/2$. The most striking effects is that we can see substantial recombination above the classical ionization limit, through the following mechanism. The classical limit is only important in non hydrogenic atoms in which the presence of the ionic core couples the blue and red hydrogenic states. Specifically, it couples rapidly ionizing red states of high n to blue states which would be stable in hydrogen.[8] In hydrogen the blue Stark states are often stable in spite of lying far above the classical limit. In any atom states of high m resemble hydrogen and can be stable above the classical limit. With the above ideas in mind we can see that the perpendicularly polarized microwave field leads to DR above the classical ionization limit by driving transitions from unstable low m to stable high m states, all of which are above the classical limit. A similar phenomenon has been observed using half cycle pulses polarized perpendicular to a static field.[9]

A final interesting feature of these experiments is that even the extreme blue Ba $m = 0$ states in some cases exhibit hydrogen-like spectra. Usually Ba states of $m = 0$ exhibit completely irregular spectra due to the numerous avoided crossings. However in high field the bluest $m = 0$ states find themselves degenerate with only continuum red states, which do not noticeably perturb their energies, and they appear hydrogenic, at least qualitatively.

During the past year we have begun experiments using the Ba $6p_{3/2}8g$ state as the CFB. The motivation for this is that DR occurs in this case via the $6p_{1/2}ng$ states which have very small quantum defects, ~0.02.[10] With this entrance channel the enhancement by an E field should begin at much lower fields than it does when using the $6p_{3/2}11d$ state, from which DR occurs via the $6p_{1/2}nd$ states, with quantum defects of 0.75. If this suggestion is correct, it suggests that using an E field is a way to determine the ℓ contributions to DR without having to resolve the $n\ell$ states energetically. More generally, this method is one which allows us to explore a collision process, DR in this case, one partial wave at a time, and it is equivalent to doing a collision experiment with control of the impact parameter.

Our plans for the future include completing the experiments in which we compare DR from the $6p_{3/2}11d$ and $6p_{3/2}8g$ CFB in E fields. We then plan to compare the microwave enhancement from the two CFB. Our present model suggests that using the $6p_{1/2}nd$ states with their large quantum defects should require a larger microwave field than the $6p_{1/2}ng$ states. Is this true?

Our microwave enhancement measurements are stimulated in part by the desire to mimic the high frequency fields of electron collisions in a plasma. In a plasma the electron fields are high frequency but not monochromatic or well polarized. Consequently it would be most interesting to compare the enhancement produced by a static field, a monochromatic microwave field, and broad band microwave noise.

Finally, we would like to return to the crossed E and B field problem. In particular, we would like to extend our measurements into the strong B field regime, where we expect to see a decrease in the DR rate with increasing field.

References

1. C.M. Evans, E.S. Shuman, and T.F. Gallagher, "Microwave-induced dielectronic recombination above the classical ionization limit in a static field," Phys. Rev. A 67, 043410 (2003).
2. J.P. Connerade, Proc. R. Soc. London, Ser. A, 362, 361 (1978).
3. V. Klimenko, L. Ko, and T.F. Gallagher, Phys. Rev. Lett. 83, 3808 (1999).
4. F. Robicheaux and M.S. Pindzola, Phys. Rev. Lett. 79, 2237 (1997).
5. V.L. Jacobs, J. Davis, and P.C. Kepple, Phys. Rev. Lett. 37, 1390 (1976).
6. T. Bartsch, S. Schippers, A. Muller, C. Brandau, G. Gwinner, A.A. Saghiri, M. Beutelspachier, M. Grieser, D. Schwalm, A. Wolf, H. Danared, and G.H. Dunn, Phys. Rev. Lett. 82, 3779 (1999).
7. V. Klimenko and T.F. Gallagher, Phys. Rev. Lett. 85, 3357 (2000).
8. M.G. Littman, M.L. Zimmerman, and D. Kleppner, Phys. Rev. Lett. 37, 486 (1976).
9. J.G. Zeibel and R.R. Jones, Phys. Rev. Lett. 89, 093204 (2002).
10. S.M. Jaffe, R. Kachru, H.B. van Linden van den Heavell, and T. F. Gallagher, Phys. Rev. A 32, (1985).

Publications 2001-2003

1. H. Maeda and T.F. Gallagher, "Inner-electron ionization for wave packet detection," Phys. Rev. A 64, 013415 (2001).
2. H. Maeda and T.F. Gallagher, "Inner electron ionization of Sr 5s16ℓ states," Phys. Rev. A 65, 053405 (2002).
3. V. Klimenko and T.F. Gallagher, "Resonant enhancement of dielectronic recombination from a continuum of finite bandwidth," Phys. Rev. A 66, 023401 (2002).
4. C.M. Evans, E.S. Shuman, and T.F. Gallagher, "Microwave-induced dielectronic recombination above the classical ionization limit in a static field," Phys. Rev. A 67, 043410 (2003).
5. V. Klimenko, L. Ko, and T.F. Gallagher, "Enhancement of dielectronic recombination in crossed electric and magnetic fields," Phys. Rev. A (accepted for publication).

Program Title:

"Ion/Excited-Atom Collision Studies with a Rydberg Target and a CO_2 Laser"

Principal Investigator: Stephen R. Lundeen,
Dept. of Physics
Colorado State University
Ft. Collins, CO 80523
Lundeen@Lamar.colostate.edu

Program Scope:

The program involves three projects, two involving the interaction of multiply-charged ion beams with a Rydberg target, and one involving multiply-excited Rb atoms in a MOTRIMS target.

1) Studies of the fine structure of high-L Rydberg ions, in order to extract measurements of dipole polarizabilities and quadrupole moments of the positive ion cores.

2) Studies of X-rays emitted from the highly-excited Rydberg ions formed in charge capture collisions by highly-charged ions on Rydberg atoms.

3) Stepwise excitation of a Rb MOT to high Rydberg states within a MOTRIMS apparatus in order to study the n-dependence of charge capture cross sections.

Recent Progress and Immediate Plans:

Project 1) We have made substantial progress in this area over the past year. We continue to be hopeful that our RESIS/microwave technique will be a practical method of studying the fine structure of a wide range of Rydberg ions, eventually including ions of Thorium and Uranium. During the past year, we completed our first study of a Rydberg ion's fine structure pattern, measuring the intervals between n=29 Rydberg levels of Si^{2+} with L of 8 to 14[1]. For these high-L levels, the fine structure pattern is relatively simple, dominated by the dipole polarization energies. In the highest L levels studied, Stark shifts due to small ambient electric fields become significant, but these can be recognized by their characteristic effect on the fine structure pattern. Figure 1 illustrates the scaled plot of all the measured intervals from which the dipole polarizability of the core ion, Si^{3+} can be extracted. The result, α_s=7.404(11) a_0^3, is comparable in precision to the best measurements of polarizabilities of neutral atoms, and provides a stringent test of the most advanced atomic structure theories of this Na-like ion. As a further test of this experimental method, we are continuing to explore the fine structure patterns in other Rydberg ions of Silicon. The results of these preliminary studies should provide valuable guidance in planning experiments with heavier ions.

In addition to the purely experimental challenges posed by heavier ions, another issue is the potential complications in the theoretical interpretation of Rydberg ion fine structure that may be encountered in heavier systems. We stumbled upon one aspect of this in our studies of Si^{2+} fine structure. Since the Na-like Si^{3+} core of this system is a $^2S_{1/2}$ state, we expected to observe spin fine structure similar to that which we had previously studied in the helium atom, where spin-orbit interactions produce a four-fold splitting of each transition. Our observations, such as those illustrated in Figure 2, were completely inconsistent with this expectation, causing us to think more deeply about the spin structure issue[2]. In this connection, we noticed that previous studies of Rydberg

states of the Barium atom, which also has a $^2S_{1/2}$ core, had reported large unexplained doublet splittings[3]. Like our own observations in Si^{2+}, this was in stark contrast to our expectation that all Rydberg states based on $^2S_{1/2}$ cores would show the four-fold splitting seen in helium. We were eventually able to reconcile observations of spin structure in all three of these superficially similar Rydberg systems (helium, Si^{2+} , and barium) by calculating the "indirect spin orbit" effects produced by core-excited admixtures in the Rydberg wave function. The effect in question is common to all three systems, but varies in importance by more than six orders of magnitude as the systems become heavier[2].

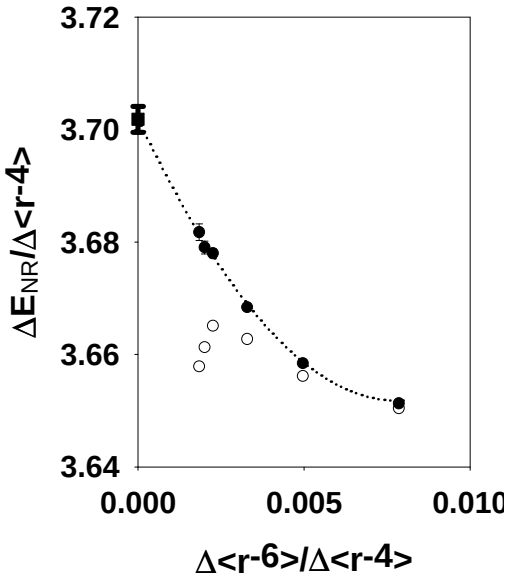

Fig. 1. Scaled fine structure interval measurements in the n=29 level of Si^{2+}. The open circles represent the directly measured intervals. The solid circles have been corrected for Stark shifts inferred from the fine structure pattern. The square point is the fitted intercept which determines the Si^{3+} dipole polarizability.

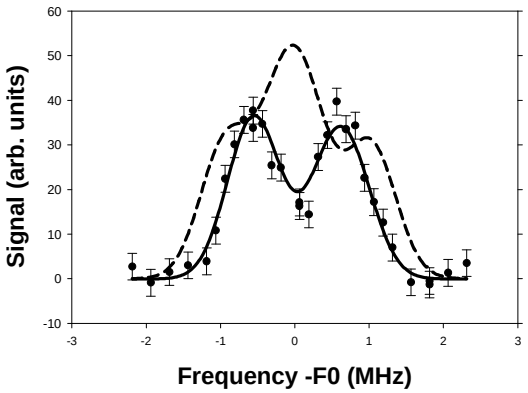

Fig. 2. Observed spin structure of the L=9 to 10 transition in n=29 of Si^{2+}. The dashed line shows a composite curve expected if the underlying spin structure is helium-like. The solid curve shows the composite structure expected when the effects of indirect spin orbit interactions are included.

One result of our experience with the indirect spin orbit splittings has been to encourage us to explore heavier Rydberg systems sooner, rather than later. We expect that there will be other aspects of the interpretation of heavy Rydberg fine structure that will need to be explored carefully. Although we are limited in the range of Rydberg ions that can be studied with the facilities at Kansas State, it should be possible to study fine structure in some heavier neutral atoms using existing facilities at Colorado State. One example is the barium atom. This is another Rydberg system with an alkali-like core for which precise polarizability measurements can be compared with mature theoretical calculations. We are planning to begin such a study within the next year.

Project 2) A paper reporting the first results of this experiment was published this year. By studying the variation with electric field of the X-ray spectrum emitted by H-like and He-like Silicon after electron capture from our Rydberg target, we were able to deduce the fraction of those captures which resulted in a state of low m (-1, 0, 1) with respect to the beam axis. The result, about 40%, was much higher than a statistically-distributed population would imply (4%)[4].

A further study, extending the range of Rydberg targets and the range of bare ions studied, has now been completed. This study checks the scaling with target n and ion charge Q of the critical electric field needed to induce the direct decay to the ground state. A report describing this study and comparing with the predictions of CTMC calculations is in preparation.

Beyond this, we are working on the design of a "Stark Barrel" type apparatus which will allow application of electric fields at arbitrary angles to the beam direction. The rate of X-ray emission to the ground state as a function of electric field direction should give additional information about the emitting populations.

Project 3) As a first step in this project, we used our diode laser at 1529 nm to excited the Rb MOT to the $4^2D_{5/2}$ level. The MOTRIMS spectrometer was able to distinguish collision events coming from all three initial states, 5S, 5P, and 4D. When the 1529 laser was off, the 4D events rapidly disappear, along with the 4D population. This observation was extremely suggestive, and it led us to realize the potential of the MOTRIMS technique for simultaneous measurement of relative cross sections and relative populations. A short paper describing this idea has been submitted for publication and is under review. It is included in our publication list.

In preparation for further studies of this type, we have installed fiber-optic links between the Rydberg target area and the MOTRIMS apparatus that will allow shared use of the 1529 nm and TiSaphire lasers between these two experiments. We hope to excite the Rb MOT to a range of nF states using these lasers, and utilize the MOTRIMS spectrometer to measure the relative capture cross section as a function of n.

References

[1] R.A. Komara, et. al. Phys. Rev. A 67, 062502 (2003)
[2] E.L. Snow, et. al., (to be published Phys. Rev. A, August, 2003)
[3] T.F. Gallagher, et. al., Phys. Rev. A 26, 2611 (1982)
[4] M.A. Gearba, et. al., Phys. Rev. A 66, 032705 (2002)

Recent Publications:

1) "State selective charge transfer cross sections for Na^+ with excited rubidium: A unique diagnostic of MOT population dynamics," X. Flechard, H. Nguyen, S.R. Lundeen, M. Stauffer, H.A. Camp, C.W. Fehrenbach, and B.D. DePaola, submitted to Phys. Rev. Letters.

2) "Stark-induced X-ray emission from high Rydberg states of H-like and He-like Si", R.A. Komara, S.R. Lundeen, C.W. Fehrenbach, and B.D. DePaola , Phys. Rev. A 66, 032705 (2002)

3) "Determination of the polarizability of Na-like Silicon by study of the fine structure of high-L Rydberg states of Si^{2+}", R.A. Komara, M.A. Gearba, S.R. Lundeen, and C.W. Fehrenbach, Phys. Rev. A 67, 062502 (2003)

4) "Indirect spin orbit interaction in high *L* Rydberg states with $^2S_{1/2}$ cores", E.L Snow, R.A. Komara, M.A. Gearba, and S.R. Lundeen, to be published Phys. Rev. A, Aug.,2003

Localized emission from sharp metal tips

Lukas Novotny (novotny@optics.rochester.edu)
University of Rochester, The Institute of Optics, Rochester, NY, 14627.

1 Program Scope

In an effort to push *spatial* resolution of optical spectroscopy into the length scale of quantum confinement in semiconductors or the size-range of proteins in biological membranes we are investigating light confinement at a laser-irradiated metal tip. Suitably polarized excitation light gives rise to field enhancement at the metal tip thereby creating a light source with dimensions determined by the tip size [1, 2]. This nanoscale light source interacts with a sample surface at close proximity and by raster scanning the tip over the sample surface an optical scan image can be recorded. In the past we have investigated different optical interactions between tip and sample, such as two-photon excited fluorescence [3], second-harmonic generation [4], and Raman scattering [5]. The spatial resolution in these experiments was $10 - 20nm$, consistent with theoretical predictions [1, 2].

The goal of this project is to establish a solid understanding of the optical interaction between a laser-irradiated metal tip and and a single molecule. Single molecules are well defined systems in terms of their chemical structure and electronic/vibrational states and they are well approximated by elementary two-level systems. As such, they are ideal probes for measuring optical field distributions [6, 7], and for investigating lifetime variations and emission properties near nanostructures [8, 9]. Once we understand the interaction with single molecules we are in a better position to understand interactions with more complex systems such as molecular aggregates, proteins in biological membranes, or semiconductor nanostructures. The research is aimed at gaining deeper insight into optical interactions on the nanometer scale.

2 Recent Progress

We observed that a sharp gold tip generates different kinds of luminescence when irradiated with femtosecond laser pulses at $\lambda \approx 830nm$. A strong peak appears at the second harmonic (SH) frequency at $\lambda \approx 415nm$. We have demonstrated that this SH light is generated at the tip surface thereby creating a highly confined photon source [4]. A theoretical model for the excitation and emission of SH radiation at the tip was developed and it was found that this source can be represented by a single on-axis oscillating dipole. The model was experimentally verified by imaging the spatial field distribution of strongly focused laser modes [4]. The dimensions of the SH source are defined by the sharpness of the tip which can be as small as 10nm. In future experiments we intend to use this confined photon source to perform local absorption spectroscopy with unprecedented spatial resolution.

Besides the SH peak, the luminescence spectrum from a gold tip is characterized by a broad visible and infrared continuum which is also observed for gold nanostructures. We determined that the ratio of generated infrared to visible emission is much stronger for gold nanostructures than for smooth gold films. While visible emission is well explained by interband transitions of d-band electrons into the conduction band and subsequent radiative recombination, the strong infrared emission cannot be accounted for by the same mechanism. We proposed that the infrared

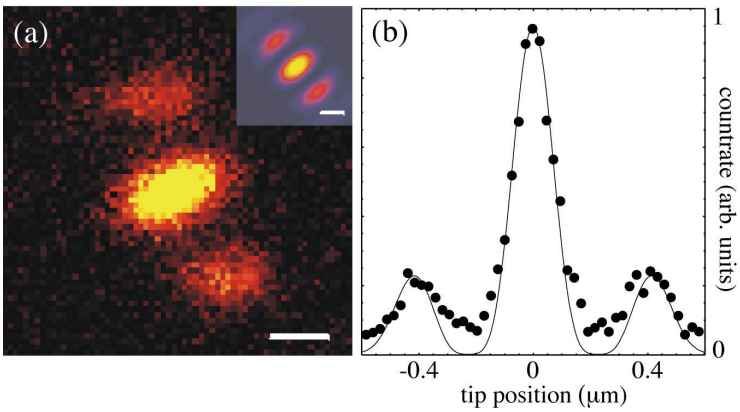

Figure 1: (a) *Tip-induced SH image of the focal fields of a strongly converging Gaussian HG_{10} beam. The recorded pattern indicates that SH is predominantly generated by fields polarized along the tip axis ($E_{o,z}$). The inset shows the calculated longitudinal field distribution ($E^2_{o,z}$) of a focused HG_{01} beam . (b) Comparison of $E^4_{o,z}$ (solid line) with the experimentally detected SH signal (dots). Scale bars: 250 nm. From [4].*

emission is generated by intraband transitions mediated by the strongly confined fields near metal nanostructures (localized surface plasmons) [10]. These fields possess wavenumbers that are comparable to the wavenumbers of electrons in the metal and the associated field gradients give rise to higher-order multipolar transitions. We compared photoluminescence spectra for single gold spheres, smooth and rough gold films, and sharp gold tips and demonstrated that the infrared signal is only present for surfaces with nanometer scale roughness.

We determined that the photoluminescence at shorter wavelengths than the $\lambda = 830nm$ excitation wavelength (visible luminescence) follows a quadratic intensity dependence consistent with a two-photon process. On the other hand, photoluminescence at longer wavelengths than the the excitation wavelength (infrared luminescence) shows a linear intensity dependence indicating a different origin [10]. We also measured the transient decay of the infrared photoluminescence from gold films using a streak camera at DOE's Environmental Molecular Sciences Laboratory (PNNL, Richland, WA). The infrared photoluminescence signal resulted in the instrument response function of 2.3 ps from which we concluded that the radiative recombination rate is competitive with non-radiative decay channels [10]. This is reasonable considering that the energy is coupled out through the fast surface plasmon decay rate, which from the spectral width of individual nanoparticles is of the order of 2-20 fs.

In a related effort, we compared light scattering from sharp metallic and dielectric tips [11]. The tips were raster scanned through the beam waists of tightly focused laser beams and the backscattered light was detected to record an optical scan image. We found that regardless of the tip material, the recorded scattering signal is always a measure of the spatial distribution of the longitudinal field, i.e. the field polarized along the tip axis. A surprising contrast reversal was observed between the images obtained with a metallic tip and the images obtained with a dielectric tip [11].

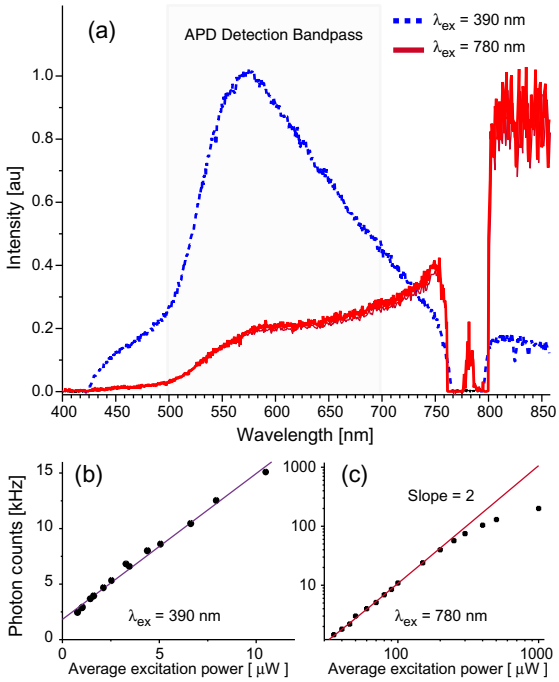

Figure 2: *(a) One and two-photon excited emission spectra from a sharp gold tip. The detection range of the APD is indicated by the shaded box. (b) The APD signal dependence for* $\lambda = 390$ *nm excitation, shown with a linear curve-fit. (c) The APD signal dependence for* $\lambda = 780$ *nm excitation, with a quadratic curve fit. Strong infrared luminescence is only observed for very sharp gold tips. From [10].*

3 Future Plans

In the next funding period we intend to perform first nanoscale absorption measurements using the confined second-harmonic photon source created by a laser-irradieted metal tip. As model sytem we will use molecules that are used as saturable absorbers with an absorption peak near $\lambda = 400nm$. In parallel to this effort we will perform first measurements on single molecules and investigate the trade-off between enhancement and quenching.

References

[1] J. Wessel, *J. Opt. Soc. Am. B*, **2**, 1538, 1985.

[2] L. Novotny, R. X. Bian, and X. S. Xie, *Phys. Rev. Lett.* **79**, 645, 1997.

[3] E. J. Sanchez, L. Novotny, and X. S. Xie, *Phys. Rev. Lett.* **82**, 4014, 1999.

[4] A. Bouhelier, M. R. Beversluis, A. Hartschuh, and L. Novotny, "Near-field second-harmonic generation induced by local field enhancement," *Phys. Rev. Lett.* **90**, 13903, 2003.

[5] A. Hartschuh, E. J. Sanchez, X. S. Xie, and L. Novotny, "High-resolution near-field Raman microscopy of single-walled carbon nanotubes," *Phys. Rev. Lett.* **90**, 95503, 2003.

[6] J. K. Trautman, J. J. Macklin, L. E. Brus, and E. Betzig, "Near-field spectroscopy of single molecules at room temperature," *Nature* **369**, 40-42, 1994.

[7] L. Novotny, M. R. Beversluis, K. S.Youngworth, and T. G. Brown, "Longitudinal field modes probed by single molecules," *Phys. Rev. Lett.* **86**, 5251-5254, 2001.

[8] R. X. Bian, R. C. Dunn, X. S. Xie, and P. T. Leung, "Single molecule emission characteristics in near-field microscopy," *Phys. Rev. Lett.* **75**, 4772-4775, 1995.

[9] H. Gersen, M. F. Garca-Parajo, L. Novotny, J. A. Veerman, L. Kuipers, and N. F. van Hulst , "Influencing the angular emission of a single molecule," *Phys. Rev. Lett.*, **85**, 5312-5315, 2000.

[10] M. R. Beversluis, A. Bouhelier, and L. Novotny, "Continuum generation from single gold nanostructures through near-field mediated intraband transitions," *Phys. Rev. B*, in print, 2003.

[11] A. Bouhelier, M. R. Beversluis, and L. Novotny, "Near-field scattering of longitudinal fields," *Appl. Phys. Lett.* **82**, 4596-4598, 2003.

[12] A. Bouhelier, J. Renger, M. Beversluis, and L. Novotny, "Plasmon coupled tip-enhanced near-field microscopy," *J. Microsc.* **210**, 220-224, 2003.

[13] A. Bouhelier, M. R. Beversluis, and L. Novotny,, "Applications of field-enhanced near-field optical microscopy," *Ultramicroscopy*, submitted, 2003.

[14] A. Hartschuh, M. R. Beversluis, A. Bouhelier, and L. Novotny, "Tip-enhanced optical spectroscopy," *Phil. Trans. R. Soc. Lond. A*, submitted, 2003.

[15] J. Zurita-Sanchez and L. Novotny, "Multipolar interband absorption in a semiconductor quantum dot: I. Electric quadrupole enhancement," *J. Opt. Soc. Am. B* **19**, 1355, 2002.

[16] J. Zurita-Sanchez and L. Novotny, "Multipolar interband absorption in a semiconductor quantum dot: II. Magnetic dipole enhancement," *J. Opt. Soc. Am. B* **19**, 2722, 2002.

DOE sponsored publications (2002-2003): Refs. [4], [5], [10], [11], [12], [13], [14], [15], [16].

Time-dependent treatment of electron capture in $\alpha + H_2^+$ collisions

B.D. Esry
J.R. Macdonald Laboratory, Kansas State University, Manhattan, KS 66506
esry@phys.ksu.edu, 785-532-1620
Collaborators: Shu-chun Cheng

While adequate theoretical descriptions of single electron capture in ion-atom collisions are available, similar quality treatments of capture in ion-molecule collisions are not. We have been working on providing just such a treatment for the process

$$\alpha + H_2^+ \longrightarrow \mathrm{He}^+ + p + p.$$

This system was recently the subject of an experiment in which the capture probability was measured as a function of the molecular orientation [1]. This experiment motivated us to calculate precisely this probability.

We have solved the three-dimensional time-dependent Schrödinger equation on a grid for the electronic motion. At the collision energies considered, the α can accurately assumed to travel along a straight line and the nuclei in H_2^+ can be assumed fixed in space. The problem is thus a three-center problem, but this fact is of little import for the grid method employed. There are, however, five parameters upon which the capture probability depends. They are the three H_2^+ nuclear coordinates, the impact parameter, and the impact velocity. Given that the calculation for a single set of parameters takes on the order of 10 hours, filling out this parameter space is a computationally expensive proposition.

Nevertheless, we have carried out a series of calculations for an impact velocity of 0.41 a.u. The main qualitative result is that capture is largest when the molecule is aligned perpendicular to the projectile direction — exactly the opposite of the experimental result!

The only other calculations carried out for this system are based on an old model from C.D. Lin's group that coherently superposes individual ion-atom scattering amplitudes [1,2]. In principle, our calculation includes fewer approximations than this interference model, but implementing it on a grid introduces other approximations that perturb the spectrum of the constituent particles on the order of a few percent. Interestingly, the interference model predictions agree with the experiment for this system, but agree qualitatively with ours for other projectiles. This raises the question of whether a resonance effect is responsible for our disagreement with experiment. Since the grid perturbs the spectra of the He^+ and H_2^+ by a few percent, this could be enough to shift them out of any near resonance. We are in the process of evaluating this speculation as well as other sources of the discrepancy.

As long as only one electron is active, there is, in principle, no difficulty to extend the method to a polyatomic target, or even a molecular projectile. These cases would, of course, require careful modeling to reduce them to one active electron, but they could be quite interesting to study. Further, with a working three-dimensional time propagation code, other non-perturbative processes — such as atoms or molecules in intense laser fields — can be tackled.

---

[1] Ingrid Reiser, Ph.D. Thesis, Kansas State University (2002); I. Reiser, C.L. Cocke, and H. Bräuning, Phys. Rev. A **67**, 062718 (2003).
[2] R. Shingal and C.D. Lin, Phys. Rev. A **40**, 1302 (1989).

X-ray processes in the presence of strong optical fields

L. Young, R. W. Dunford, D. L. Ederer, E. P. Kanter, B. Krässig, S. H. Southworth

Argonne National Laboratory, Argonne Illinois 60439

We have begun to investigate how a high-field/ultrafast laser modifies the x-ray photoionization and vacancy decay of an isolated atom. Since many proposed experiments for the next generation x-ray sources, e.g. Linac Coherent Light Source, LCLS, involve laser/x-ray pump–probe techniques on the ≈100 fs timescale, it is important to understand how the x-ray physics of an atom is perturbed due to the presence of a high-power laser. Two effects have been theoretically predicted and observed for valence electrons: 1) a ponderomotive shift of the ionization threshold, and, 2) the appearance of sidebands in the photoelectron spectrum. The shifts may be sizable with readily-available laser intensities; at 10^{14} W/cm^2 (1mJ/100ps/10μm^2) for 800 nm light, the ponderomotive energy is 6 eV. These shifts have never been observed in the x-ray region or at an inner-shell threshold. In addition, free-free transitions in the continuum will modify the photoelectron and Auger electron energy spectra, producing sidebands spaced by the laser photon energy. So, at high field strengths, we expect modifications in the absorption spectrum, in the photoelectron spectrum, in the vacancy cascade process, as well as some surprises. To probe the atom at these field strengths, we have designed and are testing an apparatus which aims for the spatial and temporal overlap of focused x-ray and laser beams to ≈3 μm and ≈10 ps in an effusive beam while being simultaneously viewed by ion-imaging and electron time-of-flight spectrometers. These studies are being conducted at the MHATT-CAT at the Advanced Photon Source, where the output of an amplified Ti:sapphire – based laser system, (1 kHz, 1 mJ/pulse), has been synchronized to the x-ray pulses. A preliminary run demonstrated that the undulator x-ray beam, focused by a Kirkpatrick-Baez mirror pair, provides sufficient count rate for the experiment. We plan to study high-field effects first at the Kr 1s edge, 14.4 keV, where we have extensive knowledge of the weak-field physics and beamline performance is well characterized.

In collaboration with D. Reis, E. Dufresne (University of Michigan), E. Landahl (Advanced Photon Source), R. Crowell and D. Gosztola.

Energetic Photon and Electron Interactions with Positive Ions

Ronald A. Phaneuf,
Department of Physics /220
University of Nevada
Reno NV 89557-0058
phaneuf@physics.unr.edu

Program Scope

This experimental program investigates processes leading to ionization of positive ions by photons and electrons. The objective is a deeper understanding of both ionization mechanisms and multielectron interactions of atomic and molecular ions. Mononergetic beams of photons and electrons are crossed or merged with ion beams to selectively probe their internal electronic structure and the interaction dynamics. In addition to precision spectroscopic data for ionic structure, measurements of absolute cross sections for photoionization and electron-impact ionization provide critical benchmarks for the theoretical calculations that generate opacity databases. The latter are critical to models of astrophysical, fusion-energy and laboratory plasmas. Examples of particular relevance to DOE include the Z pulsed-power facility at Sandia National Laboratories, which is the world's brightest and most efficient x-ray source, and the National Ignition Facility under development at Lawrence Livermore National Laboratory for high-energy-density science, fusion energy and defense-related research.

Recent Progress

Photoionization of Ions at the Advanced Light Source

The major thrust of this research program has been the application of an ion-photon-beam (IPB) research endstation to experimental studies of photoexcitation and photoionization of singly and multiply charged positive ions using synchrotron radiation. The high photon beam intensity and energy resolution available at ALS undulator beamline 10.0.1 make photoion spectroscopy a powerful probe of the internal electronic structure of atomic ions, permitting tests of sophisticated atomic structure and dynamics codes at unprecedented levels of detail and precision. Photon-ion measurements using the IPB endstation at ALS have advanced the state of the art with respect to energy resolution by an order of magnitude or more, and have helped to attract new independent investigators to the ALS. Research using the IPB endstation *for high-resolution photo-ion spectroscopy with positive and negative ion beams* was selected for the David A. Shirley Award for Outstanding Scientific Achievement at the ALS in 2002. Specific accomplishments of the past year are highlighted below.

- A detailed spectroscopic analysis was completed of high-resolution absolute measurements of cross sections for photoionization of O^+ in an admixture of the ground and metastable states. The measurements were compared with two state-of-the-art R-matrix theoretical calculations and with the TOPBase opacity database. This analysis, which constituted part of the Ph.D. dissertation of A. Aguilar, includes a tabulation of energies, quantum defects and oscillator strengths for the observed resonances, and was published in the Astrophysical Journal [9].

- Measurements at ALS of photoionization of Sc^{2+} were compared with measurements at the TSR heavy-ion storage ring of the time-reversed process of photorecombination of electrons with Sc^{3+}, permitting determination of metastable fractions and absolute resonance strengths by application of the principle of detailed balance. This research was performed in collaboration with A. Müller and S. Schippers of the University of Giessen, Germany, G. H. Dunn of JILA and M. E. Bannister of Oak Ridge National Laboratory. Following an initial report in Physical Review Letters [6], a detailed analysis of the photoionization experiment and a comparison with photorecombination measurements was published in Physical Review A [10].
- L-shell photoionization of an admixture of the ^1S ground state and $^3P^o$ metastable states of B^+ was studied in collaboration with the Giessen group. The measurements benchmark new Breit-Pauli R-Matrix calculations of McLaughlin, and test an analytic formula based on quantum defect theory. Fano lineshape parameters were determined for Rydberg series of resonances originating from the ground and mestastable states. These results were recently published in the Journal of Physics B [11].
- High-resolution measurements were made of photoionization of the Na-isoelectronic ions, Mg^+ and Al^{2+}, in collaboration with J. B. West of Daresbury Laboratory, U.K. and H. Kjeldsen and F. Folkmann of Århus University, Denmark. The ALS measurements were successful in resolving fine structure in the photoionization cross section that was not seen in previous measurements at the Århus synchrotron light source, and in determining oscillator strengths for them. These results were published in Physical Review A [8].
- High-resolution absolute photoionization measurements were completed for ions of the nitrogen isoelectronic sequence (F^{2+}, Ne^{3+}) to complement initial measurements on O^+. A systematic analysis of these measurements based on quantum-defect theory and their comparison with the TOPBase opacity database constituted the Ph.D. dissertation of A. Aguilar [14].
- Photoionization studies of ions of the Fe-isonuclear sequence were initiated. Measurements for Fe^{3+} reveal extremely broad PEC (photoexcitation of the core) resonance features attributed to 3p - 3d excitation of ground-state and metastable Fe^{3+}, followed by rapid autoionization via a super-Coster-Kronig transition. The population of 16 metastable states in the Fe^{3+} ion beam complicates the data analysis and comparison with R-matrix theoretical results from S. Nahar of Ohio State University. Photoionization of ions of the Fe-isonuclear sequence constitutes the Ph.D. dissertation research of M. Gharaibeh.
- Measurements were initiated of photoionization of ions of the Xe-isonuclear sequence. Data for Xe^{3+} reveal a broad PEC resonance feature attributed to 4d - 4f excitation from the ground state, followed by rapid autoionization. This work is part of the M.S. thesis research of E. Emmons.
- Successful experiments were completed by four different groups of independent investigators or participating research team members using the ALS ion-photon-beam (IPB) endstation for experiments with both positive and negative ions. In most cases, technical support was provided by personnel supported by this project. Those resulting in publications involving negative ions are not reported here.

Electron-Impact Ionization of Multiply Charged ions at the University of Nevada

- To complement photoionization measurements made at ALS, detailed energy-scan measurements were made of electron-impact ionization of Xe^{3+} using the crossed-beams apparatus at the University of Nevada. This work is part of the M.S. thesis research of E. Emmons.

Future Plans

The first seven ionization stages of the iron isonuclear sequence are characterized by a partially filled 3d shell, giving rise to a complex energy-level structure and strong configuration interaction. Measurements of photoionization of Fe^{q+} ions will be continued, with emphasis on control and quantification of metastable-state populations in the primary ion beams. These will be complemented by energy-scan measurements of electron-impact ionization of Fe^{q+} ions at UNR using small energy steps to elucidate the role of excitation-autoionization. This investigation will constitute the Ph.D. dissertation of M. Gharaibeh.

The dominant feature ionization of ions of the Xe isonuclear sequence is the collapse of the 4f wave function as the ion charge is increased, leading to an increased relative importance of discrete 4d - nf resonances compared to the 4d - ϵf continuum "giant" resonance that dominates photoionization of neutral Xe. Guided by the photoionization data, electron-impact measurements are expected to elucidate the role of 4d - np and 4d - nf excitation-autoionization. ionization of Xe^{3+}, and together they will constitute the M.S. thesis of E. Emmons. Xe^{3+} is a candidate for the first detection of Auger electrons from electron-ion collisions.

Photoionization of fullerine ions remains unexplored, and will be a new subject of quantitative investigation. The energy range and high spectral resolution of ALS beamline 10.0 are ideally suited to studies of photoionization and photofragmentation of C_{60}^{q+} and C_{70}^{q+} in the threshold energy region (20 – 50 eV), and in the vicinity of the carbon K-edge (270 – 340 eV). High-resolution measurements of 1s – 2p excitation of fullerine ions are of particular interest because of the distinct classes of bonding sites of C atoms in these cluster ions, which should be manifested in high-resolution photoion-yield spectra.

References to Publications of DOE-Sponsored Research (2001-2003)

1. *Photoionization of metastable O^+ ions: experiment and theory,* A.M.Covington, A. Aguilar, I.R. Covington, M. Gharaibeh, C.A. Shirley, R.A. Phaneuf, I. Álvarez, C. Cisneros, G. Hinojosa, J.D. Bozek, I. Domínguez, M.M. Sant'Anna, A.S. Schlachter, N. Berrah, S.N. Nahar and B.M. McLaughlin, Phys. Rev. Lett. 87, 243002-1 (2001).
2. *Correlated processes in inner-shell photodetachment of the Na^- ion*, A.M. Covington, A. Aguilar, A.; V.T. Davis, I. Álvarez, H.C. Bryant, C. Cisneros, M. Halka, D. Hanstorp, G. Hinojosa, A.S. Schlachter, J.S.Thompson and D.J. Pegg, J. Phys. B 34, L735 (2001).
3. *Photoionization of Ne^+ using synchrotron radiation,* A.M. Covington, A. Aguilar, I.R. Covington, M.F. Gharaibeh, G. Hinojosa, C.A. Shirley, R.A. Phaneuf, I. Álvarez, C.

Cisneros, I. Domínguez-Lopez, M.M. Sant'Anna, A.S. Schlachter, B.M. McLaughlin and A. Dalgarno, Phys. Rev. A 66, 062710 (2002).

4. *Formation of long-lived CO^{2+} via photoionization of CO^{+},* G. Hinojosa, A.M. Covington, R.A. Phaneuf, M.M. Sant'Anna, R. Hernandez, I.R. Covington, I. Domínguez, J.D. Bozek, A.S. Schlachter, I. Álvarez and C. Cisneros, Phys. Rev. A 66, 032718 (2002).

5. *Photoionization of C^{2+} ions: time-reversed recombination of C^{3+} with electrons,* A. Müller, R.A. Phaneuf, A. Aguilar, M.F. Gharaibeh, A.S. Schlachter, I. Álvarez, C. Cisneros, G. Hinojosa and B.M. McLaughlin, J. Phys. B 35, L137 (2002).

6. *Experimental link of photoionization of Sc^{2+} to photorecombination of Sc^{3+}: an application of detailed balance in a unique atomic system,* S. Schippers, A. Müller, S. Ricz, M.E. Bannister, G.H. Dunn, J. Bozek, A.S. Schlachter, G. Hinojosa, C. Cisneros, A. Aguilar, A.M. Covington, M.F. Gharaibeh and R.A. Phaneuf, Phys. Rev. Lett. 89, 193002 (2002).

7. *Electron spectroscopy of Na-like autoionizing metastable ions,* M. Lu and R.A. Phaneuf, Phys. Rev. A 66, 012706 (2002).

8. *Photoionization of isoelectronic ions: Mg^{+} and Al^{2+},* A. Aguilar, J.B. West, R.A. Phaneuf, R.L. Brooks, F. Folkmann, H. Kjeldsen, J.D. Bozek, A.S. Schlachter and C. Cisneros, Phys. Rev. A 67 012701 (2003).

9. *Absolute photoionization cross section measurements of OII ions from 29.7 eV to 46.2 eV,* A. Aguilar, A.M. Covington, G. Hinojosa, R.A. Phaneuf, I. Álvarez, C. Cisneros, J.D. Bozek, I. Dominguez, M.M. Sant'Anna, A.S. Schlachter, S.N. Nahar and B.M. McLaughlin, Astrophys. J (Supplement Series) 146, 467 (2003).

10. *Photoionization of Sc^{2+} ions by synchrotron radiation: high-resolution measurements and absolute cross sections in the photon energy range 23-68 eV,* S. Schippers, A. Müller, S. Ricz, M.E. Bannister, G.H. Dunn, A.S. Schlachter, G. Hinojosa, C. Cisneros, A. Aguilar, A.M. Covington, M.F. Gharaibeh and R.A. Phaneuf, Phys. Rev A 67, 032702 (2003).

11. *Photoionization studies of the B^{+} valence shell: experiment and theory*, S. Schippers, A. Müller, B.M. McLaughlin, A. Aguilar, C. Cisneros, E.D. Emmons, M.F. Gharaibeh and R.A. Phaneuf, J. Phys. B: At. Mol. Opt. Phys. 26, 3371 (2003).

12. *Photoionization of C^{2+} ions*, A. Müller, R.A. Phaneuf, A. Aguilar, M.F. Gharaibeh, A.S. Schlachter, I. Álvarez, C. Cisneros, G. Hinojosa and B.M. McLaughlin, Nucl. Instrum. Methods Phys. Res. B 205, 301 (2003).

13. *Photoionization of Sc^{2+}: experimental link with photorecombination of Sc^{3+} by application of detailed balance*, S. Schippers, A. Müller, S. Ricz, M.E. Bannister, G.H. Dunn, J. Bozek, A.S. Schlachter, G. Hinojosa, C. Cisneros, A. Aguilar, A.M. Covington, M.F. Gharaibeh and R.A. Phaneuf, Nucl. Instrum. Methods Phys. Res. B 205, 297 (2003).

14. *Photoionization of positive ions: the nitrogen isolectronic sequence,* A. Aguilar, Ph.D. Dissertation, University of Nevada, Reno (May, 2003).

Note: Participation of those underlined was supported wholly or in part by this DOE program.

Physics of Correlated Systems

Chris H. Greene
Department of Physics and JILA
University of Colorado, Boulder, CO 80309-0440
chris.greene@colorado.edu

1. Program scope and overview

This project aims at the development of theoretical tools that can describe complex phenomena relating to the exchange of energy among different degrees of freedom in small or modest-sized atomic or molecular systems. When such energy exchanges occur readily, those systems are said to exhibit strong correlations. The systems studied are primarily those for which a nonperturbative quantum mechanical description is essential. The following sections describe the specific areas that have been the focal points of our study during the past year.

2. Energy interconversion between the electronic and nuclear degrees of freedom in an electron collision with a polyatomic molecule

Our calculations during the past year have concentrated on testing as carefully as possible our recently proposed method for describing the competition between ionization and dissociation channels in triatomic species. We have implemented our nonperturbative approach which appears to be the first such treatment of a polyatomic molecule that incorporates all vibration, rotation, and electronic degrees of freedom quantum mechanically. The main calculations for H_3^+ were completed during the past year and published in two articles that have convincingly demonstrated that Jahn-Teller dynamics control the dissociative recombination (DR) process.[1,2] These publications present the first theoretical treatment capable of describing the correct order of magnitude of the low energy DR rate coefficient, as they have demonstrated agreement with the newest storage ring experiments carried out in Stockholm by the group of Mats Larsson and with an even newer unpublished storage ring experiment by Daniel Zajfman and his coworkers.

This work shows the power of high-end scientific parallel computation, because one complete set of final calculations requires around 10,000 cpu hours. It was thus important to be able to divide that calculation among hundreds of processors at NERSC, in order for this to be completed in a manageable amount of real time (approximately 80 hours of wall clock time).

Our work in the immediate future will focus on additional tests intended to sharpen our understanding of the strengths and limitations of these calculations for H_3^+ and its isotopomers. One detailed test underway is a calculation of the accurate H_3 photoionization spectrum in energy ranges that have been measured by Hanspeter Helm's group. A longer-term project underway is a study of the dissociative recombination of HCO^+ triggered by an electron collision. This will be an important test of whether our method has a general applicability to other species of chemical interest. A specific question that we hope to answer is whether the Renner-Teller effect controls the DR rate for linear molecular ions, analogous to the now-demonstrated importance of Jahn-Teller coupling for H_3^+. Although V. Kokoouline is no longer supported by this project, having recently assumed a faculty position at the University of Central Florida, he plans to continue collaborating on these problems for the foreseeable future.

One thing required in most photoionization and electron-molecule collision calculations is a reliable method to compute the clamped-nuclei electron scattering amplitudes. A graduate student supported by this project, Stefano Tonzani, will continue developing the capability to carry out such calculations. He has already developed a fully three-dimensional electron-molecule scattering code, at the static-exchange level. The method and some initial calculated results for specific systems will probably be published some time during the coming year.

3. Long range interactions and collisions between metastable alkaline-earth atoms

A new postdoctoral associate, Robin Santra, joined the group in the autumn of 2003 and began to investigate the long-range interaction between two excited, anisotropic strontium atoms. A first detailed study, which develops a concise spherical tensor description of these long range interactions, was published this year.[3] That was followed by a study of inelastic collisions between two strontium atoms in their $^3P_2$ states in the presence of an external magnetic field, in which V. Kokoouline took the lead role in developing a coupled-channels solution. This is an interesting system that had been proposed by A. Derevianko, P. Julienne, and their collaborators as a plausible candidate for forming an excited state Bose-Einstein condensate, because quadrupole-quadrupole coupling generates a long range potential barrier that appeared to suppress inelastic collisions. This had led some experimental groups to begin attempts to form such a condensate. Our more complete analysis of the collision dynamics, based on the formal derivation of the long-range Hamiltonian presented in [3], was published this year in [4], and showed that such a condensate has far stronger inelastic losses than had been estimated in the earlier theoretical proposals. This study appears to have already had some impact in persuading experimental groups that this system and other anisotropic systems of the same class are almost always likely to have too much inelastic decay to permit the creation of a long-lived condensate.

4. Extending closed-orbit theory to include nonclassical pathways

The strong doctoral dissertation research of Brian Granger rederived closed-orbit theory within the context of a semiclassical approximation to quantum defect theory. That derivation provided a deeper understanding of standard semiclassical approximations, and it identified a previously overlooked cancellation effect that occurs for atomic hydrogen. The main new physics to emerge from this work was s a new interpretation of the nonclassical "ghost orbits" that have been observed in scaled-variable spectroscopy of diamagnetic Rydberg states. A new method was proposed for implementing closed-orbit theory for any atom possessing more than one nonzero quantum defect (for the relevant symmetry of interest), a key example being the rubidium atom. Previous methods were plagued by an unphysical divergence of the recurrence spectrum, but with the new techniques, a convergent cross section and recurrence spectrum emerge. The results show reasonably good agreement with large-scale quantum calculations performed independently, using quantum defect and R-matrix techniques. This work appeared during 2003 in paper [5] below. Note that Brian Granger has now completed a two-year ITAMP postdoctoral stint, and will start this fall in a tenure-track faculty position at Santa Clara University.

5. Clusters in an intense VUV laser field

At Robin Santra's initiative, we have recently begun to develop a theoretical description of xenon clusters that are exposed to intense VUV radiation, of the type provided by the free-electron laser at the TESLA Test Facility (TTF) in Hamburg. This is a new regime of strong photon-cluster interactions, very different from the physics of infrared lasers that are directed at such clusters. For instance, theory has not previously been able to explain why approximately 30 photons per atom are absorbed, in a 100 femtosecond pulse of intensity 7.3×10^{13} W/cm^2. [The experimental research was published by H. Wabnitz *et al*., Nature **420**, 482 (2002).] Our preliminary calculations suggest that this absorption of many VUV photons can be understood, once realistic screened potentials are used to describe the behavior of the electrons, in addition to plasma screening effects, and once free-free radiative absorption or inverse bremsstrahlung is inccorporated. We will pursue this in the near future, and attempt to develop a more complete and quantitative description of this new regime of laser-cluster interaction dynamics.

6. Coherent control of rotational wave packets

During 2001 we began a collaboration with the experimental group of Kapteyn and Murnane at JILA. In a first combined experimental and theoretical study [6], we examined the use of femtosecond laser pulses to form coherent rotational wave packets of CO_2 molecules. Rotational revivals were then be used to produce a negative chirp that ultimately increased the bandwidth of a probe pulse and allowed it to be shortened

temporally by almost an order of magnitude, from 270 fs down to about 30 fs duration. Our theoretical calculations implemented a simple rigid rotor model that has been able to reproduce the experimental spectrum for gas-phase CO_2 in detail.

Following that initial joint experimental and theoretical paper on the subject[6] we extended our studies to molecules other than CO_2 to look for different species that appear to be promising for future experiments. Another collaborative study carried out with the same JILA experimental group was an investigation of whether the molecular rotational alignment can provide a way to coherently control the phase-matching in a third-harmonic generation experiment.[7]

Papers published since 2001 that were supported at least in part by this grant

[1] *Theory of dissociative recombination of D_{3h} triatomic ions applied to H_3^+*, V. Kokoouline and C. H. Greene, Phys. Rev. Lett. **90**,133201-1 to -4 (2003).

[2] *Unified theoretical treatment of dissociative recombination of D_{3h} triatomic ions: Application to H_3^+ and D_3^+*, Phys. Rev. A **68**, 012703-1 to -23 (2003).

[3] *Tensorial analysis of the long-range interaction between metastable alkaline-earth-metal atoms*, R. Santra and C. H. Greene, Phys. Rev. A **67**, 067213-1 to -15 (2003).

[4] *Multichannel cold collisions between metastable Sr atoms*, V. Kokoouline, R. Santra, and C. H. Greene, Phys. Rev. Lett. **90**, 253201-1 to -4 (2003).

[5] *Nonclassical paths in the recurrence spectrum of diamagnetic atoms*, B. E. Granger and C. H. Greene, Phys. Rev. Lett. **90**, 043002-1 to -4 (2003).

[6] *Phase modulation of ultrashort light pulses using molecular rotational wave packets*, R.A. Bartels, T.C. Weinacht, N. Wagner, M. Baertschy, C.H. Greene, M.M. Murnane, and H.C. Kapteyn, Phys. Rev. Lett. **88**, 013903-1 to 013903-4 (2002).

[7] *Phase matching conditions for nonlinear frequency conversion by use of aligned molecular gases*, R.A. Bartels, N.L. Wagner, M.D. Baertschy, J. Wyss, M.M. Murnane, and H.C. Kapteyn, Optics Letters 28, 346-348 (2003).

[8] *Excitation of the $3p^4(4s,3d,4p)$ Ar^+ states during Ar photoionization: Intensity, alignment, and orientation*, H.W. van der Hart and C.H. Greene, Phys. Rev. A **65**, 062509 (2002).

[9] *Regularities and irregularities in partial photoionization cross sections of He*, H.W. van der Hart and C.H. Greene, Phys. Rev. A **66**, 022710 (2002).

[10] *Quantum and semiclassical analysis of long-range Rydberg molecules*, B. E. Granger, E.L. Hamilton, and C. H. Greene, Phys. Rev. A. **64**, 042508-1 to 042508-9 (2001).

[11] *Multiphoton processes in a two-dimensional model of helium, in "Correlations, Polarization, and Ionization in Atomic Systems"*, C.H. Greene, M. Baertschy, A.L. Young, and B.E. Granger, in , AIP Conference Proceedings, **604**, pp.1-5, (2002),. edited by D.H. Madison and M. Schulz.

[12] *Accurate amplitudes for electron-impact ionization*, M. Baertschy, T.N. Rescigno, and C.W. McCurdy, Phys. Rev. A **64**, 002709 (2001).

[13] *Ejected-energy differential cross sections for the near threshold electron-impact ionization of hydrogen*, M. Baertschy, T.N. Rescigno, C.W. McCurdy, J. Colgan, and M.S. Pindzola, Phys. Rev. A **63**, 050701R (2001).

[14] *Doubly differential cross sections for the electron-impact ionization of hydrogen*, W.A. Isaacs, M. Baertschy, C.W. McCurdy, and T.N. Rescigno Phys. Rev. A, **63**, 030704R (2001).

[15] *Electron-impact ionization of atomic hydrogen*, M. Baertschy, T.N. Rescigno, W.A. Isaacs, X. Li, C.W. Phys. Rev. A **63**, 022712 (2001).

[16] *Time-dependent close-coupling calculations of the triple-differential cross section for electron-impact ionization of hydrogen*, J. Colgan, M. S. Pindzola, F. J. Robicheaux, D. C. Griffin, and M. Baertschy, Phys. Rev. A **65**, 042721 (2002).

Time-dependent, lattice approach for atomic collisions and The ORNL MIRF upgrade

D.R. Schultz
Physics Division, Oak Ridge National Laboratory

Several recent applications of the time-dependent, lattice approach to solving the Schrödinger equation for atomic collisions will be described that illustrate progress in treating fundamental collisions. These will include the following: a study of inelastic proton-impact ionization of atomic hydrogen that extends our recent work to detailed description of the momentum distribution the ejected electrons; a four-dimensional, model of antiproton-impact ionization of helium demonstrating the ability to study fully-correlated two-electron systems; calculations of charge transfer for the (nuclear charge) asymmetric collision, Be^{4+} + H; and exploratory consideration of laser-modified charge transfer in proton-lithium collisions.

The ongoing upgrade of the ORNL Multicharged Ion Research Facility (MIRF) will also be described. This significant enhancement of the capabilities of the MIRF includes the addition of a second, all-permanent magnet ECR ion source and a 250 kV high-voltage platform. Along with installation of a floating beamline utilizing the existing CAPRICE ECR source, the project will greatly extending the range of collision energies. In particular, upgraded merged beam experiments (electron- and atom-impact of atomic and molecular ions) will be able to explore collisions at both higher and lower collision energies as well as consider new reactions (such as fragmentation). The increased availability of user ports and of beam time will also enable greater access for on-line experiments including decelerated-beam and grazing-incidence ion-surface interactions and ion-atom/molecule COLTRIMS.

Electron-Molecular Ion Fragmentation*

M. E. Bannister
Physics Division
Oak Ridge National Laboratory

Collisions of electrons with molecular ions often play crucial roles in the energy and particle balance, chemistry, and neutral transport of low-temperature plasma environments found in diverse areas such as fusion energy, aeronomy, and plasma processing. To provide enabling data for these fields, we have established a program to investigate the dissociation of molecular ions by electron impact for energies ranging from zero to several hundred electron volts. Through experiments at the Multicharged Ion Research Facility (MIRF) at ORNL and collaborative experiments at the CRYRING heavy-ion storage ring in Stockholm, we are studying the processes of dissociative excitation (DE), ionization (DI), and recombination (DR) in an attempt to form a complete picture of electron-molecular ion fragmentation for selected systems. Recent measurements on the DE and DI of the hydrocarbon ions CH^+ producing C^+ fragment ions and CH_2^+ producing CH^+ and C^+ fragment ions will be presented. We will also present results of zero-energy DR experiments performed at CRYRING including cross sections, branching fractions for the dissociation channels, and imaging studies of the fragmentation dynamics for di-hydride molecular ions. Future plans for this program will be discussed, including utilization of the upgraded MIRF ECR ion source platform to perform DR measurements using a merged electron-ion beams energy-loss apparatus.

* Please also see the Research Summary for the ORNL AMOS program.

PROGRESS REPORT

ELECTRON-DRIVEN PROCESSES IN POLYATOMIC MOLECULES

Investigator: Vincent McKoy

A. A. Noyes Laboratory of Chemical Physics
California Institute of Technology
Pasadena, California 91125

email: mckoy@caltech.edu

PROJECT DESCRIPTION

This project aims to develop and apply accurate, scalable methods for first-principles computational study of low-energy electron–molecule collisions. Because our focus in applications is on polyatomic molecules, for which calculations are highly numerically intensive, the code developed is designed to run efficiently on large-scale parallel computers, including workstation clusters as well as tightly-integrated supercomputers.

HIGHLIGHTS

Over the past year, we have continued our research into low-energy electron collision processes in larger polyatomic molecules. This work includes both applications of existing methodology and development of improved methodology, with a focus on developing methods exhibiting better scaling with molecular size.

Principal accomplishments in the past year are:

- Computation of an extensive set of electron cross sections for SF_6
- Continued research into low-energy electron collisions with DNA bases
- Initiation of work on C_{60}, buckminsterfullerene
- Presentation and publication of results
- Continued development and application of our computational methods

PLASMA PROCESSING GASES

During the past year we completed a study of collisions between low-energy electrons and SF_6. Electron collisions with SF_6 are of interest not only because of its long-standing importance as a prototypical polyatomic target and as a gaseous dielectric, but also because of its use as a feed gas in plasma-based materials processing. Our study included both elastic electron scattering (with polarization effects included) and extensive calculations of electron-impact excitation. Excitation cross sections were computed for 10 low-lying electronic states, all arising from promotion of F lone-pair electrons to the first empty a_{1g} orbital. These cross sections are being prepared for publication and are also being used in plasma simulations by our collaborator, W. Lowell Morgan, to develop a self-consistent electron cross section set for SF_6 for use by the plasma modeling community.

We also completed, in collaboration with M. H. F. Bettega of the Federal University of Paraná (Brazil), a study of elastic and inelastic electron collisions with methylsilane, CH_3SiH_3, which is used as precursor in various plasma-enhanced chemical vapor deposition applications. The results of this study recently appeared in J. Chem. Phys.

DNA BASES

During 2003 we continued our work on the DNA bases. As noted in last year's report, this work is stimulated by the observation [1] that dissociative attachment can produce single- and double-strand breaks in DNA. Because low-energy shape resonances in the elastic electron cross section are one mechanism for promoting electron attachment [2], characterizing those resonances provides basic insight into the dissociative attachment process. Accordingly, we have been computing elastic cross sections for the DNA bases, with polarization effects included, in order to obtain more reliable resonance energies. However, the major dissociative attachment peak in the condensed phase occurs at fairly high energy, 9 eV, and it has been suggested that attachment via core-excited resonances is involved [1,3,4]. In the past year we have also initiated inelastic calculations DNA bases, beginning with thymine, in order to gain some insight into the electron-impact excitation cross sections of states that may be involved in dissociation.

C_{60}

Although the properties and spectroscopy of buckminsterfullerene, C_{60}, have attracted a great deal of attention, very little is yet known of its electron scattering cross sections. Indeed, to our knowledge, only a single and very limited experimental study of the elastic cross section has been published [5], while theoretical studies [6–8] have relied on severe approximations. We have recently begun work directed at obtaining well-converged elastic electron cross sections for C_{60}. As part of this work, we have been developing a variant quadrature procedure for our electron scattering program that will allow us to take full advantage of the high symmetry of C_{60} in constructing the Green's-function term and thereby reduce the computational effort by approximately two orders of magnitude.

PROGRAM DEVELOPMENT

Most of our effort in program development focused on refining our scalable treatment of polarization effects affecting elastic scattering at the lowest energies. However, we also continued work on use of multiconfiguration target states for both elastic and inelastic collisions. Test calculations indicate that the refined treatement of elastic scattering is working correctly and exhibits, as expected, extremely favorable scaling with problem size in comparison to our original approach.

PLANS FOR COMING YEAR

We will complete our elastic calculations on the DNA bases and obtain electron-impact excitation cross sections for selected channels. We also expect to complete necessary program modifications and carry out elastic calculations on C_{60}. Program development will continue, with a focus on completing changes necessary for flexible multiconfigurational treatment of excited electronic states.

REFERENCES

[1] B. Boudaïffa, P. Cloutier, D. Hunting, M. A. Huels, and L. Sanche, Science **287**, 5458 (2000).

[2] See, *e.g.,* M. A. Huels, I. Hahndorf, E. Illenberger, and L. Sanche, J. Chem. Phys. **108**, 1309 (1998).
[3] H. Abdoul-Carime, P. Cloutier, and L. Sanche, Radiat. Res. **155**, 625 (2001).
[4] X. Pan, P. Cloutier, D. Hunting, and L. Sanche, Phys. Rev. Lett. **90**, 208102 (2003).
[5] H. Tanaka, L. Boesten, K. Onda, and O. Ohashi, J. Phys. Soc. Jpn. **63**, 485 (1994).
[6] K. Yabana and G. F. Bertsch, J. Chem. Phys. **100**, 5580 (1994).
[7] R. R. Lucchese, F. A. Gianturco, and N. Sanna, Chem. Phys. Lett. **305**, 413 (1999).
[8] F. A. Gianturco, R. R. Lucchese, and N. Sanna, J. Phys. B **32**, 2181 (1999).

PROJECT PUBLICATIONS AND PRESENTATIONS, 2001–2003

1. "Low-Energy Electron Scattering by C_2HF_5," M. H. F. Bettega, C. Winstead, and V. McKoy, J. Chem. Phys. **114**, 6672 (2001).

2. "Electron Cross Section Set for CHF_3," W. L. Morgan, C. Winstead, and V. McKoy, J. Appl. Phys. **90**, 2009 (2001).

3. "Electron Collisions with Octafluorocyclobutane, c-C_4F_8," C. Winstead and V. McKoy, J. Chem. Phys. **114**, 7407 (2001).

4. "Electron–Molecule Collisions in Processing Plasmas," V. McKoy and C. Winstead, First International Symposium on Advanced Fluid Informatics, Sendai, Japan, 4–5 October, 2001 *(invited talk)*.

5. "Electron Collisions with Hexafluorocyclobutene, c-C_4F_6," C. Winstead and V. McKoy, Fifty-Fourth Gaseous Electronics Conference, State College, Pennsylvania, 9–12 October, 2001.

6. "Electron-Molecule Collisions in Processing Plasmas," V. McKoy and C. Winstead, Forty-Eighth International Symposium of the American Vacuum Society, San Francisco, California, 28 October–2 November, 2001 *(invited talk)*.

7. "Low-Energy Electron Scattering by CH_3F, CH_2F_2, CHF_3, and CF_4," M. T. do N. Varella, C. Winstead, V. McKoy, M. Kitajima, and H. Tanaka, Phys. Rev. A **65**, 022702 (2002).

8. "Electron Collisions with Tetrafluoroethene, C_2F_4," C. Winstead and V. McKoy, J. Chem. Phys. **116**, 1380 (2002).

9. "Electron Transport Properties and Collision Cross Sections in C_2F_4," K. Yoshida, S. Goto, H. Tagashira, C. Winstead, V. McKoy, and W. L. Morgan, J. Appl. Phys. **91**, 2637 (2002).

10. "Electron Collision Cross Sections for Tetraethoxysilane (TEOS)," W. L. Morgan, C. Winstead, and V. McKoy, J. Appl. Phys. **92**, 1663 (2002).

11. "Developing Cross Section Sets for Fluorocarbon Etchants," C. Winstead and V. McKoy, *Proceedings of the Third International Conference on Atomic and Molecular Data and Their Applications, Gatlinburg, Tennessee, 24–27 April, 2002*, AIP Conf. Proc. **636**, 241 (2002) *(invited talk)*.

12. "Quickly Generating Databases," C. Winstead, Third International Conference on Atomic and Molecular Data and Their Applications, Gatlinburg, Tennessee, 24–27 April, 2002 *(panelist)*.

13. "Electron Collisions with SF_6 (Sulfur Hexafluoride)," C. Winstead and V. McKoy, Fifty-Fifth Gaseous Electronics Conference, Minneapolis, Minnesota, 15–18 October, 2002.

14. "Parallel Computations of Electron–Molecule Collisions in Processing Plasmas," V. McKoy, Ninth International Conference on High-Performance Computing, Bangalore, India, 18–21 December, 2002 *(Keynote Lecture)*.

15. "Electron–Molecule Collisions in Processing Plasmas," V. McKoy, Applied Materials, Santa Clara, California, 7 February, 2003 *(invited talk)*.

16. "Electron–Molecule Collisions in Processing Plasmas," V. McKoy, Colloquium, Departments of Physics and Materials Science, University of Southern California, 28 April, 2003.

17. "Electron–Molecule Collision Calculations on Vector and MPP Systems," C. Winstead and V. McKoy, Cray Users' Group Conference, Columbus, Ohio, 12–16 May, 2003.

18. "Low-Energy Electron Scattering by Methylsilane," M. H. F. Bettega, C. Winstead, and V. McKoy, J. Chem. Phys. **119**, 859 (2003).

Electron Emission From Atoms and Small Molecules

M.H. Prior,
Chemical Sciences Division,
Lawrence Berkeley National Laboratory

This part of the LBNL Chemical Sciences Division AMOP program has focused in recent years on the exploitation of momentum spectroscopy techniques to elucidate details of the photoionization of atoms and small molecules. Using photons from the LBNL Advanced Light Source, the technique measures the momenta of all fragments following a photoionization event with high efficiency. This provides the ability to view the relationships between the final momentum in essentially any way that provides insight into the dynamics of the breakup or which can be readily compared with advanced calculations. Originally centered on studies of single photon double ionization of the He atom, this work has progressed to include studies of the breakup of H_2 or D_2 molecules and the K-shell photoionization of heavier diatomics such as CO and N_2. This presentation will summarize recent work in this area.

Single photoionization of H_2 and D_2 molecules

We have recently applied the COLTRIMS methodology to study the single photon ionization and dissociation of H_2 and D_2 molecules. For photon energies above about 18.1 eV it is possible to ionize and dissociate H_2 or D_2 ; in the range up to about 46 eV, the products are the photoelectron and either an intact molecular ion, e.g. H_2^+ or, with considerably less probability, a dissociated molecular ion, i.e H^+ and a neutral H atom (or D^+ and D). The latter channel is particularly interesting because it includes many resonant doubly exited molecular states that decay by Auger emission. Competition between this process and direct ionization to the continuum, yields interference effects that affect the structure in the correlation between the electron energy and the kinetic energy of the heavy dissociating fragments. We have been able to map the evolution of the ionization and dissociation process over the photon range 30-60 eV for both H_2 and D_2 molecules, and we have also obtained the electron angular distributions in the molecular frame. There is a substantial body of theoretical and previous experimental studies of this process; our studies are consistent with much of the previous experimental work, but include for the first time the electron angular patterns keyed to particular channels. Because the electron emission often comes from Auger decay of unbound doubly excited molecular states (e.g. the Q1, Q2…etc… manifolds), there can be significant isotope dependencies and these appear in our measurements. Above 46 eV, it is possible to doubly ionize D_2 or H_2 with a single photon, and our measurements shows the smooth evolution from below to above the double ionization threshold. This work was carried out at the LBNL Advanced Light Source at beamline 9.3.2 during August 2002 and forms the Diplom project of visiting U. Frankfurt graduate student Lutz Foucar.

Double ionization of D_2: correlations among the four photo fragments

Our earlier studies of the single photon double ionization of the He atom, led naturally to the study of the same phenomena in the simple H_2 or D_2 molecules. The single photon, total fragmentation of these simple molecules contains the elements of electron correlation, as in the He double ionization, with the added complexity of an additional Coulomb particle in the final state. In our first approach to this problem we recorded a single electron in coincidence with the two fragment ions, the results then being an average over all the emission angles of the “missing” electron. Later experiments recorded all four fragments in coincidence and have allowed the description of the process at an unprecedented level of detail. It is instructive to compare the electron angular distributions to the case of He.

Jim Feagin (JPB **31**, L729, [1998]) has shown that the double ionization of H_2 (or D_2) can be described as a coherent sum of He-like amplitudes for driving a Σ and a Π transition (for a general orientation of the molecule with respect to the axis of linear polarization). Thus for pure Σ or Π geometries (polarization parallel or perpendicular to the molecule) one obtains electron emission patterns which are similar to those obtained from He. However for intermediate geometries, the interference of the Π and Σ amplitudes causes a marked departure from similarity to the He case. Some familiar selection rules from the He case remain in force but others dissolve to mere propensities or vanish altogether. Of course there are entirely new phenomena which can only appear in the molecular case. One striking example is the variation of the electron emission pattern with fragment ion energies within the Frank-Condon profile; the total fragment kinetic energy (called the Kinetic Energy Release, KER) is directly related to the internuclear separation via the Coulomb repulsive curve. Our measurements display the two electron distribution pattern from molecules with selected internuclear separations and selected orientation of the molecular axis with respect to the linear polarization axis. This marks the most detail description of the double electron emission from this prototypical molecular system.

This work, carried out during more than one experimental run time at the LBNL Advanced Light Source, was the U. Frankfurt, PhD project of Dr. Thorsten Weber. Reports drawn from this project are in preparation for publication.

Auger emission from "fixed-in-space" CO molecules

K-shell photo-ionization of an atom within a molecule yields a photo-electron followed by emission of at least one Auger electron and the fragmentation of the molecule. It has been generally believed that the photo-emission and Auger processes are independent so that, e.g. the Auger electron angular distribution in the molecular frame should not depend on the photon energy or the orientation of the photon's linear polarization with respect to the molecular axis apart from a scaling to reflect the cross-section for the photo-ionization. However, a recent report claimed observation of a marked difference in the Auger emission patterns following K-shell ionization of C in CO by photons polarized parallel vs. perpendicular to the molecular axis. This unexpected observation was reported to depend strongly on the particular Auger transition, and is strongest for photon energies near 305 eV, i.e. near the peak of the σ shape resonance in CO. In February 2002 we used a modified COLTRIMS setup to measure energy resolved Auger electron emission patterns from oriented CO molecules at the ALS Beam-line 4.0 These measurements were insensitive to the photoelectron distribution but the Auger electron was measured with improved collection efficiency; the C^+ and O^+ fragments were collected with 4π efficiency and their kinetic energy measurement resolves the different CO^{++} final channels. The results have conclusively shown no break down of the independence of the Auger and photo-electron emission [PRL **90**, 153003, (2003)] We obtained electron angular distributions in the molecular frame for three different Auger transitions. One of these shows a strongly peaked emission pattern in the direction of the oxygen nucleus and appears to be the result of a focusing of the electron emission by the screen coulomb potential of the oxygen ion. Superimposed on this narrow emission pattern are small but significant oscillations due to the diffraction of the Auger electron wave in the two center molecular potential.

Vibrational state resolved and satellite K-shell photo electron emission from CO molecules

We have recently utilized a portion of an experimental running period at the LBNL ALS in March 2003 to study a number of topics in the K-shell photo-ionization of the CO molecule. Although the analysis is continuing, it is clear that one of the results of this work includes the molecular frame electron distributions which resolve the vibrational state of the core excited CO molecular ion left behind by the photo-electron. Resolution of this fine scale of photoelectron energies is not unusual using modern dispersive or precision time-of-flight electron spectrometers, however combining the ability to do so with the high efficiency of the COLTRIMS methodology for mapping the full electron angular distributions is unique. The electron

distributions are dominated by the v=0 and v=1 vibrational states which show similar angular distributions. The weak v=2 state however displays a significantly changed pattern which may reflect the larger weight given to higher internuclear separations present in the v=2 wavefunction and the resulting modification to the intramolecular potential sensed by the outgoing photo-electron wave.

From the same and earlier data sets we have also obtained photoelectron satellite line angular distributions. Satellite photo-electrons refer to those emitted with simultaneous excitation of the core hole CO molecular ion. Thus these electrons appear at energies lower than the main photoelectron line by the amount of the excitation of the molecule. The electron angular distributions of these satellite photoelectrons can be markedly different from the main line photoelectrons, since the excited core ionized molecule can take up a different set of angular momentum quantum states and/or parity than the main line. In CO the ground core excited molecular ion is in a $^2\Sigma^+$ state, whereas one of the prominent satellite states observed has $^2\Pi$ symmetry. As it turns out the angular pattern of the $^2\Pi$ satellite strongly resembles that of a nearby Σ^+ satellite with respect to the molecular frame however it is only strongly excited by light polarized to perpendicular to the molecular axis as opposed to the parallel alignment favored to excite a Σ. Thus in this case, the Π character remains in the core, while the exciting electron wave resembles a pure Σ wave in the molecular frame. Full analysis of the data set obtained in March 2003 will doubtless reveal more detail regarding the emission patterns from these and other satellite states. Since one electron is emitted while also exciting the molecular ion, there is similarity to other electron-electron induced phenomena such as "shake-up" or the excitation of doubly excited states.

Future Directions

The detailed study of photo- electron and Auger emission from molecules will continue through exploitation of the power of the the COLTRIMS methodology. We hope to conduct experiments in H_2 and/or D_2 at photon energies high enough so that one of the two electrons emitted in the double ionization process has a De Broglie wavelength short enough so that diffraction effects in its propagation outward from the molecule can be observed. At the opposite extreme one would like also to reach a low energy regime near threshold for double ionization, where the electron and fragment ion velocities are similar…here one might expect to see strong four particle Coulomb effects yielding marked departure from Born-Oppenheimer approximation behavior. This will be extremely difficult but its feasibility is under study. We will also continue to exploit the rich array of processes available for study in the core ionized heavier molecules. This will likely include a complete 4 particle study in a system like CO, that is where the photoelectron, Auger electron and the two fragment ions are measured for each K-shell ionization event. The extension of the COLTRIMS method to electron impact induced processes, such as dissociation following electron attachment, remains on our list of projects and will build upon electron gun tests performed during FY 2003. In the case of K-shell ionization of atoms, we will conduct experiments in search of postcollision effects on K-shell photoelectron distribution from Neon atoms, i.e the effect of the Auger electron "scattering" the photo electron. To more efficiently pursue these goals and others we expect to assemble a new COLTRIMS apparatus during FY2004.

The COLTRIMS studies of photo-ionization are collaborative with colleagues from U. Frankfurt, Kansas State University; Western Michigan and Auburn Universities, with occasional participation by researchers from other institutions. All of this work is conducted at the LBNL Advanced Light Source.

Publications during the period 2001-2003

Landers, A.; Weber, Th.; Ali, I; Cassimi, A.; Hattass, M.; Jagutzki, O.; Nauert, A.; Osipov, T.; Staudte, A.; Prior, M.H.; Schmidt-Böcking, H.; Cocke, C.L.; Dörner, R.
Photoelectron Diffraction Mapping: Molecules Illuminated from Within
Physical Review Letters, **87**, 013002 (2001).

T. Weber, O. Jagutzki, M. Hattass, A. Staudte, A. Nauert, L. Schmidt, M.H. Prior, A.L. Landers, A. Bräuning-Demian, H. Bräuning, C.L. Cocke, T. Osipov, I. Ali, R. Díez Muiño, D. Rolles, F.J. García de Abajo, C.S. Fadley, M.A. Van Hove, A. Cassimi, H. Schmidt-Böcking and R. Dörner
K-shell Photonionization of CO and N_2: Is There a Link Between the Photoelectron Angular Distribution and the Molecular Decay Dynamics?
J. Phys. B: At. Mol. Opt. Phys, **34**, 3669 (2001)

A. Staudte, C.L. Cocke, M.H. Prior, A. Belkacem, C. Ray, H.H.W. Chong, T.E. Glover and R.W. Schoenlein
Observation of a nearly Isotropic, High Energy Coulomb Explosion Group in the Fragmentation of D_2 by Short Laser Pulses
Physical Review A (Rapid Communication), **65**, 020703(R) (2002)

A. Knapp, M. Walter, T. Weber, A.L. Landers, S. Schössler, T. Jahnke, M. Schöffler, J. Nickles, S. Kammer, O. Jagutzki, L.P.H. Schmidt, T. Osipov,
J. Rösch, M.H. Prior, H. Schmidt-Böcking, C.L. Cocke, J. Feagin, R. Dörner
Energy Sharing and Asymmetry Parameters for Photo Double Ionization of Helium 100 eV Above Threshold in Single-Particle and Jacobi Coordinates.
Journal of Physics B-Atomic Molecular & Optical Physics, **35**, L521, (2002)

T. Jahnke, Th. Weber, A.L. Landers, A. Knapp, S. Schössler, J. Nickles, S. Kammer, O. Jagutski, L. Schmidt, A. Czasch, T. Osipov, E. Arenholz, A.T. Young, R. Díez Muiño, D. Rolles, F.J. Garacía de Abajo, C.S. Fadley, M.A. Van Hove, S.K. Semenov, N.A. Cherepkov, J. Rösch, M.H. Prior, H. Schmidt-Böcking, C.L. Cocke and R. Dörner
Circular Dichroism in K-shell Ionization from Fixed-in-Space CO and N_2 Molecules
Physical Review Letters, **88**, 073002 (2002) [Figure on Journal Cover]

A. Knapp, A. Kheifets, I. Bray, T. Weber, A.L. Landers, S. Schössler, T. Jahnke, J. Nickles, S. Kammer, O. Jagutzki, L.P.H. Schmidt, T. Osipov, J. Rösch
M.H. Prior, H. Schmidt-Böcking, C.L. Cocke, R. Dörner
Mechanisms of Photo Double Ionization of Helium by 530 eV Photons.
Physical Review Letters, **89**, 033004, (2002)

Th. Weber, M. Weckenbrock, M. Balser, L. Schmidt, O. Jagutzki, W. Arnold, O. Hohn, M. Schöffler, E. Arenholz, T. Young, T. Osipov, L. Foucar, A. De Fanis, R.D. Muino, H. Schmidt-Böcking, C.L. Cocke, M.H. Prior, R. Dörner
Auger electron emission from fixed-in-space CO
Physical Review Letters, **90**, 153003, (2003)

T. Osipov, C. L. Cocke, M. H. Prior, A. Landers, Th. Weber, O. Jagutzki, L. Schmidt, H. Schmidt-Böcking, and R. Dörner
Photoelectron-Photoion Momentum Spectroscopy as a Clock for Chemical Rearrangement: Isomerization of the Di-Cation of Aceltylene to the Vinylidene Configuration
Physical Review Letters, **90**, 233002 (2003)

Research Summaries

(multi-PI programs by institution)

Ultracold Atoms: Applications

R. W. Dunford, S.H. Southworth, L. Young
Argonne National Laboratory, Argonne, IL 60439

dunford@anl.gov, southworth@anl.gov, young@anl.gov

The unique properties of cooled and trapped neutral atoms enable applications in a variety of fields. The highly-localized, low-momentum spread sample of ultracold atoms provides a well-defined target for ionization studies. Extreme isotopic selectivity combined with efficient capture probability has spurred the development of an ultrasensitive trace isotope analysis technique based upon counting individual atoms, ATTA (atom trap trace analysis). In addition, ultracold atoms are ideal for precision spectroscopy as the absence of Doppler spread simplifies the lineshape. We are currently using cooled and trapped atoms in these applications.

Triple Ionization of Lithium by Electron Impact

M.-T. Huang[1], W.W. Wong[2], M. Inokuti[3], S.H. Southworth, L. Young

Electron-impact ionization is a fundamental collision process in atomic physics. Because of importance from both applied and theoretical viewpoints, it has been the subject of study for many years. Nevertheless, the predictive power of theory remains limited. Theoretical challenges are great, as even the simplest process, electron-impact single ionization, yields a final state with three charged particles in the continuum. Over the past decade, considerable theoretical progress has been made on electron-impact single ionization based on non-perturbative methods, where calculations in the electron + hydrogen system reproduce the observed ionization cross-sections to within experimental error bars over a wide energy range. For atoms more complex than hydrogen, the agreement between theory and experiment for total ionization cross sections is somewhat less impressive, particularly when target electrons occupy more than one shell, e.g. metastable He ($1s2s\ ^3S$) and the alkalis. For electron-impact double-ionization, an *ab initio* theoretical understanding is starting to emerge, although the emphasis has been on the observed angular correlation patterns observed in (e,3e) experiments rather than the value of the absolute cross-section. To our knowledge, only one *ab initio*, fully quantal work has calculated the double-to-single ionization ratio, despite the existence of rather reliable data in, e.g., the two-electron atom helium. For triple ionization, the *ab initio* theoretical work is non-existent, and semi-empirical calculations are used for estimates. Lithium holds special interest as the simplest three-electron system and the natural progression to more complex systems.

Ejection of the three electrons from lithium in a single electron collision was observed for the first time. Triply charged lithium was observed in an ion time-of-flight spectrum following electron impact on a sample of ultracold, trapped lithium. The higher signal/background afforded by the trap environment made the observation of Li^{3+} possible. We measured the ratios of triple-to-double and double-to-single ionization at an impact energy of 1000 eV. The 3+/2+ ratio is ≈ 0:001, a value 2 orders of magnitude lower than semiempirical predictions. We demonstrated a simple method that uses photoionization data combined with sum-rule analysis to predict the asymptotic charge-state ratios. The sum-rule predictions compare reasonably with experiment and shake calculations, but disagree sharply with the semiempirical estimates. We hope that these results will motivate *ab initio* calculations for this relatively simple system.

Future plans for ultracold lithium include using the trap environment for precision spectroscopy of the 2s ^{2}S -2p ^{2}P transitions, where precise calculations by Drake are in disagreement with experimental measurements. Of particular unique interest at Argonne, vis-à-vis the active *ab initio* nuclear structure program and the availability of large fluxes of rare isotopes using the ATLAS low energy heavy ion accelerator, is the measurement of the rms charge radius of ^{8}Li, which can be obtained through accurate isotope shift measurements of the 2s ^{2}S -2p ^{2}P transitions. These experiments are planned in collaboration with the Argonne Physics Division, York University and Tokyo University.

Optical Production of Metastable Krypton

W.W.Wong[2], X. Du, R. W. Dunford, L. Young

Metastable rare gas atoms are useful in a range of important applications such as cold collision physics, optical lattices, atom lithography, rare isotope detection and Bose-Einstein condensation. Such atoms are produced by direct extraction from DC or rf discharges or by excitation of an atomic beam via electron bombardment. Metastable fractions in such beams are typically less that 0.1% and this can be a severe limitation on the applications that utilize these beams. We have investigated an optical method for excitation of the 5s, J=2 metastable level of Kr ($5s[3/2]_{J=2}$) which has the potential to significantly increase the metastable fraction available. The technique will also work for other rare gases. Kr atoms are resonantly excited to $5p[3/2]_{J=2}$ level using the 123 nm output of a Kr resonance lamp followed by the 819 nm output of a Ti:sapphire laser. From this level, the atoms radiate at 760 nm to the metastable level with a 77% branch. We demonstrated a production rate for metastable Kr of 10^{14}/s at a pressure of 1 mTorr in a gas cell. We were able to model our experiment using a Monte-Carlo simulation that accounts for the multiscattering of the uv photons in the cell. These experiments and simulations show a conversion efficiency of uv photons to metastable atoms of ≈10%. In order to use the metastable Kr for atom trapping, the cell geometry must be converted to a beam configuration. A beam apparatus and the 811 nm laser used to measure the flux and velocity distribution has been set up during this past summer. Our goal is to obtain a metastable beam flux of about 10^{14} metastables/second in a solid angle of 10^{-3} sr. Attaining this goal will enable dating of polar ice using the atom trap trace analysis method.

Atom Trap Trace Analysis

X. Du[3], K. Bailey[3], Z.-T. Lu[3], I. Moore[3], P. Mueller[3], T. P. O'Connor [3], L. Young

We have made the first practical use of Atom Trap Trace Analysis, a relatively new method for ultrasensitive trace isotope analysis based upon laser manipulation of neutral atoms. In this method, individual atoms are counted while residing in a magneto-optical trap (MOT). With no observed contamination from neighboring isotopes, the selectivity is limited primarily by the number of atoms that can be sorted during a finite operation time and has been demonstrated at the part-per-trillion level. Key technical features are an efficient capture rate and the ability to detect a single atom in the MOT. Applications involving ^{85}Kr and ^{81}Kr should be of particular interest to the DOE. Trace detection of ^{85}Kr ($t_{1/2}$ = 10.5 yrs) can be used to monitor nuclear fission activities. ^{81}Kr ($t_{1/2}$ ≈229 kyrs) is a cosmogenic nuclide and homogeneously distributed over the earth. Its concentration is unaltered by human activities

because stable ^{81}Br shields ^{81}Kr from the neutron-rich isotopes that are produced in nuclear fission. Thus, ^{81}Kr is ideal for dating polar ice and groundwater in the 100 kyr range.

This year, we have demonstrated a new method for determining the ^{81}Kr/Kr ratio in environmental samples based upon two measurements: the ^{85}Kr/^{81}Kr ratio measured by Atom Trap Trace Analysis (ATTA) and the ^{85}Kr/Kr ratio measured by Low-Level Counting (LLC). This method can be used to determine the mean residence time of groundwater in the range of $10^5 - 10^6$ years. It requires a sample of 100 µl STP of Kr extracted at an efficiency of 70% from approximately two tons of water. Using this method, the age of six samples from the Nubian aquifer in Egypt has been determined. A paper has been submitted on this result.

Detection of ^{41}Ca in biomedical samples with isotopic abundance levels between 10^{-8} and 10^{-10} using ATTA has been demonstrated. The applications for ^{41}Ca ($t_{1/2}$= 103 kyrs) and natural abundance of 10^{-15} - 10^{-14} include medical use as a tracer for osteoporosis, nuclear activity monitoring and radioisotope dating of ancient bones. ATTA was calibrated against Resonance Ionization Mass Spectrometry and a good agreement was found. The present counting efficiency is 2 x 10^{-7}. A paper has been submitted on this result. A slightly modified system could be of interest to DOE as an trace analyzer for ^{90}Sr, a fission product.

[1]Permanent address: Saginaw Valley State University, [2]Princeton University, [3]Physics Division, Argonne National Laboratory

Publications 2001-2003

A Beam of Metastable Krypton Atoms Extracted from an RF-Driven Discharge
C.Y. Chen, K. Bailey, X. Du, Y.M. Li, Z.-T. Lu, T.P. O'Connor, L. Young, G. Winkler
Rev. Sci. Instr. **72**, 271-272 (2001).

Atom Trap Trace Analysis
Z.-T. Lu, K. Bailey, C.Y. Chen, X. Du, Y.-M. Li, T.P. O'Connor, L. Young
Atomic Physics 17, Proceedings of the 17th International Conference on Atomic Physics (Eds. E. Arimondo, P. DeNatale, M. Ingusio, copyright 2001) p.367-381.

Measurements of the electron-impact double-to-single ionization ratio using trapped lithium
M.-T. Huang, L. Zhang, S. Hasegawa, S. H. Southworth, L. Young
Phys. Rev. A **66**, 012715:1-7 (2002).

Optical production of metastable krypton
L. Young, D. Yang, R.W. Dunford
J. Phys. B **35**, 1-8 (2002).

Towards ultrahigh sensitivity analysis of ^{41}Ca
I.D. Moore, K. Bailey, Z.-T. Lu, P. Müller, T.P.O'Connor and L. Young,
Nucl. Instr. Meth. B **204**, 701-704 (2003).

Triple Ionization of Lithium by Electron Impact
M.-T. Huang, W.W. Wong, M. Inokuti, S.H. Southworth, L. Young
Phys. Rev. Lett. **90**, 163201:1-4 (2003).

X-ray and Inner-Shell Interactions

R. W. Dunford, E. P. Kanter, B. Krässig, S. H. Southworth, L. Young
Argonne National Laboratory, Argonne, IL 60439

dunford@anl.gov, kanter@anl.gov, kraessig@anl.gov, southworth@anl.gov, young@anl.gov

We seek to establish a quantitative understanding of x-ray interactions with free atoms and molecules. We have explored a broad energy range where the dominant interaction evolves from photoabsorption to scattering, with careful attention to regions near resonances and thresholds. The focus has been on understanding the limitations of theory, in particular the validity of the independent particle approximation and the role of multipole effects. Multipole effects are studied using an apparatus with four photoelectron spectrometers to monitor multiple angles simultaneously. Multielectron excitation is studied as a measure of electron-electron correlation in heavy atoms. Studies of two-photon transitions address rare decay modes of inner shell vacancies produced by photoionization. We have initiated studies of the effect of strong-AC fields on the x-ray photoionization and decay of a free atom.

Nondipole Photoelectron Asymmetries

R. W. Dunford, E. P. Kanter, B. Krässig, S. H. Southworth, L. Young

New aspects of the photoionization of atoms and molecules have been investigated in recent years through measurements and theoretical calculations of the nondipole asymmetries of photoelectron angular distributions. Nondipole asymmetries result from interference between electric-dipole (E1), electric-quadrupole (E2), and magnetic-dipole (M1) photoionization amplitudes. These interactions give rise to an asymmetry between the intensities of photoelectrons emitted in the forward- and backward-hemispheres with respect to the photon propagation direction. Forward-backward (nondipole) asymmetries can be isolated from the pure-E1 anisotropy and accurately measured with suitable detection geometries. Nondipole asymmetries vary with photon energy due to variations of the magnitudes and phases of the E1, E2, and M1 photoionization amplitudes. Our research focuses on photoionization of atoms and molecules, but nondipole interactions are also being studied in solids.

Using hard x rays at Argonne's Advanced Photon Source (APS), we have measured the nondipole asymmetries of deep inner-shell photoelectrons. We recently reported on an experimental and theoretical study of Kr 1s in which we compared measurements over 11–8000 eV kinetic energy with calculations. The measured asymmetries agree well with both full multipole relativistic and nonrelativistic first-order retardation calculations within the independent-particle approximation. Deviations of the measured asymmetries from predictions of the point-Coulomb retardation correction confirm the importance of screening on the continuum-wave normalizations and phase shifts.

Using vacuum-ultraviolet radiation at Wisconsin's Synchrotron Radiation Center (SRC), we have measured nondipole asymmetries of valence photoelectrons of He, Ne, Xe and N_2. Recent publications from that work describe the effects of many-electron interactions on nondipole asymmetries. Autoionization of the $1s^2 \rightarrow 2s2p$ ($^1P_1$) (dipole allowed) and $1s^2 \rightarrow 2p^2$ ($^1D_2$) (dipole forbidden) doubly-excited states in He produce resonance structure in the nondipole asymmetry parameter. The Fano-profile parameters of both resonances were determined, and the ratio of the magnitudes of the E2 and E1 photoionization amplitudes and their relative phase

were also determined experimentally and compared with theory. To test predictions of channel-coupling effects on the nondipole asymmetry parameter of Xe 5s, our measurements were combined with higher-energy measurements made by our collaborators at Berkeley's Advanced Light Source and compared with calculations that treat interchannel coupling with the 5p, 4d, 4p, and 4s subshells. The calculations are in good qualitative agreement with measurements and confirm the importance of interchannel coupling, including coupling within the E2 channels.

For future work, we will optimize the performance of our electron spectrometer for low kinetic-energy measurements in order to better study resonance and threshold effects. A soft x-ray beamline will be used at the APS to study K shells of Ne and small molecules. At the SRC, we will measure several higher members of dipole-allowed and -forbidden doubly-excited Rydberg series converging on the He^+ n=2 ionic limit. Benchmark measurements on valence electrons of small molecules are also of great interest for comparison with theoretical calculations that are currently in progress.

Double K-photoionization of Heavy Atoms

R. W. Dunford, D. S. Gemmell[1], E. P. Kanter, B. Krässig, S. H. Southworth, and L. Young

The double K-photoionization of heavy atoms is a rare (~10^{-4}) process that produces a *hollow* atom. The process itself is of fundamental interest as a measure of electron-electron correlations in high-Z systems, but this work has several practical applications as well including a possible source of entangled electrons. We have recently completed a comprehensive study of double K-photoionization of Ag (Z=47). Measurements were carried out at several photon energies from just below the double K-ionization threshold (51.782 keV) to the region of the expected maximum in the cross-section (~90 keV). The energy-dependence of these data has been fitted with a model in which the shakeoff and scattering contributions are calculated independently. Because of extensive previous studies of this atomic system using the electron capture (EC) decay of ^{109}Cd, the shakeoff contribution is well known experimentally for the single-electron final state produced in EC. Thus, our photoionization measurements served to isolate the effects of the dynamic electron-electron scattering term. Analysis of these results demonstrates a significantly larger scattering contribution than in lighter atoms. The measured ratio (double/single ionization) in the peak region is found to agree well with the Z-dependence we had found from fitting previous measurements and is slower than the characteristic $1/Z^2$ dependence of shakeoff, further confirming the large scattering contribution in the peak region. An important goal for the immediate future is to complete this work with additional measurements beyond the peak region. Our principal goal for the future is to observe this phenomenon in Au (Z=79). This is a case where relativistic effects should be dominant.

Two-photon decay

R. W. Dunford, E. P. Kanter, B. Krässig, S. H. Southworth, L. Young, P. H. Mokler[2], and Th. Stöhlker[2]

One of the processes contributing to the decay of an inner-shell vacancy in an atom is the simultaneous emission of two photons. Although this is a rare decay mode, it is important because it contributes to the continuum radiation on the low energy side of the characteristic x-ray lines down to zero energy. Two-photon decay is also important from a theoretical standpoint

as it provides a unique way of testing atomic structure calculations. Typical measurements provide data on transition probabilities differential in the opening angle distribution and the energy of the individual photons. Together these characteristics provide a wealth of information to test the details of the calculations. We have measured two-photon decay of single K-vacancies in gold atoms following photoionization with synchrotron radiation. Our results determine differential transition probabilities for the 2s → 1s, 3d → 1s and 4sd → 1s two-photon decays for events in which the two photons share the transition energy equally and have opening angles near θ = π/2. This is the highest-Z measurement of inner-shell two-photon decay and the first to be done at a synchrotron light source. The next step in this work is to measure the spectral shape of the two-photon continuum from gold atoms. Improvements have been made to the apparatus and initial data have already been obtained. For this measurement longer integration times are needed in order to gain sufficient statistical accuracy for the differential measurements. Subsequent experiments will study heavier atoms and explore the distributions of photon opening angles.

A quantum-mechanically complete experiment on photo-double ionization of helium

B. Krässig

The dynamics of the three-body breakup of the helium atom during photo-double ionization are fully contained in two complex-valued correlation functions that only depend on the energies of the two electrons and their mutual angle. Previously I reported on how the magnitudes of the correlation functions and the cosine of their relative complex phase can be extracted from a COLTRIMS experiment performed with fully linearly polarized incoming light. This formalism has now been extended to work for arbitrary degrees of light polarization, and, if the light contains a component of circular polarization, the full complex phase (modulo 2π) and the degree of circular polarization are now obtained as well. The formalism takes advantage of the ability of COLTRIMS to record double ionization events angle- and energy-resolved with 4π-solid angle acceptances. To this end it is necessary that the detection efficiencies of the experiment are uniform over the entire parameter space, or else corrections have to be applied to the data sets. In the data set used in the present study, obtained with multi-channel plate electron detectors, the detection efficiency is dependent on the impact angle, and the absence of a capability to count double hits separately causes false identifications of such events. The development of an algorithm for the correction of these experimental imperfections is currently in progress.

[1]Physics Division, Argonne National Laboratory, [2]GSI, Darmstadt, Germany

Selected Publications 2001 – 2003

Double Electron Capture in Relativistic U^{92+} Collisions Observed at the ESR Gas-Jet Target, G. Bednarz *et al.*, Physica Scripta **T92**, 429-431 (2001).

Strong Evidence for Enhanced Multiple Electron Capture from Surfaces in 46 MeV/u Pb^{81+} Collisions with Thin Carbon Foils, H. Bräuning *et al.*, Phys. Rev. Lett. **86**, 991-994 (2001).

Multiple Electron Capture by 46 MeV/u Pb^{81+} Ions from Solid Targets,
H. Bräuning *et al.*, Physica Scripta **T92**, 43-46 (2001).

The Two-Photon Decay of the 1s2s $^1S_0$-like States in Heavy Atomic Systems,
P. H. Mokler and R. W. Dunford, Fizika A **10**, 105-112 (2001).

Near-Threshold Photoionization of Hydrogenlike Uranium Studied in Ion-Atom Collisions via the Time-Reversed Process, T. Stöhlker *et al.*, Phys Rev Lett. **86**, 983-986 (2001).

Radiative Electron Capture Studied for Bare, Decelerated Uranium Ions,
T. Stöhlker *et al.*, Physica Scripta **T92**, 432-434 (2001).

Corrections to the usual x-ray scattering factors in rare gases: experiment and theory,
L. Young *et al.*, Phys. Rev. A **63**, 052718 (2001).

Interaction of atomic systems with x-ray free-electron lasers,
M. A. Kornberg *et al.,* J. Synchrotron Rad. 9, 298-303 (2002).

Photoexcitation of a Dipole-Forbidden Resonance in Helium,
B. Krässig *et al.*, Phys. Rev. Lett. **88**, 203002 (2002).

Nondipole asymmetries of Kr 1s photoelectrons,
B. Krässig *et al.*, Phys. Rev. A **67**, 022707 (2003).

Threshold krypton charge-state distributions coincident with K-shell fluorescence,
G.B. Armen *et al.*, Phys. Rev. A **67**, 054501 (2003).

Two-photon decay in gold atoms following photoionization with synchrotron radiation,
R.W. Dunford *et al.,* Phys. Rev. A **67**, 054501 (2003).

Applications of position sensitive germanium detectors for X-ray spectroscopy of highly charged heavy ions, Th. Stöhlker *et al.,* Nucl. Instrum. Meth. B **205**, 210-214 (2003).

Double K-shell photoionization of neon,
S.H. Southworth *et al.*, Phys. Rev. A **67**, 062712 (2003).

E1-E2 interference in the VUV photoionization of He,
E.P. Kanter *et al.*, Phys. Rev. A **68**, 012714 (2003).

Dramatic nondipole effects in low-energy photoionization: experimental and theoretical study of Xe 5s, O. Hemmers *et al.*, Phys. Rev. Lett. **91**, 053002 (2003).

GENERATION AND CHARACTERIZATION OF ATTOSECOND PULSES

L. F. DiMauro[1], K. C. Kulander[2], I. A. Walmsley[3,4] and R. Boyd[4]
[1] Brookhaven National Laboratory, Upton, NY 11973
[2] Lawrence Livermore National Laboratory, Livermore, CA 94551
[3] Oxford University, Oxford, UK OX1 3PU
[4] University of Rochester, Rochester, NY 14627

PROGRAM SCOPE

The objective of this program is the complete optical characterization of high harmonics, which might be exploited in the production of an attosecond pulse, and to demonstrate the formation of such a pulse. By complete characterization we mean the extraction of the temporal or spectral amplitude and phase of a single pulse or train of pulses. The proposal has two parallel efforts (BNL/LLNL and Rochester) with the ultimate aim of generating and measuring an attosecond pulse.

RECENT PROGRESS

High harmonic (HHG) radiation, which results from atoms interacting with an intense laser field, has the potential to produce pulses of light with unprecedented durations approaching the attosecond (1 as = 10^{-18} s) time-scale. Moreover, with high conversion efficiencies (~ 10^{-5}) [1] in the XUV range and ~ 10 A [2] spectral content, HHG exhibits attractive traits for coherent XUV research. Within the past two years, two separate confirmations [3,4] of attosecond pulse formation from HHG have been reported. High harmonics are commonly generated by the interaction of intense, near visible (0.8 μm) laser field with high binding energy atoms (rare gases). However, Keldysh [5] formulated that equivalent interactions can be achieved throughout the electromagnetic spectrum. Thus, an equivalent interaction can be experimentally realized by proper choice of the field parameters, e.g. intensity, and wavelength, and atomic binding energy. We have demonstrated that the lower binding energy alkali metal atoms excited by an intense mid-infrared pulse fulfills this condition. The Keldysh framework addresses one of the most fundamental principles in strong-field physics: the invariance of a scaled interaction. Consequently, our experiments are a critical paradigm in establishing this understanding.

An important practical aspect of the aforementioned scaled interaction is the study of attosecond (10^{-18} s) pulse formation by enabling experimental accessibility to well-developed metrology for characterization of high harmonic radiation. For example, harmonics generated by a 3.4 μm mid-infrared (MIR) fundamental field have a spectrum that extends from the near-visible to the near-ultraviolet. In this regime, superior optics and nonlinear materials exist for manipulation and measurement of the high harmonic light. Furthermore, the study of alkali atoms with MIR light not only provides the necessary Keldysh scaling but also yields optical accessibility to bound-bound and bound-continuum harmonic emission. All these points are essential for establishing the

viability for using a comb of high harmonic light for generating light pulses on the attosecond time-scale and provide the major impetus for our investigations.

Our experiments are unique in that they provide a means for directly measuring the formation of attosecond light pulses. We have demonstrated that the interaction of an alkali-atom with a MIR pulse does produce a comb of high harmonic light [6] in a manner consistent with the Keldysh scaling. The viability of this approach was further demonstrated by studying the coherence properties [7] of harmonic orders 5-9 generated in a Rb atomic oven using a 3.4 μm MIR source. The study showed that sufficient high harmonic intensity could be generated allowing the application of second-harmonic autocorrelation and temporal interferometer. This is the first direct measurement of harmonic orders higher than the fifth. This has given us the ability to study in detail both the microscopic and macroscopic behavior of high harmonic generation. Currently, calculations coupling numerical solutions of the time-dependent Schrödinger equation (single-atom) and Maxwell's equation (macroscopic) within a slowly varying approximation are being performed in collaboration with Prof. K. Schafer and Prof. M. B. Gaarde of Louisiana State University. Initial studies indicate excellent quantitative agreement between experiment and theory, which would give us a powerful predictive tool.

The march towards brighter and shorter high harmonic sources inevitably involves the control of the physics of this coherent process. Control can be achieved both at the "single" atom (quantum) or macroscopic (Maxwell's equation) level. To date, it has been the latter approach that has yielded the largest gains in brightness through optimized phase-matching geometries or novel periodic fiber structures. Exploration of the atomic response has been largely unexplored and limited to the selection of a suitable ground state atom, generally a rare gas. However, HHG is a coherent process and thus sensitive to the initial atomic state. We have recently conducted the first experiment [7] that demonstrates the enhanced production of high harmonic light from a diode-laser prepared excited state of a rubidium atom exposed to a 3.5 μm laser pulse. The results clearly demonstrate large enhancements (factors of 10-1000 increase) in the excited state HHG process as compared to the ground state atom. The physics of this process has its origin in the single atom response and could provide a very viable means for optimization of high harmonic light sources.

FUTURE PLANS

Our plans for future high harmonic studies in a scaled interaction include 1) shortening of the MIR pulse into the femtosecond regime, 2) phase & amplitude characterization of high harmonics 3) harmonic generation from a "coherent" target and 4) study of more deeply bound atoms in the tunneling regime.

Generation of intense, few-cycle MIR pulses. In order to effectively study attosecond pulse formation it is necessary to increase the energy and reduce the pulse duration of the MIR fundamental field. A pulse energy increase to nearly a millijoule of MIR light will

be accomplished by adding a second titanium sapphire amplifier into the current *kilohertz* system. The reduction in the MIR pulse width is accomplished by a straightforward modification to the titanium sapphire oscillator and the chirp pulse amplification dispersion. A 40 fs titanium sapphire pulse would correspond to a 3-cycle MIR pulse. The combination of these two upgrades will increase the achievable MIR peak intensity in the 1 PW/cm^2 range. This will allow us to study the scaled physics for a broader range of atoms and molecules that satisfy the conditions for tunnel ionization.

Amplitude and phase characterization of high harmonic pulses. Our previous studies have demonstrated the utility of using a scaled interaction for generating and measuring high harmonic light. With the above mentioned laser modifications, we will be in a position for implementing advance temporal metrology for direct measurement of the amplitude and phase of the high harmonic light. In a few month visit to BNL, Ellen Kosik (U. Rochester graduate student) constructed and tested an achromatic SPIDER interferometer for this characterization. Upon completion of the laser upgrade and spectral characterization of the harmonic light generated with the few-cycle pulse we will attempt to coherently sum the harmonic comb into an attosecond pulse. Two strategies will be explored. The first approach will attempt to phase-lock as many harmonic orders as possible using the inherent atomic phase of the process. A second approach will use optical “tricks” to manipulate the phases after harmonic generation.

High harmonic generation from a coherent superposition of atomic states. The scaled alkali-mid-infrared interaction provides a prototype for studying the influence of prepared atomic states on the harmonic process. All harmonic experiments are performed on atoms initially in their ground state. However, the harmonic process is coherent and sensitive to the preparation of the initial state. Our studies have shown that by increasing the atomic polarizability through excited state excitation an enormous enhancement in the harmonic yield is possible. We will continue to study this physics by expanding the state selectivity in our experiments. An interesting physical scenario will be the preparation of a coherent atomic superposition state. The coherence of this process will not only influence the atomic response but also the macroscopic propagation. Issues such as whether a resonance can develop as the atomic transition becomes commensurate with the mid-infrared field and how does the harmonic phase change with the initial coherence, can all be addressed. If, by virtue of our studies, the atomic coherence develops into an important tool for harmonic production, it is conceivable to apply these schemes in inert gases.

High harmonic generation in the tunneling regime. By virtue of the energy and pulse duration upgrade to the MIR system it should be possible to study the ionization of atoms with more deeply bound electrons (10-15 eV), e.g. xenon. Since the ponderomotive energy scales as the square of the wavelength we will be able to study ionization and harmonic generation in an unprecedented regime of interaction energy. For example, at red wavelengths xenon experiences approximately 5 eV of quiver energy. At the same intensity of MIR light the quiver energy will be 25-times larger, that is more quiver energy than helium experiences at red wavelengths. One could expect to observe xenon

harmonic emission at wavelengths as short as 3 nm. Furthermore, all inert gas atoms interacting with MIR radiation will satisfy the tunneling limit, thus providing detailed scaling test of semi-classical models.

The ultimate objective of this research is the coherent construction of an attosecond pulse. However, it is clear that the roadmap will be established by the comprehensive investigations outlined above. The construction will be determined by the ability to monitor and control the harmonic field. Once this is accomplished, standard optical techniques for compensating amplitude and phase can be applied. We will be aided by a full complement of optical "tricks" available in this spectral region. Once we are in a better position for evaluating the attosecond construction, we can apply this knowledge at shorter wavelengths utilizing a standard inert gas harmonic source.

REFERENCES

[1] E. Constant et al., *Phys. Rev. Lett*. **82**, 1668 (1999).
[2] H. Chang et al., IEEE J. Sel. Top. QEX, **4**, 266 (1998).
[3] P. M. Paul et al., *Science* **292**, 1689 (2001).
[4] M. Hentschel et al., *Nature* **414**, 509 (2001).
[5] L. V. Keldysh, *Zh. Eksp. Teor. Fiz.* **47**, 1945 (1964) [*Sov. Phys. JETP* **20**, 1307 (1965)].
[6] B. Sheehy et al., *Phys. Rev. Lett*. **83**, 5270 (1999); M. B. Gaarde et al., *Phys. Rev. Lett.* **84**, 2822 (2000).
[7] T. O. Clatterbuck et al., *J. Mod. Optics* **50**, 441 (2003).

PUBLICATIONS RESULTING FROM THIS RESEARCH

1. "Atomic Dynamics at Long Wavelengths", B. Sheehy, J. D. D. Martin, T. Clatterbuck, Dalwoo Kim, L. F. DiMauro, K. J. Schafer, M. B. Gaarde and K. C. Kulander, in *Advances in Multiphoton Processes and Spectroscopy, Volume 14. Quantum Control of Molecular Reaction Dynamics*, eds. R. J. Gordon and A. Fujimura (World Scientific Press, Singapore), 203 (2001).
2. "Strong Field Physics in a Scaled Interaction", B. Sheehy, T. O. Clatterbuck, C. Lyngå , J. D. D. Martin, Dalwoo Kim, L. F. DiMauro, K. J. Schafer, M. B. Gaarde, P. Agostini and K. C. Kulander, *Laser Physics* **11**, 226 (2001).
3. "Absorptionless Self-Phase Modulation in a Dark-State Electromagnetically Induced Transparency System", V. Wong, R. W. Boyd, C. R. Stroud, Jr., R. S. Bennink, D. L. Aronstein, and Q.H. Park, *Phys. Rev. A* **65**, 013810, (2001).
4. "Atomic Photography", L. F. DiMauro, Nature **419**, 789 (2002).
5. "Scaled Intense Laser-Atom Physics: The Long Wavelength Regime" T. O. Clatterbuck, C. Lyngå, P. Colosimo, J. D. D. Martin, B. Sheehy, L. F. DiMauro, P. Agostini and K. C. Kulander, *J. Mod. Optics* **50**, 441 (2003).
6. "Thirteen pump-probe resonances of the sodium D1 line" Vincent Wong, R. W. Boyd, C.R. Stroud Jr., R. S. Bennink, and A. Marino, *Phys. Rev. A* 68, 012502 (2003).
7. "Characterization of attosecond electromagnetic pulses" by E. Kosik, E. Cormier, C. Dorrer, I. A. Walmsley and L. DiMauro, in *Proceedings of the IV Ultrafast Optics Conference*, eds. I. A. Walmsley and P. B. Corkum (Springer, Heidelberg, 2003).

Structure and Dynamics of Atoms, Ions, Molecules, and Surfaces:
Atomic Physics with High Velocity, Highly Charged Ion Beams

P. Richard, J. R. Macdonald Laboratory [JRML], Kansas State University
Manhattan, KS 66506 [richard@phys.ksu.edu]

The goals of this part of the JRML program are to investigate 1) strongly correlated three-electron, triply-excited [2l2l'2l"] states of ions, and the formation of two-electron, doubly-excited [nln'l'; n,n' > 2] states, 2) inelastic and super elastic electron scattering from highly charged ions and 3) ionization of atomic hydrogen and transfer ionization in fast highly charged ion collisions as well as electron capture in slow ion-atom collisions.

1. Triply excited states in Li-like ions formed in fast ion-atom collisions

The study of triply excited states of atoms and ions presents new opportunities to probe multi-particle excitations of a quantum system. Interelectronic correlation plays a crucial role in determining the properties of three-electron, triply excited states, and thus the description of their atomic structure as well as excitation and decay dynamics provide unique challenges to theory. The advances in synchrotron radiation technology in the last decade have stimulated considerable experimental and theoretical interest in the subject. In particular, the recent investigations using high-resolution photoelectron spectroscopy have provided some of the most detailed information on the partial photoionization cross sections for a number of triply excited states. Until now, however, studies of triply excited states have focused almost exclusively on neutral lithium, mostly due to the insufficient densities of ionic targets, which ruled out the possibility to investigate triply excited resonances in Li-like ions. Furthermore, the selective nature of the photoexcitation technique prohibited the population of quartet states, recently considered an ideal probe for photodetachment studies. The absence of available experimental data for three electron ions has prevented theorists from pursuing a global understanding of triply excited states, such as new classification schemes, approximate quantum numbers, and possible approximate selection rules for the formation and the decay of these states.

We have introduced two novel experimental techniques that provide efficient ways to populate triply excited states in Li-like ions as well as to study their decay dynamics. In the first approach, the $2s2p^2\ ^2D^e$ state is selectively populated by 180^o *quasi-free* resonant electron scattering (RES) from the 1s2s ^3S metastable state of He-like ions. In the second approach, all $2l2l'2l''$ intrashell states can be formed via triple electron capture to bare ions.

Study of the Z-dependent autoionization rates for the $2s2p^2\ ^2D^o$ triply excited states ---

E. P. Benis, M. Zamkov, T. J. M. Zouros, T. Gorczyca, K. R. Karim, and P. Richard

In our first method of studying triply excited states, the formation of the $2s2p^2\ ^2D^e$ state was experimentally observed in high resolution Auger spectra obtained in collisions of B^{3+} beams with H_2 targets [pub. #1]. The B^{3+} ions were prepared in mixed ($1s^2\ ^1S$, 1s2s ^3S) ground and metastable states, respectively. The $2s2p^2\ ^2D^e$ state is formed via resonant electron scattering (RES), where the loosely bound target electron interacts with the 1s projectile electron resulting in the transfer of the target electron to an excited projectile state with the simultaneous excitation of the projectile's 1s electron. Thus the ion is promoted to excited states with an empty K- shell, from which it relaxes primarily via Auger decay.

The success of the first study motivated us to proceed to the next step, i.e., to extend the investigation to ions with higher atomic numbers. The first measurement of the production and

subsequent Auger decay of Li-like triply excited states as a function of an atomic number Z=5-9 was performed. The R-matrix calculations were utilized within the electron scattering model (ESM) in which the quasi-free H_2 electrons scatter from the ion as a free particle with a momentum distribution given by their Compton profile. Auger rates for the elastic decay scattering channel also were extracted from the experimental data and compared to a number of theoretical calculations. These studies are in the publication process.

Formation of all Li-like triply excited states by triple electron capture ---
M. Zamkov, E. P. Benis, C. D. Lin, T. Morishita, T. J. M. Zouros, T. G. Lee and P. Richard

The second experimental technique relies on a strong projectile-Coulomb interaction to populate *all* triply excited states in Li-like ions. The states are produced by triple electron capture in energetic ion-atom collisions and observed by the subsequent Auger decay to the continuum states of He-like ions. The method has been demonstrated by studying triply excited $2s2p^2\ ^2S^e$, $^{2,4}P^e$, $^2D^e$, and $2p^3\ ^2P^o$, $^2D^o$ states of fluorine formed in fast collisions of bare F^{9+} ions with Ar atoms both experimentally using zero-degree Auger projectile electron spectroscopy, and theoretically using the hyperspherical close coupling method (HSCC) [pub. #2].

The Auger decay branching ratios have been extracted from the electron spectra and compared to the limited calculations available in the literature. Differential cross sections for triple electron capture are calculated in the independent electron approximation and are shown to be in good overall agreement with the experimental data. Finally, the energies for the observed triply excited states were calculated using the HSCC method and compared to both the present experimental data and other available calculations.

Formation of doubly excited states by triple electron capture ---
M. Zamkov, E. P. Benis, T. J. M. Zouros, T. G. Lee, and P. Richard

In this work, high resolution zero-degree Auger electron projectile spectroscopy was used to study true triple electron capture to doubly excited KLL states of carbon. The states are produced in fast collisions (v = 4.5-6.6 a.u.) of bare C^{6+} projectiles with Ar gas targets [pub. #3]. High resolution measurements of differential cross sections for individual KLL states provided a unique tool for testing the predictions of the independent particle model for the triple electron capture. Single electron capture probabilities, employed by the model, were calculated using the two-center semiclassical close-coupling method, based on an atomic orbital expansion. In order to allow comparison of the measured zero-degree differential cross sections with calculated total cross sections, the Auger electron emission from the doubly excited KLL states was assumed isotropic.

Production mechanism and fraction of metastable $1s2s\ ^3S$ He-like ions formed in fast cascading ion-atom collisions ---
M. Zamkov, E. P. Benis, H. Aliabadi, H. Tawara, T. Gray, T. J. M. Zouros, and P. Richard

The mechanism for the formation of $1s2s\ ^3S$ metastable beams in high velocity beams is developed in this work. Experimental measurements of various collision cross sections for He-like beams require quantitative information on the non-negligible fraction of ions in a long-lived $1s2s\ ^3S$ metastable state. The knowledge of the metastable $1s2s\ ^3S$ fraction is crucial for the absolute cross section measurements of numerous processes in He-like ions including dielectronic recombination, impact excitation, transfer excitation, capture of the target electron,

inelastic scattering or recently discovered superelastic scattering of target electrons from highly charged metastable ions.

In this work, a universal technique for the determination of the metastable 1s2s ^{3}S ion fraction, which is based on measurements of Auger electron emission from doubly excited states of Li-like ions formed in collisions of investigated beams with light targets, is outlined. The method was used to measure the fraction of metastable 1s2s ^{3}S ions in fast He-like B, C, N, O, and F beams produced in collisions with thin carbon foils as a function of both the incident energy, in the range of 0.5 to 2 MeV/u, and the foil thickness, in the range of 1-5 µg/cm^2 [pubs. #5-7]. The metastable content in C^{4+} ions produced in carbon foils was found to be significantly lower than that of other investigated beams. The observed deviation has been explained as due to K-vacancy sharing, which is known to have the highest probability for symmetric collisions.

A different experimental technique also has been developed to allow for a more accurate determination of the metastable fraction [pub. #8]. Similar to the first method, it utilizes measurements of the Auger electron yield from the doubly excited states of Li-like ions, ^{4}P and ^{2}D. However, in the new approach, the metastable beam fraction is determined by relating the Auger yields obtained in two successive measurements taken at the same beam energy but with beams having different metastable fractions.

2. Inelastic and superelastic electron scattering deduced from ion-atom collisions

In previous grant periods, we have presented absolute double differential cross sections, DDCS, for the inelastic electron scattering in $e^- + O^{7+}$ and $e^- + F^{8+}$ collision systems. The 3*l*3*l*' resonances were observed for 0^o and 180^o scattering in the c.m. frame. R-matrix calculations gave an overall good agreement with most of the observed resonances. We attempted to study the 3*l*3*l*' resonances in e^- -Mg^{11+}, -Al^{12+}, and -Si^{12+} collisions, which are of interest in fusion modeling. We were able to measure the electron elastic scattering DDCS, but had insufficient count rates from the LINAC beams to be able to successfully observe the electron inelastic scattering channels. As a recourse, we did measure the resonances in e^- -B^{4+} collisions. The energy resolution required to separate the resonances in this system is difficult to reach. To obtain higher resolution data, attempts were made to measure inelastic electron scattering spectra with an off-center hemispherical spectrometer, which has a zoom lens and a position sensitive detector. These efforts failed due to the large background of electrons coming from cusp electrons hitting the plates of the analyzer and scattering onto the position sensitive detector.

We have also reported for the first time the measurement of electrons scattered superelastically from highly charged ions having an initial K-shell vacancy. In this process, the scattered electron gains ~725 eV of energy from the deexcitation of an excited He-like F^{7+}(1s2s ^{3}S) metastable ion to its ground state. A theoretical calculation based on an R-matrix approach agrees well in position, shape, and magnitude with the experimental results [pub. #4].

3. Ionization of atomic hydrogen, molecular hydrogen, and helium and transfer ionization with highly charged ions at high velocity; and electron capture with highly charged ions at low energy collisions

These three projects are either completed or nearly completed. Due to lack of space, write-ups are not provided, but a list of the published results sorted by the projects is given: High velocity ionization [pubs. #9-10]; high velocity transfer ionization [pub. #11]; and low energy electron capture [pubs. #12-13].

Publications on resonance excitation and triple electron capture:

1) "Absolute Cross Sections and Decay Rates for the Triply Excited $B^{2+}(2s2p^2\ ^2D)$ Resonance in Electron-Metastable-Ion Collisions," M. Zamkov, H. Aliabadi, E. P. Benis, P. Richard, H. Tawara, and T.J.M. Zouros, Phys. Rev. A **65**, 032705-1 (2002).
2) "Experimental Observation and Theoretical Calculations of Triply Excited $2s2p^2\ ^2S^e$, $^{2,4}P^e$, $^2D^e$ and $2p^3\ ^2P^o$, $^2D^o$ States of Fluorine," M. Zamkov, E. P. Benis, C. D. Lin, T. G. Lee, T. Morishita, P. Richard, and T.J.M. Zouros, Phys. Rev. A **67**, 050703-1 (2003).
3) "Triple Electron Capture in Fast 0.5-1.1 MeV/u C^{6+} on Ar Collisions," M. Zamkov, E. P. Benis, P. Richard, T. G. Lee, and T.J.M. Zouros, Phys. Rev. A **66**, 042714 (2002).
4) "Superelastic Scattering of Electrons from Highly Charged Ions with Inner Shell Vacancies," P. A. Zavodszky, H. Aliabadi, C. P. Bhalla, P. Richard, G. Toth, and J. A. Tanis, Phys. Rev. Letters **87**, 033202 (2001).

Publications on metastable ion production

5) "Stripping Energy Dependence of a $B^{3+}(1s^2\ ^1S, 1s2s\ ^3S)$ Beam Metastable Fraction," M. Zamkov, H. Aliabadi, E. P. Benis, P. Richard, H. Tawara, and T.J.M. Zouros Application of Accelerators in Research and Industry – XVIth Int'l Conf., ed. by J. L. Duggan and I. L. Morgan (American Institute of Physics, 2001) p. 149.
6) "Energy Dependence of the Metastable Fraction in $B^{3+}(1s^2\ ^1S,1s2s\ ^3S)$ Beams Produced in Collisions with Thin-Foil and Gas Targets," M. Zamkov, H. Aliabadi, E. P. Benis, P. Richard, H. Tawara, and T.J.M. Zouros, Phys. Rev. A **64**, 052702-1 (2001).
7) "Fraction of Metastable $1s2s\ ^3S$ Ions in Fast He-like Beams (Z=5-9) Produced in Collisions with Carbon Foils," M. Zamkov, E. P. Benis, P. Richard, and T.J.M. Zouros, Phys. Rev. A **65**, 062706-1 (2002)
8) "Technique for the Determination of the $1s2s\ ^3S$ Metastable Fraction in the Two-Electron Ion Beams," E. P. Benis, M. Zamkov, P. Richard, and T.J.M. Zouros, Phys. Rev. A **64**, 042712-1 (2002).

Publications on ionization, transfer ionization and single electron capture

9) "Two-Center Effect on Low-Energy Electron Emission in Collisions of 1-MeV/u Bare Ions with Atomic Hydrogen, Molecular Hydrogen, and Helium: I. Atomic Hydrogen," Lokesh C. Tribedi, P. Richard, L. Gulyás, M. E. Rudd, and R. Moshammer, Phys. Rev. A **63**, 062723-1 (2001).
10) "Two-Center Effect on Low-Energy Electron Emission in Collisions of 1-MeV/u Bare Ions with Atomic Hydrogen, Molecular Hydrogen, and Helium: II. H_2 and He," Lokesh C. Tribedi, P. Richard, L. Gulyás, and M. E. Rudd, Phys. Rev. A **63**, 062724-1 (2001)
11) "Transfer Ionization to Single Capture Ratio for Fast Multiply Charged Ions on He," R. Ünal, P. Richard, H. Aliabadi, H. Tawara, C. L. Cocke, I. Ben-Itzhak, M. J. Singh, and A. T. Hasan, Application of Accelerators in Research and Industry – XVIth Int'l Conf., ed. by J. L. Duggan and I. L. Morgan (American Institute of Physics, 2001) p. 36.
12) "L X Rays from Low-Energy (~2-keV/u) Ions with L-Shell Vacancies Produced in Single Collisions with Atoms and Molecules," H. Tawara, P. Richard, U. I. Safronova, A. A. Vasilyev, S. Hansen, and A. S. Shiyaptseva, Phys. Rev. A **65**, 042509-1 (2002).
13) "Observation and Analysis (Synthesis) of X-Ray Spectrum Originated from Electron Capture of Low-Energy, Highly Charged Xe^{q+} (q=26-43) Ions in Single Collisions with Ar Atoms," A. A. Vasilyev, H. Tawara, P. Richard, and U. I. Safronova, Can. J. Phys. **80**, 65 (2002).

Structure and Dynamics of Atoms, Ions, Molecules and Surfaces: Atomic Physics with Ion Beams, Lasers and Synchrotron Radiation

C.L.Cocke, Physics Department, J.R. Macdonald Laboratory, Kansas State University, Manhattan, KS 66506, cocke@phys.ksu.edu

The goals of this aspect of the JRML program are to explore mechanisms of ionization of atoms, ions and small molecules by intense laser pulses, to identify and explain basic mechanisms whereby electrons are removed from simple systems in capture and ionization processes and to investigate the dynamics of photoelectron emission from small molecules interacting with synchrotron radiation.

Recent progress and future plans:

1) Photoelectron diffraction from C_2H_2, C_2H_4 and other small molecules, *T. Osipov, C.L. Cocke (KSU), A. Landers (Western Mich. Univ.), R. Doerner, Th. Weber, L. Schmidt, A. Staudte, H. Schmidt-Boecking (U. Frankfurt), M.H. Prior (LBL).* Using beamlines 4.0 and 9.3.2 at the Advanced Light Source, we have measured the correlated momentum-space distributions of photoelectrons and charged photofragments ejected when the K-shells of acetylene and ethylene are photoionized. During the past year our work has centered on the analysis of diffraction patterns from these molecules. Our attempt to identify, in acetylene, an f-wave shape resonance, well known in N_2 and CO but controversial for C_2H_n, was initially frustrated by the interesting observation that the dication of this molecule often undergoes isomerization to the vinylidene configuration before it dissociates. Separating these two channels shows that the photoelectron distributions in the acetylene channel show a strong f-wave character near the "resonance" region, but the vinylidene channel does not. The photoelectron distribution was used as a clock to measure the time the isomerization process takes. By analyzing the degree to which the photoelectron angular distribution was "washed out" (Fig. 1) in the latter channel we were able to deduce that the time scale for isomerization is no longer than approximately 60 fs. A Phys. Rev. Lett. on this work has been published [3].

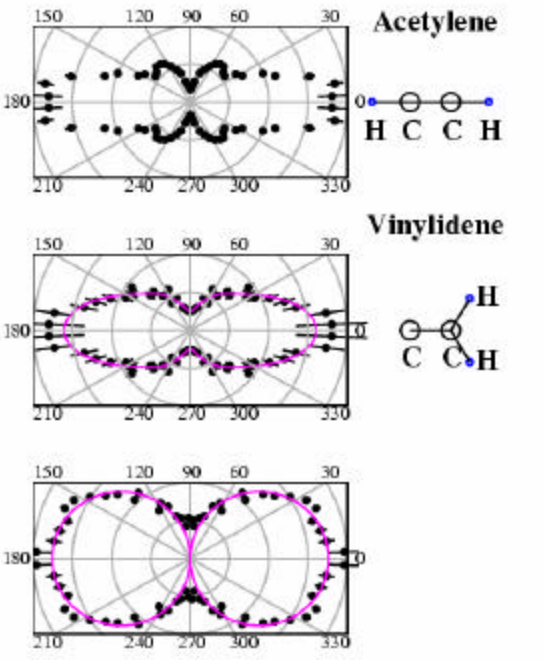

Figure 1. Body-fixed photoelectron angular distributions for acetylene photoionized at 310 eV and decaying through though the (a) acetylene (b) vinylidene channels.

For the case of C_2H_4, no such complication occurs, and full photoelectron angular distributions for fixed-in-space molecules have been taken as a function of photoelectron energy spanning the range of the expected shape resonance. The data are extremely high quality and comprehensive. The angular distributions show definite enhancement

of the f-wave partial wave in the "resonance" region for the sigma alignment, but strong enhancement in the p-wave channel as well. In spite of the high quality of the data, no unique extraction of the dipole matrix elements and phases from the data is possible, due to the symmetric nature of the collision system. Contact with two theoretical groups has been initiated to calculate the photoelectron angular distribution *ab initio*. This work is being written up in the Ph.D. thesis of Timur Osipov and a Physical Review article is in preparation. Future work by this collaboration includes completion of the hydrocarbon analysis and detailed examination of the ionization of "fixed-in-space" molecular hydrogen near the series limit for double ionization. Examination of angular distributions of Auger electrons from such collision studies are also underway.

2) Identification of a rescattering mechanism in the double ionization of D_2 and H_2 by intense laser pulses, *T. Osipov, E.P. Benis, A. Wech, C. Wyant, B. Shan, Z. Chang and C.L. Cocke.* It is now well established that so-called "non-sequential" ionization of neutral atoms by femtosecond laser pulses with intensities in the range 10^{13}-10^{15} watts/cm^2 can occur through a rescattering mechanism whereby the electron liberated in the single ionization process returns to the ion with sufficient energy to further ionize the singly charged ion. Using the newly installed fs light source in the JRM laboratory and COLTRIMS techniques, we have found, using linearly and circularly polarized light, that a high energy d^+ group in the double ionization of D_2 by 36 fs pulses in the 1-5 x 10^{13} -10^{15} watts/cm^2 range is caused by a rescattering process. The energy distribution of the resulting deuterons is consistent with the picture that the vibrational wave packet created in the single ionization of the D_2 molecule, trapped in the gerade potential well of the D_2^+ ion, is further ionized by the returning electron. Figure 2 shows the KER for the rescattering process for deuterium and hydrogen targets. The structure is interpreted as due to the excitation on the first, third, fifth (etc.) return times of the electron. It is different for D_2 and H_2 because the evolution of nuclear wave packet in the $1s\sigma$ potential curve is different for the two cases, being slower for D_2. The rescattering process is believed to be a rescattering excitation of the $1s\sigma$ electronic state of D_2^+ to either the $2p\sigma$ or $2p\pi$ state, followed by ionization to the continuum by the laser field. A theoretical model based on this interpretation has been developed by Tong and Lin and the results of this model are also shown in the figure. This work has been submitted to Phys. Rev. Lett.. Future plans for this program include measurements with full kinematic control over reaction products using COLTRIMS techniques on neutral targets, investigation of ultra-fast-rise-time pulses and the role of sequential ionization processes and ionization of fast beams from our accelerator facilities.

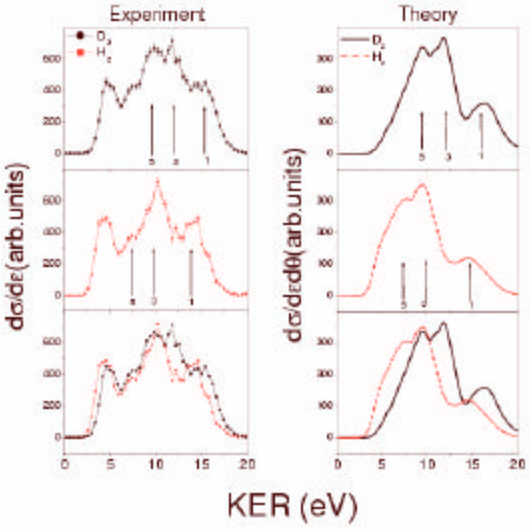

Figure 2. KER distributions of deuterons(protons) from double ionization of D_2 (H_2) by fast laser pulses.

3) COLTRIMS measurements of electron spectra from low energy ionization of atomic H and He targets, *E. Edgu-Fry and C. L. Cocke.* The goal of this project was to identify and characterize the process whereby a slow charged projectile promotes into the continuum an electron from a neutral target. The projectile velocity is sufficiently low that direct kinematic ionization is forbidden, and saddle-point electron promotion, in some form, is expected to the major process. Theoretical analyses of this process and previous data indicated that the major mechanism should be the rotational coupling of the $2p\sigma$ and $2p\pi$ orbitals, followed by a saddle-like promotion of the π orbital into the continuum. Structure of the electron momentum distributions indicating this structure had been measured by several groups, including ours. However, quantitative theoretical analysis of this had always been frustrated by the fact that the calculations could only be done for a true one-electron system, whereas the experiments were always carried out for multielectron targets. Therefore we invested the effort to develop a COLTRIMS-compatible target of atomic hydrogen to study this problem.

The experiment has finally been to some extent successful, following the development of a microwave discharge source geometrically cooled to provide partially adequate atomic hydrogen recoil resolution. The ionization experiment was carried out for p on atomic hydrogen at v= 0.77, 1.0 and 1.4 a.u. Unfortunately, because of limited momentum resolution along the jet, it was not possible to obtain full impact-parameter information, and this limits the detail of the momentum-space images. In particular, only a washed-out π structure was observed, since it was not possible to clearly distinguish transverse direction of the recoil ion. Thus the comparison between experiment and theory remains somewhat compromised, although for a different reason than had previously been the case. Dr. Edgu-Fry has written this up as part of her Ph.D. thesis, a paper is in preparation, and additional experimental work is continuing still.

The presence on the EBIS of a working COLTRIMS atomic hydrogen target led us to carry out measurements of electron capture on this target as well. Previous COLTRIMS studies of this process have been carried out by us and others but never with a true one-electron target. Theoretical treatments of this process have become quite mature, but, as in the case of ionization discussed above, the comparison between theory and experiment was regularly compromised by the need to model a multielectron target with a core-plus-one-electron model. We therefore took advantage of our atomic H target to measure Q value distributions for Ar^{8+} on atomic hydrogen with a true one-electron target. The choice of Ar^{8+} was made because it is a closed-shell projectile which, at the large impact parameters for which capture occurs, appears nearly point-like to the target, yet it has sufficiently large quantum defects for the penetrating orbits for n=5 and 6 (where the capture occurs) to allow us to resolve the ℓ values for capture. Cross sections were measured for v=0.3, 0.5 and 0.7 a.u. A sample spectrum is shown in Fig. 3. Since the coupled channel approach of Lin et al. to the analysis of such collisions has in the past appeared to be of high precision, it was expected that these spectra, for a true atomic hydrogen target, would be exactly described by the calculations. To our surprise, the theory appears to predict much too weak population of n=6. The reason for this discrepancy remains unidentified. These data are described in the Ph.D. thesis of Erge Edgu-Fry, and are being prepared for publication. Future plans are to exploit this source for further capture experiments and to try to extend the ionization work to lower velocities for which the recoil momentum resolution will be adequate.

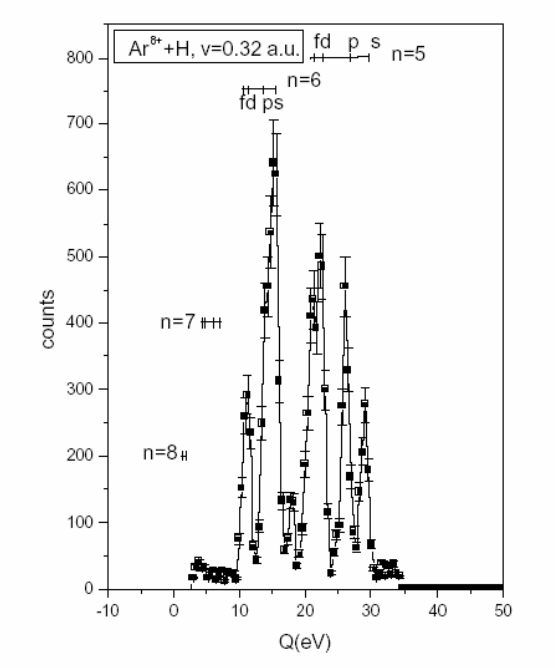

Figure 3. Q value spectra for capture from atomic hydrogen by Ar^{8+} ions from COLTRIMS measurements.

Publications 2002-2003 not previously cited:

1. Double-to-Single Target Ionization Ratio for Electron Capture in Fast ρ-He Collisions, H.T. Schmidt, A. Fardi, R. Schuch, S.H. Schwartz, H. Zettergren, and H. Cederquist, L. Bagge, H. Danared, A. Källberg, J. Jensen, and K.-G. Rensfelt, V. Mergel, L. Schmidt, and H. Schmidt-Böcking, C.L. Cocke, Phys. Rev. Lett. **89**, 163201-3 (2002).
2. Alignment Measurements in Collisions of D_2^+ with Doubly Charged Projectiles, I. Reiser and C.L. Cocke, Nucl. Inst. Meth. B **205**, 614 (2003).
3. Photoelectron-Photoion Momentum Spectroscopy as a Clock for Chemical Rearrangements: Isomerization of the Dication of Acetylene to the Vinylidene Configuration, T. Osipov, C.L. Cocke, M.H. Prior, T. Weber, O. Jagutzki, L. Schmidt, H. Schmidt-Böcking, R. Dörner and A. Landers, Phys. Rev. Lett. **90**, 233002 (2003).
4. Auger Electron Emission from Fixed-in-Space CO, Th. Weber, M. Weckenbrock, M. Balser, O. Jagutzki, W. Arnold, O. Hohn, M. Schöffler, E. Arenholz, T. Young, T. Osipov, L. Foucari, A. De Faria, R. Diez-Munos, H. Schmidt-Böcking, C.L. Cocke, M. H. Prior and R. Dörner, Phys. Rev. Lett. **90**, 153003 (2003).
5. Alignment Effects in Electron Capture from D_2^+ Molecular Ions by Ar^{2+}, N^{2+}, and He^{2+}, I. Reiser, C.L. Cocke and H. Bräuning, Phys. Rev. A **67**, 062719 (2003).

Structure and Dynamics of Atoms, Ions, Molecules, and Surfaces:
Molecular Dynamics with Ion and Laser Beams

Itzik Ben-Itzhak, J. R. Macdonald Laboratory, Kansas State University
Manhattan, Ks 66506; ibi@phys.ksu.edu

The goals of this part of the JRML program are to study the different mechanisms leading to molecular dissociation and charge exchange following fast collisions, slow collisions, or interactions with an intense short-pulse laser.

Photo ionization and photo dissociation of H_2^+ by an intense short pulse laser, *J. Xia, A.M. Sayler, M.A. Smith, K.D. Carnes, and I. Ben-Itzhak* – partly in collaboration with *Z. Chang's* group, *C. Fehrenbach*, and *C.L. Cocke.*

Interrogating molecules with intense short-pulse lasers has resulted in a multitude of interesting new phenomena because the strength of the interactions of the electrons with the nuclei and the laser field are comparable. Among these phenomena are: tunneling ionization, above threshold dissociation (ATD), bond softening and bond hardening, charge resonance enhanced ionization (CREI), molecular alignment, and many more (see for example the review by Giusti-Suzor *et al*. [1]). The simplest molecular ion, H_2^+, is commonly studied by theorists, while experimentalists, for obvious reasons, prefer to study the naturally abundant H_2 molecule. In some of the experimental studies of H_2 the experimental conditions have been tailored to enable the study of the behavior of the transient H_2^+ formed early in the laser pulse [2,3]. However, some of the predictions about the H_2^+ behavior are better tested using the molecular ion itself, and similar arguments hold for many-electron molecular ions. Only a handful of experimental studies of molecular ions have been conducted so far [4-7].

We have recently begun measurements of ionization and dissociation of keV H_2^+ beams crossed by an intense short-pulse laser beam using 3D molecular-dissociation imaging. The triple coincidence (laser-pulse, ion, ion/atom) and the initial motion of the fragments separate them from ions produced by ionizing the much denser residual gas. These measurements provide detailed information about each reaction, e.g.: (1) the kinetic energy release upon dissociation, from which we expect to learn about the vibrational states involved as well as the net number of photons absorbed; (2) the alignment and orientation (?,f) of the molecular ion relative to the polarization vector; to this end we use linearly polarized light. In addition, we separate the dissociation and ionization channels using a longitudinal electric field in the interaction region.

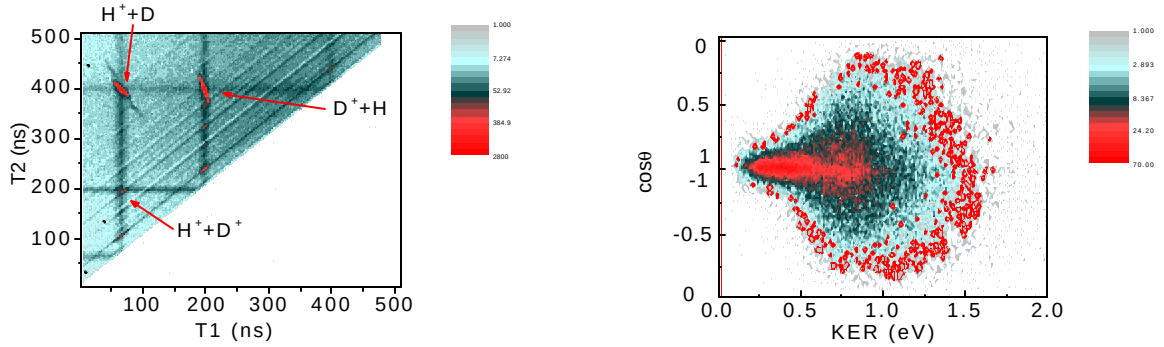

Figure 1. *Left*: Time correlation plot for HD^+ exposed to a 45fs, 3.9×10^{14} W/cm^2 laser pulses. *Right*: A density plot of the angular dependence of HD^+ dissociation for different KER values.

It can be seen from Fig. 1(*Left*) that the ionization of HD^+ is much smaller than its laser induced dissociation. Further data analysis is needed in order to compare quantitatively the measured ionization to dissociation ratio to previous measurements of Williams *et al*. [4] and to theoretical predictions of Kulander *et al*. [8], for example. In Fig. 1(*Right*) we show preliminary results for the angular distributions for different values of KER, i.e. different vibrational states. Our results are in qualitative agreement with 2D-imaging measurements of Sändig *et al*. [5] who used longer pulses (of about 130-600 fs). It can be clearly seen that the lower vibrational states associated with lower KER values are aligned much more than the higher vibrational states, which exhibit approximately a $\cos^2(?)$ distribution. One would expect the vibrational states that dissociate immediately when the energy gap between the dressed states opens to be less aligned, since they start dissociating way before the laser pulse reaches its peak intensity. In contrast the lower states are exposed to higher intensity before they dissociate and thus should be more aligned. Though the qualitative picture seems right, there is still much to do before we can predict quantitatively what would be the outcome of such interactions.

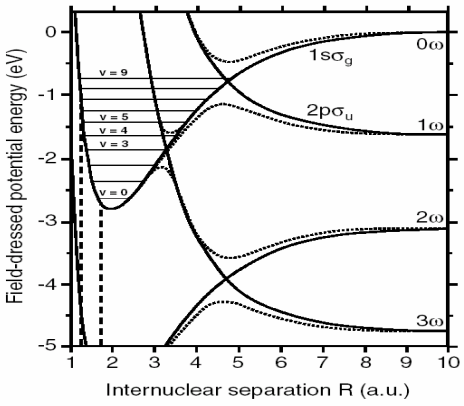

Figure 2. A schematic view of the dressed states of H_2^+, from Ref. [4]. Note that vibrational states around v=9 will dissociate immediately as the energy gap opens, i.e. at lower laser intensities.

Future plans: We plan to measure the dependence of ionization and dissociation of H_2^+, and other simple molecular ions, on the duration of the intense laser pulse. It has been predicted that the ratio of ionization to dissociation will change with increasing number of laser cycles, i.e. pulse width [8].

1. A. Giusti-Suzor, F.H. Mies, L.F. DiMauro, E. Charron, and B. Yang, J. Phys. B **28**, 309 (1995).
2. G.N. Gibson, M. Li, C. Guo, and J. Neira, Phys. Rev. Lett. **79**, 2022 (1997).
3. J.H. Posthumus, J. Plumridge, L.J. Frasinski, K. Codling, E.J. Divall, A.J. Langley, and P.F. Taday, J. Phys. B **33**, L563 (2000).
4. I.D. Williams, P. McKenna, B. Srigengan, I.M.G. Johnston, W.A. Bryan, J.H. Sanderson, A. El-Zein,, T.R.J. Goodworth, W.R. Newell, P.F. Taday, and A.J. Langley, J. Phys. B **33**, 2743 (2000).
5. K. Sändig H. Figger, and T.W. Hänsch, Phys. Rev. Lett. **85**, 4876 (2000).
6. C. Wunderlich, H. Figger, and T.W. Hänsch, Phys. Rev. A **62**, 023401-1 (2000).
7. A. Assion, T. Baumert, U. Weichmann, and G. Gerber, Phys. Rev. Lett. **86**, 5695 (2001).
8. K.C. Kulander, F.H. Mies, and K.J. Schafer, Phys. Rev. A **53**, 2562 (1996).

Molecular dissociation imaging of collision induced dissociation and dissociative capture in slow H_2^+ + Ar (He) collisions, *D. Hathiramani, J.W. Maseberg, A.M. Sayler, M.A. Smith K.D. Carnes and I. Ben-Itzhak*

The dissociation of hydrogen molecular ions following a slow collision (keV) is studied by 3D momentum imaging of the fragments. The two main processes at this collision energy, collision-

induced dissociation (CID, e.g. $H_2^+ + Ar \rightarrow H^+ + H + Ar$) and dissociative capture (DC, e.g. $H_2^+ + Ar \rightarrow H + H + Ar^+$), are experimentally separated in the method we have recently developed. Using a longitudinal electric field in the target region followed by a field free region, we managed to separate the CID from the DC in time. Thus, it is possible to evaluate the relative importance of these two processes, because both CID and DC are measured simultaneously. The same is true for the ratio of the two possible CID channels for heteronuclear molecules, i.e. $A^+ + B$ or $A + B^+$. Moreover, this method allows one to distinguish experimentally between two different mechanisms of CID, namely, (i) CID caused by an electronic excitation to a repulsive state, and (ii) CID caused by a vibrational/rotational excitation. These mechanisms differ in the kinetic energy release upon dissociation (KER) and the momentum transfer to the projectile. For the first the KER is relatively large while the momentum transfer to the projectile is very small. In contrast the latter is associated with small KER and very large momentum transfer. This distinguishes the present work from previous studies [1], in which no such separation was possible.

The electronic excitation to a repulsive state (mostly the first excited state of H_2^+) is the dominant CID mechanism for 3 keV H_2^+ + Ar collisions. The angular dependence of this CID mechanism depends on the "bond length". Explicitly, the dissociating fragments align along the beam direction for "short" molecular ions and perpendicular to the beam for "long" ones, as predicted by Green and Peek [2]. The vibrational/rotational dissociation mechanism shows very strong alignment effects. First, molecular ions aligned perpendicular to the beam velocity (i.e. $\theta = 90°$) are much more likely to dissociate by this mechanism. Second, the dissociation velocity is preferentially aligned along the momentum transfer. The first distribution is much narrower than the latter.

More recently we have conducted studies of CID of HD^+ in similar collisions in search of the isotopic effects observed previously for this molecular ion [see, for example, Refs. 3,4], namely, that *the dissociation into $H + D^+$ was favored over $H^+ + D$.* Preliminary results indicate that such effects, if they exist, are much smaller than those reported in previous work. These results were presented as invited talks in the CAARI 2002 and DAMOP 2003 meetings.

Future plans: Systematic studies of DC and CID caused by either electronic or vibrational excitation will be conducted focusing on the effect of the target species and the collision energy. Our preliminary results indicate significant differences in vibrational CID between Ar and He targets. Furthermore, we plan to investigate both these processes for a few additional simple molecular ions, such as HeH^+, He_2^+ and H_3^+. While conducting these studies on the existing system, an improved setup, which includes a cold jet target, will be assembled and tested. This will enable the simultaneous measurement of the recoil ion momentum for DC reactions, thus providing kinematically complete information about the process.

1. J. Los and T.R. Govers, in *Collision Spectroscopy* (ed. R.G. Cooks, Plenum Press, NY 1978) p-289
2. T.A. Green and J.M. Peek, Phys. Rev. **183,** 166 (1969)
3. T.A. Lehman et al. Int. J. Mass Spectrom. Ion Proc. **69**, 85 (1986)
4. R.W. Rozett and W.S. Koski, J. Chem. Phys. **49**, 2691 (1968)

Isotopic effects and asymmetries in bond-rearrangement and bond-breaking processes in water ionized by fast proton impact. *A.M. Sayler, M. Leonard, J.W. Maseberg, D. Hathiramani, K.D. Carnes, B.D. Esry, and I. Ben-Itzhak*. Studies of ionization and fragmentation of water molecules by fast protons and highly charged ions have revealed an interesting isotopic

preference for H-H bond rearrangement. Specifically, the dissociation of $H_2O^+ \rightarrow H_2^+ + O$ is about twice as likely as $D_2O^+ \rightarrow D_2^+ + O$, with $HDO^+ \rightarrow HD^+ + O$ in between. Further investigations of this isotopic effect lead us to discover a similar isotopic effect following double ionization of water, i.e. in $H_2O^{2+} \rightarrow H_2^+ + O^+$, although these results are preliminary. Calculations are underway to determine the relative production rates for the different isotopes from the overlap of the initial and final vibrational wave functions and the time evolution of the final wave function.

Future plans: The isotopic enhancement in the $H_2O^{2+} \rightarrow H_2^+ + O^+$ dissociative double ionization channel requires further investigation to determine if it is similar in magnitude to that found in single ionization. Furthermore, we are also exploring the likelihood of this bond-rearrangement mechanism occurring in multiple ionization, i.e., does $H_2O^{3+} \rightarrow H_2^+ + O^{2+}$ truly occur as our preliminary data suggests.

Publications:

1. "Probing very slow H^+ + D(1*s*) collisions using the ground state dissociation of HD^+", E. Wells, K.D. Carnes, and I. Ben-Itzhak, Phys. Rev. **67**, 032708 (2003).
2. "Bond-Rearrangement in Water Ionized by Ion Impact", A.M. Sayler, J.W. Maseberg, D. Hathiramani, K.D. Carnes, and I. Ben-Itzhak, **Application of Accelerators in Research and Industry**, edited by J.L. Duggan and I.L. Morgan (AIP press, New York 2003), vol. 680.
3. "A comparative study of the ground state dissociation of H_2^+ and D_2^+ induced by ionizing and electron capture collisions with He^+ at velocities of 0.25 and 0.5 a.u.", W. Wolff, I. Ben-Itzhak, H.E. Wolf, C.L. Cocke, M.A. Abdallah, and M. Stöckli, , Phys. Rev. A **65**, 042710 (2002).
4. "A kinematically complete charge exchange experiment in the Cs^+ + Rb collision system using a MOT target", X. Flechard, H. Nguyen, E. Wells, I. Ben-Itzhak, and B.D. DePaola, Phys. Rev. Lett. **87**, 123203 (2001).
5. "Charge exchange and elastic scattering in very slow H^+ + D(1*s*) "half" collisions", E. Wells, I. Ben-Itzhak, K.D. Carnes, and B.D. Esry, Phys. Rev. Lett. **86**, 4803 (2001).
6. "Transfer Ionization to Single Capture Ratio for Fast Multiply Charged Ions on He", R. Ünal, P. Richard, H. Aliabadi, H. Tawara, C.L. Cocke, I. Ben-Itzhak, M.J. Singh, and A.T. Hasan, **Application of Accelerators in Research and Industry**, edited by J.L. Duggan and I.L. Morgan (AIP press, New York 2001), p. 36.
7. "Velocity Dependence of Electron Removal and Fragmentation of Water Molecules Caused by Fast Proton Impact", A.M. Sayler, E. Wells, K.D. Carnes, and I. Ben-Itzhak, **Application of Accelerators in Research and Industry**, edited by J.L. Duggan and I.L. Morgan (AIP press, New York 2001), p. 33.
8. "Double and single ionization of hydrogen molecules by fast proton impact", I. Ben-Itzhak, E. Wells, D. Studanski, Vidhya Krishnamurthi, K.D. Carnes, and H. Knudsen, J. Phys. B **34**, 1143 (2001).
9. "Measurements of the mean lifetime and kinetic energy release of metastable CO^{2+}," J.P. Bouhnik, I. Gertner, B. Rosner, Z. Amitay, O. Heber, D. Zajfman, E.Y. Sidky, and I. Ben-Itzhak, Phys. Rev. A **63**, 032509 (2001).

Femtosecond X-ray Detectors and High Field Atomic Physics

Z. Chang
J. R. Macdonald Laboratory, Department of Physics,
Kansas State University, Manhattan, KS 66506, chang@phys.ksu.edu

The goals of this aspect of the JRML program are (1) to develop a femtosecond x-ray detector for time-resolved x-ray spectroscopy at the 3rd and 4th generation x-ray sources facilities, (2) to study femtosecond and attosecond x-ray sources based on high order harmonic generation, and (3) to study the ionization of atoms and molecules by a strong laser field.

1. A sub-600 femtosecond x-ray streak camera with <100 fs timing jitter, *Mahendra Shakya, Bing Shan, Chun Wang, Jinyuan Liu (ANL), Jin Wang (ANL) and Zenghu Chang*

The application of a picosecond streak camera developed by the PI's group at the *Advanced Light Source* synchrotron facility on ultrafast time-resolved x-ray scattering and spectroscopy has been proven to be powerful to study structural dynamics during laser-matter interactions [1- 3]. However, the temporal resolution of the experiments was about 2 ps, set by the streak camera. Due to the relatively low instantaneous x-ray intensity of the 3rd generation source, the accumulation of over thousands of x-ray shots is of absolute necessity. In the accumulation mode, the temporal resolution of a streak camera is normally limited by the timing jitter caused by the shot-to-shot pulse energy fluctuation of the lasers.

Recently, we demonstrated that the timing jitter of a classic streak camera can be reduced to 50 fs, even triggered by a laser with 1.2% rms fluctuation [4, 5]. In such a system, the timing jitter becomes irrelevant to the temporal resolution of x-ray streak camera operated in the accumulation mode. Therefore, the time resolution of an accumulation streak camera is only determined by the intrinsic or the so-called single-shot resolution. Such a small jitter was the result of the extremely fast response time from the combination of the improved switch/deflection plates. The sub-100 fs jitter is achieved with a laser that has similar fluctuations (1.2% rms) to most of the commercial lasers, therefore, it is easier to be implemented in synchrotron facilities.

After reducing the timing jitter to less than 100 fs, it was found that sweeping aberrations of the deflection plates limited the time resolution of our camera. We observed that the effect of the aberrations is significant for photoelectrons with large emission angles, which can be significantly reduced by collimating the electron bunches with a slit. Figure 1 shows the lineout of the streak image accumulated with the 6000 UV shots. After proper calibration, 30-fs UV pulses were recorded by the streak camera as 590 fs wide (full-width-at-half-maximum) streak strips. This shows that the x-ray streak camera has better than 600 fs time resolution operating in the accumulation mode.

Since the streak camera can be operated reliably in the sub-ps regime, it will not only make a significant impact on ultrafast science using the 3rd generation synchrotron x-ray

sources but also will play an important role in the timing diagnosis for 4th generation x-ray sources. We have continued the collaboration with camera users to conduct research at ALS and APS synchrotron facilities [7-9].

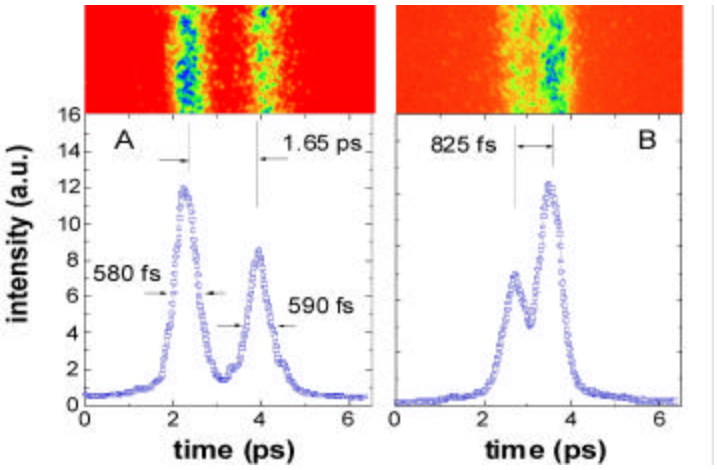

Fig. 1. Averaged lineout of the streak images with corresponding actual images (top) of two 30 fs UV pulses separated by 1650 fs (A) and 825 fs (B).

We plan to improve the temporal resolution of the streak camera down to 100 fs.

2. The effect of orbital symmetry on high harmonic generation, *Bing Shan, Ghimire Shambhu, Chun Wang, and Zenghu Chang*

Molecules are interesting candidates for producing ultrafast x-rays through high harmonic generation. We have found harmonic generation from molecules is different from that of atoms. Far example, the ionization suppression of O_2 leads to a significant cutoff extension as compared to Xe atoms [9]. To further understand the mechanism of the harmonic generation process with molecules, the dependence of harmonic yield on the ellipticity of the driving laser field for O_2 and N_2 were compared experimentally for the first time. The results were also compared with that of Ar. It was found that the 45th order harmonic signal decreases slower for O_2 than that for N_2 with laser ellipticity, while that of Ar is in between. We believe that this is caused by the difference in the orbital symmetry between the two molecules. The ellipticity dependence was measured using the *Kansas Light Source*. Figure 2 (a) shows the results for the 45th order harmonics.

To understand what caused the difference, we applied the Lewenstein model to simulate high harmonic generation from *molecules*. The Lewenstein model can be considered as the quantum treatment of the three-step semiclassical model, i.e. the electron first tunnels out the field-suppressed barrier of the atom, then the freed electron is accelerated in the laser field, and finally it recombines with the parent ion and emits a photon. Figure 2(b) shows the simulation that sums up the contribution from molecules with random orientation angles. It is clear that the ellipticity difference between bonding and anti-bonding molecules exist for arbitrarily aligned molecules. This is consistent with our experimentally measured results.

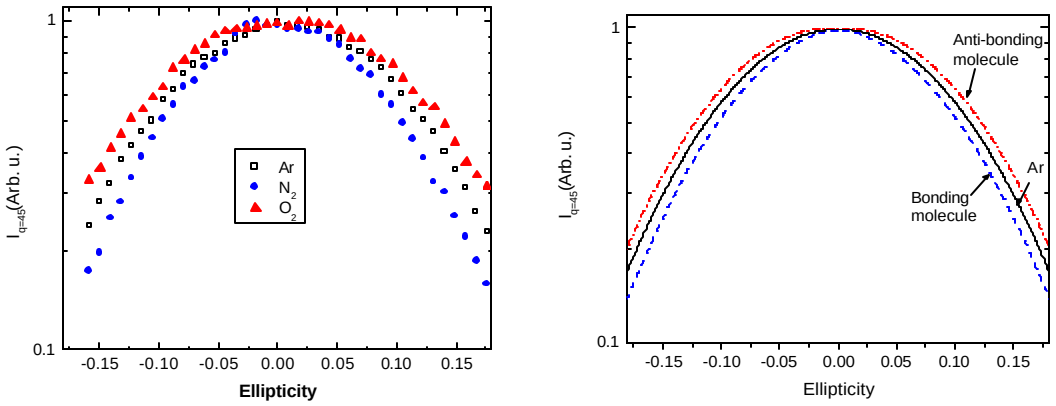

(a) (b)

Fig. 2. (a). The measured ellipticity dependence for the 45th order harmonics. (b) The simulation results for the 45th order harmonics

The ellipticity dependence can be explained by the interference of wave packets from the two atomic centers of the molecules. For an anti-bonding molecule, the electron tunnels out with a larger initial transverse velocity due to the destructive interference. For a linearly polarized laser pulse, the electron will drift away transversely from the parent ions, resulting in a very small recombination probability in the recollision process. With an appropriate amount of ellipticity, the vertical component of the electric field can compensate for the effect of the transverse initial velocity and drive the drifting electron back to the parent ion, thus enhancing the recombination probability. For a bonding molecule with axis oriented perpendicular to the electric field of a linear light, the probability of an electron tunneling out with initial velocity along the electric field is larger than in the other direction as the result of the constructive interference. In this case, when the electric field drives the electron back to the parent ion, the recombination probability is high for a linearly polarized light pulse. The work was submitted to PRL.

3. Suppression of laser field ionization of Cl_2 molecules, *M. Benis, Jiangfan Xia, M. Faheem, Xiao-min Tong, M. Zamkov, Bing Shan, P. Richard, C.D. Lin, Zenghu Chang*

The puzzling question of why O_2 molecules exhibit ionization suppression has created a lot of attention. The ionization potential of O_2 is almost the same as that of Xe, but the measured ionization probability of O_2 is almost an order of magnitude smaller than that of Xe. Both the interference model and the molecular ADK model attribute the suppression to the anti-bonding nature of O_2 and predicted that other anti-bonding molecules such as F_2 should also show ionization suppression. The experiments, however, did not show such suppression. We measured the ionization probability of the Cl_2 molecule that is also an anti-bonding molecule.

The laser field ionization of Cl_2 experiments were conducted at the Kansas Light Source facility. A spatial imaging ion time-of-flight spectrometer was developed for the ionization experiments. The spatially resolved ionization signals along the laser beam propagation direction allow us to obtain the intensity-dependent ionization probability

without changing the laser pulse energy. The ionization probability of Cl_2 was compared with that of Xe. The ionization potentials of Cl_2 and Xe are 11.48 eV and 12.13eV, respectively. According to the atomic PPT model, the ionization signal of Cl_2 should be two times *higher* than that of Xe at 1×10^{14} W/cm^2, whereas the measurements show that the former is in factor of two *lower* than the latter. It therefore demonstrated that the field ionization of Cl_2 is suppressed. The ionization probability of Cl_2 vs. Xe was calculated with a molecular PPT model. The calculated results agreed well with the experiments, which supported the idea that the ionization suppression is caused by the anti-bonding structure of the molecules. Our results suggest that the field ionization of anti-bonding molecules is generally suppressed while the case of F_2 is an exception.

PUBLICATIONS

1. A. M. Lindenberg, I. Kang, S. L. Johnson, R. W. Falcone, P. A. Heimann, Z. Chang, R. W. Lee, J. S. Wark, *"Coherent control of phonons probed by time-resolved x-ray diffraction,"* Optics Letters **27**, 869 (2002).
2. P. A. Heimann, A. M. Lindenberg, I. Kang, S. Johnson, T. Missalla, Z. Chang, R.W. Falcone, R.W. Schoenlein, T.E. Glover, H.A. Padmore, *"Ultrafast X-ray diffraction of laser-irradiated crystals,"* Nuclear Instruments & Methods in Physics Research Section Accelerators Spectrometers Detectors and Associated Equipment **467**, 986 (2001).
3. J. S. Wark, A. M. Allen, P. C. Ansbro, P. H. Bucksbaum, Z. Chang, M. DeCamp, R. W. Falcone, P. A. Heimann, S. L. Johnson, I. Kang, H. C. Kapteyn, J. Larsson, R. W. Lee, A. M. Lindenberg, R. Merlin, T. Missalla, G. Naylor, H. A. Padmore, D. A. Reis, K. Scheidt, A. Sjoegren, P. C. Sondhauss, M. Wulff, *"Femtosecond X-ray diffraction: experiments and limits,"* Proceedings-of-the-SPIE--The-International-Society-for-Optical-Engineering **4143**, 26 (2001).
4. Jinyuan Liu, Jin Wang, Bing Shan, Chun Wang, Zenghu Chang, *"An accumulative x-ray streak camera with sub-600 fs temporal resolution and 50 fs timing jitter"*, Applied Physics Letters, **82**, 3553 (2003).
5. J. Liu, A. G. MacPhee, C. Liu, B. Shan, Z. Chang and J. Wang, *"New approach to jitter reduction of an x-ray streak camera in accumulation mode,"* Proceedings of SPIE **4796**, 184 (2003).
6. M. F. DeCamp, D. A. Reis, A. Cavalieri, P. H. Bucksbaum, R. Clarke, R. Merlin, E.M. Dufresne, and D. A. Arms, A. Lindenberg and A. Macphee, Z. Chang, J. S. Wark and B. Lings**,** *"Supersonic strain front propagation in a dense electron-hole plasma,"* submitted to PRL.
7. S. L. Johnson, P. A. Heimann, A. M. Lindenberg, H. O. Jeschke, M. E. Garcia, Z. Chang, R.W. Lee, J. J. Rehr, and R. W. Falcone, *"Properties of liquid silicon observed by time-resolved x-ray absorption spectroscopy,"* submitted to PRL.
8. S. L. Johnson, P. A. Heimann, A. G. MacPhee, A. M. Lindenberg, O. R. Monteiro, Z. Chang, R. W. Lee, and R. W. Falcone, *"Bonding in liquid carbon studied by time-resolved x-ray absorption spectroscopy,"* submitted to Nature.
9. Bing Shan, Xiao-Min Tong , Zengxiu Zhao, Zenghu Chang and C. D. Lin, *"High harmonic cutoff extension of O_2 molecule due to ionization suppression,"* PRA, **66**, 061401(R) (2002).

Theoretical Studies of Interactions of Atoms, Molecules and Surfaces

C. D. Lin
J. R. Macdonald Laboratory
Kansas State University
Manhattan, KS 66506
e-mail: cdlin@phys.ksu.edu

In this abstract we report progress and future plans in the theoretical developments in three areas: (1) Interaction of intense laser fields with atoms and molecules; (2) Hyperspherical close coupling method for ion-atom collisions and other three-body systems at low energies and (3) Classifications of multiply excited states of atoms. Other works related to experiments will also be summarized.

1.1. Alignment dependence of tunneling ionization rates of molecules in an intense laser field.

In the previous year we had developed a tunneling ionization theory for molecules, called MO-ADK theory. The ionization rate of a molecule in a laser field clearly will depend on the alignment or orientation of the molecule with respect to the polarization of the laser. Since in the experiment the molecules are randomly distributed initially, the measured ionization rate of molecules in a short laser pulse is obtained by averaging over the orientation of molecules. The MO-ADK theory makes definite predictions of the dependence of ionization rates on the alignment of molecules. To test the theoretical prediction we proposed a pump-probe experiment where a short weak pulse is used to induce alignment of the molecules and another more intense laser to ionize it. Molecules can be periodically aligned at rotational revival times during that time period the alignment changes rapidly. We proposed to ionize molecules during these time intervals. Our calculations show that the ionization rate will depend sensitively on the time delay between the two pulses, from which one can extract the dependence of ionization rates on the alignment of molecules. Although no such experiments have been carried out yet, an experiment with similar idea has been performed recently by Corkum's group on N_2 and their deduced alignment dependence is in agreement with the MO-ADK theory. Our theoretical paper has appeared, see Pub. #A1.

1.2. Rescattering dynamics of H_2 and Molecular Clock at sub-fs resolution.

Following two recent Nature papers from Corkum's group [Niikura et al., Nature 417, 917 (2002); 421, 826 (2003)] and the experimental work of Cocke's group, we had initiated a theoretical program for simulating the details of the ionization of H_2 in an intense laser field. We focused on processes which result in the emission of H^+ with large kinetic energies (greater than 5 eV per ion). In particular, we concentrated on molecules which are aligned perpendicular to the direction of the linearly polarized laser field. This special geometry eliminates complications from the strong bond softening and enhanced ionization processes of H_2^+ which would result in lower kinetic energies of the protons. The laser intensity was chosen at where the rescattering mechanism is important, i.e., in the nonsequential ionization regime.

The H_2 molecule is ionized near the peak of the laser pulse. We then follow the physical processes that lead to the production of H^+ ions. First the ionization rate of H_2 is calculated using the MO-ADK theory. This initial ionization creates a correlated electron wave packet, and a vibrational wave packet which propagates and broadens in the s_u potential curve of H_2^+. The electron, which is in the field of the molecular ion and the laser field, will return to collide with the H_2^+ ion at about 2/3 cycle of the optical period later and every ½ period after that, to excite or ionize the other electron. The excited H_2^+ will dissociate into $H+H^+$ if it is not further ionized by the laser. If it is further ionized by the laser, then two H^+ ions are formed. Since the rescattering and/or ionization occur at relatively well-defined times, the dissociation or ionization energy of each H^+ ion has its own characteristic value. By

measuring the kinetic energy of the H^+ ion, the recollision time can be read if the physical processes leading to the dissociation and the ionization are properly understood.

From our simulation we concluded that for H_2 at peak field near $2x10^{14}$ w/cm^2, a large fraction of H^+ ions are produced by the ionization of excited H_2^+, in agreement with the recent experiment from Cocke's group at the JRM laboratory. This result is in contradiction with the assumptions made in the experiment of Niikura et al., where the H^+ ions were assumed to come from the dissociation of H_2^+. Thus they attributed the peaks in the D^+ ion kinetic spectra (the experiment of Niikura et al., used D_2 target) to incorrect physical processes and hence the molecular clocks were not read correctly. We have used the rescattering model to simulate the kinetic energy spectra of the ions for different laser peak intensities, and have also shown that a shorter laser pulse would allow the clock to be read more accurately. Based on our analysis, we showed indeed that the molecular clock can be measured with attosecond accuracy. A report on this work has been submitted to Physical Review Letters.

We anticipate that additional works in these two areas will be continued in the coming years as more experiments are being carried out. In particular, the idea of measuring times to sub-femtosecond accuracy using existing femtosecond lasers is a very attractive field. Similarly, knowing the alignment dependence of the ionization probability of a molecule is the first step in understanding molecules in an intense laser field.

1.3. Attosecond lasers and atomic physics in the time domain.

Attosecond lasers where laser pulses last for less than one femtosecond will be the next frontier in laser technology. The current method is to use high harmonic generation from short femtosecond lasers on rare gas atoms. There are many experimental issues such as the stabilization and the determination of the absolute phase of the femtosecond laser, the characterization of the attosecond laser and what exciting new physics that can be probed when such attosecond lasers become available. Since the time scale of the electronic motion is in the order of attoseconds, clearly that is where the possible applications will be in the future with attosecond lasers. However, unlike the use of femtosecond lasers in chemistry to probe dynamics of atoms in a molecule, the pump-probe physics involving attosecond lasers is different since uncertainty principle becomes significant. We are beginning to build the theoretical tools needed for such studies. In particular, the characterization of attosecond lasers so far is based on measuring photoelectrons in a combined XUV or X-ray attosecond laser with a femtosecond IR laser. We will be developing the theory for such experiments and then move on to multielectron atomic systems where we will address how "electron correlation" can be probed directly in the time domain with attosecond lasers.

2.1. Hyperspherical approach to ion-atom collisions at low energies.

Ion-atom collisions at low energies are usually carried out using close-coupling method with molecular orbitals. This “standard” approach has serious difficulties since the theory is not Galilean invariant. In the past few decades electron translational factors were introduced in an ad hoc manner to account for such deficiency. The validity of such an approach is difficult to assess. We have developed a new approach for ion-atom collisions at low energies based on hyperspherical coordinates, which bypasses the need of electron translational factors. In the last year, we finally got all the programs developed and a first calculation on ion-atom collisions using hyperspherical coordinates had been carried out.

In the new HSCC package, we employed modern powerful computational techniques in the formulation. This includes using the B-spline basis functions to obtain adiabatic hyperspherical potential curves (from Brett Esry), and the R-matrix propagation method and the slow-variable discretization method (SVD) in the solution of hyperradial functions. We have also employed rigid-rotor approximation which allows us to calculate partial wave cross sections without the need to solve the adiabatic channel functions for each partial wave, and a two-dimensional interpolation procedure within the SVD method so calculations can be carried out at higher energies.

So far we have studied a few collision systems: He^{2+}+H, H^++D, H^++Na, Si^{4+}+H and Be^{4+}+H, from a few meV/amu to about 1 keV/amu. These collision systems have been studied by other theorists using reaction coordinates or switching functions and these calculations are considered to be the more reliable ones available. In general, we did not find great discrepancies between the present HSCC calculations and results from using the reaction coordinates for the total cross sections or cross sections to the dominant channels. However, we did find discrepancies in the small channels and in the partial wave cross sections. Thus it appears that calculations based on the reaction coordinate method are capable of providing reliable cross sections for ion-atom collisions, despite that ad hoc switching functions have been used in the formulation of the theory

In the coming year, we expect to continue using the HSCC theory to study a few ion-atom collision systems. We are comparing the partial wave cross sections obtained from HSCC with results from other method. For this purpose we are collaborating with Luis Mendez using the reaction coordinate method and with Pradrag Krstic using the hidden crossing theory. We will extend the method to systems involving multiply charged ions where the number of channels becomes large. We will be testing the method of eliminating the unimportant channels in the calculation. Since the present HSCC code is a robust code for doing collisions in any three-body systems, we expect to apply the method to collisions of atoms with positrons, in particular those involving excited states. If the method works well, we will look at processes involving antiprotons which are relevant in the current effort for making copious amount of antihydrogen atoms for spectroscopic studies.

3. Multiply excited states of atoms--triply and quadruply excited states.
(with T. Morishita, University of Electrocommunications, Tokyo, Japan)

In this grant period, we have also investigated the correlation of electrons in intershell triply excited states. We have used hyperspherical coordinates to calculate the wavefunctions and analyzed the hyperspherical channel functions for the intershell states. Due to the large multiplicity of the number of states, we focused only on the 223 intershell states, i.e., two of the electrons in the n=2 shell and the other in the n=3 shell. Within this group, there are already 49 states. We have been able to show that in addition to A, B and C, which classify the bending motions of the three electrons, additional "+" and '-" quantum numbers are needed to describe the symmetric or antisymmetric stretches of the outer electron with respect to the two inner ones. The "+" and "-" are similar to those used earlier in the classification of doubly excited states. The full report of this work has now appeared in Pub. #A4.

In the coming year we will start looking into quadruply excited states of an atom using hyperspherical approach. Because of the complexity, we will start with the so-called s^4 model where all the four electrons have angular momentum equal to zero. We will first obtain hyperspherical potential curves and from there to disentangle the singly, doubly, triply and quadruply excited states.

4. Total and differential charge transfer cross sections from MOTRIM experiments.

We have used the close-coupling code to obtain total and angular differential charge transfer cross sections for ions on Rb targets that have been measured at the J.R. Macdonald Laboratory in DePaola's group. We have found general good agreement with experiments. But discrepancies were found at the lower energies. The angular resolution from the experiment is still not good enough to test the oscillatory structure predicted by the theory. In the low energy end we also see some discrepancy, which may be due to the limitation of calculations based on the atomic orbital model. We will use the newly developed hyperspherical code to repeat the calculations. Improved resolution from the experiment is also expected.

Publications (A1- 14) and preprints (B1- 4) (2002-2003). There are 28 publications for 2000-2002.

A1. Z. X. Zhao, X. M. Tong and C. D. Lin, "Determination of the alignment dependent ionization probability of molecules in a double pulse laser experiment", Phys. Rev. A67, 043404 (2003).
A2. X. M. Tong, Z. X. Zhao and C. D. Lin, "Abnormal pulse duration dependence of ionization probability of Na atoms in intense laser fields", J. Phys. B36, 1121 (2003).
A3. C. N. Liu, A.T. Le, Toru Morishita, B. D. Esry and C. D. Lin, "Hyperspherical Close Coupling Calculations for Charge Transfer Cross Sections in He^{2+}+H(1s) Collisions at Low Energies," Phys. Rev. A67, 051801 (2003)
A4. Toru Morishita and C. D. Lin, "Radial and Angular Correlations and the classification of intershell 2l2l'3l" triply excited states of atoms," Phys. Rev. A67, 022511 (2003).
A5. M. Zamkov, E. P. Benis, C. D. Lin, T. Morishita, P. Richard, T. G. Lee and T. J. M. Zouros, "Experimental observation and theoretical calculations of triply excited $2s2p^2$ (S, P, D) and $2p^3$(P,D) states of fluorine," Phys. Rev. A67, 050703 (2003).

A6. X. M. Tong, Z. X. Zhao, and C. D. Lin, "Theory of Molecular Tunneling Ionization," Phys. Rev. A 66, 033402 (2002).
A7. Bing Shan, Xiao-Min Tong, Zengxiu Zhao, Zenghu Chang, and C. D. Lin, "High-Order Harmonic Cutoff Extension of the O_2 Molecule Due to Ionization Suppression," Phys. Rev. A 66, 061401 (2002).
A8. E. Edgu-Fry, C. L. Cocke, E. Sidky. C. D. Lin, and M. Abdallah, "Intermediate Energy Ionization of Helium by Proton Impact," J. Phys. B 35, 2603 (2002).
A9. C. D. Lin and Ingrid Reiser, "Alignment-Dependent atomic Model for Electron Transfer in Ion-Molecule Collisions," Int. J. Mol. Sci. 3, 132 (2002).
A10. Z. X. Zhao, B. D. Esry, and C. D. Lin, "Boundary-Free Scaling Calculation of the Time-Dependent Schrödinger Equation for Laser-Atom Interactions," Phys. Rev. A 65, 023402-1 (2002).
A11. "Fast and Slow Collisions of Ions, Atoms, and Molecules," C. D. Lin and F. Martin in "Scattering and Inverse Scattering in Pure and Applied Science," ed. by R. Pike and P. Sabatier for Academic Press (2002) p. 1025.
A12. E. Edgu-Fry, C. L. Cocke, E. Sidky, C. D. Lin and M. Abdallah, "Intermediate Energy Ionization of Helium by Proton Impact," J. Phys. B 35, 2603 (2002).
A13. T. Y. Shi and C. D. Lin "Double Photoionization and Transfer Ionization of He: Shakeoff Theory Revisited," Phys. Rev. Lett. 89, 163202 (2002).
A14. T. G. Lee, H. Nguyen, X. Flechard, B. D. DePaola, and C. D. Lin, "Differential Charge-Transfer Cross Sections for Na^+ with Rb Collisions at Low Energies," Phys. Rev. A 66, 042701 (2002).

B1. Z. X. Zhao, X. M. Tong and C. D. Lin, "Probing Molecular Dynamics at Attosecond Resolution with Femtosecond Laser Pulses," submitted to PRL.
B2. A. T. Le, M. Hesse, T. G. Lee and C. D. Lin, "Hyperspherical close coupling calculations for charge transfer cross sections in Si^{4+}+H(D) and Be^{4+}+H collisions at low energies," to be published in J. Phys. B.
B3. A. T. Le, C. N. Liu and C. D. Lin, "Charge transfer in slow collisions between H^+ with Na," to be published in Phys. Rev. A.
B4. T. G. Lee, A. T. Le and C. D. Lin, "Charge transfer and excitation in slow 20eV-2 keV H^++D(1s) collisions," submitted to J. Phys. B.

Interactions of Ions and Photons with Surfaces, and Molecules

Uwe Thumm
J.R. Macdonald Laboratory
Manhattan, KS 66506
thumm@phys.ksu.edu
(785) 532-1613

1. Neutralization of Negative Hydrogen Ions near Metal Surfaces (T. Niederhausen, H. Chakraborty, U. Thumm)

Project scope: The goal of this project is to study in detail the resonant transfer of a single electron, initially bound to the projectile, during the reflection of a slow incoming ion or atom on a metal surface. Apart from contributing to the qualitative understanding of the interaction mechanisms through computer animations, this project contributes to the quantitative assessment of charge transfer and wave function hybridization in terms of level shifts, decay widths, and ion-neutralization probabilities.

Recent progress: We find that resonant neutralization of H^- near a Cu(111) surface is strongly influenced by transient hybrid states. We represented H^- by an effective potential that models the interaction of the active electron with a polarizable core and yields the correct affinity. We used a one-dimensional single-electron effective potential, constructed from pseudo-potential local-density-functional calculations to model the surface-electronic structure along the surface normal. This potential correctly reproduces the L-band gap position, surface state and image states for zero electron-momentum component parallel to the surface. We employed a wave packet propagation approach of the initially free H^- wave function, over a two-dimensional numerical grid in which the metal continuum is approximated by free electronic motion in a direction parallel to the surface.

For fixed ion-surface distances, the numerical propagation over time yields the ionic survival amplitude. The real part of the Fourier transform (FT) of this amplitude yields the projected density of states (PDOS) that exhibits resonance structures. From the position, width, and amplitude of these resonances, we obtained the energy, lifetime, and population of affinity level, surface, and image states [1].

The transient hybrid states originate from an ion-induced confinement parallel to the surface. The lowest members of this set of states have lifetimes of the order of the ion-surface interaction time. The propagation of the electron probability density provides clear evidence for this confinement effect in visualizing the evolution and the decay of these states (Fig. 1).

Interestingly, the existence of these laterally confined states is linked to the existence of a Cu(111) surface state within the projecteds L-band gap of bulk states and results in a

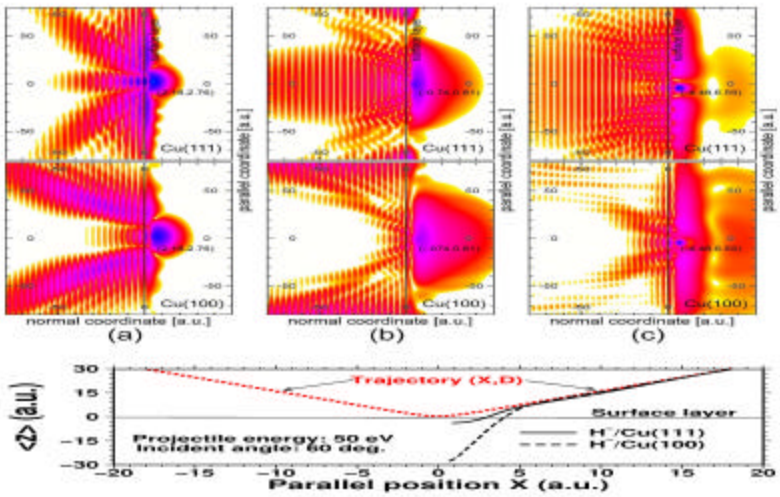

Fig.1. *Wave packet densities (logarithmic scale) for Cu(111) (upper panel) and Cu(100) (lower panel) at times -110 a.u.(a), 20 a.u.(b), and 180 a.u.(c), relative to the time at which the point of closest approach is reached. The ion approaches the surface at an angle of 60^o with respect to the surface and with an energy of 50 eV. Positions (X,D) are given in parenthesis, with X being relative to the point of closest approach* ***(a)****: incident trajectory, (X,D)=(2.2,2.8);* ***(b)****: exit trajectory, (-0.7,0.8);* ***(c)****: exit trajectory, (-4.5, 6.6).* ***Top row****: Cu(111);* ***bottom row****: Cu(100).*
Bottom panel*: The expectation value of z, the electronic coordinate along the surface normal, as a function of the parallel position X of the ion along the trajectory.*

strong increase of the negative ion survival probability in comparison with (under otherwise identical conditions) the neutralization of H near Cu(100), where the surface state is degenerate with the valence band. This leads to the simple interpretation that long-lived laterally confined states at the Cu(111) surface retain electronic probability density that eventually swaps back to the reflected projectile.

Future plans: We plan to extend our Cu(111/100) calculations to three dimension. We will try to quantify to what degree the inclusion of the active electron's motion in the surface plane affects resonance widths, and shifts. Furthermore, we intend to investigate the neutralization dynamics of H^- near the (111) and (100) surfaces of Al, Ag, and Pt. Taking advantage of the flexibility of our wave-packet-propagation codes with regard to the choice of an effective surface potential, we plan to investigate resonance formation and charge exchange near near vicinal and nano-structured surfaces.

2. Laser-Matter Interactions (B. Feuerstein, U. Thumm).

Project scope: In this project we investigate the fragmentation and vibrational excitation of simple molecules during and after their exposure to ultrashort intense laser pulses by means of wave-packet propagation calculations.

Recent progress: We have investigated the fragmentation of the H_2^+ and D_2^+ molecular ions in 25 fs, 800 nm laser pulses in the intensity range 0.05 to 0.5 PW/cm^2. We used a collinear reduced-dimensionality model that represents both the nuclear and electronic motion by one degree of freedom, including non-Born-Oppenheimer couplings. In order to reproduce accurately the properties of the "real" 3D molecule, we introduced a modified "soft-core" Coulomb potential with a softening function that depends on the internuclear distance [2].

We solved the time-dependent Schrödinger equation on a two-dimensional numerical grid and calculated the outgoing flux of emitted electrons and nucleons by means of „virtual detectors" for electrons and protons or deuterons. These detectors are placed outside the excursion range of the electron and at a distance R where the amplitudes of bound vibrational states have become irrelevant [3].

Our calculated fragmentation probabilities and kinetic energy spectra reproduce the main features of measured spectra, support a previously postulated "charge-resonance enhanced" ionization mechanism, and allow us to clearly distinguish between molecular dissociation (MD) into field-dressed final channels and fast, ionization-induced Coulomb explosion (CE). For 25fs, 0.2 PW/cm^2, 800nm pulses, we find that MD dominates for molecular ions that are prepared in the two lowest vibrational states only, while CE becomes increasingly dominating for higher vibrational states.

Fast ionization of D_2 leads to the coherent population of stationary vibrational states of D_2^+. Usually, only the squared absolute values of the vibrational state amplitudes (Franck-Condon factors) are observed since insufficient experimental time resolution averages out all coherence effects. We proposed a Coulomb explosion imaging method to visualize the coherent motion of bound nuclear wave packets using ultrashort (5 fs), intense pump-probe laser pulses. With this type of experiment decoherence times in the fs to ps range may become directly observable and provide relevant information for coherent control (Fig. 2) [4].

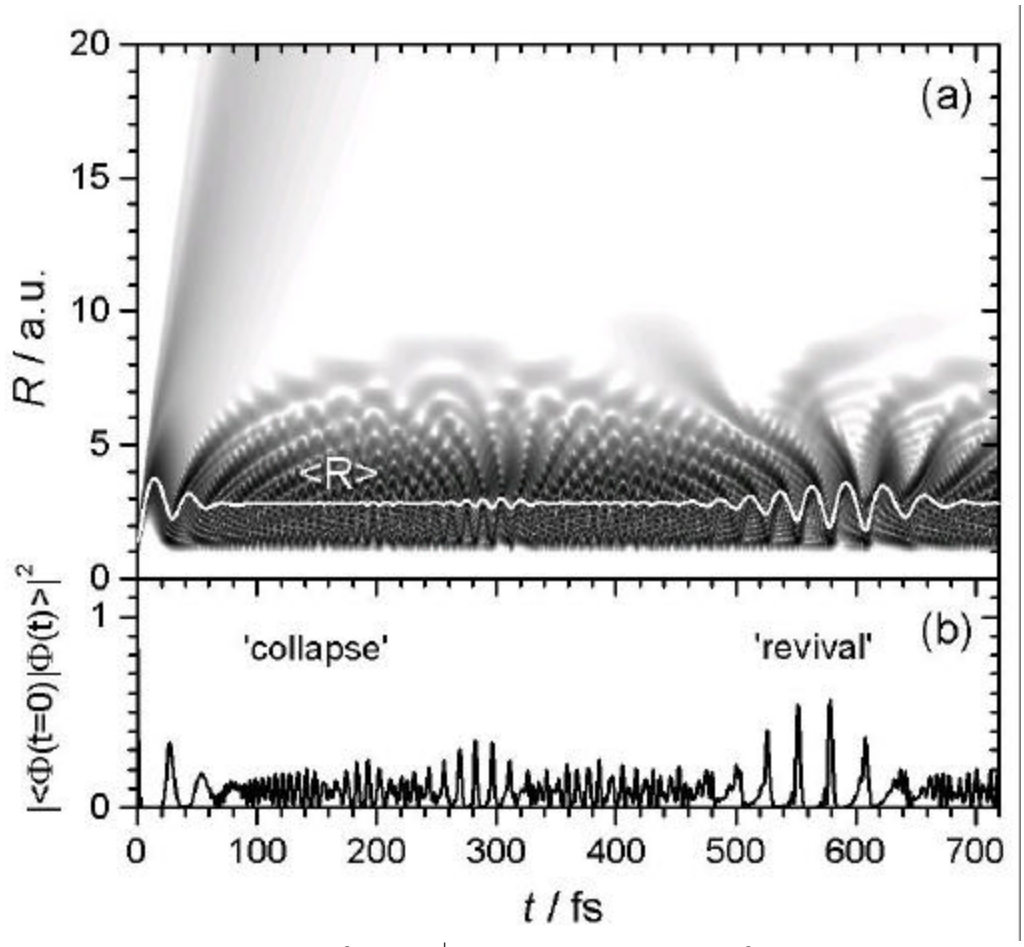

Fig. 2*. Coherent motion of the D_2^+ nuclear wave packet following ionization of D_2 (v = 0) in a 5 fs, 1 PW/cm^2 laser pulse. (a): Probability density $|F(R,t)|^2$ (logarithmic gray scale) and expectation value <R>. (b): Autocorrelation function.*

Future plans: We intend to extend our calculations by adding a second electron thereby describing the interaction of a linearly polarized, short laser pulse with neutral molecules (H_2 and D_2). Our model molecule will be assumed to be one-dimensional, with both electrons restricted to move along the internuclear axis. The electron-nucleus and electron-electron model interaction potentials will be carefully adjusted to reproduce accurate electronic potential curves of the neutral molecule. We plan to examine the rescattering dynamics after single ionization of H_2 and D_2 and its contribution to double ionization and fragmentation for different pulse intensities, lengths, and phases of the laser pulse. Furthermore, we have in mind to study the decoherence of the nuclear motion in D_2^+ due to ro-vibrational couplings.

[1] U. Thumm, Book of invited papers, XXII ICPEAC, eds. S. Datz et al., Santa Fe, NM (Rinton Press, 2002) p. 592.
[2] B. Feuerstein and U. Thumm, Phys. Rev. A **67**, 043405 (2003).
[3] B. Feuerstein and U. Thumm, J. Phys. B **36**, 707 (2003).
[4] B. Feuerstein and U.Thumm, Phys. Rev. A **67**, 063408 (2003).

Multiparticle Processes and Interfacial Interactions in Nanoscale Systems Built from Nanocrystal Quantum Dots

Victor Klimov
Chemistry Division, C-PCS, MS-J567, Los Alamos National Laboratory
Los Alamos, New Mexico 87545, klimov@lanl.gov

Program Scope

Controlling functionalities of nanomaterials requires a detailed physical understanding from the level of the individual nanoscale building blocks to the complex interactions in the nanostructures built from them. This project concentrates on electronic properties of semiconductor quantum-confined nanocrystals (NCs) and the electronic and photonic interactions in NC nanoscale assemblies. Specifically, we study multiparticle processes in individual NCs and interfacial interactions in NC-based "homogeneous" and "hybrid" structures. Multiparticle states (e.g., quantum-confined biexcitons) and multiparticle interactions (e.g., Auger recombination) play an important role in both optical gain and band-edge optical nonlinearities in NCs. Interfacial interactions (e.g., electrostatic coupling) can enable communication between NCs (homogeneous systems) or between NCs and other inorganic or organic structures (hybrid systems), leading to such important functionality as energy transfer. The ability to understand and control both multiparticle processes and interfacial interactions developed in this project will lead to such new NC-based technologies as solid-state optical amplifiers and lasers, nonlinear optical switches, and electrically pumped tunable light emitters.

Recent Progress

1. Multiparticle interactions and optical gain in shape-controlled CdSe NCs

Because of size-controlled spectral tunability (achieved via the quantum confinement), high photoluminescence (PL) efficiencies, and chemical flexibility, semiconductor NCs are very attractive for applications in various optical technologies including optical amplification and lasing [1]. Optical gain in ultrasmall (sub-10 nm) NCs relies on emission from multi-exciton states [2, 3]. However, the decay of these states is dominated by nonradiative Auger processes rather than by radiative recombination [4], which makes them nominally non-emissive species. One approach to force these non-emissive multi-excitons to lase is by increasing the NC density in the sample until the rate of stimulated emission becomes greater than the rate of Auger decay [5, 6]. Although this straightforward approach does work (Figure 1), the suppression of Auger recombination remains an important current challenge in the field of NC lasing.

In our work, we explore the effect of NC "geometry" (e.g., NC shape) on the rates of the multi-particle decay. In particular, we study the influence of the zero- to one-dimensional (1D) transformation on multi-particle Auger recombination using a series of elongated semiconductor NCs (quantum rods). We observe an interesting new effect, namely, the transition from the three- to two-particle recombination process as the nanocrystal aspect ratio is increased [7]. This transition implies that in the 1D

confinement limit, Auger decay is dominated by Coulomb interactions between 1D excitons that recombine in a bimolecular fashion. One consequence of this effect is

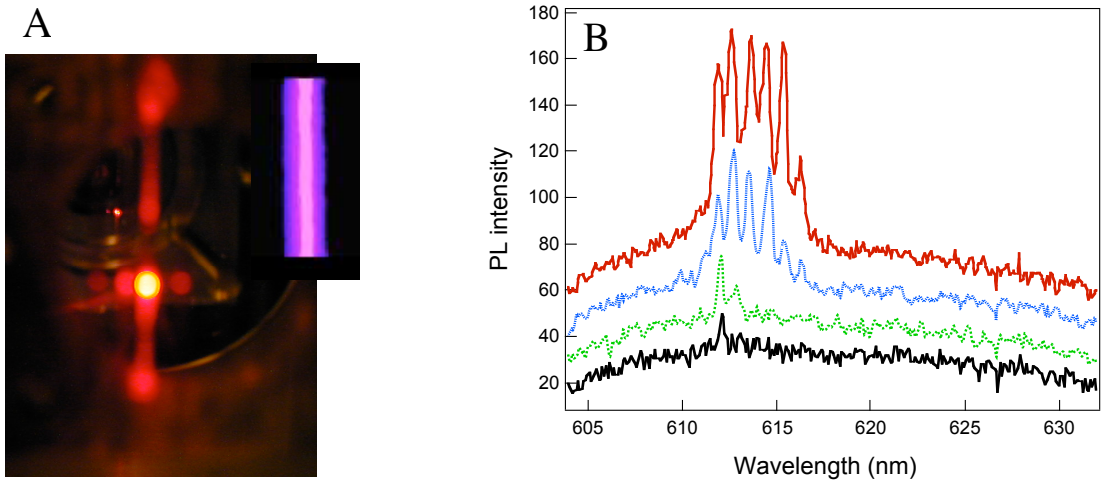

Figure 1. (A) Microring lasing in the NC solid incorporated into a microcapillary cavity (400 nm pump) and a microphotograph of the device (the NC layer on the inner side of the microcapillary tube appears pink). (B) The development of the "lasing" whispering gallery modes with increasing pump level.

strongly reduced decay rates of higher multi-particle states that lead to increased optical gain lifetime and efficient light amplification due to transitions involving excited electronic states [8]. These unique rod properties suggest that shape control may be key to developing practical lasing applications of NCs.

2. High-performance NC-based nanocomposites for optical gain applications

A significant challenge for realizing optical applications of NCs is their incorporation into transparent host matrices while preserving size monodispersity and high PL quantum yields (QYs). Additional challenges are associated with achieving high NC filling factors, which are essential for enhancing optical nonlinearities and obtaining large gain magnitudes. During the last year, we developed a generalized approach for the preparation of NC-based nanocomoposites designed in such a way as to provide high volume loading (up to 20%) and to preserve the size monodispersity (<7%) and the large PL QYs (>10% at room temperature) of the NCs in the matrices [9].

Our strategy involves decoupling the synthesis of NCs from the preparation of the matrix. In this method, high quality NCs with high fluorescence efficiency and a narrow size distribution are first prepared using previously established literature procedures. The organic, surface-passivating ligands are then exchanged to stabilize the nanoparticles in polar solvents and also to provide a tether through which the NCs are incorporated into the titania sol-gel matrix. This route produces high optical quality films with stability which is significantly improved in comparison with matrix-free solids. Additionally, the new method also provides a high volume fraction of NCs, which is sufficient to observe stimulated emission and large optical nonlinearities.

3. Energy transfer dynamics in NC assemblies

Understanding and ultimately controlling communication and coupling between NCs is of significant fundamental and technological interest. One mechanism for inter-NC coupling is via electrostatic Coulomb interactions. Such interactions can allow communication between nanoparticles via *incoherent* exciton transfer. Even for NC assemblies that are not optimized structurally (such as nominally monodispersed NC solids), exciton transfer has a dramatic effect on NC optical properties leading, *e.g.*, to a strong red shift of the emission band. Although they provide strong indication for interactions between NCs, PL red shifts can not be used to directly evaluate the strength

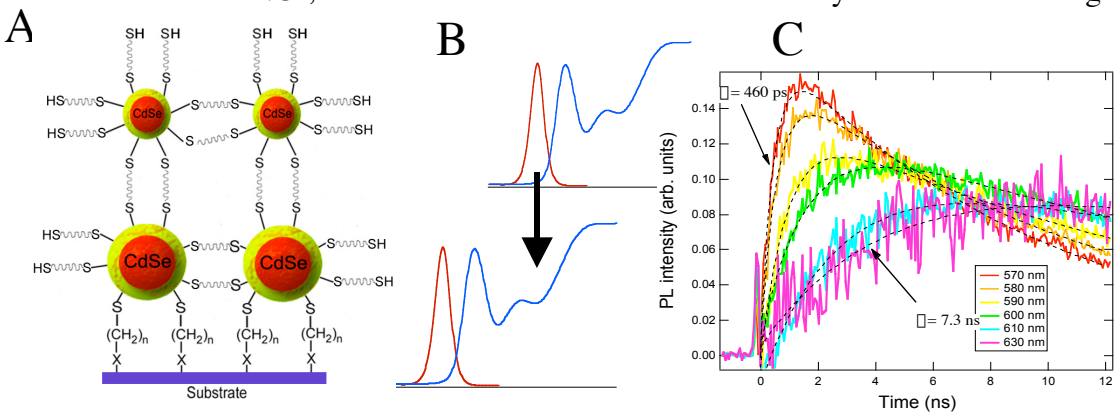

Figure 2. (A) A prototype NC energy-gradient bilayer structure for directed energy flow: NCs with 1.3 nm radius are assembled onto a layer of 2.05 nm NCs. (B) Schematics of energy transfer in this structure: The emission from small "donor" NCs efficiently couples to a dense manifold of high-energy absorbing states in large "acceptor" NCs. (C) Time-resolved emission spectra reveal fast "vertical" transfer from small to large dots with a 460 picosecond time constant.

of these interactions. To obtain more direct information about time scales characteristic of the energy transfer in NC materials, we have recently performed spectrally selective time-resolved PL studies within the inhomogeneously broadened emission line of NC solids [10]. We observe that inter-NC energy migration is dominated by direct energy transfer from "blue" to "red" sides of the emission band across an energy range on the order of tens of meV, which corresponds to the transition between NCs with a relatively large size difference. The high efficiency of this process is due to a strong coupling between the lowest "emitting" transition in a donor NC and a higher energy, strongly "absorbing" transition in an acceptor NC. We performed phenomenological modeling of exciton inter-NC dynamics that provides important insights into optimization of NC assemblies with respect to energy transfer efficiencies. Furthermore, we demonstrate a prototype energy-gradient structure (a NC bilayer) which is engineered in such a way as to boost the rate of the unidirectional (vertical) transfer (Figure 2). Studies of these gradient structures indicate that inter-NC transfer can approach ultrafast picosecond time scales in structurally optimized assemblies.

Future Plans

We are planning to extend our studies of mutiparticle effects in quantum confined NCs to the problem of impact ionization (the inverse Auger effect). This process results in the

generation of biexcitons from high-energy single excitons and can be used for, e.g., improving the efficiency of NC-based solar sells. In our optical gain work, we will explore the use of IV-VI semiconductor NCs for optical amplification in the infra-red (IR) spectal range. Tunable NC-based media for producing optical gain at a specific near- or mid-IR wavelength are highly desirable for a number of applications ranging from optical communication and remote sensing to a recent proposal on coherent plasmon generation. As a next step in our energy transfer studies, we will use well-defined Langmuir-Blodgett assemblies of NCs in order to directly study relationships between the sample morphology (inter-NC separation and NC arrangement) and the energy transfer dynamics/efficiencies. We will also attempt to study energy transfer in single NC donor-acceptor pairs using near-field optical measurements.

Publications

1. V. I. Klimov and M. G. Bawendi, Ultrafast carrier dynamics, optical amplification, and lasing in nanocrystal quantum dots, *MRS Bulletin*, Feature Issue on *New Aspects of Nanocrystal Research,* **26**, 998 - 1004 (2001).
2. A. A. Mikhailovsky, A. V. Malko, J. A. Hollingsworth, M. G. Bawendi, and V. I. Klimov, Multiparticle interactions and stimulated emission in chemically synthesized quantum dots, *Appl. Phys. Lett.* **80**, 2380 - 2382 (2002).
3. M. Achermann, J. A. Hollingsworth, and V. I. Klimov, Multiexcitons confined within "sub-exciton" volume: Spectroscopic and dynamical signatures of biexcitons and triecitons in sub-10 nanometer quantum dots, *Phys. Rev. B* (in press, 2003).
4. S. A. Crooker, T. Barrick, J. A. Hollingsworth, and V. I. Klimov, Multiple temperature regimes of radiative decay in CdSe nanocrystal quantum dots: Intrinsic limits to the dark-exciton time, *Appl. Phys. Lett.* **82**, 2793--2795 (2003).
5. A. V. Malko, A. A. Mikhailovsky, M. A. Petruska, H. Htoon, J. A. Hollingsworth, M. G. Bawendi, and V. I. Klimov, From amplified spontaneous emission to microring lasing using nanocrystal quantum dot solids, *Appl. Phys. Lett.* **81**, 1303 - 1305 (2002).
6. H.-J. Eisler, V. C. Sundar, M. G. Bawendi, M. Walsh H. I. Smith and V. I. Klimov, Color-selective semiconductor nanocrystal laser, *Appl. Phys. Lett.* **80**, 4614 – 4616 (2002).
7. H. Htoon, J. A. Hollingsworth, R. Dickerson, and V. I. Klimov, Zero- to one-dimensional transition and Auger recombination in semiconductor quantum rods, (submitted to *Phys. Rev. Lett.*)
8. H. Htoon, J. A. Hollingsworth, A. V. Malko, R. Dickerson, and V. I. Klimov, Light amplification in semiconductor nanocrystals: Quantum rods vs. quantum dots, *Appl. Phys. Lett.* 82, 4776 – 4778 (2003).
9. M. A. Petruska, A. V. Malko, P. M. Voyles, and V. I. Klimov, High-performance, quantum-dot nanocomposites for nonlinear-optical and optical-gain applications, *Advanced Materials* **15**, 610–613 (2003).
10. S. A. Crooker, J. A. Hollingsworth, S. Tretiak, and V. I. Klimov, Spectrally-resolved dynamics of energy transfer in quantum-dot solids: Towards engineered energy flows in quantum-dot assemblies, *Phys. Rev. Lett.* **89**, 186802-1(2002).

Inner-shell photoionization of atoms and small molecules

A. Belkacem, M. Prior and M. Hertlein

Chemical Sciences Division

Lawrence Berkeley National Laboratory

Berkeley, CA 94720

Email: abelkacem@lbl.gov

mphertlein@lbl.gov

mhprior@lbl.gov

Objective and Scope

The goal of this part of the LBNL AMOS program is to understand the structure and dynamics of atoms and molecules using photons as probes. The current research carried at the Advanced Light Source is focused on studies of inner-shell photoionization and photo-excitation of atoms and molecules, as well as breaking new ground in the interaction of x-rays with atoms and molecules dressed with femto-second laser fields. These studies can be divided into three complementary parts, a) dynamics of x-ray ionization of atoms and small molecules (see *parts of this work in Michael Prior's talk and abstract for the talk*), b) intense-field, two-color (x-ray + laser) inner-shell photoionization, c) inner-shell photoionization at high energies. The low-field photoionization work seeks new insight into atomic and molecular processes and tests advanced theoretical treatments by achieving new levels of completeness in the description of the distribution of momenta and/or internal states of the products and their correlations. The intense-field two-color research is designed to provide new knowledge of the evolution on a femto-second time scale (ultimately atto-second) of atomic and molecular processes as well as the relaxation of atomic systems in intense transient fields. The third part of this research seeks to expand the knowledge of atomic physics into new frontiers in the relativistic regime and very strong fields where the negative energy continuum plays a major role in photo-ionization and charge transfer processes.

X-ray ionization of laser dressed atoms and molecules (gas phase).

An atom is a multielectron system that responds as a whole when perturbed by a strong laser field. The modifications to the atomic structure by the femto-second laser (acting on the outer electrons only) can indirectly extend to inner-shells through electron correlation. In particular the presence of the laser during relaxation of an atom with an inner-shell hole will modify the autoionization of the upper states as well as the post-collision interactions (e.g. between photo- and Auger electrons) changing the end products.

First we performed static measurements without the laser. We measured the charge state distribution when the x-ray energy is tuned around the K-edge of K and Ar ions. The potassium atomic structure is similar to the argon atomic closed-shell structure with an additional electron in the 4s state. The measured charge state distributions exhibit markedly different shapes but close mean values of the charge state. A strong single-photon two-electron excitation (1s4s)4p5s located 1 eV above the K-edge ionization energy is visible for potassium. We systematically measured the charge distribution of potassium ions around the double-excitation resonance where we expect a strong effect on the shape of the charge state distribution and post-collision interaction effects in potassium. The strength of the double excitation is approximately 10% that of the 1s-4p resonance in agreement with previous measurements recently reported in the literature using an absorption technique in a vapor cell.

We used a 1 mJ femtosecond laser pulse to remove or excite the 4s-electron of K and used the x-rays delayed by 100ps and tuned around the 1s-4p excitation as a probe. We measured the charge state distribution with laser-on and compared it to laser-off. We also measured the charge state distribution for laser-on and laser-off as the x-ray energy is scanned through the K-edge. We see small differences but these initial laser-on/laser-off measurements are still dominated by background associated with the very large number of singly-charged potassium ions created by the high power laser. We modified our experimental set up and developed a time-of-flight technique based on a pulsed-extraction and pulsed acceleration to use the multi-bunch mode. This technique allows the extraction of ions created in a single-camshaft pulse of the ALS train of pulses. This is despite the long time-of-flight and time spread of different charge states (up to 10 microsecond) that the ions take to reach the detector. A combination of nanosecond-switching high-voltage extraction allowed us to sort with very high efficiency the high charge-state ions (K^{2+} and up) from the very large number of K^{+}.

Metal-insulator transition in an expanding metallic fluid: particle formation kinetics.

This Work is done in collaboration with T.E. Glover at the ALS and published in PRL in 2003. Core level photoemission spectroscopy provides a local probe of expansion dynamics and associated transient chemical properties as a highly pressurized metallic fluid expands into vacuum following impulsive heating of a semiconductor by an intense, ultrashort laser pulse. These experiments probe constituent species and solidification kinetics occurring in the early moments of material ejection and provide insight into how particles arise in the current laser ablation regime.

Laser pump (12 J/cm2) and x-ray probe photoemission experiments are performed at the Advanced Light Source (ALS) using a laser system (800 nm, 200fs, 1kHz) synchronized to the ALS storage ring. Femtosecond laser pulses impulsively heat a silicon wafer to produce a hot, pressurized fluid which expands into vacuum. Vacuum expansion is probed by time-delayed synchrotron pulses (400eV) with 2p core spectra recorded using a hemispherical analyzer. The synchrotron fill mode isolate a single x-ray pulse whose photoelectrons are electronically gated so measurements at a fixed pump-probe delay reflect spectral evolution over a time-window set by a single x-ray pulse (~80 ps). Photoemission transients shorter than 80 ps (ALS pulse length) can be observed. A temporal sequence of Si 2p photoelectron spectra reveals a transient peak shift; an initial shift to lower binding energy followed by a return to higher binding energy.

The measured time width of the peak shift indicates a spectral transient shorter than the x-ray pulse width (~80 ps).

Inner-shell photoionization at high energies

Detailed studies of single and double ionization mechanisms, electron correlation effects, post-collision interaction effects have resulted in major advances of our understanding of photoionization mechanisms in the soft and hard x-ray regime. The situation is quite different at relativistic energies. When the photon energy exceeds twice the rest mass of the electron, the negative energy continuum will play an additional important role. Photoionization can now proceed through a new channel in which the excess energy is taken by one of the negative-energy continuum electrons. The final result is the creation of an inner-shell vacancy (K, L,….) along with the creation of an electron-positron pair on the same atom.

We performed the first measurement of vacuum-assisted photoionization in the GeV energy range for Au and Ag targets. This work was published in PRL in 2003. The experimental work is carried out at the European Synchrotron Radiation Facility (ESRF) in Grenoble, France. High energy photons are produced by Compton backscattering of laser photons from the 6 GeV electron beam (GRAAL beamline). A signature of VAP is given by a simultaneous detection of a K- or L-vacancy in coincidence with the production of an electron-positron pair. These values are a factor of 5 to 10 larger than contributions from Compton scattering and photoelectric effect. Our experimental results constitute the first absolute measurement of VAP cross section and are used as benchmark values for theory. Initial calculations of VAP predict that the contribution to the VAP cross section, for tightly bound Au K-shell, comes mainly from the mechanism that involves pair creation on the nucleus. Our experimental value of VAP appears to be smaller than theory for Au K-shell and in agreement for Ag K-shell. This may be an indication that the contribution from VAP that involves pair creation on the nucleus is smaller than predicted by theory. This could be due to e^+/e^- mutual screening at the Au K-shell orbital scale. A more involved theoretical model than found in the literature is needed to account for our experimental measurements.

Electron impact ionization at relativistic energies.

We used the 1.5 GeV electron beamline at the ALS booster and time-of-flight technique to measure multiple ionization of helium, neon and argon. In this relativistic limit the electron is equivalent to a half-cycle pulse-of-light, the perturbation by the projectile is small and the probability for a simultaneous and independent interaction with many electrons of the target is usually neglected. Double ionization of He for instance is induced by only one single interaction of the projectile with one target electron. It solely occurs due to the electron-electron interaction and the ratio $R = \sigma^{2+}/\sigma^{1+}$ reaches an asymptotic value between 0.24% and 0.28% already at lower impact energies (about 100 keV). Our measurement of the ratio R at 1.5 GeV yields a value of about 0.25% confirming that relativistic effects do not affect the asymptotic values for He. However the situation appears to be different for Neon and Argon. The fraction for higher charge states (2+ and up) increases for higher electron impact energies. The rate of increase is higher for the highest charge states. One possible explanation would be a faster increase of electron impact ionization cross section for inner shells than for outer shell.

We are currently analyzing the data to extract quantitative numbers to compare to calculations.

Future Plans

We plan to continue the pump-probe experiments at the ALS. We will continue our studies with potassium and extend the measurements to molecules such as H-Cl and I-Br. Time-resolved XANES has the capability to observe the degree of charge transfer by making use of the intensity of bound-bound transitions to monitor the whereabouts of the photoexcited electron. Interhalogens like I-Br are suitable for this because we can monitor the intensity of the 2s-4p absorption intensity. In the initial phase we will use our 5-kHz laser system to develop the detection technique most suitable for this experiment (direct absorption technique or detection of fragments along the polarization axis).

We plan to continue the measurements of photo-ionization and electron impact ionization at high energies. We will make use of the COLTRIMS detection technique to study the recoil taken by the nucleus and ultimately discriminate between the two vacuum-assisted photo-ionization mechanisms.

Recent Publications

''Metal-insulator transitions in an expanding metallic fluid: particle formation kinetics"
T.E. Glover, G. D. Ackerman, A. Belkacem, P. A. Heimann, Z. Hussain, R. W. Lee, H. A. Padmore, C. Ray, R. W. Schoenlein, W. F. Steele, and D. A. Young
Phys. Rev. Lett, 90, 23102-1 (2003)

"Measurement of vacuum-assisted photoionization at 1 GeV for Au and Ag targets"
D. Dauvergne, A. Belkacem, F. Barrue, J. P. Bocquet, M. Chevallier, B. Feinberg, R. Kirsch, J. C. Poizat, C. Ray, and D. Rebreyent
Phys. Rev. Lett. 90, 153002 (2003)

"Dynamics of ionization mechanisms in relativistic collisions involving heavy and highly charged ions"
D. C. Ionescu and A. Belkacem
Eur. Phys. J. D18, 301-307 (2002).

"Observation of a nearly isotropic, high energy Coulomb explosion group in the fragmentation of D2 by short laser pulses"
A. Staudte, C.L. Cocke, M.H. Prior, A. Belkacem, C. Ray, H.H.W Chong, T.E. Glover, R.W. Schoenlein,
Phys. Rev A65, (2002) 020703(R)

"Measurement of synchrotron pulse durations using surface photovoltage transients",
T.E. Glover, G.D. Ackermann, A. Belkacem, B. Feinberg, P.A. Heimann, Z. Hussein, C. Ray, R.W. Schoenlein, W. F. Steele, *Nucl. Instr. Meth. in Phys. Res*. A467-468 (2001) 1438

"Photoionization at relativistic energies"
D.C. Ionescu, A. Belkacem and A. Sorensen
Physics Scripta, Vol. T92, R. Swedish Acad. Sci., (2001) 330

Electron-Atom and Electron-Molecule Collision Processes

C. W. McCurdy and T. N. Rescigno
Computing Sciences, Lawrence Berkeley National Laboratory, Berkeley, CA 94720
cwmccurdy@lbl.gov, tnrescigno@lbl.gov

Program Scope: This project seeks to develop theoretical and computational methods for treating electron collision processes that are currently beyond the grasp of first principles methods, either because of the complexity of the targets or the intrinsic complexity of the processes themselves. We are developing methods for treating low energy electron collisions with polyatomic molecules, complex molecular clusters and molecules bound to surfaces and interfaces, for studying electron-atom and electron-molecule collisions at energies above that required to ionize the target and for calculating detailed electron impact ionization and double photoionization probabilities for simple atoms and molecules.

Recent Progress and Future Plans: We report progress in three distinct areas covered under this project, namely electron-polyatomic molecule collisions, electron impact ionization and double photoionization.

1. Electron-Molecule Collisions

A major goal of our research in the area of electron-polyatomic molecule scattering is to explore the mechanisms that control the flow of energy from electronic to nuclear degrees of freedom in such collisions. To this end, we have been studying the electron-CO_2 system. Earlier this year, we completed a major study of resonant vibrational excitation in the 4 eV energy region; the results of this study, which have been published in Physical Review A, explore details of the nuclear vibrational dynamics on the two components of the $^2\Pi_u$ resonance surfaces, which are strongly coupled by non-adiabatic (Renner-Teller) forces. This study represents the first time that all aspects of an electron-polyatomic collision, including not only the determination of the fixed-nuclear electronic cross sections, but a treatment of the nuclear dynamics in multiple dimensions on coupled resonance surfaces, has been carried out entirely from first principles. Our calculations have produced vibrational excitation cross sections that are in excellent agreement with experiments and reveal the origin of the subtle interference effects observed in the most recent experimental studies.

We have extended our treatment of CO_2 to look at threshold vibrational excitation in the virtual state region, which lies well below the energy range dominated by negative ion resonances. We have developed a virtual state model, based on an extension of the zero-range theory of Gauyacq and Herzenberg, that can be implemented in a completely *ab initio* fashion by using mathematical properties of the long-range dipole interaction to construct a complex anion potential surface that determines the nuclear dynamics. The theory was first tested on the electron-HCl problem and then applied to CO_2. The theory explains, for the first time, the selectivity recently observed in the threshold excitation of the Fermi dyad, as well as the pattern of peaks and oscillations observed in the higher polyads. The have submitted this work to Physical Review Letters.

Cross sections for excitation of the Fermi polyads in CO_2 in the threshold region. *Ab initio* results (solid lines) are compared with recent experiment.

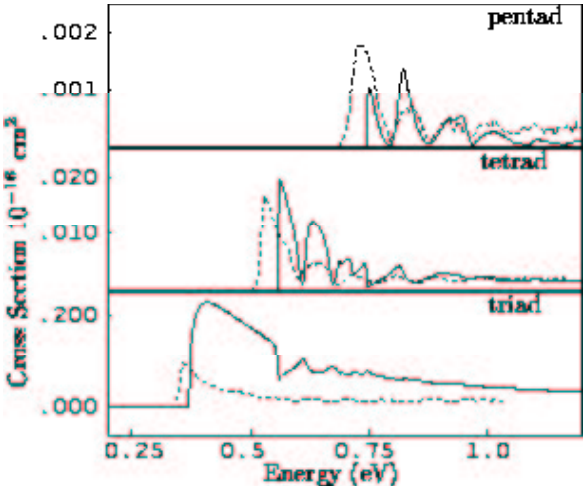

We have continued with our studies of dissociative electron attachment to water. Using the Complex Kohn Variational method, augmented with large-scale configuration-interaction studies, we have constructed a complete, three-dimensional complex energy surface for the lowest ($^2A_1$) resonance and have initiated multi-dimensional studies of the dissociation dynamics using the MCTDH method. The Complex Kohn method continues to serve as our principal tool for studying electron-molecule scattering. We have initiated theoretical studies of low-energy electron scattering by ethylene and NO, prompted by the appearance on new experimental studies on these target gases. We have also initiated, in collaboration with Prof. A. E. Orel at UC Davis, an effort to modify and extend the Kohn method to handle positron-molecule scattering and excitation, since this is an area where there is considerable experimental activity and relatively little corresponding theory.

2. Electron-Impact Ionization

The computational approach we have developed to study electron impact ionization, which has provided the only *complete* solution to the quantum mechanical three-body Coulomb problem at low collision energies to date, relies on a mathematical transformation of the Schrödinger equation called *exterior complex scaling* (ECS) that allows us to solve for the wave function without detailed specification of complicated asymptotic boundary conditions. Over the past year, we have continued with our studies of ionization of an atomic target with two active electrons. The extraction of breakup amplitudes from multi-electron wave functions is considerably more difficult than what is encountered in two-electron systems and continues to be a topic of ongoing research in our group. Using a time-dependent version of the basic ECS approach, which uses accurate Lanczos propagation techniques and was designed to avoid the solution of large systems of complex linear equations, we have completed a study of electron-helium ionization within the S-wave model. This work was carried out by UC Berkeley graduate student Dan Horner as part of his doctoral research.

3. Double Photoionization

We initiated a new theoretical effort in FY03 directed at studying double photoionization (one photon in, two electrons out) of atoms and molecules. Like electron-impact ionization, double photoionization is a sensitive measure of electron-electron correlation. Moreover, optical selection rules, and the fact that it is a 'half-collision' process with no free electrons in the initial state, make it computationally more tractable to study than collisional ionization. The fact that this is an active area of experimental research at the Advanced Light Source, and that there are presently no credible first-principles studies for any molecule, has provided additional motivation for this effort.

Our initial efforts in this area were carried out in collaboration with Prof. Fernando Martin (Universidad Autónoma de Madrid), who has implemented the use of B-splines for atoms (and 2-electron diatomics). We have demonstrated that B-splines can be used to implement exterior complex scaling of electronic coordinates, allowing the correct application of outgoing boundary conditions for scattering problems with multiple electrons in the continuum. We have modified the atomic B-spline codes to implement ECS and have used them successfully in calculating triple differential cross sections for double photoionization of helium. We have undertaken a similar effort that we hope will provide the first results for H_2. Our future plan in this area is to develop a hybrid approach that combines the use of molecular Gaussian basis sets with the discrete variable representation and ECS. Such an approach avoids the use of single-center expansions, simplifies the computation of two-electron integrals and paves the way for studies of double photoionization of more complex molecules.

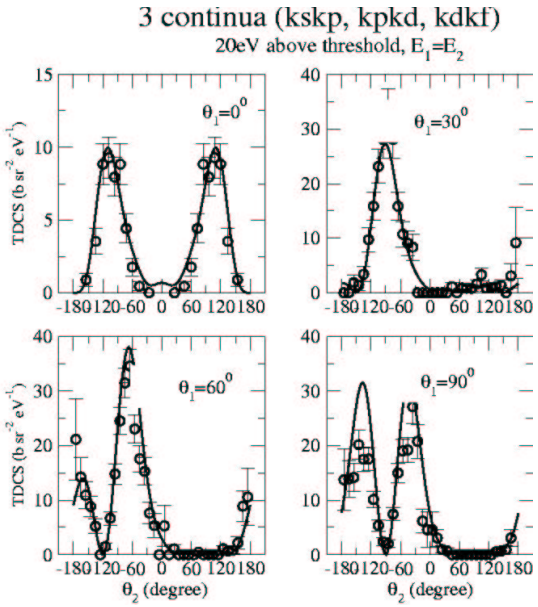

Triple differential cross sections for He double photoionization at equal energy sharing, 20 eV above threshold. Comparison of experiment and ab initio results.

Publications (2001-2003):

1. C. W. McCurdy, D. A. Horner and T. N. Rescigno, "Practical Calculations of Amplitudes for Electron Impact Ionization", *Phys. Rev. A* . **63**, 022711 (2001).
2. M. Baertschy, T. N. Rescigno, W. A. Isaacs, X. Li and C. W. McCurdy, "Electron Impact Ionization of Atomic Hydrogen", *Phys. Rev. A* **63**, 022712 (2001).
3. W. A. Isaacs, M. Baertschy, C. W. McCurdy and T. N. Rescigno, "Doubly Differential Cross Sections for the Electron Impact Ionization of Hydrogen", *Phys. Rev. A* **63**, 030704 (2001).
4. M. Baertschy, T. N. Rescigno, C. W. McCurdy, J. Colgan and M. S. Pindzola, "Ejected-Energy Differential Cross Sections for the Near Threshold Electron-Impact Ionization of Hydrogen", *Phys. Rev. A* **63**, 050701 (2001).
5. M. Baertschy, T. N. Rescigno and C. W. McCurdy, "Accurate Amplitudes for Electron Impact Ionization", *Phys. Rev. A* 64, 022709 (2001).
6. T. N. Rescigno, "The Three-Body Coulomb Problem", in "Yearbook of Science and Technology", (McGraw Hill, New York, 2001).
7. T. N. Rescigno, W. A. Isaacs, A. E. Orel, H.-D. Meyer and C. W. McCurdy, "Theoretical Studies of Excitation in Low-Energy Electron-Polyatomic Molecule Collisions", in *Photonic, Electronic and Atomic Collisions, Invited Papers* , *Proceedings of the XXII International Conference on Photonic, Electronic and Atomic Collisions,* Santa Fe, NM 2001 (Rinton Press, Princeton 2002).
8. C. W. McCurdy, M. Baertschy, W. A. Isaacs and T. N. Rescigno, "Reducing Collisional Breakup of a System of Charged Particles to Practical Computation: Electron-Impact Ionization of Hydrogen", in *Photonic, Electronic and Atomic Collisions, Invited Papers* , *Proceedings of the XXII International Conference on Photonic, Electronic and Atomic Collisions,* Santa Fe, NM 2001 (Rinton Press, Princeton 2002).
9. T. N. Rescigno, W. A. Isaacs, A. E. Orel, H.-D. Meyer and C. W. McCurdy, "Theoretical Study of Resonant Vibrational Excitation of CO_2 by Electron Impact", *Phys. Rev. A* **65**, 032716 (2002).
10. C. W. McCurdy, D. A. Horner and T. N. Rescigno, "Time-dependent approach to collisional ionization using exterior complex scaling", *Phys. Rev. A* **65**, 042714 (2002).
11. W. Vanroose, C. W. McCurdy and T. N. Rescigno, "On the Interpretation of Low Energy Electron-CO_2 Scattering", *Phys. Rev. A* **66**, 032720 (2002).
12. T. N. Rescigno and C. W. McCurdy, "Collisional Breakup in Coulomb Systems", in *Many-Particle Quantum Dynamics in Atoms and Molecules* , edited by V. Shevelko and J. Ullrich (Springer-Verlag, Heidelberg, 2003).
13. C. W. McCurdy, W. A. Isaacs, H.-D. Meyer and T. N. Rescigno, "Resonant Vibrational Excitation of CO_2 by Electron Impact: Nuclear Dynamics on the Coupled Components of the $^2\Pi_u$ resonance", *Phys. Rev. A* **67**, 042708 (2003).
14. T. N. Rescigno, M. Baertschy and C. W. McCurdy, "Resolution of phase ambiguities in electron-impact ionization amplitudes", *Phys. Rev. A* **68**, xxxx (2003).

Femtosecond X-ray Beamline for Studies of Structural Dynamics

Robert W. Schoenlein

Materials Sciences Division
Lawrence Berkeley National Laboratory
1 Cyclotron Rd. MS:2-300
Berkeley, CA 94720
email: rwschoenlein@lbl.gov

Background and Program Scope

Modern synchrotrons providing high-brightness, tunable x-ray beams, have driven rapid advances in our understanding of the atomic and electronic structure of condensed-matter via x-ray diffraction and spectroscopy techniques such as EXAFS and XANES. The fundamental time scale on which atomic structural changes can occur is the time scale of a vibrational period, ~100 fs. This is the limiting time scale for atomic motion that determine the course of phase transitions in solids, the kinetic pathways of chemical reactions, and even the function and efficiency of biological processes. The direct study of structural dynamics is a frontier research area in physics, chemistry, materials science and biology. However, the development of this research area has been limited by the lack of suitable tools for probing structural dynamics on the femtosecond time scale. A significant limitation of synchrotron sources is the pulse duration (~100 ps) as determined by the duration of the stored electron bunch. In contrast, advanced femtosecond laser technology now enables the measurement of dynamic processes on time scales shorter than 10 fs. However, femtosecond lasers probe the extended electronic states of condensed matter (using low-energy visible photons) and such states are only indirect indicators of atomic structure.

Our research group has pioneered the development of a novel technique for generating femtosecond x-ray pulses from a synchrotron storage ring by using femtosecond optical pulses to modulate the energy (and time structure) of a stored electron bunch[1]. A simple bend-magnet beamline, incorporating this technique, has been constructed at the Advanced Light Source. The beamline provides ~100 fs x-ray pulses over an energy range of 0.1-12 keV with a flux of $\sim 10^4$ ph/sec/0.1% BW.

The scope of this research program includes the development and characterization of a unique synchrotron bend-magnet beamline for generating 100 fs x-ray pulses based on laser modulation of the stored electron beam. In addition to providing for the development of femtosecond x-rays, this beamline will be a proving ground for time-resolved x-ray science incorporating femtosecond laser systems and end stations suitable for time-resolved x-ray diffraction, EXAFS, XANES, and photoionization measurements. Finally, this research program seeks to develop scientific applications and associated measurement techniques including pump-probe with femtosecond visible and x-ray pulses, ultrafast x-ray streak camera detectors, and dispersive measurement schemes. Initial research will focus on ultrafast solid-solid phase transitions in crystalline solids, light-induced structural changes in molecular crystals, and x-ray interactions with atoms in the presence of strong laser fields.

Recent Progress

During this past year, there has been considerable scientific progress by various beamline users. The dynamics of the charge transfer reaction of photoexcited aqueous $[Ru(bpy)_3]^{2+}$ has been measured. A clear dynamic shift of the Ru L-edge has been observed at the 80 ps

resolution of a full ALS bunch. This shift is associated with the metal-to-ligand charge transfer. This work has been based on the development of a novel scheme for x-ray absorption spectroscopy in the hard x-ray range, providing sensitivity to within a factor of two of the shot-noise limit.

The electronic structure of high-temperature volatile liquids (silicon and carbon) has been studied via x-ray absorption spectroscopy. Measurements at short time scales have enabled the observation of molten liquid at densities near that of the solid. Measurements at the L-edges of liquid silicon, were accurately modeled by a combination of molecular dynamics simulations and the *ab initio* x-ray scattering code FEFF. Measurements at the K-edge of liquid carbon (pre-edge π^* and complementary σ^* absorption features) reveal that the low-density form of liquid carbon is primarily sp-bonded (2-fold coordination), and that the average coordination number increases significantly as the density approaches that of solid forms of carbon.

Gas phase experiments have been developed to probe x-ray interaction with atomic systems in the presence of a strong laser field. Experiments this past year have focused on potassium. A novel time-of-flight apparatus has been developed to measure the charge-state distribution while isolating the interaction of a single ALS pulse. The optical pulse was used to remove the K 4s electron, and the x-rays were tuned to the 1s-4p resonance. Evidence of the laser/x-ray interaction has been observed, and the data is currently being analyzed.

Initial time-resolved measurements (using the full ALS pulse duration) have been made of the thermally-driven solid-solid phase transition in VO_2, and of the photo-induced spin crossover transition in $Fe[tpen]^{3+}$ molecular crystals. In the case of VO_2, we observe a transient increase in absorption at the V L-edge, associated with the formation and growth of the metallic state on the time scale of the 80 ps x-ray pulses. We are presently working on applying these measurements using the femtosecond x-ray pulses in order to probe the fundamental dynamics of the phase transition.

Our current achievements make efficient use of only $\sim 10^4$ x-ray photons per pulse (at 80 ps duration) provided by the 5.3.l bend magnet. The average flux is a significant limitation for nearly all experiments, and this underscores the scientific need for the additional flux provided by a femtosecond undulator beamline. This new beamline is now under development, and is a fundamental component of the future plans for this research program.

During this past year, beamline development has focused on improving the capability for generating femtosecond x-rays. We have characterized the femtosecond x-ray flux and contrast (relative to the long-pulse background). We have demonstrated for the first time that the femtosecond x-ray flux per pulse is comparable to the integrated long-pulse background. A more complete analysis of the laser/e-beam interaction gives confidence that this may be further improved. Another important area of beamline development has been the improvement in the efficiency and resolution of the soft-x-ray spectrometer. (This is an inherited instrument, originally designed for low-resolution spectroscopy.) Specifically, the spectrometer has been reconfigured to accommodate a ruled grating at grazing incidence, and the detector mounting has been re-designed to allow for complete adjustment of the included angle of diffraction.

Considerable progress has been made in the development of an ultrafast x-ray streak camera with a target resolution approaching 100 fs. In comparison with previous cameras, this device will provide enhanced electron detection efficiency and spatial resolution, and will incorporate an improved photoconductive switch design. Many of the camera components have been assembled and tested, including the x-ray photocathode and anode, the electron imaging optics and the electron detection and data storage.

Future Plans

The primary objectives of this research program are: (a) to develop a unique femtosecond bend-magnet beamline and associated instrumentation for time-resolved x-ray research, and (b) to develop and support scientific applications and experiments in time-resolved x-ray science. This program covers the commissioning and characterization of the beamline, development of time-resolved x-ray measurement techniques and instrumentation, and staff effort in operating the beamline and in providing scientific support for time-resolved x-ray research using the beamline.

We will develop advanced diagnostics and instrumentation for femtosecond operation of the beamline including a gated x-ray CCD camera and photodetectors for isolating single synchrotron pulses. This development will build on the techniques currently being employed for the x-ray streak camera. The development of the streak camera will continue. Specifically, we expect to incorporate a new high-speed/high-voltage pulser, streak plates, and photoconductive switch, and test the assembled unit.

Time-resolved NEXAFS measurements in VO_2 will investigate changes in short-range order and bonding following laser excitation. Measurements using the full 80 ps duration of the ALS pulses will be pursued and optimized with the goal of eventually utilizing the high time resolution (and relatively low flux) provided by the femtosecond x-rays. VO_2. is a correlated electron system which is an insulator at room temperature (rutile structure), and undergoes an insulator-metal transition at ~340 K (monoclinic structure). Previous time-resolved optical and x-ray (Bragg) measurements indicate that the phase transition can be induced electronically on a sub-picosecond time scale. Time-resolved absorption measurements on the V L-edge will provide complementary information about the electronic dynamics and on the short-range structural dynamics, and may elucidate the role of the V-O bonding on the phase transition.

AMO research on BL5.3.1 will investigate the bound-state structure of a laser-dressed atom and the resulting perturbations to the x-ray scattering with such dressed atoms. Experiments will focus on the modification of the absorption of x-rays resulting from the laser excitation of the outer electron of Na and K atoms.

Time-resolved L-edge x-ray absorption measurements in molecular crystals of the $[Fe(tpen)]^{2+}$ complex will address fundamental questions about the role of structural dynamics in the ultrafast spin-crossover transition in these molecules. This research builds on previous time-resolved optical studies and static x-ray studies. Optical measurements indicate a sub-picosecond transition from the metal-to-ligand charge-transfer (^{1}MLCT) state to the high-spin ligand-field state ($^5T_2$). Static x-ray measurements indicate a ~15% dilation of the metal-ligand bond distance in the high-spin state, and it has been suggested that this structural change may facilitate the spin-crossover transition.

In order to meet the stringent flux requirements for future x-ray spectroscopy on the femtosecond time scale, we are developing an undulator beamline (the Ultrafast X-ray Science Beamline) at the ALS, which will be dedicated for time-resolved x-ray research. The development, commissioning, operation, and scientific support of this beamline are important components of the future plans for this research program. The beamline will consist of a 1.5 T undulator/wiggler providing femtosecond x-rays for two branchlines: a soft x-ray branchline operating in the 0.3-2 keV range, and a hard x-ray branchline operating in the 2-10 keV range. The soft x-ray branchline will include a spectrograph providing <1 eV resolution for single-wavelength experiments, and ~100 eV bandwidth for dispersive spectroscopic measurements.

The hard x-ray branchline will include a double-crystal monochromator providing ~2 eV resolution. The beamlines will include a high repetition rate (40 kHz) femtosecond laser system with an average power approaching 100 W. The average flux from this beamline is expected to be $10^7 - 10^8$ ph/sec/0.1% BW (with roughly 100x increase in flux from the insertion device relative to the current bend-magnet, and another 10x increase over the present laser repetition rate). The beamline will provide ~200 fs duration x-ray pulses for a wide range of experiments in ultrafast x-ray science.

Publications from DOE Sponsored Research (since 2000)

R.W. Schoenlein, S. Chattopadhyay, H.H.W. Chong, T.E. Glover, P.A. Heimann, C.V. Shank, A. Zholents, and M. Zolotorev, "Femtosecond x-rays from a synchrotron: A new tool for ultrafast time-resolved x-ray spectroscopy," *Science*, **287**, 2237, (2000).

R.W. Schoenlein, S. Chattopadhyay, H.H.W. Chong, T.E. Glover, P.A. Heimann, C.V. Shank, A. Zholents, and M. Zolotorev, "Generation of x-ray pulses via laser-electron beam interaction," *Appl. Phys. B*, **71**, 1, (2000).

R.W. Schoenlein, H.H.W. Chong, T.E. Glover, P.A. Heimann, C.V. Shank, A.A. Zholents, and M.S. Zolotorev, "Femtosecond x-ray pulses from a synchrotron," **Ultrafast Phenomena XII**, T. Elsaesser, S. Mukamel, M.M. Murnane, N.F. Scherer, Eds., Springer-Verlag, 271, (2000).

P.A. Heimann, A.M. Lindenberg, I. Kang, S. Johnson,T. Missalla, Z. Chang, R.W. Falcone, R.W. Schoenlein, T.E. Glover, H.A. Padmore, "Ultrafast x-ray diffraction of laser-irradiated crystals," *Nuclear Inst. and Methods A*, **467**, 986, (2001).

R.W. Schoenlein, H.H.W. Chong, T.E. Glover, P.A. Heimann, W.P. Leemans, H.A. Padmore, C.V. Shank, A. Zholents, M. Zolotorev, and J.S. Corlett, "Femtosecond x-rays from relativistic electrons: New tools for probing structural dynamics," *Comtes Rendus de l'Académie des Sciences IV Physique Astrophysique, **2***, 1371, (2001).

C. Bressler, M. Saes, M. Chergui, D. Grolimund, R. Abela, in: Femtochemistry and Femtobiology: Ultrafast Dynamics in Molecular Science, A. Douhal, J. Santamaria, Eds., World Scientific Publishing Co., Singapore, 449-458 (2002).

C. Bressler, M. Saes, M. Chergui, D. Grolimund, R. Abela, and P. Pattison, "Towards Structural Dynamics in Condensed Chemical Systems Exploiting Ultrafast Time-Resolved X-Ray Absorption Spectroscopy," J. Chem. Phys., **116**, 2954 (2002).

M. Saes, C. Bressler, R. Abela, D. Grolimund, S. Johnson, P.A. Heimann, and M. Chergui, "Observing Photochemical Transients by Ultrafast X-Ray Absorption Spectroscopy," *Phys. Rev. Lett.*, **90**, 047403, 2003.

References

[1] A.A. Zholents and M.S. Zolotorev, *Phys. Rev. Lett.*, **76**, 912, (1996).

ATOMIC AND MOLECULAR PHYSICS RESEARCH AT OAK RIDGE NATIONAL LABORATORY

David R. Schultz, Task Leader, Atomic Physics
ORNL, Physics Division, P.O. Box 2008
Oak Ridge, TN 37831-6372

Principal Investigators

M. E. Bannister [bannisterme@ornl.gov]
C. C. Havener [havenercc@ornl.gov]
H. F. Krause [krausehf@ornl.gov]
J. H. Macek [macek@utk.edu]
F. W. Meyer [meyerfw@ornl.gov]
C. Reinhold [reinhold@ornl.gov]
D. R. Schultz [schultzd@ornl.gov]
C. R. Vane [vanecr@ornl.gov]

OVERVIEW

The ORNL atomic physics program has as its overarching goal the understanding and control of interactions and states of atomic-scale matter. The scientific objective is to enhance progress toward development of detailed understanding of the interactions of multicharged ions, charged and neutral molecules, and atoms with electrons, atoms, ions, surfaces, and solids. Towards this end, a robust experimental program is carried out by our group centered at the ORNL Multicharged Ion Research Facility (MIRF) and as needed at other world-class facilities such as the ORNL Holifield Radioactive Ion Beam Facility (HRIBF) and the CRYRING heavy-ion storage ring in Stockholm. Closely coordinated theoretical activities support this work as well as lead investigations in complementary research. Specific focus areas for the program are broadly classified as particle-surface interactions, atomic processes in plasmas, and manipulation and control of atoms, molecules, and clusters, the latter focus area cross cutting the first two.

The MIRF Upgrade Project – *F. W. Meyer, M. E. Bannister, C. C. Havener, H. F. Krause, R. Rejoub, C. R. Vane, and L. Vergara*

In order to expand the range of energies of intense beams of multicharged ions for atomic collision experiments at MIRF, a two-part upgrade project is currently underway. The first part consists of installation of a 250 kV high-voltage platform with an all permanent magnet Electron Cyclotron Resonance (ECR) ion source. The ECR ion source, designed and fabricated by CEA, Grenoble will operate in the frequency range 12.75 – 24.5 GHz. The higher-energy multicharged ion beams will significantly enhance the capabilities of present online experiments, and make possible investigations at here-to-fore inaccessible energies. For example, the higher energy center-of-mass energies available for the merged electron-ion beams energy loss (MEIBEL) experiment studying electron-impact excitation cross sections, will enable measurements of very low threshold excitation cross sections as well as extension of cross-section measurements to higher energies above threshold. In addition, the higher beam energies will make possible new lines of investigation with this apparatus, such as measurements of dissociative recombination of molecular ions with mass >30, which are difficult with the present generation of storage rings.

For the ion-atom merged beams experiment, the higher energy beams will make possible achievement of velocity matching conditions for higher-Z multicharged projectiles, and, after suitable increase of the neutral beam energies, measurements at higher center-of-mass energies with a correspondingly larger collection solid angle in the laboratory frame.

The second part of the MIRF upgrade project entails fabrication of a floating beamline for the existing CAPRICE ECR ion source, to permit deceleration of extracted ion beams to energies as low as a few eV/q

during injection into grounded experimental chambers. This scheme simplifies the present approach of studying low energy ion-surface interactions, which employs a floating scattering chamber. The new approach will also expand the range of ion-surface investigations in the very low-energy-impact regime, to include, e.g., X-ray spectroscopy studies.

Installation of the 250-kV high-voltage platform and the 30-kW isolation transformer has been completed. Delivery and installation of the new all-permanent-magnet ECR source are planned for late fall of 2003. First delivered beam from the platform is anticipated early in 2004. Implementation of the floating beam line for the CAPRICE ECR source is planned toward end of 2004.

1. F. W. Meyer, "ECR-based Atomic Collision Physics Research at ORNL MIRF", in *Trapping Highly Charged Ions: Fundamentals and Applications,* J. Gillaspy, ed., Nova Science Pub, New York, 2000, pp. 117-164.
2. E. W. Bell et al., *Phys. Rev. A* **49**, 4585 (1994).
3. C. C. Havener, in "*Accelerator Based Atomic Physics Techniques and Applications*", ed. S. Shafroth and J. Austin, (Woodbury New York: AIP Press), pp. 117-145 (1997).
4. V. A. Morozov, and F. W. Meyer, *Rev. Sci. Inst.* **70**, 4515 (2000); *Phys. Rev. Lett.* **86**, 736 (2001).

Low-Energy Multicharged Ion-Surface Interactions – *F. W. Meyer, H. F. Krause, and L. Vergara*

This section deals with investigations at the ORNL MIRF studying the interactions of slow, highly charged ions with metal, semiconductor, and insulator surfaces. We are also interested in surface science that is relevant to controlled fusion devices. Our goal is to improve fundamental understanding of neutralization, energy dissipation, physical and chemical sputtering processes occurring in such interactions, and subsequently to apply the knowledge gained to probe and modify surfaces of amorphous materials, single crystals, thin films, and nanostructures.

We have continued studies and analyses of site-specific neutralization of slow (E~ 4 keV) multicharged F^{q+} and Ne^{q+} ions in large-angle (120^0) collisions on a RbI(100) surface.[1,2] Previous studies of insulator surfaces have employed the grazing incidence approach where the projectile interacts with a large number of target atoms at large impact parameters (b). Our unique large-angle scattering approach greatly limits the number of surface interactions and provides site-specific information. For incident ions normal to the surface (a blocking direction), for example, this arrangement provides final charge-state distributions where most projectile-target interactions essentially occur in either one "hard" collision (b ~ 0.004 nm) or in a "hard-soft" quasi-binary collision on the surface, where the "soft" interaction is distant (b ~ 0.1 nm). Simultaneous recoil energy-loss information identifies the atomic site (Rb or I) associated with each "hard" collision. Rotation of the crystal in the azimuthal direction also allows the selection of different quasi-binary collision sequences (i.e., Rb-I, I-Rb, Rb-Rb, and I-I). In addition, for off-normal projectile beam incidence, the same information is obtained involving some subsurface atomic sites. Numerous Monte Carlo trajectory studies performed in the last year, using the MARLOWE code[3,4] recently ported to the high-performance Macintosh-OSX UNIX platform, have shown that these simple trajectory descriptions are indeed valid. Continuing analyses of our large RbI data sets have shown that the average recoil charge-state from an insulator is considerably higher than that obtained in our previous studies of a corrugated Au(110) surface.[5] In general, yield in the lowest charge states ($q' < 3$) does not depend significantly on whether a hard collision occurs either on Rb or I, despite a significant difference in the number of localized electrons at these different atomic sites. Modeling calculations for the normal incidence cases show that azimuthal variations of the charge state fraction observed between the <100> and <110> axes are the consequence of quasi-binary collisions, prevalent near the <100> direction. Our results on F^{q+} ions also show for the first time that a large recoil anion yield can occur on RbI in just one or two collisions, in contrast to grazing incidence studies. Continuing analyses for off-normal projectile incidence will allow us to assess the role of sequential binary collisions involving the first and second layer of RbI. We will be able to compare and contrast the different neutralization pathways that occur on a flat insulator surface with those that occur on a corrugated Au(110) metal surface.

We also initiated studies of low-energy atomic and molecular hydrogen ions on graphite. There is considerable interest in the surface physics of amorphous graphite hydrogenated by ion beam bombardment because of its relevance in understanding atomic and molecular collisions that occur in divertor regions of controlled fusion devices and in other carbon ablation environments. The full breadth of atomic-scale surface interactions taking place under low-energy (E ~ 10 eV) particle bombardment, an energy regime

that has not been well studied, still remains unclear. A recent molecular dynamics simulation,[6] for example, indicated that physical sputtering yields are seriously underestimated in this low impact energy regime using standard binary ion-atom codes such as TRIM. An understanding of chemical sputtering effects, unpredictable at present, is also needed. Our experience using low-energy ion beams with careful surface preparation techniques at ultra-high vacuum provides the opportunity to perform surface experiments under pristine conditions rarely used in previous studies of graphite and only at much higher beam energy. In our inaugural chemical sputtering study, a beam of D_2^+ ions (1.6 x 10^{14} D/cm^2/s, E ~ 32 eV/D ion) impacts a clean heated surface of ATJ graphite (commonly used in fusion devices) where the ambient pressure is below 2 x 10^{-10} Torr. A quadrupole mass spectrometer samples a small fraction of the slow neutral species emitted from the graphite surface, cleaned and baked at 800 ^{0}C. In the presence of beam, the most interesting changes in mass spectra (1-75 amu range) occur for hydrocarbon species such as CD, CD_2, CD_3, CD_4 and C_2D_2. Preliminary mass spectra recorded when the graphite is heated to 600 ^{0}C, indicate that the yields of CD_3 and CD_4 increase by about a factor of 2 after a deuterium beam integrated flux of only 1–2 x 10^{18} D/cm^2 and an estimated penetration depth below 5 nm. No significant rise in the yield of CH_n species is observed for graphite at room temperature using the same deuterium beam dose. We plan to vary the beam energy, density, D/D_2 composition, and target temperature and study the linearity of these chemical-sputtering processes. Potential saturation effects for the CD_2 and C_2D_2 species may also be studied as our techniques are further developed. Our goal is to fundamentally explain and predict absolute yields for these large molecular species in terms of the ion beam energy and integrated flux.

1. F. W. Meyer, H. F. Krause, and C. R. Vane, *Nucl. Instrum. Meth. Phys. Res.* **B203**, 231 (2003).
2. F. W. Meyer, H. F. Krause, and C. R. Vane, *Nucl. Instrum. Meth. Phys. Res.* **B205**, 700 (2003).
3. H. F. Krause and M. T. Robinson, *MARLOWE Version* **15b**, (2003).
4. M. T. Robinson, *Rad. Effects and Defects in Solids* **130**, 3 (1994); *Phys. Rev. B* **40**, 10717 (1989).
5. V. A. Morozov and F. W. Meyer, *Phys. Rev. Letters* **86**, 736 (2001).
6. E. Salonen et al., *Journal of Nucl. Materials* **290**, 144 (2001).

Electron-Molecular Ion Fragmentation – *M. E. Bannister and C. R. Vane*

A program of electron-molecular ion interaction research has been initiated, complementary to our continuing studies of zero energy dissociative recombination (DR) of relatively simple tri-atomic ions being pursued in collaborative measurements at the CRYRING heavy-ion storage ring at Stockholm University. At the ORNL Multicharged Ion Research Facility (MIRF), we are experimentally investigating low-to-moderate energy electron-molecular ion collisions leading to dissociative excitation (DE), ionization (DI), and recombination (DR). Systems being investigated are of particular relevance to fusion-energy research, plasma-processing applications, and aeronomy. For example, measurements employing the MIRF crossed-beams apparatus[1] have been completed this year for 3 to 100 eV, e^- + CH^+, and CH_2^+ collisions resulting in dissociation through DE and DI channels leading to C^+ ions[2], and to CH^+ ions,[3] respectively. Unexpected resonance structures have been observed in the cross sections vs. collision energy for CH^+ products indicting significant populations of CH_2^+ excited states in the incident beam. The MIRF CAPRICE ECR was used in these measurements, providing 10-keV ions.

A novel source of cold molecular ions is being developed for use in collision studies with well-characterized initial-state ions. The studied interactions will be primarily with electrons, but also with atoms, neutral molecules, and surfaces. This source, known as a surfajet, is based on the expansion of a surface-wave-sustained discharge through a supersonic nozzle to adiabatically relax the vibrational and rotational modes of the extracted ions. Hydrodynamic and spectroscopic diagnostics are being developed in parallel to measure the degree of cooling given by the source, providing initial-state characterization of the target molecular ions.

Electron-molecular ion experiments performed at MIRF and at CRYRING are being coordinated to enable inter-comparisons of results from these complementary experimental approaches. For example, the coordination will help characterize electronic and rovibronic-state distributions of molecular ions extracted from the ECR source at MIRF, where ions normally too heavy for routine measurements at CRYRING will be investigated. A current area of ongoing research at CRYRING involves developing a reliable base of accurate data on fragmentation of cold triatomic di-hydride ions in DR at zero energy. DR results from recombination of a molecular ion with a free electron, leading to disintegration of the molecular ion into several neutral fragments. A complete analysis of measured DR cross sections, fragmentation fractions, and

dynamics for vibrationally cold H_2O^+ ions has recently been published.[4] Analyses of similar measurements for DR of vibrationally cold $NH_2^+$and CH_2^+ are proceeding, especially comparing results for these systems with H_2O^+, and new experimental studies of dissociation fractions and dynamics in DR of H_2S^+ have begun at CRYRING. Studies of more complex molecular ion systems, e.g., heavier hydrocarbons, will also be initiated using existing techniques, modified to accept heavier ions and more channels of decay. The scientific goal is to develop a systematic base of reliable state-specific data for relatively simple molecular ions, sufficient to support progress toward a fundamental understanding of DR, and especially of the roles of initial internal state populations on the routes of mass and energy dissipation in fragmentation. Progress toward that goal has been especially rapid this year with theoretical work[5] on the simplest triatomic H_3^+ at last matching DR rates measured at CRYRING[6] for rotationally and vibrationally cold ions.

1. D. C. Gregory, F. W. Meyer, A. Müller, and P. Defrance, *Phys. Rev. A* **34,** 3657 (1986).
2. M. E. Bannister et al., *Contributed Abstracts*, ICPEAC 2003, Stockholm, Sweden, and to be published in Phys. Rev. A (2003).
3. C. R. Vane et al., *Contributed Abstracts*, ICPEAC 2003, Stockholm, Sweden.
4. Richard Thomas et al., *Phys. Rev. A* **66**, 032715 (2002).
5. V. Kokooutine and C. H. Greene, *Phys. Rev. A* **68**, 012703 (2003).
6. M. Larsson et al., *Contributed Abstracts*, ICPEAC 2003, Stockholm, Sweden.

Ultra-Fast Electron Dynamics in Nanostructures and Bulk Solids – *C. R. Vane and H. F. Krause*

This section deals with investigations of the transport and energy loss of Ti ions in mescopic structures. This is the first step toward forming sufficiently aligned, arrayed, parallel carbon nanotubes through which heavy ions may be channeled. Measurements of channeled bare ion scattering, energy loss, and radiative electron-capture X rays will provide the means to determine the electron densities and Compton profiles inside nanotubes grown in these channels. This is collaborative research with members of the ORNL Condensed Matter Sciences and Chemical Sciences Divisions who supply and characterize nanostructured materials.

In the past, guided transmission of 3-keV Ne^{7+} ions was observed in 100-nm-diameter capillaries of length 10 μm produced by etching ion tracks in a polyethlyene polymer film.[1] To determine whether the phenomenon occurs for highly charged ions at a much higher energy, we attempted to guide fully-stripped 200-MeV Ti ions through an aluminum-oxide array having capillaries of diameter 100 nm and 60 μm length. In the experiment, a small highly collimated beam impinged on the array held by a precision goniometer (i.e., very low-projectile transverse energy). The energy of transmitted ions was detected using a solid-state detector. The capillary length was sufficient to stop ions that passed completely through 60 μm of bulk material. Precise alignment of the nanopores to the beam direction was easily accomplished by monitoring the count rate of transmitted ions in computerized angular scans of the goniometer.

In these initial experiments, no characteristic evidence of channeled or guided 200-MeV Ti ions was observed. Although a fraction of the transmitted ions did traverse capillary channels with full beam energy, the measured average beam energy was below half the incident energy. This finding indicates that virtually all transmitted ions underwent one or more violent collisions in the capillary, thus redirecting each ion through capillary walls and a significant amount of bulk material. Also, no evidence of improved "guidance" was observed by first conditioning the sample with an intense projectile beam.[1] Future experiments at much lower energy and with other mesoscopic materials are planned using our upgraded MIRF.

1. N. Stolterfoht *et al., Phys. Rev. Letters* **88,** 133201 (2002); N. Stolterfoht *et al., Nucl. Instrum. Meth. Phys. Res. B* **203,** 246 (2003).

Near-Thermal Collisions of Multicharged Ions with H and Multi-Electron Targets – *C. C. Havener, R. Rejoub, C. R. Vane, P. S. Krstic*

The merged-beams technique[1] is being used to explore near-thermal collisions (meV/u – keV/u) of multicharged ions with neutral atoms and molecules, providing benchmark measurements for comparison with state-of-the-art theories. Electron capture by multicharged ions from neutrals is important in many technical plasmas including those used in materials processing, lighting, ion-source development, and for

spectroscopic diagnostics and modeling of core, edge, and diverter regions of magnetically confined fusion plasmas.

For endoergic electron capture where the cross section decreases with decreasing energy as the threshold energy is approached, the functional form of the cross section provides a sensitive test of our understanding of collision dynamics. For our recent Ne^{2+} + H measurements,[2] the cross section was expected to show a simple exponential decrease due to the predicted radial coupling between initial and final states. However, a "change of slope" was observed in the decreasing cross section, similar to predictions for the He^{2+} + H system, where the change in slope is attributed to the onset of rotational coupling. The importance of rotational coupling for Ne^{2+} + H system was confirmed with a careful analysis of all the potential energy curves. To further explore rotational coupling, we have initiated merged-beams measurements and a vigorous theoretical study[3] for the fundamental He^{2+} + H system where, below 300 eV/u, the contribution due to rotational coupling dominates the cross section.

Previous measurements for Ne^{3+} + H suggest the electron capture cross section sharply decreases toward lower energies in contrast to theoretical estimates. Our recently completed merged-beams measurements show an increasing cross section toward lower energies with a sharp increase below 1 eV/u. Such a sharp increase is indicative of trajectory effects due to the ion-induced dipole attraction. State-of-the-art molecular-orbital close-coupling calculations have been performed by P. Stancil at the University of Georgia and show good agreement at the lower collision energies.

The new Cs sputter source allows merged-beams measurements to be performed with a variety of neutral beams other than H and D, such as Li, B, Na, Cr, Fe,… , and molecular beams such as O_2, CH_2,… Last year, improvements in our Li beam intensity allowed for absolute measurements[4] with Ar^{2+} + Li, which showed similar energy dependence but a factor of two differences with previous measurements. The Li beam optics has been improved further and will allow additional testing. Our goal is to measure He^{2+} + Li where strong shape resonances are predicted due to the strong ion-induced dipole attraction.

Modifications to the merge-beams apparatus to take advantage of the ECR upgrade project are under way. The upgrade will allow direct observation of isotope effects at low energy, allowing measurements with both H and D. Also, due to the availability of higher energy beams and a shortened merge-path, the apparatus will have an increased angular collection ensuring full collection of the signal at eV/u energies.

1. C. C. Havener in "T*he Physics of Multiply and Highly Charged Ions,*" ed. Fred J. Currell, Kluwer Academic Publishers, Dordreecht, September 2003.
2. T. Mroczkowski, D. W. Savin, R. Rejoub, P. S. Krstic, and C. C. Havener, to be published in Physical Review A.
3. P. Krstic, R. Rejoub, and C. C. Havener, *Abstracts of Contributed Papers,* XXIII ICPEAC, Stockholm, Sweden, 2003, p. 155.
4. R. Rejoub and C. C. Havener, *Abstracts of Contributed Papers,* XXIII ICPEAC, Stockholm, Sweden, 2003, p. 154.

Theoretical Atomic Physics – C. *Reinhold, J. Macek, D. R. Schultz, S. Ovchinnikov, T. Minami, and J. Burgdörfer*

Open quantum systems are usually described by their reduced density matrices. Their dynamics is governed by a Lindblad master equation that can be solved in terms of quantum trajectory Monte Carlo (QTMC) sampling. For systems involving a high-dimensional Hilbert space, QTMC methods are advantageous in terms of computer storage compared to a direct solution of the Lindblad equation. One key feature of the standard Lindblad equation is that it describes strictly unitary time transformations of the reduced density matrix. This property is of limited value in simulations of atomic systems when only finite subspaces can be represented within any realistic finite basis size and the coupling to the complement cannot be neglected. We have derived a generalized Lindblad form (and its QTMC implementation) that accounts for the outgoing flux of probability out of the finite Hilbert subspace while neglecting the back flow. For the case of multi-level radiative decay of an ion, where the exact solution can be obtained, our approach yields the correct result. We are implementing the new approach to describe multiple collisions with particles in a solid and the line emission intensities arising from the transmission of fast Ar^{18+} ions through amorphous carbon foils in an attempt to explain recent experimental data.

The production of selected Stark states at high n ($n > 100$) remains a challenge because the oscillator strengths associated with their excitation are small, and because the Stark energy levels are closely spaced

requiring the use of narrow line-width frequency-stabilized lasers and the minimization of Doppler effects. We have demonstrated that strongly polarized quasi-one-dimensional very-high-*n* (potassium) Rydberg atoms can be produced by photoexcitation of an ensemble of Stark states in the presence of a weak *dc* field. Calculations and experiment show that states located near the Stark-shifted *d*-level have sizable polarizations. We plan to study the non-linear dynamics of these polarized states under the influence of a train of unipolar pulses. Depending on the orientation of the Rydberg states, the dynamics is expected to be regular or chaotic and should yield clear differences in the survival probability of Rydberg atoms. When the dynamics becomes globally chaotic, the resulting system provides a low-dimensional laboratory to study quantum localization.

We have developed a Liouville master equation approach to describe the interaction of highly charged ions with insulator surfaces including the close-collision regime above the surface. Our approach employs a Monte-Carlo solution of the master equation for the joint probability density of the ionic motion and the electronic population of the projectile and the target surface. It includes single as well as double particle-hole de-excitation processes and incorporates electron correlation effects through the conditional dynamics of population strings. The input in terms of elementary one- and two-electron transfer rates is determined from CTMC calculations as well as quantum mechanical Auger calculations. For slow projectiles and normal incidence, the ionic motion depends sensitively on the interplay between image acceleration towards the surface and repulsion by an ensemble of positive hole charges in the surface ("trampoline effect"). For Ne^{10+} ions we find that image acceleration dominates and no collective backscattering high above the surface takes place. For grazing incidence, our simulation delineates the pathways to complete neutralization, in accordance with recent experimental observations.

Theoretical Atomic Physics: Recent Progress – *J. H. Macek and S. Yu. Ovchinnikov*

We have extended the advanced adiabatic theory to allow for processes such protonium formation in the collisions of antiprotons with atomic hydrogen. Our modification extends the scope of the advanced adiabatic theory to include ion-atom collision processes where the heavy particles bind and one or more free electrons leave. We have applied the theory to protonium formation and find good agreement with previous calculations for total ionization, and protonium formation. In the latter case we extract the *n* and *l* distribution of the protonium states. These distributions are used to estimate annihilation cross sections relevant to the formation of antihydrogen.[1]

Future plans: Top of barrier propagation is a crucial element in bringing exact calculations of electron energy and angular distributions into agreement with observations. This aspect of the electron motion in ion-atom collisions can be treated using the top of barrier propagator. Initial applications of this propagator, however, overcompensates for top-of-barrier motion at low energies. We will derive a version of this propagator applicable at low energies and apply this revised propagator to previously published electron distributions computed using nearly exact numerical solutions of the time dependent Shrödinger equation.

1. S. Yu. Ovchinnikov and J. H. Macek, "Anniilation of Low-energy Antiprotons in Hydrogen," CAARI 2002, AIP Conference Proceedings **680** (2003).

References to Publications of DOE Sponsored Research from 2001-2003 (decending order)

Year 2003 publications

"Absolute Measurements of Cross Sections for Near-Threshold Electron-Impact Excitation of Na-like and Mg-like Multiply Charged Ions," A.C.H. Smith, M. E. Bannister, Y.-S. Chung, A M. Derkatch, N. Djuric, H. F. Krause, D. B. Popovic, B. Wallbank, and G. H. Dunn, Nucl. Instrum. Methods Phys. Res. B **205**, 421 (2003).

"Electron-Impact Dissociation of CH^+ Ions: Measurements of C^+ Fragment Ions," M. E. Bannister, H. F. Krause, C. R. Vane, N. Djuric, D. B. Popovic, M. Stepanovic, G. H. Dunn, Y.-S. Chung, A.C.H. Smith, and B. Wallbank, Phys. Rev. A (to be published 2003).

"Observation of Trielectronic Recombination in Be-like Cl Ions," M. Schnell, G. Gwinner, N. R. Badnell, M. E. Bannister, S. Böhm, J. Colgan, S. Kieslich, S. D. Loch, D. Mitnik, A. Müller, M. S. Pindzola, S. Schippers, D. Schwalm, W. Shi, A. Wolf, and S.-G. Zhou, Phys. Rev. Letters **91**, 043001 (2003).

"Elastic Processes Involving Vibrationally Excited Molecules in Cold Hydrogen Plasmas," P. S. Krstic, D. R. Schultz, J. Phys. B **36**, 385 (2003).

"Production of Quasi-One-Dimensional Very-High-n Rydberg Atoms," C. L. Stokely, J. C. Lancaster, F. B. Dunning, D. G. Arbo, C. O. Reinhold, J. Burgdörfer, Phys. Rev. A **67**, 013403 (2003).

"Liouville Master Equation for Multi-Electron Dynamics: Neutralization of Highly Charged Ions Near an LiF Surface," K. Wirtz, C. O. Reinhold, C. Lemell, J. Burgdörfer, Phys. Rev. A **67**, 012903 (2003).

"Quantum Trajectory Monte Carlo Method for Internal State Evolution of Fast Ions Traversing Amorphous Solids," T. Minami, C. O. Reinhold, J. Burgdörfer, Phys. Rev. A **67**, 022902 (2003).

"Ionization of Helium by Antiprotons: Fully Correlated, Four-Dimensional Lattice Approach," D. R. Schultz, P. S. Krstic, Phys. Rev. A **67**, 022712 (2003).

"Elastic and Transport Cross Sections for Argon in Hydrogen Plasmas," P. S. Krstic, D. R. Schultz, T. Chung, Phys. Plasmas **10**, 869 (2003).

"Site-Resolved Neutralization of Slow Singly and Multiply Charged Ions during Large-Angle Backscattering Collisions with RbI(100)," F. W. Meyer, H. F. Krause, C. R. Vane, Proceedings, 14th International Workshop on Inelastic Ion-Surface Collisions, Ameland, The Netherlands, Sept. 8-13, 2002, Nucl. Instrum. Methods Phys. Res. B **203**, 231 (2003).

"Projectile Neutralization in Large-Angle Back-Scattering of Slow F^{q+}, Ne^{q+}, and Ar^{q+} Incident on RbI(100)," F. W. Meyer, H. F. Krause, C. R. Vane, Nucl. Instrum. Methods Phys. Res. B **205**, 700 (2003).

"Highly Transverse Velocity Distribution of Convoy Electrons Emitted by Highly Charged Ions," M. Seliger, K. Tokesi, C. O. Reinhold, J. Burgdörfer, Nucl. Instrum. Methods Phys. Res. B **205**, 830 (2003).

"Pulse-Induced Focusing of Rydberg Wavepackets," D. G. Arbo, C. O. Reinhold, J. Burgdörfer, A. K. Pattanayak, C. L. Stokely, W. Zhao, J. C. Lancaster, F. B. Denning, Phys. Rev. A **67,** 063401 (2003).

"Annihilation of Low Energy Antiprotons in Hydrogen," S. Yu. Ovchinnikov and J. H. Macek, *CAARI 2002*, AIP Conference Proceedings **680** (2003).

"Quantum Trajectory Monte Carlo Method Describing the Coherent Dynamics of Highly Charged Ions," T. Minami, C. O. Reinhold, and J. Burgdörfer, Nucl. Instrum. Meth. Phys. Res. **B205**, 818 (2003).

"Liouville Master Equation for Multi-electron Dynamics: Neutralization of Highly Charged Ions near a LiF Surface," L. Wirtz, C. O. Reinhold, C. Lemell, and J. Burgdörfer, Phys. Rev. A **67**, 012903 (2003).

"Interaction of Highly Charged Ions with Insulator Surfaces at Low Velocities: Estimates for Auger Rates," J. Burgdörfer, C. O. Reinhold, and F. Meyer, Nucl. Instrum. Meth. Phys. Res. **B205**, 690 (2003).

"The Kicked Rydberg Atom: A New Laboratory for Study of Non-Linear Dynamics," F. B. Dunning, C. O. Reinhold, and J. Burgdörfer, Physica Scripta **68**, C44 (2003).

Year 2002 publications

"Transport Cross Sections Relevant to Cool Hydrogen Plasmas Bounded by Graphite," D. R. Schultz, P. S. Krstic, Phys. Plasmas **9**, 64 (2002).

"Charge Transfer Processes in Slow Collisions of Protons with Vibrationally Excited Hydrogen Molecules [Invited Presentation]," P. S. Krstic, D. R. Schultz, R. K. Janev, Proceedings, Workshop on Molecule Assisted Recombination and Other Processes in Fusion Divertor Plasmas, Oak Ridge, Tenn., Sept. 8-9, 2000, Physica Scripta **T96**, 61 (2002).

"Lassettre's Theorem for Excitation of Ions by Charged Particle Impact," J. H. Macek, and N. Avdonina, J. Phys. B **35**, 1775 (2002).

"Electron Capture in Collisions of S^{4+} with Helium," J. G. Wang, A. R. Turner, D. L. Cooper, D. R. Schultz, M. J. Rakovic, W. Fritsch, P. C. Stancil, B. Zygelman, J. Phys. B **35**, 3137 (2002).

"Working Group on Collision Processes," D. R. Schultz, P. C. Stancil, Rep. Astron. XXVA, 1001 (2002).

"Merged-Beams Measurements of Electron-Impact Excitation of $Al^{2+}(3s^2S \rightarrow 3p^2P)$," M. E. Bannister, H. F. Krause, N. Djuric, D. B. Popovic, G. H. Dunn, Y.-S. Chung, A.C.H. Smith, Phys. Rev. A **66**, 032707 (2002).

"Atomic and Molecular Databases for Fusion Divertor Plasma [Invited Presentation]," P. S. Krstic, D. R. Schultz, pp. 277-286 in Proceedings, 3rd International Conference on Atomic and Molecular Data and Their Applications, Gatlinburg, Tenn., April 24-27, 2002, AIP Conference Proceedings **636**, American Institute of Physics, Melville, N.Y., 2002.

"Ion-Implantation-Related Atomic Collision Studies at the ORNL MIRF [Invited Presentation]," F. W. Meyer, M. E. Bannister, C. C. Havener, H. F. Krause, P. Krstic, D. R. Schultz, A. Aggarwal, D. Swensen, F. Yan, pp. 125-134 in Proceedings, 13th APS Topical Conference on Atomic Processes in Plasmas, Gatlinburg, Tenn., April 22-25, 2002, AIP Conference Proceedings **635**, American Institute of Physics, Melville, N.Y., 2002.

"Proceedings of Third International Conference on Atomic and Molecular Data and Their Applications (ICAMDATA)," Gatlinburg, Tenn., April 24-27, 2002, D. R. Schultz, P. S. Krstic, F. Ownby (editors) AIP Conference Proceedings **636**, American Institute of Physics, Woodbury, N.Y., 2002.

"Proceedings of 13th APS Topical Conference on Atomic Processes in Plasmas," Gatlinburg, TN, April 22-25, 2002, D. R. Schultz, F. W. Meyer, F. Ownby (editors), AIP Conference Proceedings **635**, American Institute of Physics, Woodbury, N.Y., 2002.

"Quantum Localization in the High Frequency Limit," E. Persson, S. Yoshida, X.-M. Tong, C. O. Reinhold, J. Burgdörfer, Phys. Rev. A **66**, 043407 (2002).

"Electromagnetically Induced Nuclear-Charge Pickup Observed in Ultrarelativistic Pb Collisions," C. Scheidenberger, I. A. Pshenichnov, T. Aumann, S. Datz, K. Sümmerer, J. P. Bondorf, D. Boutin, H. Geissel, P. Grafström, H. Knudsen, H. F. Krause, B. Lommel, S. P. Møller, G. Münzenberg, R. H. Schuch, E. Uggerhøj, U. Uggerhøj, C. R. Vane, Ventura, Z. Z. Vilakazi, and H. Weick, *Phys. Rev. Lett.* **88**, 042301 (2002).

"Photonic, Electronic, and Atomic Collisions," *Proceedings of the Invited Talks, XXII ICPEAC*, Editors, J. Burgdörfer, J. S. Cohen, S. Datz, and C. R. Vane (Rinton Press, Princeton, NJ, 2002).

"Laboratory Measurements of Charge Transfer on Atomic Hydrogen at Thermal Energies," C. C. Havener, C. R. Vane, H. F. Krause, P. C. Stancil, T. Mrodzkowski, and D. Savin, *Proceedings, NASA Laboratory Astrophysics Workshop*, NASA-Ames Research Center, CA May 2002.

"Ejected-Electron Spectrum in Low-Energy Proton-Hydrogen Collisions," D. R. Schultz, C. O. Reinhold, P. S. Krstic, and M. R. Strayer, Phys. Rev. A **65**, 052722 (2002).

"Exact Electron Spectra in Collisions of Two Zero-Range Potentials with Non-Zero Impact Parameters," S. Yu. Ovchinnikov, D. B. Khrebtukov, and J. H. Macek, Phys. Rev. A **65**, 032722 (2002).

"Evidence of Collisional Coherences in the Transport of Hydrogenic Krypton Through Amorphous Carbon Foils," T. Minami, C. O. Reinhold, M. Seliger, J. Burgdörfer, C. Fourment, B. Gervais, E. Lamour, J. P. Rozet, and D. Vernhet, Nucl. Instrum. Meth. Phys. Res. **193**, 79 (2002).

"Time Dependent Dynamics of Atomic Systems," M. S. Pindzola, F. J. Robicheaux, J. Colgan, D. M. Mitnik, D. C. Griffin, and D. R. Schultz, in *Photonic, Electronic & Atomic Collisions, Proceedings of the XXII ICPEAC*, J. Burgdörfer, J. S. Cohen, S. Datz, and C. R. Vane, eds. (Rinton Press, Princeton, 2002), p. 483.

"Recent Advances and Applications of Lattice, Time-Dependent Approaches: Fundamental One- and Two-Electron Collision Systems," D. R. Schultz, P. S. Krstic, C. O. Reinhold, M. R. Strayer, M. S. Pindzola, and J. C. Wells, in *Photonic, Electronic & Atomic Collisions, Proceedings of the XXII ICPEAC*, J. Burgdörfer, J. S. Cohen, S. Datz, and C. R. Vane, eds. (Rinton Press, Princeton, 2002), p. 536.

"Comparative Study of Surface-Lattice-Site Resolved Neutralization of Slow Multicharged Ions During Large-Angle Quasi-Binary collisions with Au(110): Simulation and Experiment," F. W. Meyer and V. A. Morozov, Nucl. Inst. Methods Phys. Res. **B193**, 530 (2002).

"Large-Angle Backscattering of Ar^{q+} (q = 1 – 13) During Quasi-Binary Collisions with CsI(100) in the Energy Range 10 eV/q – 2.8 keV/q: Energy Loss Analysis and Scattered Charge-State Distributions," W. Meyer, V. A. Morozov, J. Mrogenda, C. R. Vane, S. Datz, Nucl. Instrum. Meth. Phys. Res. **B193**, 508 (2002).

Quantum Localization in the High Frequency Limit," E. Persson, S. Yoshida, X. Tong, C. O. Reinhold, and J. Burgdörfer," *Phys. Rev. A* **66**, 043407 (2002).

"Quantum Transport of Kr^{35+} Ions through Amorphous Carbon Foils," T. Minami, C. O. Reinhold, M. Seliger, J. Burgdörfer, C. Fourment, B. Gervais, E. Lamour, J.-P. Rozet, and D. Vernhet, Phys. Rev. A **65**, 032901 (2002).

"Transient Phase Space Localization," C. L. Stokely, F. B. Dunning, C. O. Reinhold, and A. K. Pattanayak, Phys. Rev. A **65,** 021405 (2002).

"Absolute Cross Sections for Electron-Impact Excitation of the $3d^2\ ^3F \rightarrow 3d4p\ ^3D,\ ^3F$ Transitions in Ti^{2+}," Popovic, D. B., M. E. Bannister, R.E.H. Clark, Y.-S. Chung, N. Djuric, F. W. Meyer, A. Müller, A. Neau, M. S. Pindzola, A.C.H. Smith, B. Wallbank, and G. H. Dunn, Phys. Rev. A **65**, 034704/1-4 (2002).

"Three-Body Recombination of Ultracold Atoms Near a Feshbach Resonance," O. J. Kartavtsev and J. H. Macek, Few-Body Systems **31**, 249 (2002).

Year 2001 publications

"Excitation of He^+ to the $2\ ^2S$ and $2\ ^2P$ States by Electron Impact," A.C.H. Smith, M. E. Bannister, Y.-S. Chung, N. Djuric, G. H. Dunn, A. Neau, D. Popovic, M. Stephanovic, and B. Wallbank, J. Phys. B **34**, L571 (2001).

"Breakup and Recombination of Identical Bosons: He Dimer-Monomer Collisions" [Invited Presentation], J. H. Macek, pp. 130-132 in Proceedings, 16th International Conference on the Application of Accelerators in Research and Industry (CAARI 2000), Denton, Texas, Nov. 1-4, 2000, American Institute of Physics Conference Proceedings **576**, Melville, N.Y., 2001.

"Path-Dependent Neutralization of Multiply Charged Ar Ions Incident on Au (110)," V. A. Morozov and F. W. Meyer, Phys. Rev. Lett. **86**, 736 (2001).

"Target Orientation Dependence of the Backscattered Intensities and Charge Fractions Observed for Large-Angle Quasi-Binary Collisions of Ar^{q+} Ions with Au(110)," A. Morozov and F. W. Meyer, Phys. Scripta **T92**, 31 (2001).

"Electrostatic Trap for keV Ion Bemas," H. F. Krause, C. R. Vane, and S. Datz, in Proceedings, 16th Intl. Conf. On Application of Accelerators in Research and Industry, Editors – J. L. Duggan and I. L. Morgan, AIP Press, New York, AIP Conferences **576,** 126-129 (2001).

"Charge Transfer Experiment," C. C. Havener, in Spectroscopic Challenges of Photoionized Plasmas, Editors, G. Ferland and D. Savin, ASP Conference Series, 2001.

"Charge Fraction Measurements for 2.4 – 35 keV Ar^{q+} (q = 2–13) Projectile Backscattered from Au(110)," F. W. Meyer, V. A. Morozov, S. Datz, and R. Vane, Phys. Scripta **T92**, 182 (2001).

"Adiabatic Limit of Inelastic Transitions," P. Krstic, C. O. Reinhold, and J. Burgdörfer, Phys. Rev. A **63** 032103 (2001).

"Autoionization of Doubly and Triply Excited States of Li^+ and Li Produced in Li^{3+} Ion Collision with C_{60}, Ar, and Xe," D. V. Lukic, P. R. Focke, C. Koncz, V. A. Morozov, F. W. Meyer, and I. A. Sellin, Physica Scripta **T92**, 174 (2001).

"Relativistic Electron Transport Through Carbon Foils," M. Seliger, K. Tökesi, C. O. Reinhold, J. Burgdörfer, Y. Takabayashi, T. Ito, K. Komaki, T. Azuma, and Y. Yamazaki, Physica Scripta **T92**, 211 (2001).

"Low-Energy Electron Capture by Cl^{7+} from D Using Merged Beams," J. S. Thompson, A. M. Covington, P. S. Krstic, Marc Pieksma, J. L. Shinpaugh, P. C. Stancil, and C. C. Havener, Phys. Rev. A **63**, 012727 (2001).

"Dynamics of Dissociative Recombination of Molecular Ions: Three-body Breakup of Triatomic Di-Hydrides," S. Datz, J. Phys. Chem. A **105**, 2369 (2001).

"Electron Capture and Ionization of 33-TeV Pb Ions in Gas Targets," H. F. Krause, C. R. Vane, S. Datz, P. Grafström, H. Knudsen, U. Mikkelsen, C. Scheidenberger, R. H. Schuch, and Z. Vilakazi, Phys. Rev. A **63**, 032711 (2001).

"Random and Channeled Energy Loss of 33.2-TeV Pb Nuclei in Silicon Single Crystals," S. Pape Møller, V. Biryukov, S. Datz, P. Grafström, H. Knudsen, H. F. Krause, C. Scheidenberger, U. I. Uggerhøj, and C. R. Vane, Phys. Rev. A **64**, 032902 (2001).

"Inelastic Transitions in Slow Heavy-Particle Atomic Collisions," P. S. Krstic, C. O. Reinhold, and J. Burgdörfer, Phys. Rev. A **63**, 052702 (2001).

"Designing Rydberg Wave Packets Using Trains of Pulses," C. O. Reinhold, J. Burgdörfer, S. Yoshida, B. E. Tannian, C. L. Stokely, and F. B. Dunning, J. Phys B. **34,** L551 (2001).

"Probing Coordinates of Rydberg Wave Packets," B. E. Tannian, C. L. Stokely, F. B. Dunning, C. O. Reinhold, and J. Burgdörfer, Phys. Rev. A **64,** 021404 (2001).

"Transport of Kr^{35+} Inner-Shells through Thin Carbon Foils," D. Vernhet, C. Fourment, E. Lamour, J.-P. Rozet, B. Gervais, L. J. Dube, F. Martin, T. Minami, C. O. Reinhold, M. Seliger, and J. Burgdörfer, Physica Scripta **T92**, 233 (2001).

"Vertical Incidence of Slow Ne^{10+} Ions on a LiF Surface: Suppression of the Trampoline Effect," L. Wirtz, C. Lemell, J. Burgdörfer, L. Hagg, and C. O. Reinhold, Nucl. Instrum. Meth. Phys. Res. **182**, 36 (2001).

"Siegert-Pseudostate Representation of Quantal Time-Evolution: A Harmonic Oscillator Kicked by Periodic Pulses," S. Tanabe, S. Watanabe, N. Sato, M.Satsuzawa, S. Yoshida, C. O. Reinhold, and J. Burgdörfer, Phys. Rev. A **63**, 052721 (2001).

"Time-Dependent Treatment of Electron-Hydrogen Scattering of Higher Angular Momenta (L>0)," D. O. Odero, J. L. Peacher, D. R. Schultz, and D. H. Madison, Phys. Rev. A **63**, 022708 (2001).

"On Quantum-Classical Correspondence in Classical Studies of Atomic Processes," M. Rakovic, D. R. Schultz, P. C. Stancil, and R. K. Janev, J. Phys. A **34**, 473 (2001).

"Classical/Quantal Correspondence in State-Selective Charge Transfer for Partially Stripped Ion Impact on Atomic Hydrogen: Improvements to the CTMC Method," D. R. Schultz, P. C. Stancil, and M. J. Rakovic, J. Phys. B **34**, 2739 (2001).

Research Summaries

(single-PI grants by PI)

Properties of Transition Metal Atoms and Ions

Donald R. Beck
Physics Department
Michigan Technological University
Houghton, MI 49931
e-mail: donald@mtu.edu

Program Scope

Transition metal atoms are technologically important in plasma physics (e.g. as impurities in fusion devices), Atomic Trap Trace Analysis (detection of minute quantities of radioactive species), astrophysical abundance (e.g. Fe II) and atmospheric studies, deep-level traps in semiconductors, hydrogen storage devices etc. The more complicated rare earths which we are beginning to study are important in lasers, high temperature super-conductivity, advanced lighting sources, magnets, etc.

Because of the near degeneracy of nd and $(n+1)$s electrons in lightly ionized transition metal ions and the differing relativistic effects for d and s electrons [1], any computational methodology must simultaneously include the effects of correlation and relativity from the start. We do this by using a Dirac-Breit Hamiltonian and a Relativistic Configuration Interaction (RCI) formalism to treat correlation. Due to the presence of high-l (d) electrons, computational complications are considerably increased over those in systems with just s and/or p valence electrons. These include the following: (1) larger energy matrices (5-10x larger) because the average configuration can generate many more levels [2]. Multi-root RCI calculations with matrices of order 20,000 are becoming common. With the use of REDUCE [3], these can be equivalent to calculations 10 times (or more) larger, (2) increased importance of interactions with core electrons (d's tend to be more compact, and there can be more of them), (3) a significant variation of the d radial functions with level (J), which either requires the presence of second order effects. Methodological improvements are most needed in the treatment of second order effects.

We desire to develop the methodology to a point where properties of $(\mathrm{d+s})^n$ states can be treated accurately and efficiently. To date, this is only possible for $n < 5$. A systematic knowledge of which basis functions are crucial to a physical property can allow us to limit basis set sizes, while retaining accuracy. To this end, contributions to properties are generated at all computational stages. These are particularly helpful in determining where the saturation of radial basis sets may need further exploration.

Recent Progress

A. Zr III and Nb IV Energy Levels, Oscillator Strengths, Landé g-values

Zr III is an astrophysically important species whose energy levels have been recently remeasured [4], for which there exists some semi-empirical predictions of f-values. For the isoelectronic Nb IV energy levels, a modern measurement exists [5], but with few f-value predictions. In both species the $5s^2$ and 5s5p levels have been hard to locate; they are excited, are involved in few strong transitions,

and for 5s5p embedded in two nearly degenerate (1-2000 cm^{-1} separations) 4d np and 4d nf Rydberg series.

Even though the number of valence electrons is low ($N = 2$), the near degeneracy presents a challenge to the computationalist. Second order effects are important if the reference space is restricted to just 5s5p and the 4d5p ($J = 1$) states below it. These are harder than first order effects to treat systematically, as it is not possible to include them all. Here, we have mostly avoided this problem by enlarging the reference space to include the 4d6p, 4d7p, 4d4f and 4d7p levels. This required extending and automating the analysis part of the codes [3] to make sure each of the reference functions received "equal treatment". E.G. if the excitation $4p^2 \rightarrow 4d^2$ appeared for the 4d5p and 5s5p functions, it was also included for the 4d6p$\cdots$ functions. This maintains the correct separation between the basis functions, so necessary to their correct mixing in the final wavefunction. We were able to accurately extract 17 levels from the $J = 1$ RCI matrix, and perhaps another 6-12 additional levels could have been accurately extracted. For the more complicated (higher N) Fe ions, for example, one can not be as optimistic.

The net result is perhaps our most accurate calculations on Transition Metal atoms. Energy separation errors between adjacent $J = 1$ energy levels average 210 cm^{-1} for Zr III (300 cm^{-1} for Nb IV). One striking improvement is in our repositioning of the Nb IV $5s^2$ $J = 0$ level. In the prior work [5], this position was predicted, not measured. The RCI result is in good agreement with a very recent measurement [6].

Length and velocity gauge agreements average 3% for the larger f-values ($> .01$). The semi-empirical f-values are mainly somewhat smaller than the RCI ones, except in two cases where the discrepancies are quite large (Zr III). In the one case, this is probably because two levels are extremely close (300 cm^{-1}), so that their RCI and semi-empirical identities are flipped. The source of the discrepancy in the second case is not so obvious, but we note the absence of the $4f^2$ $J = 0$ basis function in the semi-empirical work, whose inclusion is called for [7], when 4d nf basis functions are important for the odd parity levels. The RCI results, which have been submitted for publication [8], also include Landé g-values.

B. Tc I lifetimes

The most complex calculation undertaken during this project was to obtain accurate f-values for $(d+s)^7 \rightarrow (d+s)^6p$ Tc I transitions. No prior *ab initio* results exist. The specific goal was to find a strong transition involving just two levels (absorption and emission), which could be used in Atomic Trap Trace Analysis (ATTA) studies [9]. One was found: $4d^6\ 5s\ {}^6D_{9/2} \rightarrow 4d^6\ 5p\ {}^6F_{11/2}$ with $f \sim 0.3$, with the ${}^6D_{9/2}$ having a long lifetime (decays via $E2$).

We calculated wavefunctions for all $J = 5/2$-$11/2$ odd parity levels below 34516 cm^{-1}, and all even parity $J = 3/2$-$9/2$ levels below 17330 cm^{-1}, a total of 42 levels [10]. The average energy difference error between adjacent levels is 536 cm^{-1}. This is considerably higher than for Zr III, due to the greatly increased complexity of the calculations, arising from the higher N. There are more basis functions, each expanded in more determinants. Radial functions (particularly 4d) can vary significantly with configuration ($d^5\ s^2$ *vs* d^6 s), and even with term. Errors as large as 5000 cm^{-1} can be introduced using just a single set of 4d, 5s radials (generated from $d^5\ s^2$). Such errors are reduced by using a second set of radials ($4d'$,$5s'$) generated from d^6 s .

Without correlation, errors in absolute energy differences can exceed 7500 cm^{-1}. Correlation effects can be not only differentially large, but absolutely large. Since Tc I has a spectrum [10]

whose levels are frequently nearly degenerate (2-3000 cm^{-1}), the absolutely large correlation effects can require inclusion of second order effects, which are difficult to handle (large number of basis functions, large number of determinants). Presently, only the energetically largest of these could be included directly, even with extensive use of REDUCE [3]. For f-values the average gauge agreement was 19%, again considerably higher than for Zr III due to the poorer quality of the wavefunctions. For the velocity operator, excitations from 4p should be included, and indeed some of the most important ones [7] have been inserted in the even parity states.

Despite these additional complications which grow rapidly with N [2], the Tc I results are the only *ab initio* ones available, and represent state of the art. What has been learned will be used in our study on the homologous Fe II f-values to be begun this fall. Fe II is very important to astrophysicists, and its f-values are not well established.

C. Previously Completed Work, Now Published

C.1 *K* II $3p^6 \rightarrow 3p^5(4s+3d)$ $J = 1$ *f-values*

Ab initio f-values for K II were in poor agreement with experiment [11]. The problem lies with the near degeneracy of the levels [as close as ~ 1300 cm^{-1}] and the great variation of the d radial function with level [^{3}P *vs* ^{3}D *vs* ^{1}P]. A thorough *ab initio* treatment involves the presence of considerable second order effects-matrices of order 10 000 are utilized. Agreement with 2 of the 3 measured f-values is excellent, with the 3rd it is fair. F-values to the two uppermost levels are newly predicted. The work has now been published [11].

C.2 *Lifetimes of* np^5 $(n+1)s$ $J = 2$ *Rare Gas States*

There was a factor of 2 discrepancy between theory and experiment for Magnetic Quadruple ($M2$) lifetimes in np^5 $(n+1)s$ $J = 2$ states. This grew worse as correlation effects were added. We identified the problem with missing second order effects associated with the np^5 nd basis function. Both np^5 nd and np^5 $(n+1)s$ basis functions must be treated on an equal footing with respect to correlation. This work has now been published [12].

C.3 *Er*$^{3+}$ $^4f^{11}$ $^4S_{3/2} \rightarrow {}^4I_{15/2}$ *Transition Energy*

It is the ultimate intention of the PI to extend this project to include studies of rare earth properties. Presently, such projects need to be selected with care by the *ab initio* computationalist, due to the complexity of these species. Positive ion energy differences with no configuration change are easier to treat than many other properties. This transition in GaN is important in high temperature optoelectronic device applications. Correlation effects contribute ~ 5000 cm^{-1} to to the $4f^{11}$ energy differences, which should be little affected by the host [13]. Transition probabilities are clearly strongly host dependent. RCI calculations have accounted for most of the correlation energy, and this work has now been published [14].

C.4 *Other DOE publications*

In addition to references 2, 11, 12, and 14 which were DOE supported, Fe V f-values [15] and Ta II lifetimes [16] have been published.

Future Plans

Near future applications include beginning a study of Fe II f-values, and completing calculations on Mo V f-values.

References

[1] R. L. Martin and P. J. Hay, J. Chem. Phys. **75**, 4539 (1981).

[2] S. M. O'Malley and D. R. Beck, "Lifetimes of Tc I $(4d+5s)^6$ 5p and $4d^6 5s\ ^6D$ States, Phys. Scr. (in press).

[3] The RCI program suite consists of 3 unpublished programs written by D. R. Beck over a period of years. RCI calculates the bound state wavefunctions, hyperfine structure, and Landé g-values. RFE uses RCI wavefunctions and computes $E1$, $E2$, $M1$ and $M2$ f-values, including the effects of non-orthonormality. REDUCE minimizes the number of eigenvectors needed for a correlation manifold by rotating the original basis to maximize the number of zero matrix elements involving the reference functions; only rotated vectors having non-zero reference interactions are retained.

[4] J. Reader and N. Acquista, Phys. Scr. **55**, 310(1997).

[5] E. Meinders, F. G. Meijer, and L. Remijn, Phys. Scr. **25**, 527(1982).

[6] T. Ahmad and J. Reader, unpublished. J. Reader, private communication.

[7] C. A. Nicolaides and D. R. Beck, Chem. Phys. Letts. **36**, 79(1975).

[8] D. R. Beck and L. Pan, "*Ab Initio* Energy Levels, Oscillator Strengths, and Landé-g Values for $J = 0, 1$ States of Zr III and Nb IV", Physica Scripta, submitted for publication.

[9] C. Y. Chen, Y. M. Li, K. Bailey, T. P. O'Connor, L. Young, and Z. T. Lu Science **286**, 1139 (1999).

[10] C. E. Moore, Atomic Energy Levels, Volume II, NSRDS-NBS 35, US GPO, Washington D.C., Reissued Dec. 1971.

[11] D. R. Beck, J. Phys. B**35**, 4155(2002).

[12] D. R. Beck, Phys. Rev. A**66**, 034502 (2002).

[13] W. C. Martin, R. Zalubas, and L. Hagan, Atomic Energy Levels-The Rare Earth Elements, NBS, USGPO , Washington, DC (1978).

[14] D. R. Beck, Int. J. Quant. Chem. **90**, 439(2002).

[15] S. M. O'Malley, D. R. Beck and D. P. Oros, Phys. Rev. A**63**, 032501(2001).

[16] P. L. Norquist and D. R. Beck, J. Phys. B**34**, 2107 (2001).

Molecular Structure and Electron-Driven Dissociation and Ionization

Kurt H. Becker and Vladimir Tarnovsky
Department of Physics and Engineering Physics and Center for Environmental Systems,
Stevens Institute of Technology, Hoboken, NJ 07030
phone: (201) 216-5671; fax: (201) 216-5638; kbecker@stevens-tech.edu

Program Scope:

This program is aimed at investigating the molecular structure and the collisional dissociation and ionization of selected molecules and free radicals. The focus areas are (1) ionization studies of selected molecules and free radicals and (2) the study of electron-impact induced neutral molecular dissociation processes. Targets of choice for ionization studies include WF_6, $SiCl_4$ and BCl_3 and their radicals, the molecular halogens Cl_2, Br_2, and F_2 and the radicals SF, SF_2, and SF_4. Targets of choice for the neutral molecular dissociation studies include $SiCl_4$, BCl_3, NO_2, and N_2O. The fragments to be probed include Si(^{1}S), Si(^{1}D), Si(^{3}P), BCl(X $^1\Sigma$), B($^2P^o$), and NO (X $^2\Pi$). This choice is motivated on one hand by the relevance of these species in specific technological applications involving low-temperature processing plasmas and, on the other hand, by basic collision physics aspects (WF_6 is similar in its structure to SF_6, $SiCl_x$ and BCl_x are similar to $TiCl_x$ and SiF_x).

The scientific objectives of the research program can be summarized as follows:

(1) to provide the atomic and molecular data that are required in efforts to understand the properties of low-temperature processing plasmas on a microscopic scale

(2) to identify the key species that determine the dominant plasma chemical reaction pathways

(3) to measure cross sections and reaction rates for the formation of these key species and to attempt to deduce scaling

(4) to establish a broad collisional and spectroscopic data base which serves as input to modeling codes and CAD tools for the description and modeling of existing processes and reactors and for the development and design of novel processes and reactors

(5) to provide data that are necessary to develop novel plasma diagnostics tools and to analyze more quantitatively the data provided by existing diagnostics techniques

Specific Recent Progress:

Ionization of NO, NO_2, and N_2O. We carried out absolute partial ionization cross section studies for the 3 nitrogen-oxygen compounds NO, NO_2, and N_2O. These measurements constitute the first effort to measure absolute partial ionization cross sections for all three nitrogen-oxygen compounds in the same apparatus using the same experimental technique. NO and NO_2 are considered oxides of nitrogen. Both molecules have an unpaired electron and are thus classified as radicals. N_2O is a symmetric non-linear molecule with a bond angle of about 134^o. N_2O, "laughing gas", is a linear molecule which cannot easily be represented by a single valence bond picture. The molecule has the O atom at one end and "oscillates" between three resonance structure involving double and triple bonds. Several persistent ambiguities that existed in the literature regarding the ionization properties of NO, NO_2, and N_2O were addressed in the course of our work and open/unresolved questions were answered.

Ionization of B_2H_6. Diborane has a very unusual molecular structure, which is very different from other molecules such as C_2H_6, C_2F_6 and Si_2H_6. There is no direct chemical bond between the two B atoms in B_2H_6. Two BH_2 groups lie in a plane with the B atoms facing each other.

The molecule is held together by 2 B-H-B lobes which are perpendicular and on opposite sides of that plane. The B-H-B lobes are so-called "three-center orbitals" or "banana bonds. Each bond is formed via a linear combination of a sp^3 from each B atom and the (1s) electron of the H atom. The intensities of the ions BH_3^+, BH_2^+, and BH^+ are distinctly higher in our mass spectrum compared to the NIST standard data table, which may be attributable to a higher detection efficiency in our experiment for ions formed with significant excess kinetic energy. We also found ion signals for the three ions H^+, H_2^+, and H_3^+. No appreciable ion signals were detected that corresponded to the formation of doubly charged ions. The formation process leading to H_3^+ fragment ions could not be uniquely identified. The cross-section curves of all ions show a very similar shape as a function of impact energy. The cross sections increase rapidly from threshold to a maximum and then decrease slightly with higher impact energy. The maximum for the B_2-containing ions was found to be in the range between 40 and 70 eV and at higher energies around 80 eV for the B-containing ions and H^+. The total ionization cross-section curve of diborane exhibits a maximum at 70 eV with a peak value of 10.74×10^{-16} cm^2.

Ionization of SF_3 and SF_5 Radicals: When the measured total single ionization cross sections for SF_3 and SF_5 were compared to BEB and DM calculations, it was found that much like in the case of the CF_x and NF_x radicals there was a serious discrepancy between experimentally determined and calculated cross section. The recent work of Dr. Huo in conjunction with a thorough re-analysis of our earlier data has demonstrated that the use of a modified and improved siBEB method has resolved this issue (as in the case of the CF_x and NF_x species).

Ionization Cross Section Calculations. All experimental ionization studies were also supported by our continuing effort to extend and refine our semi-classical approach to the calculation of total single ionisation cross sections for molecules and free radicals. In general, we now have a achieved a level of agreement between calculation and experiment of better than 20% (and in many cases of better than 10%). This level of agreement gives us confidence as to the predictive capabilities of our approach for molecules for which no experimental data are available.

Neutral Molecular Dissociation Studies. We are in the final stages of completing a comprehensive study of neutral molecular dissociation of SiH_4, SiF_4, and several Si-organic compounds (TMS, HMDSO, TEOS) with particular emphasis on the determination of final-state specific cross sections for the formation of $Si(^1S)$ and $Si(^1D)$ atoms. In the case of the formation of $Si(^1S)$ atoms from SiH_4, we found a peak cross section of about 5×10^{-17} cm^2 at an impact energy of 60 eV. The formation of $Si(^1D)$ atoms when compared to $Si(^1S)$ atoms has a somewhat larger cross section (by about 40%). Cross sections for $Si(^1S, ^1D)$ formation from SiF_4 have absolute values comparable to those from SiH_4, but a distinctly different energy dependence and they showed a reverse cross section ordering for $Si(^1S)$ vs. $Si(^1D)$ formation. Preliminary relative measurements for the formation of CH from CH_4 (and other hydrocarbon compounds) have also been carried out and relative cross sections have been obtained.

Ongoing studies and future work - Ionization

$SiCl_4$ and the $SiCl_x$ radicals: $SiCl_4$ has a similar structure to fluorinated and hydrogenated targets that we studied in the past (SiF_4, SiH_4). No ionization cross section data are available for the molecule. Perhaps most importantly, the $SiCl_4$ molecule is a candidate for electron-impact ionization studies on thin deposited $SiCl_4$ films (T. Orlando, private communication, 2002). This affords a unique opportunity to explore how the ionization properties of a molecule change from the gas phase to the condensed phase. We are in the process of carrying out a comprehensive series of absolute partial ionization cross section measurements for $SiCl_4$ and for the $SiCl_x$ (x=1-

3) radicals using (i) the TOF-MS apparatus at the INP Greifswald (complemented by high mass resolution studies for isotope separation using the double-focusing MS) for the stable $SiCl_4$ molecule and (ii) our fast-beam apparatus for the $SiCl_x$ radicals. Preliminary results for $SiCl_4$ show some interesting similarities to our previous results for $TiCl_4$. The experimental results will be complemented by semi-classical calculations of the total single ionization cross sections.

SF, SF_2, and SF_4 Free Radicals: The recent work of Dr. Huo has demonstrated that the use of a modified and improved siBEB method has resolved this earlier discrepancy between measured and calculated ionization cross sections for and SF_5. We now re-visit the experimental determination of the ionization properties of the remaining 3 radicals SF, SF_2, and SF_4 and determine a comprehensive set of cross sections for the ionization and dissociative ionization.

Cl_2, Br_2, and F_2: As far as ionization of Cl_2 is concerned, the only available data are total ionization cross sections in addition to ionization cross sections for atomic chlorine, Cl. No information is available as to the partial ionization cross sections Cl_2^+ from Cl_2 and Cl^+ from Cl_2. Information on negative ion formation (Cl_2^- and Cl^-) and positive-negative ion pair formation processes are available for Cl_2 (as well as for F_2 and Br_2). The status of the collisional and spectroscopic data bases for F_2 and Br_2 are in general much more fragmentary than those for Cl_2. The main emphasis of our work will be on Cl_2 where we will first measure partial cross sections for the formation of Cl_2^+ parent ions and Cl^+ fragment ions from Cl_2 from threshold to 200 eV using the fast-beam apparatus. Subsequently, we will carry out similar studies for the Br_2 and F_2 molecules in an attempt to establish common trends and similarities (or a lack thereof) in the data for the 3 molecular halogens F_2, Cl_2, and Br_2.

BCl_3 and the BCl_x radicals: There is some information in the literature on the formation of positive and negative ions formed by electron impact on BCl_3 and on the spectroscopy of BCl_3 and the BCl free radical, which is widely used in optical diagnostics studies of BCl_3-containig plasmas. There have also been some recent calculations of electron collisions with BCl_3. Earlier ionization studies used Fourier transform mass spectrometry (FTMS) to obtain absolute partial ionization cross sections. Results obtained by this technique can be plagued by serious systematic errors. We are in the process of measuring a complete set of absolute partial ionization cross sections for BCl_3 and for the BCl radical with special emphasis on the low-energy, near-threshold region using the fast-beam technique. Based on some preliminary studies we will be using pure BCl_3 or a defined mixture of BCl_3 and Ar to produce the primary ions.

<u>Ongoing studies and future work – Neutral Dissociation</u>

$SiCl_4$: This molecule is a natural choice as a target for the neutral dissociation studies leading to final-state specific Si cross sections as it extends the sequence of SiH_4 and SiF_4 to the chlorine-containing compound. Moreover, similar to SiH_4 and SiF_4, we also measure ionization and dissociative ionization cross sections for $SiCl_4$, so that this becomes another molecule for which we will have a broad data base of collisional data on ionization and dissociation.

***BCl_3*:** The significance and importance of the BCl_3 molecule in various applications has already been discussed in the previous section. We will investigate the two neutral dissociation channels which have most likely the largest partial dissociation cross sections, (i) the break-up of the parent molecule into a ground-state BCl fragment in the ($X\ ^1\Sigma$) state which will be detected by pumping and probing the strong $X\ ^1\Sigma \rightarrow A\ ^1\Pi^+$ transition near 272 nm and (ii) the boron atom in its ($^2P^o$) ground-state which will be probed via the (2p) $^2P^o \rightarrow$ (3s) ^2S transition at 250 nm. Both measurements will require the use of the frequency doubler.

NO_2 and N_2O: The studies of the neutral molecular dissociation of NO_2 and N_2O into NO complement the (dissociative) ionization studies for these compounds that were carried out recently. The formation of NO from these molecules is an important reaction pathway in combustion processes and in atmospheres.

Publications Acknowledging DOE Support (2000 – present)

1. "Calculations of Cross Sections for the Electron Impact Ionization of Molecules", Int. J. Mass Spectrom. 197, 37 (2000), with H. Deutsch, S. Matt, and T.D. Märk (Invited Topical Review)
2. "Elementary Electron Collision Processes in Plasmas", in "Low-Temperature Plasma Physics: Fundamental Aspects and Applications", editors: R. Hippler, S. Pfau, M. Schmidt, and K.H. Schoenbach, Wiley-VCH Publishing, Berlin/New York (2001), p. 55-77
3. "Calculation of Absolute Electron-Impact Ionization Cross Sections of Dimers and Trimers", Europ. Phys. J. D 12, 283 (2000), with H. Deutsch and T.D. Märk
4. "Calculated Cross Sections for the Multiple Ionization of N and Ar Atoms by Electron Impact Using the DM Formalism", Plasma Phys. Controlled Fusion 42, 489 (2000), with H. Deutsch and T. Märk
5. "Electron-Impact Ionization of $TiCl_4$", Thin Solid Films 374, 219 (2000), with R. Basner, M. Schmidt, V. Tarnovsky, and H. Deutsch
6. "Absolute Cross Section for the Formation of Si(^{1}S) Atoms Following Electron Impact Dissociation of SiH_4", J. Chem. Phys. 113, 2250 (2000), with N. Abramzon and K. Martus
7. "Calculated Absolute Electron Impact Ionization Cross Sections for AlO, Al_2O, and WO_x (x=1-3)", J. Appl. Phys. 89, 1915 (2001), with H. Deutsch, K. Hilpert, M. Probst, and T.D. Märk
8. "Calculations of Absolute Electron Impact Ionization Cross Sections for Molecules of Technological Relevance Using the DM Formalism", Int. J. Mass Spectrom. 206, 13 (2001), with M. Probst, H. Deutsch, and T.D.Märk
9. "Absolute Total and Partial Cross Sections for the Electron Impact Ionization of SiF_4", J. Chem. Phys. 114, 1170 (2001), with R. Basner, M. Schmidt, E. Denisov, and H. Deutsch
10. "Electron Impact Ionization of the $TiCl_x$ (x=1-3) Free Radicals" Int. J. Mass Spectrom. 208, 1, (2001), with V. Tarnovsky, R. Basner, and M. Schmidt
11. "Calculated Cross Sections for the Multiple Ionization of Krypton and Chromium Atoms by Electron Impact", Contr. Plasma Phys. 41, 73 (2001), with H. Deutsch and T.D. Märk
12. Calculated Cross Sections for the K-Shell Ionization of Cr, Ni, Cu, Sc, and Va Using the DM Formalism", J. Phys. B 34, 3377 (2001), with B. Gstir, H. Deutsch and T.D. Märk
13. "Calculated Absolute Cross Section for the Electron-Impact Ionization of CO_2^+ and N_2^+", J. Phys. B 35, L65, (2002), with H. Deutsch, P. Defrance, U. Onthong, R. Parajuli, M. Probst, S. Matt, and T. Märk
14. "Calculated Cross Sections for the K-Shell Ionization of Fe, Co, Mn, Ti, Zn, Nb, and Mo Using the DM Formalism", Int. J. Mass Spectrom. 213, 5 (2002), with H. Deutsch, B. Gstir, and T.D. Märk
15. "Calculated Absolute Electron Impact Ionization Cross Sections for the Molecules CF_3X (X=H,Br,I)", Int. J. Mass Spectrom. 214, 53 (2002), with U. Onthong, H. Deutsch, S. Matt, M. Probst, and T. Märk
18. "Total Electron Impact Ionization Cross Sections of CF_x and NF_x (x=1-3)", Chem. Phys. Lett. 358, 328 (2002), with W.M. Huo and V. Tarnovsky
17. "Absolute Total and Partial Electron-Impact Ionization Cross Sections for C_2F_6", Int. J. Mass Spectrom. 214, 365 (2002), with R. Basner, M. Schmidt, E. Denisov, P. Lopata, and H. Deutsch
18. "Electron Impact Ionization of NO, N_2O, and NO_2", Int. J. Mass Spectrom. 225, 25 (2003), with J. Lopez and V. Tarnovsky
19. "Calculated Absolute Cross Sections for the Electron-Impact Ionization of Simple Molecular Ions", Int. J. Mass Spectrom. 223/224, 639 (2003), with H. Deutsch, P. Defrance, U. Onthong, M. Probst, S. Matt, P. Scheier, and T.D. Märk
20. "Absolute Total and Partial Electron-Impact Ionization Cross Sections for B_2H_6", J. Chem. Phys. 118, 2153 (2003), with R. Basner and M. Schmidt

+ 2 manuscripts submitted for publication

PROBING DYNAMICS AND STRUCTURE IN ATOMS, MOLECULES AND NEGATIVE IONS USING THE ADVANCED LIGHT SOURCE

Nora Berrah
Physics Department, Western Michigan University, Kalamazoo, MI 49008
e-mail:Berrah@wmich.edu

Program Scope

The objective of the research program is to advance fundamental understanding of the interaction between vuv/soft x-ray photons and gas-phase targets as well as to achieve a better understanding of the dynamics and electronic structure of atoms, molecules, clusters and negative ions. These studies allow an understanding, at the atomic and molecular level, of many processes important to the understanding of the properties of complex materials and of strongly correlated systems. We use photons from the Advanced Light Source as our probe because they provide the photon energy range that accesses inner-shells light targets as well as tunability and resolution necessary to obtain detailed knowledge with an impressive degree of precision. We have also improved our experimental techniques to achieve high detection efficiency and high precision measurements. We present here results completed and underway this past year and plans for the immediate future.

Recent Progress

1) K-Shell Photodetachment Studies of Negative Ions

Negative ions are special targets since they contain confined electrons but do not exhibit Rydberg series, like neutral targets or positive ions. The reason is that after photodetachment, the electron does not experience the long range Coulomb force. Instead, it experiences a short range force due to a polarization potential that can hold only a finite number of bound states, which are a direct measure of their binding strength. This attribute is a blessing since it provides simple spectra, which are not overcrowded with overlapping Rydberg series, but it is also a curse because it provides formidable experimental and theoretical challenges because the independent-electron model is inadequate for even a qualitative description of their properties. From an experimental point of view, unlike outer-shell studies, inner-shell photodetachment is a largely unexplored territory; only a few negative ion targets have been investigated, and that only these past two years.

a) K-shell photodetachment of He^-

Inner-shell photodetachment of He^- is very markedly different from Li^- and significantly more complicated. He^- does not form a stable ground state; the lowest extant state is $1s2s2p\ ^4P$, bound by only 77 meV relative to the excited $1s2s\ ^3S$ He state. The situation is also much more complicated because the ^4P symmetry of the initial state of He^- allows ^4S, ^4P and ^4D final states, while the initial ^1S state of Li^- allows only ^1P final states. In addition, the photoexcitation of the 1s electron in He^- leads primarily to a "hollow" ion,

i.e., in the 1s photoexcitation region "hollow" resonances dominate the cross section, thereby allowing detailed study of these highly unstable states.

We have undertaken K-shell photodetachment measurements of He^- to probe for the first time both triply excited states in the metastable He^- ions and doubly excited states in the neutral He atoms [1]. Our motivation was in part due to a theoretical controversy; two calculations [a,b] disagreed with each other in many ways, both qualitatively and quantitatively. One of them uses a multiconfiguration Hartree-Fock (MCHF) methodology [a] while the other one uses the R-matrix formalism with an upgraded asymptotic part to handle the negative ion system [b]. However, both of these calculations predicted that the response of inner-shell electrons to ionizing radiation does indeed differ both qualitatively and quantitatively from neutral atoms and positive ions, just like the case of Li^-. Also, the two theories disagreed about the interpretation of the predicted structure.

The experiments were performed on the HRAMO undulator beamline 10.0.1 at the Advanced Light Source at Lawrence Berkeley National Laboratory. Two sets of data were recorded with low (100 meV) and intermediate (70 meV) photon resolution, in the 38-44 eV photon energy range. The experimental data show a peak of about 15 Mb at 38.88 eV, just above the first (He $2s2p\ ^3P$) 1s detachment threshold. Also, below the first 1s threshold, the experimental cross section is, within errors bars, zero as expected. Above the peak is a long tail and a broad flat region, up to about 42.8 eV. Then we move into a region of structures, up to 44 eV. Comparison of the experimental results with the theoretical spectra [b] is fairly good overall, except for the large discrepancy between all calculations and the measurements at the first threshold maxima above the first 1s detachment threshold, $2s2p\ ^3P$, at 38.88 eV. It provides the poorest agreement between experiment and theories; the latter are a factor of two larger than experiment. This is reminiscent of an even larger discrepancy between theory and experiment at the first 1s threshold in Li^- photodetachment [c] as discussed last year.

This work attracted new theories since recently two new calculations, based on different methodologies, but each of them introduced similar correlation effects have been performed [d,e]. The Zatsarinny et al. [d] theory employs an R-matrix calculations with a spline basis and the Sanz-Vicarrio and Lindroth [e] calculation uses a complex scaled configuration interaction. Nevertheless, the agreement between the measurements and all calculations [b,d,e] is mixed because, as discussed above, negative ion photodetachment provides an extreme theoretical challenge since the wave functions of both initial and final states are so very sensitive to electron correlation effects, much more than for neutral or positive ions targets. In fact, all calculations overestimated the strength of the first threshold and disagreed on the nature of the structures above 42.8 eV.

According to recent work by Sanz-Vicario et al. [f], the basic cause of this discrepancy in He^- is the same as the one in Li^- [c]. Namely, PCI electron recapture effect is indeed very strong near the first threshold; ie a large Auger width that leads to a wide recapture energy window. Sanz-Vicario et al. [f] added a classical damping factor to his ab-initio calculations that suppressed the first threshold. The agreement between the calculation that includes PCI recapture and measurements is now very good [f].

b) K-shell photodetachment of C^-

In a recent study, we investigated K-shell photoexcitation of C^- over the photon energy range 280-285 eV and measured the relative cross section for C^+ production by double detachment. [2] The measured spectrum showed the first experimental evidence for a $1s2s^22p^4(^4P)$ shape resonance near 281.8 eV, which was in excellent agreement with R-matrix calculations. In the present study, we measured higher resolution spectra of this resonance to determine its parameters with substantially improved accuracy and measured the absolute cross sections for C^+ production. These new measurements permit quantitative comparison to theory for this more complex negative ion.

Recent high resolution measurements show that the resonance is quite narrow; the full-width of the resonance is close to the nominal photon bandwidth and is well represented by the Breit-Wigner resonance formula. Preliminary analysis of the absolute cross section measurements indicates that the cross section is on the order of several tens of Mb at the resonance peak. This value is in rough agreement with the calculated peak cross section of 15-18 Mb.

2) Experimental Evidence of a Dynamic Jahn-Teller Effect in C_{60}^+

Detailed analysis of the Highest Occupied Molecular Orbital bandshape in the photoelectronspectrum of gaseous C_{60} reveals a *dynamic* Jahn-Teller effect in the ground state of C_{60}^+. The direct observation of three tunneling states asserts a $D3d$ geometry for the isolated cation, originating from a strong vibronic coupling. These results show that the ionic motion plays an important role in the electron-phonon interaction. [3]

3) Spin-polarization measurements of the krypton $M_{4,5}NN$ and xenon $N_{4,5}OO$ Auger electrons: Orientation and intrinsic parameters

In the framework of the two-step model of Auger decay the orientation of the krypton $3d^{-1}$ and xenon $4d^{-1}$ primary hole states has been determined as a function of photon energy. This was achieved by carrying out spin-polarization measurements of the Kr $M_{4,5}N_{2,3}N_{2,3}$ and Xe $N_{4,5}O_{2,3}O_{2,3}$ Auger electrons after ionization of free atoms by circularly polarized synchrotron radiation of 130–530 eV photon energy. The orientation parameter is found to be strongly influenced by the Cooper minimum in the Xe $4d$ photoionization cross section as demonstrated by the comparison of the Kr and Xe data. Furthermore, the intrinsic parameters for all lines in the Kr $M_{4,5}N_{2,3}N_{2,3}$ and Xe $N_{4,5}O_{2,3}O_{2,3}$ Auger groups and for several lines in the Kr $M_{4,5}N_{2,3}N_{2,3}$ Auger group were determined with high accuracy and are compared with previous experiments and calculations. We were also able to measure the spin polarization of most of the low kinetic-energy Kr $M_{4,5}N_{2,3}N_{2,3}$ and Xe $N_{4,5}O_{2,3}O_{2,3}$ lines, showing that the assignment of one of the lines should be revisited. [4]

Future Plans

The principal areas of investigation planned for the coming year are: (1) Test the neutral detector built this past year to measure the neutral decay channel in the photodetachment

experiments of negative ions; Li^-, He^-, B_2^-. 2) Analyze recent high-resolution measurements in He^- in order to resolve discrepancies among 3 different calculations [b,d,f]. 3) Analyze the measurements of the absolute photodetachment cross section in the case of He^- and Si^- since our measurements were relative. (4) Measure in detail the absolute photodetachment cross section of B^- as well as the photodissociation and photodetachment mechanism in the case of B_2^- as well as B_3^-.

Publications from DOE sponsored research.

[1] N. Berrah, J. D. Bozek, G. Turri, G. Akerman, B. Rude, H.-L Zhou, and S. T. Manson, " K-Shell Photodetachment of He^-: Experiment and Theory", Phys. Rev. Lett. **88**, 093001 (2002).

[2] N. D. Gibson, C. W. Walter, O. Zatsarinny, T. W. Gorczyca, G. D. Ackerman, J. D. Bozek, M. Martins, B. M. McLaughlin, and N. Berrah Phys. Rev. A **67**, 030703 (2003).

[3] S. E. Canton, A. J. Yencha, E. Kukk, J. D. Bozej, M. C. A. Lopes, G. Snell, and N. Berrah, "Experimental Evidence of a Dynamic Jahn-Teller Effect in C_{60}^+", Phys. Rev. Lett. **89**, 045502-1 (2002).

[4] G. Snell, B. Langer, A. T. Young and N. Berrah, "Spin polarization measurements of the Kr $M_{4,5}NN$ and Xe $N_{4,5}$ Auger electrons:orientation and intrinsic parameters", Phys. Rev. A **66**, 022701 (2002).

[5] T. Karlsen, L. J. Saethre, K. J. Borve, N. Berrah, E. Kukk, J. D. Bozek, T. X. Carroll and T. D. Thomas, J. Phys. Chem. A **105,** 7700 (2001).

[6] L. J. Saethre, N. Berrah, J. D. Bozek, K. J. Borve, T. X. Carroll, E. Kukk, and T. D. Thomas, "Chemical insights from high-resolution x-ray photoelectron spectroscopy and ab initio theory: Propyne, trifluoropropyne and ethynylsulfur pentafluoride", J. Am. Chem. Soc. **123**, (43) 10729 (2001).

[7] A. A. Wills, E. Sokell, T. W. Gorczyca, X. Feng, M. Wiendenhoeft, S. E. Canton and N. Berrah, "Importance of spin-orbit interactions for the He 2lnl' states revealed by a novel use of angle-resolved photoelectron spectroscopy", J. Phys. B. Lett. **35**, L367 (2002).

[8] J. D. Bozek, S. E. Canton, E. Kukk and N. Berrah, "Vibrationally resolved resonant Auger spectroscopy of formaldehyde at the C 1s-1* resonance", Chemical Physics, **289**, pages 149-161 (2003).

References:

[a] J. Xi, and C. Froese Fischer, Phys. Rev. A **59**, 307 (1999).

[b] H.-L., Zhou, S. T. Manson, L. Vo Ky, A. Hibbert, N. Feautrier, Phys Rev. A 64, 01271 (2001).

[c] N. Berrah, J. D. Bozek, A. Wills, G. Turri, H.L. Zhou, S. T. Manson, B. Rude, N. D. Gibson, C. W. Walter, L. Voky, A. Hibbert, and S. Fergusson, Phys. Rev. Lett. **87,** 253002-1 (2001).

[d] O. Zatsarinny, T. Gorczyca, and C. Froese-Fisher, J. Phys. B **35**, 4161 (2002).

[e] J. Sanz-Vicario, and E. Lindroth, Phys. Rev. A **65**, 060703(R (2002).

[f] J. Sanz-Vicario, E. Lindroth, and N. Brandefelt, Phys. Rev. A **66**, 052713 (2002).

Coherent Control of Ultrafast X-rays

P.H. Bucksbaum and D.A. Reis
FOCUS Center, Physics Department, University of Michigan,
Ann Arbor, MI 48109-1120 phb@umich.edu Grant DEFG02-00ER15031

This is a program to develop ultrafast x-ray physics at synchrotrons and linear accelerators. The research is carried out at the Advanced Photon Source sector 7, with the MHATT-CAT collaboration; and at the Stanford Linear Accelerator Center, with the SPPS collaboration.

Program Scope

Modern third-generation synchrotrons are many orders of magnitude brighter than laser-based laboratory sources of x-ray radiation (see figure 1). Their importance in *ultrafast* x-ray science has been limited in the past, because the x-ray pulse duration is generally no shorter than the electron bunch lengths in synchrotrons, which are constrained by various technical considerations in electron storage rings to a range of tens of picoseconds or longer. Some important dynamical phenomena can be studied in this sub-nanosecond time range; however, the fundamental motion of interatomic bonds is in the range of 10's to 100's of femtoseconds. Therefore there is a strong research incentive to find new ways to shorten the pulse duration of x-rays from synchrotron radiation.

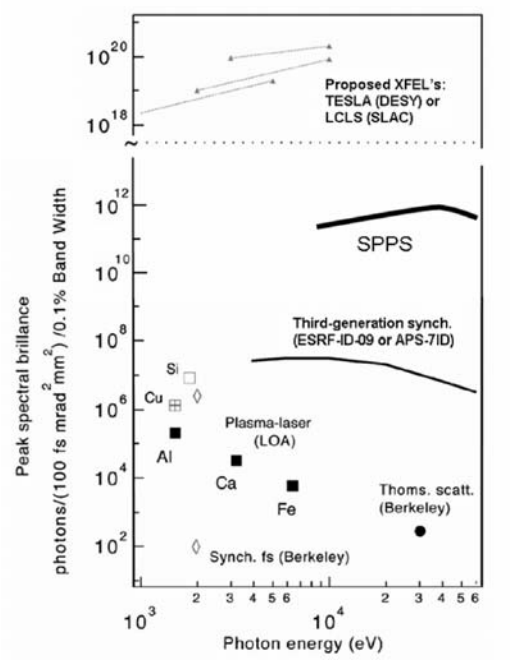

Fig. 1: Comparison of the peak brilliance of laser-based and accelerator-based sources of x-rays. This graph was adapted from [A. Rousse et al., Rev. Mod. Phys., **73**, 17-32 (2001)] and modified to include the SPPS source.

Our program is presently developing three approaches to this problem. The first approach is an ultrafast x-ray switch, based on coherent control of high amplitude phonons in Bragg scattering mirrors or filters. A switch based on the highest frequency optical phonons could in principle create x-rays as short as 12 fs. A second approach is to use an x-ray streak camera with approximately 1 ps resolution to observe transient phenomena illuminated by the 100 ps APS x-ray beam. Both of these methods are under development in parallel at the APS.

Alternatively, we can compress highly relativistic electrons in a linear accelerator, where bunch lengths can be shortened to less than 100 fsec. When these ultrashort electron bunches travel through an undulator, they produce ultrafast pulses of x-rays. We have recently demonstrated this as part of the Sub-Picosecond Pulse Source (SPPS) experiment at the Stanford Linear Accelerator Center (SLAC). The physics studied at the two sources is complementary, and will help define the new field of ultrafast x-ray physics that will be one of the frontier areas for 4th generation sources at LCLS.

Recent Progress:

Ultrafast Bragg Switch: X-ray pulse switching experiments are performed on the Sector 7 MHATT-CAT undulator beam line at the APS. The principle of the x-ray switch is laser-excitation of Bragg crystals. The excitation produces a transient change in the scattering condition, leading to a switch action. The change can either be incoherent (e.g., simple laser heating), or coherent excitation of motion (coherent phonons) in the crystal. Several physical mechanisms have been demonstrated or proposed for this transient excitation, and the switch time scale can range from nanoseconds to less than 1 ps, depending on the details of the switch material and geometry.

We have been concentrating on an x-ray switch using anomalous transmission (Borrmann effect), in which lattice planes form parallel plate waveguides for the x-rays. Since the x-ray electric field nodes are located at these atomic planes, absorption is minimized in this geometry. Nearly 50% transmission (the theoretical maximum) is possible for 10keV x-rays traversing a 300 micron thick silicon wafer. When the x-rays exit the crystal, the transverse standing wave in the crystal waveguides becomes two traveling waves in free space, so that the crystal is a coherent beamsplitter for x-rays. The angle between the two exiting waves can be conveniently large, since it is the twice the Bragg angle.

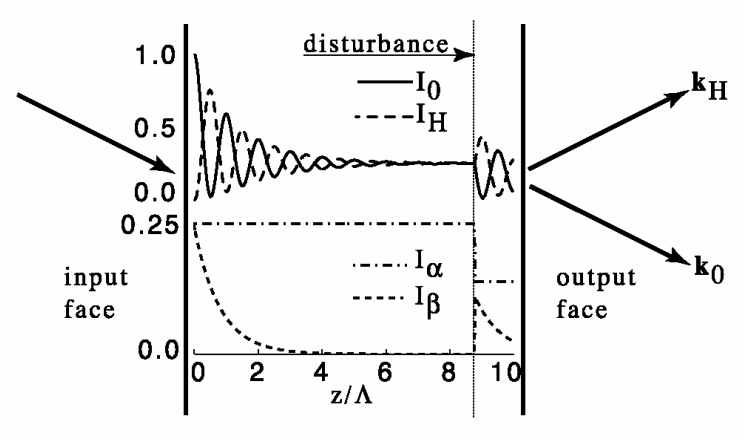

FIG. 2: Intensities of the forward- and deflected-diffracted beams (upper) and the interior solutions α and β (lower) as a function of depth inside a thick crystal. A lattice disturbance near the exit couples the two solutions, regenerating β.

We can coherently redistribute the x-ray field inside the crystal by inducing a transient shift in the lattice. If the lattice shift is near the exit face of the crystal, this leads to a corresponding redistribution of the energy between the two exiting beams. Alternately, both beams can be switched on and off simultaneously by arranging the redistribution near the input face. We have studied both of these effects in crystalline Ge, using laser absorption to launch acoustic waves in the crystal. The acoustic wave created by an ultrafast laser travels into the crystal with very little dispersion or attenuation. When the x-rays intercept the acoustic disturbance, their field is redistributed from the transmission waveguide mode into an orthogonal mode where the antinodes are on the crystal planes. These two modes then coherently interfere at the exit face to change the distribution of energy into the two free space x-ray beams.

We have been studying the initial fast transient response following laser excitation. The speed of the transient switch depends on several factors. Through both streak camera measurements and simulations, we can now show how the transient strain in ultrafast laser-excited Ge creates a rapid change in the x-ray anomalous transmission. The development of the coherent strain pulse is dominated by rapid ambipolar diffusion. This pulse extends considerably longer than the laser penetration depth because the plasma initially propagates faster than the acoustic modes. X-ray diffraction simulations are in agreement with the observed dynamics.

SPPS: The Sub-Picosecond Pulse Source is a new experiment at the Stanford Linear Accelerator Center (SLAC), which employs relativistic chirped pulse compression of the SLAC beam to produce sub-100 femtosecond bunches of electrons. These in turn produce pulses of ultrafast x-ray radiation by passing through an undulator. With 3.4 nC per bunch accelerated to 28 GeV and a 2.5 m long undulator, SPPS is designed to generate 80 fsec pulses of 10^7 8-10 keV x-rays. The peak brightness is 10^{25} photons/(s-mm^2 -mrad^2-0.1% bandwidth) (See Fig. 1).

The collaboration recently completed its first six-week operating period, when the x-ray and optical beams were installed, synchronized, and tested. The primary goals for the initial run were to test the operation of the new SPPS x-ray beam line, to measure x-ray pulse parameters, to evaluate the synchronization of the new ultrafast laser system with the x-ray pulses, and to measure the scattered x-ray intensity from a variety of samples. The measured x-ray intensity, 2×10^7 photons per pulse in 1% bandwidth, agrees well with predictions. The x-ray scattering power and background rates for single crystal, powder, and liquid samples were measured and feasibility for pump-probe experiments was established.

Measurement of the electron beam pulse length after the first stage of compression demonstrated a pulse length of ~300 fs, with beam parameters such that the final compression reduces this by a factor of 4. Direct measurements of this compressed electron bunch length and the final x-ray pulse width are planned for the next run. Since the x-rays are not generated directly by the laser at SPPS, ultrafast timing is not automatic. Synchronization is maintained by feedback to the laser oscillator cavity length, referenced to the rf that controls SLAC. The short-term synchronization jitter between laser and x-ray pulses was found to be less than 2 ps over 10-50 s. Residual jitter on this order may be very difficult to reduce. In that case ordinary pump-probe spectroscopy would not be possible at the 100 fs level, so we are developing new sampling methods based on single-shot measurements of the laser-x-ray relative delay.

To measure the arrival time and bunch duration of the x-rays, we use single shot electro-optic sampling of the coherent terahertz radiation from the relativistic electron bunch. An ultrafast laser pulse from the same oscillator that supplies light for the pump-probe experiments is transmitted through a 150m polarization-preserving optical fiber. We have demonstrated that we can compensate for the dispersion of a 100 fs pulse with a combination grating compressor and liquid-crystal pulse shaper, together with active compensation for the optical path length of the fiber.

Future plans:
We are developing an x-ray streak camera based on the traveling wave design of Z. Chang. The camera uses a novel compact layout that can be placed directly on the arm of a small goniometer. We also employ a modular design, so upgrades or replacements of defective parts should be straightforward.

We have plans to scale the Bragg switch to sub-picosecond duration, and also to begin applications. Of particular interest is work on energy transport across heterostructure interfaces and in laser-excited semiconductor multilayers. We have made preliminary measurements on epitaxial AlGaAs on GaAs. Other ideas include studies of diffusive elastic scattering in liquids under the influence of strong laser fields. It may be possible to align molecules in liquids using the molecular polarizibility. This could lead to a new series of ultrafast x-ray studies of liquids undergoing diffusion or chemical reactions.

The SPPS will share SLAC with other experiments in accelerator and high energy physics until 2006. We intend to extend our materials and chemical studies performed at the APS to higher resolution studies at SPPS. Following its 2-year run, the SPPS will be dismantled to make way for the construction of a much more powerful ultrafast x-ray source, the LCLS x-ray free-electron laser.

Publications, 2001-2003:

[1] M. F. DeCamp, D. A. Reis, P. H. Bucksbaum, B. Adams, J. M. Caraher, R. Clarke, C. W.S. Conover, E. M. Dufresne, R. Merlin, V. Stoica, and J. Wahlstrand, "Coherent Control of Pulsed X-ray Beams," *Nature* **413**, 825-828(2001).

[2] M. F. DeCamp, D. A. Reis, P. H. Bucksbaum, and R. Merlin. Dynamics and coherent control of high - amplitude optical phonons in bismuth. *Phys. Rev. B* **64,** 092301 (2001).

[3] D. A. Reis, M. F. DeCamp, P. H. Bucksbaum, R. Clarke, E. Dufresne, M. Hertlein, R. Merlin, R. Falcone, H. Kapteyn, M. M: Murnane, J. Larsson, Th. Missalla, and J. S. Wark. Probing impulsive strain propagation with x-ray pulses. *Phys. Rev. Lett.,* **86**(14):3072-3075, 2001.

[4] J. S. Wark, et al. Femtosecond x-ray diffraction: experiments and limits. In D. M. Mills, H. Schulte-chrepping, and J. R. Arthur, editors, X-ray FEL Optics and Instrumentation, SPIE International Symposium on Optical Science and Technology, San Diego, CA, 2000, **4143**, 26-37. Proceedings of the SPIE, 2001.

[5] J. Larsson, A. Allen, P.H. Bucksbaum, R.W. Falcone, A. Lindenberg, G. Naylor, T. Missala, D.A Reis, K Scheidt, A. Sjögren, P. Sondhauss, M. Wulff, and J.S. Wark, "Picosecond X-ray diffraction studies of laser-excited acoustic phonons in InSb," *Appl. Phys. A* **75**, 467–478 (2002).

[6] B. A. Adams, M. F. DeCamp, E. M. Dufresne, and D. A. Reis. Picosecond laser pump, x-ray probe spectroscopy of GaAs. *Rev. Sci. Inst.* **73** 4150-4156 (2002).

[7] D.A. Reis, M. DeCamp, P.H. Bucksbaum, R. Clarke, R. Merlin, E.M. Dufresne, B. "Time-resolved studies of acoustic phonons" *In preperation*, 2002.

[8] M. F. DeCamp, D. A. Reis, A. Cavalieri, P. H. Bucksbaum, R. Clarke, R. Merlin, E. M. Dufresne, D. A. Arms, A. M. Lindenberg, A. G. MacPhee, Z. Chang, B. Lings, J. S. Wark, S. Fahy, Supersonic strain front driven by a dense electron-hole plasma, cond-mat/0301002 (2002) to be published in Phys. Rev. Letters .

[9] M. F. DeCamp et al. Acoustic phonon dispersion measured with time-resolved x-ray diffraction. *QELS Technical Digest, Long Beach, CA*, 2002.

[10] D. A. Reis, M. F. DeCamp, et al. Time-resolved x-ray Pendellösung oscilations in impulsively strained crystals*,(invited). QELS Technical Digest, Long Beach, CA, 2002.*

[11] M. F. DeCamp et al. Time-resolved anomalous transmission of x-rays in laser heated germanium. *QELS Technical Digest, Baltimore, MD*, 2001.

[12] D. A. Reis, M. F. DeCamp, et al. Time-resolved Pendellösung oscillations. *DAMOP technical digest,London, Ontario, Canada*, 2001.

[13] M.F. DeCamp, "Seeing sound: dynamical effects in ultrafast x-ray diffraction," Ph.D. Thesis, University of Michigan, 2002 (unpublished).

[14] D.A. Reis, et al. Picosecond Dynamics Probed by X-ray Diffraction, APS Forfront, **1**, 134 (2001).

[15] P.H. Bucksbaum, D.A. Reis, and J. Hastings, Ultrafast Hard X-Rays from Electron Accelerators, *Ultrafast Optics,* Springer-Verlag, to be published (2003).

[16] D.A. Reis, Picosecond X-ray Dynamical Diffraction, in *Synch Rad News* **16,** 21-23 (2003).

[17] D.A. Reis, Ultrafast X-ray Physics, in Indo-US workshop on radiation physics with synchrotrons and other new sources (2003).

[18] D.A. Reis Ultrafast Laser-Switching of Synchrotron X-ray Pulses, Bull. Am. Phys. Soc. http://www.aps.org/meet/MAR03/baps/abs/S7740001.html (2003)

[19] P.H. Bucksbaum, Ultrafast x-ray science, proceedings of Synchrotron Radiation Instrumentation Conference, San Francisco, August 2003

[20] S.H. Lee, A.L. Cavalieri, D.M. Fritz, and D.A. Reis, Transport of near-transform limited ultrafast pulses through optical fiber, in preparation (2003).

Low-energy ion-surface and ion-molecule collisions

R. L. Champion
Department of Physics
College of William and Mary
Williamsburg, VA 23187-8795
champion@physics.wm.edu

Program Scope The present experimental research program is focused upon low-energy, ion-surface and ion- molecule collisions. In the case of the ion-surface collisions, it has been observed that the secondary electron and anion emission depends markedly upon the surface condition. The goal of the present studies has been to examine and understand the effects of adsorbates upon these secondary emission properties for both metallic and semiconductor substrates. Secondary emission is induced by positive and negative ion impact, and the systems examined include metallic, semiconductor, and insulative substrates. Both single crystal and polycrystalline substrates have been examined in an effort to identify the role of surface morphology in these secondary emission properties. The adsorbate coverage - typically oxygen - is indirectly determined and ranges from none up to a few monolayers; "low energy" implies collision energies ranging from a few up to 500 eV. The effect of adsorbates can also be anticipated to be substantial in the phenomenon of field emission, as the barrier through which near-surface electrons must tunnel to reach the vacuum is altered considerably by the presence of an adsorbate. We have examined this phenomenon for a molybdenum surface where the adsorbate-altered surface properties are fairly well understood. In a different vein, we have identified the role of ion-molecule reactions in Fourier-transform mass spectrometry where hydronium (H_3O^+) is formed via collisions of H_2O^+ with H_2O, leading to a signal at 19 amu, often mistaken for F^+ . Brief discussions of these experimental projects will be presented in what follows.

Recent Progress

Surface studies - Negative and positive ion projectiles A number of experiments utilizing a multi-purpose ion source to study secondary emission from metallic substrates and the effects of adsorbates upon those processes have been completed. One of the principal motivations for studying *negative-ion* - induced emission was to completely eliminate the role of potential energy (such as the recombination energy associated with the neutralization of an impacting positive ion) as a precursor for the secondary emission processes. An

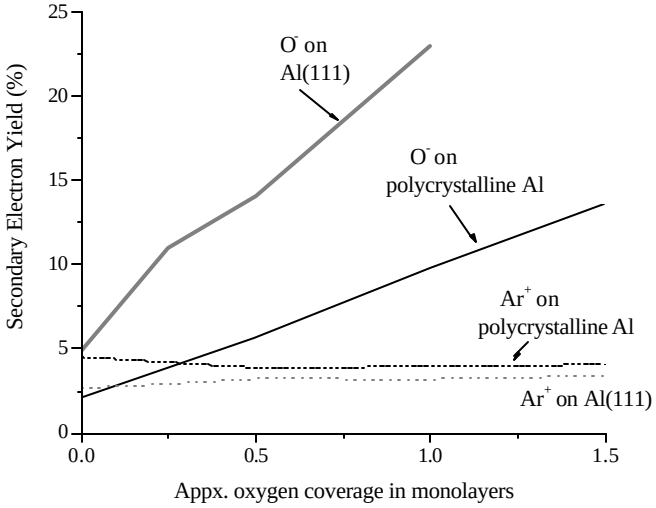

Figure 1 *The secondary electron probability is shown for an Al substrate upon which resides oxygen. The impact energy is 250 eV.*

example of the results of these experiments is shown in Fig. 1 in which the probability for secondary electron emission is shown for 250 eV O^- ions impacting both a polycrystalline and an (111) aluminum surface upon which resides various amounts of adsorbed oxygen. Also shown in the figure are the results for Ar^+ impacting the same aluminum surfaces. The results are striking in that the former (secondary emission initiated by O^-) depends markedly on the amount of adsorbed oxygen whereas the latter (initiated by Ar^+) show essentially no adsorbate-related dependence. We postulate that secondary emission initiated by the anion occurs through the collisional excitation of AlO^- to an anti-bonding state which subsequently decays yielding, among other things, electrons ejected into the vacuum. We have shown that the vertical excitation energy of AlO^- is about 8 ± 1eV. On the other hand the emission due to Ar^+ occurs via the well-known "potential" emission mechanism. Presumably, collisional excitation of the AlO^- surface state is not feasible for the Ar^+ projectile as the energy available from neutralizing Ar^+ exceeds that required for the AlO^- excitation mechanism.

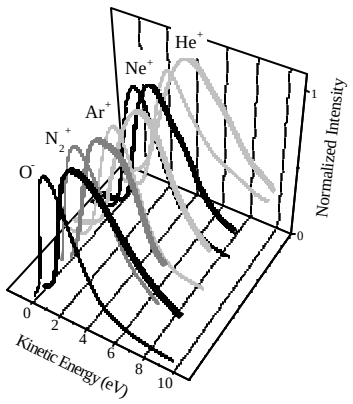

Figure 2 *Kinetic energy spectra for secondary electrons (wide ribbons) and anions are shown for various projectiles impacting a MgO surface at 250 eV.*

We have also measured the kinetic energy distributions of the secondary electrons (and secondary anions) for a number of projectile/ substrate systems; some results are seen in Fig. 2. The example chosen is for a Mg/O substrate in which about one monolayer of oxygen resides on the surface. An interesting feature of these measurements is that the spectra are all so similar; the results for the O^- projectile are consistent with our model developed for ion-induced, adsorbate-altered secondary emission. The proposed mechanism involves electronic excitation of a metal(M)-adsorbate(X) complex, e.g. MX^-, to a higher, repulsive potential, $(MX^-)^*$. This excitation can result in anion desorption into the vacuum, $(M + X^-)$, or, as mentioned above, decay of the system to yield a free electron: (M + X + e or MX + e).

The effects of adsorbates on field emission.

- The effect of adsorbates on field emission can be anticipated to be substantial as the barrier through which near-surface electrons must tunnel to reach the vacuum may actually be lowered by the presence of an adsorbate. The effects of adsorbates on the emission characteristics of Spindt-type molybdenum field emission cathode arrays have been examined. Surface "cleaning" via electron-stimulated desorption (ESD) was used in an attempt to remove adsorbed molecules from the surface of the field emitter (i.e., the

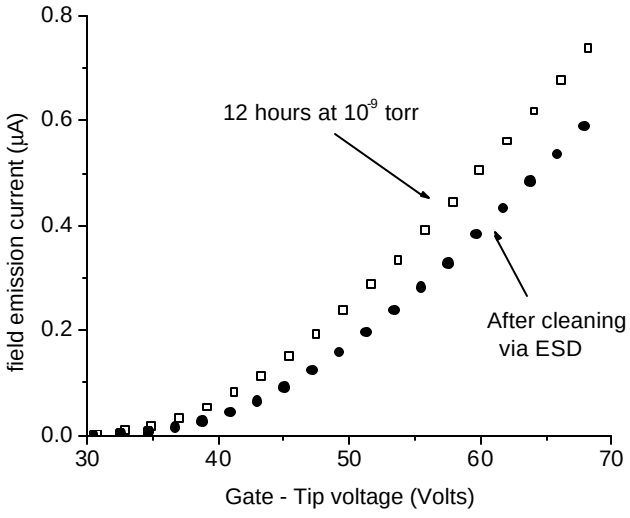

Figure 3 *A plot of the I-V characteristic for a field-emitting array is shown for "before/after" adsorbate removal.*

molybdenum tips). If, as suggested above, the barrier is lowered by the presence of an adsorbate, emission should *decrease* when the surface is relatively free of adsorbates. As may be seen in Fig. 3, the effect of removing adsorbates from the surface was indeed to diminish the field emission The re-introduction of an adsorbate to a surface cleaned via ESD was precisely controlled with the gas-handling system. It was our goal to correlate the field emission with the amount of adsorbate on the surface and compare the results with that predicted for field emission from an adsorbate-free surface as described in the seminal work of Fowler and Nordheim. The investigations of adsorbate-altered field emission are still in progress.

The origin of mass 19 in vacuum systems. The hydronium ion is readily formed via the ion-molecule reaction $H_2O^+ + H_2O \rightarrow H_3O^+ + OH$, with a rate constant k . 2 x 10^{-9} cm^3/ s. The presence of water vapor in most vacuum systems will lead to the production of H_2O^+ in any mass spectrometric ion detection scheme. Subsequent conversion of this parent ion to hydronium occurs rapidly and can (mistakenly) lead one to think that F^+ is present implying that, alas, fluorocarbons reside in the system. Below is a mass spectrum from a high resolution Fourier transform mass spectrometer (a.k.a. ion-cyclotron resonance) in which the two ions are clearly resolved. Fluorine is purposely introduced into the vacuum system through CF_4. If one varies the partial pressure of water in the vacuum system the magnitude of the H_3O^+ peak is observed to vary as the square of that pressure, in accordance with pathway suggested above.

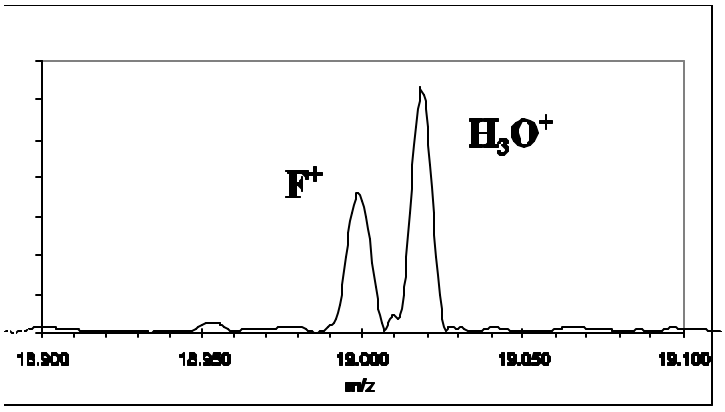

Figure 4 *A mass spectrum using a chirped, notched rf pulse in a FTMS to separate F^+ from H_3O^+.*

Future directions During the coming contract period we will complete several experiments involving particle-induced secondary emission processes on surfaces. In particular we will employ a neutral beam - with kinetic energy in the vicinity of 300-600 eV - to initiate secondary emission. By comparing these results to those of the parent positive ion, the precise role of the ion's recombination energy in the secondary emission process can likely be determined. We will also continue to investigate the role of adsorbates on field emission by a variety of means. In addition to examining field emitting arrays, we have initiated a series of experiments in which individual emitters can be probed in substantial detail.

Recent Publications

Collisional decomposition of the sulfur hexafluoride anion (SF_6^-)
R. L. Champion, I.V. Dyakov, B.L. Peko, and Y. Wang
Journal of Chemical Physics **115**, 1765 (2001).

Oxygen adsorption on a Si(100) substrate: Effects on secondary emission properties
W.S. Vogan and R.L. Champion
Surface Science **492,** 83 (2001).

Measured cross sections and ion energies for a CHF_3 discharge
B. L. Peko, R. L. Champion, M. V. V. S. Rao and J. K. Olthoff
Journal of Applied Physics **92**, 1657 (2002).

The role of an oxygen adsorbate on the secondary emission properties of low energy ion-bombarded magnesium
W. S. Vogan, R. L. Champion, and V. A. Esaulov
Surface Science **538**, 211 (2003).

Mass spectral resolution of F^+ and H_3O^+ in very high vacuum.
C. R. Cole, R. A. Outlaw, R. L. Champion, D. H. Baker, and B. C. Holloway
J. Vac. Sci. Tech. **A21**, xxx, (2003).

Multiphoton Quantum Dynamics and Optimal Generation of Coherent X-Ray Harmonic Emission

Shih-I Chu
Department of Chemistry, University of Kansas
Lawrence, Kansas 66045
E-mail: sichu@ku.edu

Program Scope

In this research program, we address the fundamental physics of the interaction of atoms and molecules with intense ultrashort laser fields. The main objectives are to develop new theoretical formalisms and accurate computational methods for *ab initio* comprehensive investigations of multiphoton quantum dynamics and very high-order nonlinear optical phenomena of one- and multi- electron quantum systems in intense and superintense laser fields, taking into account detailed atomic and molecular structures. Particular attention will be paid to the exploration of novel new physical mechanisms, time-frequency spectrum, and coherent control of multiple high-harmonic generation (HHG) processes for the development of tabletop x-ray laser light sources. Also to be investigated is the fundamental AMO theory on the interactions of ultrafast, intense x-ray pulses with atomic and molecular systems, including multiphoton and high-field effects.

Recent Progress

1. Development of Self-Interaction-Free Time-Dependent Density Functional Theories (TDDFT) for Nonperturbative Treatment of Multiphoton Processes of Many-Electron Quantum Systems in Intense Laser Fields

To study multiphoton processes of many-electron quantum systems in strong fields using the *ab initio* wave function approach, it is necessary to solve the time-dependent Schrödinger equation of 3N spatial dimensions in space and time (N = the number of electrons), which is beyond the capability of current supercomputer technology. The *single-active-electron* (SAE) model with *frozen core* is commonly used and has been successful for some strong-field processes where only one valence electron plays the dominant role. However, within the SAE model, important physical phenomena such as excited state resonances, dynamical response from different valence spin-orbitals, inner core excitation, and the dynamical electron correlations cannot be treated. Clearly, a more complete formalism beyond the SAE and other phenomenological models is very desirable for further progress in the exploration of the atomic and molecular physics in strong fields. Recently we have initiated a series of new developments of *self-interaction-free* time-dependent density functional theory (TDDFT) for probing strong-field processes of many-electron atomic systems, taking into account electron correlations and detailed electronic structure [1-3]. Since 2001, we have also begun to develop self-interaction-free TDDFT for the two-center diatomic molecular systems as well [4,6]. Given below is a brief summary of the progress in 2001-2003.

a) High-Order Harmonic Generation of Rare Gas Atoms in Intense Laser Pulsed Fields

We perform a detailed *all-electron* study of multiphoton ionization (MPI) and high-order harmonic generation (HHG) processes of rare gas atoms (He, Ne, and Ar) in intense pulsed laser fields [3] by means of the *self-interaction-free* TDDFT recently developed in our group. The time-dependent exchange-correlation (xc) potential with proper short- and long- range potential is constructed by means of the *time-dependent optimized effective potential* (TD/OEP) method and the incorporation of an explicit *self-interaction-correction* (SIC) term. The TD/OEP-SIC equations are solved accurately and efficiently by the use of the *time-dependent generalized pseudospectral* technique [7]. In this study, all the valence electrons are treated explicitly and nonperturbatively and their partial contributions to the ionization and

HHG are analyzed. The results reveal qualitatively different behavior from each subshell orbital. Moreover, we found that the HHG yields from Ne and Ar atoms are considerably larger than that of the He atom in strong fields. Two main factors are identified for accounting the observed phenomena: (a) the binding energy of the subshell valence electron, and (b) the orientation of the valence electron orbital (with respect to the electric field polarization).

b) Multiphoton and High-Order Harmonic Generation of H_2 in Intense Laser Fields

While the study of atomic processes in intense laser fields has been a very active field of strong field AMO physics research both experimentally and theoretically in the last decade, the study of strong-field molecular progress begins to receive more attention only quite recently. The high-field phenomenon in molecular systems is a largely unexplored area of frontier research. *Ab initio* theoretical studies of many-*electron* molecular processes in strong fields are considerably much more challenging than the corresponding atomic processes due to the multi-center problems and the additional nuclear degrees of freedom. Thus most theoretical studies on strong-field molecular processes up to today were based on simple models and did not take into account the effect of detailed molecular structure.

We have recently initiated the development of general *self-interaction-free* TDDFT for nonperturbative and comprehensive treatment of multiphoton processes of *multi*-electron *molecular* systems in intense laser fields [4]. The resulting TDDFT equations are structurally similar to the time-dependent Hartree-Fock equations, but include the many-body (electron-correlated) effects through an orbital-independent single-particle *local* time-dependent exchange-correlation (xc) potential. The latter is constructed by means of the time-dependent OEP/SIC method. A numerical time-propagation technique is introduced for accurate and efficient solution of the TDDFT/OEP-SIC equations for two-center diatomic molecular systems. The procedure involves the use of a *generalized pseudospectral method* for *nonuniform* optimal grid discretization of the Hamiltonian in prolate spheroidal coordinates [5] and a split-operator scheme in the *energy* representation for the time development of individual electron orbital wave functions. High-precision time-dependent wave functions can be obtained by this procedure with the use of only a modest number of grid points. The theory is applied to the first *all-electron* study of HHG processes of H_2 molecules in intense pulsed laser fields. Particular attention is paid to the exploration of the spectral and temporal structures of HHG by means of the wavelet time-frequency analysis. The results reveal striking details of the fine structures (sub-peaks) of the time profile of individual harmonic, providing new insights regarding the underlying HHG mechanisms in different energy regimes, including low-lying multiphoton dominant regime, near ionization-threshold regime, plateau regime, and near cut-off regime, for a molecular system for the first time [4].

c) Multiphoton Processes and Dynamical Response of Individual Valence Electrons of N_2, O_2, F_2 Molecules in Intense Laser Fields

Recently we have developed a molecular TDDFT with proper long-range potential for the first *all-electron* nonperturbative detailed study of multiphoton ionization (MPI) and high-order harmonic generation (HHG) of N_2 (with fixed nuclei) in intense laser fields [6]. A time-dependent generalized pseudospectral method is extended for precision solution of the TDDFT equations for two-center diatomic systems. The results reveal unexpected and intriguing nonlinear optical response behaviors of the individual valence spin orbital to strong fields. In particular, it is found that the dominant contribution of total HHG power spectrum of N_2 is due to the constructive and destructive interferences of the induced dipoles of the two highest-occupied bonding ($3\sigma_g$) and antibonding ($2\sigma_u$) molecular orbitals in the presence of intense laser fields [6]. Extension to the study of ionization and HHG of O_2 and F_2 is in progress [8].

2. *Quantum Fluid Dynamics Approach to Strong-Field Processes*

We have explored the feasibility of extending the quantum fluid dynamics (QFD) approach for nonperturbative investigation of many-electron quantum systems in strong fields. Through the amalgamation of

the QFD and density functional theory (DFT), a single time-dependent hydrodynamic equation can be derived. This equation has the form of a generalized nonlinear Schrodinger equation (GNLSE) but include the many-body effects through a local time-dependent exchange-correlation potential. A time-dependent generalized pseudospectral method is developed to the solution of the GNLSE in spherical coordinates, allowing *nonuniform* and optimal spatial discretization and accurate solution of the hydrodynamic wave function and density in space and time. The procedure is applied to the study of MPI and HHG of He and Ne atoms in intense laser fields [9]. Excellent agreement with the *ab initio* TDDFT/OEP-SIC calculations [3] is obtained for He, and for Ne, good agreement is achieved. The QFD/DFT method offers a conceptually appealing and computational practical approach for nonperturbative treatment of complex many-electron systems well beyond the time-dependent Hartree-Fock level. More exploration of this formalism is in progress.

3. Generalized Floquet Formulation of TDDFT for Intense-field Multiphoton Processes of Atomic Systems

Recently we have initiated the development of the generalized Floquet formulation of TDDFT for general nonperturbative treatment of multiphoton processes of many-electron atomic systems [10,11]. Further we have determined exact relations of the quasienergy functional and the exchange-correlation potential [11]. The Floquet-TDDFT approach allows exact transformation of the *periodically* (one-color) or *quasi-periodically* (multi-color) time-dependent Kohn-Sham equation into an equivalent time-independent generalized Floquet eigenvalue problem. Furthermore, we have developed an exterior-complex scaling (ECS) – generalized pseudospectral (GPS) method for accurate solution of the non-Hermitian Floquet-TDDFT Hamiltonian [12]. We applied the new procedure to the study of one- and two-photon detachment of Li^- negative ions. For the one-photon case, the photodetachment cross sections are in good agreement with experimental data. In the two-photon case, both the partial detachment rates and electron angular distributions for the dominant and above-threshold channels are determined for a range of laser frequencies and intensities. Dramatic transformation of the angular distributions in the vicinity of the two-photon threshold are observed and analyzed in details [12]. An account of the recent development of generalized Floquet formulations of TDDFT is given in a recent invited article [13]. An extensive review article on the generalized Floquet formulations and complex quasienergy methods for atomic and molecular processes in intense laser fields has been recently completed [14].

4. Optimization of Multiple High-Order Harmonic Generation by Genetic Algorithm and Wavelet Time-Frequency Analysis

The study of coherent control of atomic and molecular processes is a subject of much current interest in science and technology. In the area of the interaction of atoms with intense laser pulse, the optimization of high-order harmonic generation (HHG) is a topic of particular interest to the future technological development of x-ray laser, attosecond laser pulse generation, and many other applications. Recently the JILA high-field experimental group has shown that it is possible to perform "intra-atomic" phase matching, allowing the enhancement of the intensity of a specific harmonic [15]. Although qualitative picture of such an intra-atomic phase matching may be roughly explained by the quasi-classical electron trajectory picture [16], the quantum nature of this process such as the time-dependent quantum wave function, and the delicate quantum interference pattern, etc., is not yet known. To advance this important field, we have recently pursued the first fully *ab initio* quantum 3D study of the coherent control of HHG in intense laser fields by means of the *genetic algorithm* (GA) of the laser-pulse amplitude and phase [17]. Accurate time-dependent wave function and HHG power spectrum of atomic H are obtained by the *time-dependent generalized pseudospectral method* [7] and the *wavelet transform* is used to obtain the quantum dynamical phase associated with the dipole-emission time profile. It is shown that "intra-atomic" dynamical phase matching on the sub-optical cycle, atto-second, time scale can be achieved, leading to nearly perfect constructive interference between different returning quantum electronic wave packets and marked improvement in both emission intensity and purity of a given harmonic [17].

5. Spectral and Temporal Structures of High-Order Harmonic Generation of Na Atoms in Intense Mid- IR Laser Fields

The recent advancement of mid-IR laser technology [18] opens the possibility of studying multiphoton processes in systems with lower binding energies (such as alkali atoms) and allows the exploration of fundamentally different strong-field phenomena at longer wavelengths. Recently it has been also suggested that an intense mid-IR laser light source may be used to generate HHG in the visible to UV regime, allowing the application of frequency resolved optical grating [19] for the full characterization of the harmonic's amplitude and phase. Motivated by such recent experimental advances, we have performed a 3D precision quantum study of HHG of Na atoms in mid-IR laser fields [20]. The HHG power spectrum shows fine structure and significant enhancement of intensities of the lower harmonics due to the strong coupling of the 3s-np states and the 3s-3p multiphoton resonance. We extend the wavelet transform to perform a detailed time-frequency analysis for the whole range of HHG power spectrum. The results reveal unexpected details of the spectral and temporal fine structures of individual harmonic, providing insights regarding different HHG mechanisms in different frequency regime of Na atoms at longer wavelengths [20].

Future Research Plans

In addition to continuing the ongoing researches discussed above, we plan to initiate the following several new project directions: (a) Extension of the genetic algorithm and wavelet time-frequency analysis to the optimization of HHG processes of many-electron atomic systems. (b) Development and extension of self-interaction-free TDDFT to diatomic molecular systems including the vibrational and rotational degrees of freedom for the study of the ionization suppression and HHG phenomena in strong fields. (c) Development and extension of the Floquet formulation of TDDFT to the molecular systems. (d) Further exploration of the quantum-fluid dynamics/DFT approach for the investigation of multiphoton processes of complex many-electron quantum systems in strong fields.

References Cited (* Publications supported by this DOE program.)

[1] X. M. Tong and S. I. Chu, Phys. Rev. A**57**, 452 (1998).
[2] X. M. Tong and S. I. Chu, Int. J. Quantum Chem. **69**, 305 (1998).
*[3] X. M. Tong and S. I. Chu, Phys. Rev. A**64**, 013417 (2001).
*[4] X. Chu and S. I. Chu, Phys. Rev. A**63**, 023411 (2001).
[5] X. Chu and S. I. Chu, Phys. Rev. A**63**, 013414 (2001).
*[6] X. Chu and S. I. Chu, Phys. Rev. A**64**, 063404 (2001).
[7] X. M. Tong and S. I. Chu, Chem. Phys. **217**, 119 (1997).
*[8] X. Chu and S. I. Chu, Phys. Rev. A (submitted).
*[9] A. K. Roy and S. I. Chu, Phys. Rev. A**65**, 043402 (2002).
[10] D. Telnov and S. I. Chu, Chem. Phys. Lett. **264**, 466 (1997).
*[11] D. Telnov and S. I. Chu, Phys. Rev. A**63**, 012514 (2001).
*[12] D. Telnov and S. I. Chu, Phys. Rev. A**66**, 043417 (2002).
*[13] S. I. Chu and D. Telnov, J. Chinese Chem. Soc. **49**, 737 (2002).
*[14] S. I. Chu and D. Telnov , Physics Reports (submitted).
[15] R. Bartels, S. Backus, E. Zeek, L. Misoguti, G. Vdovin, I. P. Christov, M. M. Murnane, and H. C. Kapteyn, Nature (London) **406**, 164 (2000).
[16] I. P. Christov, R. Bartels, H. C. Kapteyn, and M. M. Murnane, Phys. Rev. Lett. **86**, 5458 (2001).
*[17] X. Chu and S. I. Chu, Phys. Rev. A **64**, 021403 (R) (2001).
[18] B. Sheehy, *et al*., Phys. Rev. Lett. **83**, 5270 (1999).
[19] R. Trebino, *et al*., Rev. Sci. Instrum. **68**, 3277 (1997).
*[20] X. Chu, S. I. Chu, and C. Laughlin, Phys. Rev. A**64**, 013406 (2001).

Optical Two-Dimensional Fourier Transform Spectroscopy of Disordered Semiconductor Quantum Wells and Quantum Dots

Steven T. Cundiff
JILA/University of Colorado and NIST
Boulder, CO 80309-0440
cundiffs@jila.colorado.edu

Program Scope: The goal of this program is to implement optical 2-dimensional Fourier transform spectroscopy and apply it to semiconductors. Specifically of interest are quantum wells that exhibit disorder due to well width fluctuations and quantum dots. In both cases, 2-D spectroscopy will provide information regarding coupling among excitonic localization sites.

Progress: Activities since the start of the program consisted of the following: (1) converting the existing 2-pulse four-wave-mixing setup to a 3-pulse setup; (2) exercising the 3-pulse setup by simultaneously measuring the Raman and optical decoherence rates for the heavy and light hole excitons and (3) developing the technology to be able to scan the delays by a large amount, but with subwavelength resolution and repeatability.

2D-FTS is an enhanced version of transient four-wave-mixing (TFWM). A 2-pulse TFWM setup existed in the PI's laboratory. Two-pulse TFWM is the traditional technique for studying coherent light-matter interactions in semiconductors. 2D-FTS is based on 3-pulse TFWM, thus the first step was to convert the 2-pulse setup into a 3-pulse setup. This has been completed.

To test out the 3-pulse TFWM setup, we measured the decoherence of the "Raman" transition between heavy-hole (*hh*) and light-hole (*lh*) excitons. Such a measurement cannot be performed using a 2-pulse TFWM experiment. Prior measurement of the Raman decoherence in semiconductors have used a transient-absorption configuration. The disadvantage of a transient-absorption configuration is that the Raman signal rides on a strong background from the ordinary signal due to saturation. The 3-pulse TFWM experiment has the additional advantage that it can simultaneously measure the Raman and optical decoherence rates.

Figure 1 shows the comparison of the optical [Fig. 1(a)] and Raman [Fig. 1(b)] decoherence rates, which yielded the surprising conclusion that the Raman decoherence was "anomalously" fast. In a 3-pulse experiment, the decay of beats as function of delay between 2nd and 3rd pulses (T) is due to Raman decoherence whereas the decay of the signal as function of delay between 1st and 2nd pulses (τ) is due to optical decoherence. Specifically, the Raman decoherence is anomalous because it is faster than the sum of the individual optical decoherence rates for the *hh* and *lh* excitons. This indicates that anti-correlated scattering events are contributing to the dephasing. In an anti-correlated scattering event, the frequency perturbation of the *hh* and *lh* levels have the opposite signs, thus the accumulated phase shift is larger for the Raman transition than for either optical transition.

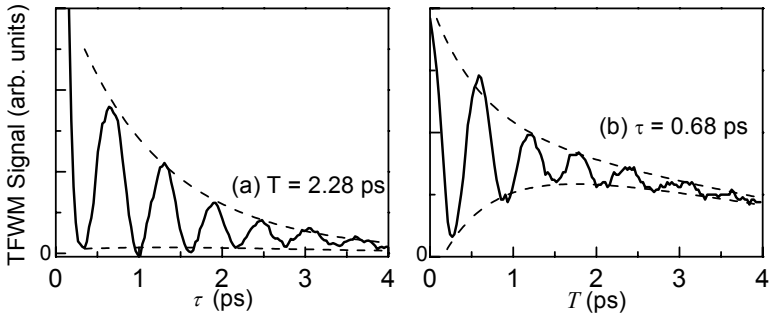

Fig. 1. Typical TFWM signal upon simultaneous excitation of both the *lh* and *hh* exciton resonances. The experimental configuration for the 3-pulse TFWM is shown as an inset to Fig. 1(a). In (a), the τ is varied with $T = 2.28$ ps. In (b), $\tau = 0.68$ ps, and the T is varied.

The fact that a larger scattering rate is actually observed also yields insight into the strength of the scattering. In the limit that the scattering is very strong, i.e. the accumulated phase shift is larger than 2π, then the maximum decoherence rate for the Raman coherence should be the sum of the rates for the two optical transitions. The fact that it exceeds this means that the scattering must weaker. This is borne out by simple simulations shown in Fig. 2. The decay of the coherence of an ensemble of 3-level system is plotted as function of time. The time derivative of the natural log is taken as a measure of the "local" decay rate. It is found that for the Raman transition, this can only exceed the sum of the decoherence rates for the optical transitions if the scattering amplitude is less than 2π. These results were presented at the workshop in Nonlinear Optics and Excitation Kinetics in Semiconductors in Karlsruhe last February and published in physica status solidi (b).[1]

Currently we are working on wrapping this up by using the formalism developed by Mukamel for calculating TFWM signals including memory effect. We have extended the theory to include population decay and will be comparing it to the experimental results.

Two more modifications to the 3-pulse TFWM setup are needed to be able to use it to perform 2D-FTS. One is to use spectral interferometry for detection. Spectral interferometery allows full phase information about the emitted signal to be obtained. This

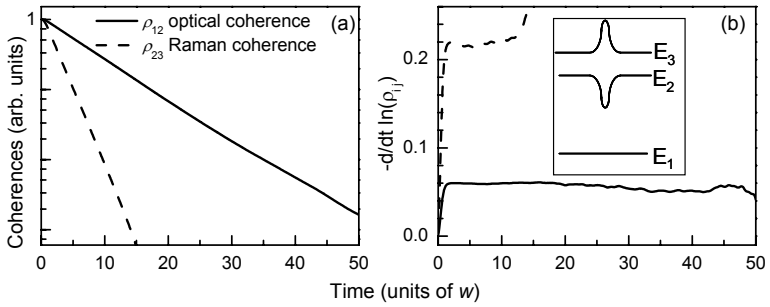

Fig. 2. Simulation results for anti-correlated exciton scattering processes in a weak scattering approximation. (a) The optical coherence, ρ_{12}, is shown as a continuous line, while the Raman coherence, ρ_{23}, is plotted with a dashed line. (b) The local dephasing rates for these two transitions. The inset shows a schematic diagram of the energy level shifts that occur for an anti-correlated scattering process.

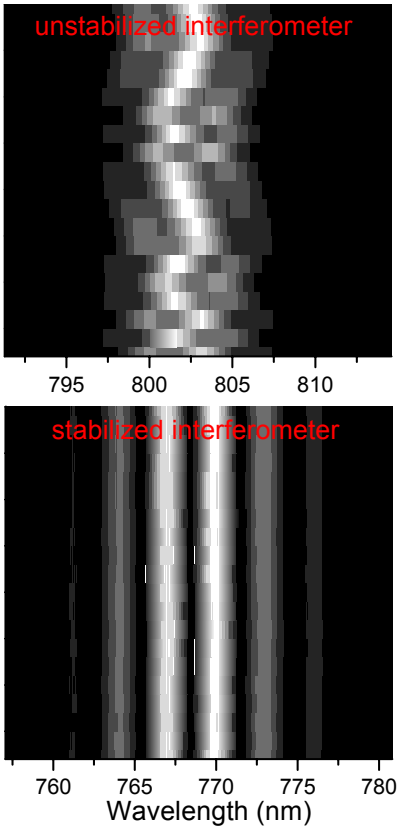

Fig 3. A series of spectral interferograms for an unstabilized and stabilized inteferometer. The shift of the peaks in the unstablized case shows the phase fluctuations.

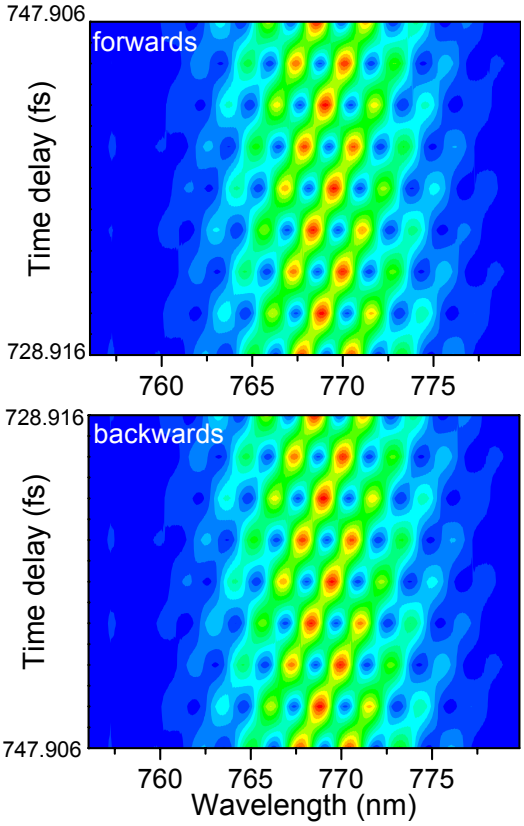

Fig 4. Spectral interferograms showing scanning of stabilized interferometer forwards and backwards.

is fairly straightforward and already implemented. The data shown in figures 3 & 4 are spectral interferograms. The second, much harder step, is to make it so that the delay between the first and second pulses is interferometrically stable and also can be scanned over several to tens of picoseconds. This requires that a servo loop be used to lock the path length difference. Furthermore, it requires an actuator, or combination of actuators, that can both make fast small motions to implement the servo lock as well as the long travel need for scans.

The second step is needed for 2D-FTS, which requires that the emitted signal be measured, including the phase, as function of the phase-delay between the first two excitation pulses. This presents a challenge for resonant excitation (approximately 800 nm) of excitons in GaAs based semiconductor heterostructures as the passive stability is usually insufficient. Prior work on molecules at these wavelengths by the Jonas group have relied on measuring the delays at each step, but this has been found to introduce artifacts in the results, thus active stabilization is preferred.

Our initial approach was to use a single actuator based on a voice-coil to fulfill both requirements. However achieving a sufficiently tight lock with the voice-coil proved prohibitively difficult. There were a variety of reasons for this, including the electrical

characteristics of the voice-coil, the fact that it acts like a microphone and that it had to move a fairly large mass. After several months, we abandoned this and switched to a different configuration.

The current configuration uses two actuators, a small piezo-electric transducer provides rapid, small corrections to implement the servo lock. A "Pico-motor" from NewFocus is used to implement the scanning. The pico-motor has a step size of 30 nm, which has sufficient accuracy to make sure that the correct fringe will be acquired when the servo loop is enabled. A HeNe laser is used to monitor fluctuations and provide an error signal to the feedback loop. The effect of stabilization at a fixed position is shown in Fig. 3. It shows a series of interferograms (vertical axis), without stabilization, the fringe position clearly fluctuates.

At this point, we have tested this system in a simplified setup. The HeNe and a femtosecond laser are combined and sent through a Michelson interferometer. After the interferometer, they are separated by a dichroic mirror. The HeNe is detected by a balanced detector, which provides the error signal to the servo loop. The spacing between the resulting pair of femtosecond pulses is measured using spectral interferometry. The spectral interferogram also gives the relative phase between the pulses. At this point, we have been able to step 100 HeNe fringes, and then return to the original point and obtain an identical interferogram, which means that the phase is being tracked and controlled during the scan. Figure 4 shows a forward and backward scan over 4.5 HeNe wavelengths. The steps are ½ a HeNe wavelength (316.5 nm). To make a step, the servo loop is disabled, the PicoMotor moved the correct number of steps, the gain sign of the servo loop changed and then the loop is re-enabled. The perfect pattern of shifting fringes shown that the steps are being taken correctly and that the servo loop is relocking correctly.

Currently we are putting this system through some further tests and making improvements to the software. Once this is complete, we will implement it on the actual TFWM setup. This requires some changes, primarily because it is not a simple Michelson interferometer. Specifically, the output beams are not collinear, thus do not interfere. In order to obtain interference, we will retro-reflect the HeNe beams with a dichroic mirror. The two output ports of the HeNe interferometer will then be the second port of the 50/50 beam splitter and the reflection of the initial dichroic that combines the HeNe and femtosecond ti:sapphire pulses.

[1] C.N. Borca, A.G. VanEngen Spivey and S.T. Cundiff, "Anomalously fast decay of the LH-HH exciton Raman coherence," phys. stat. sol. (b) **238**, 521-524 (2003).

July 2003

Theoretical Investigations of Atomic Collision Physics

A. Dalgarno

Harvard-Smithsonian Center for Astrophysics
Cambridge, MA 02138
adalgarno@cfa.harvard.edu

Our research effort develops and applies theoretical methods for the quantitative predictions of atomic, molecular and optical phenomena. The program is responsive to experimental advances and influences them. A particular emphasis has been the study of collisions in ultracold atomic and molecular gases.

We continue with the development and application and methods for calculating the long-range interactions between atoms and molecules. We are exploring the application of time-dependent density functional theory to obtain values of van der Waals coefficients for pairs of complex atoms. We are also investigating the modifications that occur when one of the atoms is in an excited state and the interaction is anisotropic.

The dynamics of the elastic and inelastic scattering of helium atoms in collision with oxygen atoms in different fine-structure levels O(^3P_J) at cold and ultracold temperatures was studied. Scattering resonances occur. The positions and shapes of the resonances do not always mirror those in the elastic channels. The real parts of the scattering lengths are all positive and small. The rate coefficients for the quenching of O($^3P_1$) and O($^3P_0$) the zero temperature are 3.1×10^{-12}cm^{3}s^{-1} and 3.3×10^{-12}cm^{3}s^{-1} respectively. Quenching of C($^3P_1$) is interesting in comparison. We have shown that its quenching rate coefficient vanishes in the limit of zero temperature.

Collisions in which the projection quantum number m of a paramagnetic atom like oxygen are changed lead to trap loss. The behavior of the cross sections near zero energy depends on the total change Δm in the collision. The cross sections actually vary with velocity v in the threshold region as $v^{2\Delta m}$ for even Δm and as $v^{2(\Delta m+1)}$ for odd Δm. For elastic collisions, $\Delta m = 0$ and Wigner's law is recovered.

Measurements have been carried out of the spin-flip transitions in collisions of ^{3}He atoms with CaH molecules in the ground rotational N=0 state at a temperature of 0.4 K. Doyle et al. find that spin-flip does occur with a rate coefficient of $10^{-17\pm1}$cm^{3}s^{-1}. The mechanism through which the change in spin projection quantum number occurs is not immediately obvious. We have used a close-coupling formalism to demonstrate that the spin-flip is driven by an electrostatic coupling of the N = 0 and N = 1 rotational states and spin-rotation interaction in the virtual N = 1 state. We confirm the mechanism by calculating the cross section for different values of the spin-rotation interaction. We predict a rate coefficient of 1.2×10^{-17}cm^{3}s^{-1}. We make predictions as to which molecules have the least probability of spin-flip. We also calculate the cross sections for elastic scattering and for vibrational and rotational quenching. The cross sections are sensitive to the interaction potential because of the possible presence of a shape resonance that may be accessible at

a temperature of 0.4 K. Better agreement with experiment is found by shifting the shape resonance though discrepancies between theory and measurement remain. We agree qualitatively that rotational quenching is rapid and vibrational quenching slow.

We have begun an analysis of spin-flip in collisions of structureless atoms with $^3\Sigma$ molecules. We have initiated a study of the influence of magnetic fields on collision processes in ultracold gases. Wigner's law is modified. We have identified the explicit mechanism that drives the Zeeman transitions in collisions of $^3\Sigma$ molecules with helium atoms.

Detailed investigations have been carried out of collisions of ground state hydrogen atoms and of metastable hydrogen atoms. In collisions of H(1*s*) atoms, we have carried out detailed close-coupling calculations that include hyperfine interactions and reconfirm earlier conclusions that no acceptable modification of the interactive potentials can resolve the discrepancies of the collision cross sections with experiment. In collisions of H (2*s*) atoms, we have now included the energy defects due to fine structure and the Lamb shift. We conclude that Penning ionization is the principal mode for the mutual quenching of the 2*s* atoms at ultralow temperatures but a substantial contribution comes from double excitation transfer. Above 20mK, double excitation transfer can be treated as a resonance process and it then dominates the quenching.

Some attention has been given to the scattering of neutral atoms by molecular ions at ultralow temperatures. Because of the strength of the polarization attraction, many partial waves contribute and the Wigner regime is not reached until temperatures below a mK are reached and the rate coefficients for rotational quenching are then of the order of 10^{-9}cm^{3}s^{-1}.

Some attention has been given also to chemical reactions at very low temperature and a comparative study has been carried out of the reactions of F with HD leading to HF and DF. At low temperature, HF is the preferred channel because of the more efficient tunneling of the lighter H atom.

Brief investigations were made of several other topics. A formula was developed for the behavior of molecular transition dipole matrix elements at large internuclear distances. In the case in which the excited molecule separates into a ground state atom and an excited atom, the dipole moment varies as $Do(1+2\alpha(w)/R^3)$ for Σ–Σ transitions and as $Do(1-\alpha(w)/R^3)$ for Σ–π transitions where $\alpha(iw)$ is the dynamic polarizability at the transition frequency w. I participated in the interpretation of the structures appearing in the photoionization spectrum of $Ne^+$and in an investigation of the statistical averaging procedure for the refractive index of matter waves in which we pointed out errors in earlier formulations.

Publications 2000-2003

M. J. Jamieson, A. Dalgarno and L. Wolniewicz, Calculation of Properties of Two-Center Systems, Phys. Rev. A. 61, 042705, 2000.

R. Côté, M. J. Jamieson, Z-C. Yan, N. Geum, G-H. Jeung and A. Dalgarno, Enhanced Cooling of Hydrogen Atoms by Lithium Atoms, Phys. Rev. Lett. 84, 2806, 2000.

P. Froelich, S. Jonsel, A. Saenz, B. Zygelman and A. Dalgarno, Hydrogen-Antihydrogen Collisions, Phys. Rev. Lett. 84, 4577, 2000.

R. Coté and A. Dalgarno, Ultracold atom-ion collisions, Phys. Rev. A. 62, 012709, 2000.

N. Balakrishnan, A. Dalgarno and R. C. Forrey, Vibrational Relaxation of CO by Collisions with ^{4}He at Ultracold Temperatures, J. Chem. Phys. 113, 621, 2000.

S. B. Bayram, M. Havey, M. Rosu, A. Sieradzan, A. Derevianko and W.R. Johnson, $5p\ ^2P_j \rightarrow 5d\ ^2D_{3/2}$ Transition Matrix Elements in Atomic ^{87}Rb, Phys. Rev. A. 61, R050502-1, 2000.

A. Derevianko, Reconciliation of the Measurement of Parity Nonconservation in Cs with the Standard Model, Phys. Rev. Lett. 85, 1618, 2000.

A. Derevianko and A. Dalgarno, Long-range Interaction of Two Metastable Rare-gas Atoms, Phys. Rev. A. 62, 062501-1, 2000.

C.M. Dutta, P. Nordlander, M. Kimura and A. Dalgarno, Charge-transfer Cross Sections in Collisions of Ground-state Na Atoms with H^+ at Low-eV Collision Energies, Phys. Rev. A. 65, 0022709, 2001.

N. Balakrishnan and A. Dalgarno, On the Quenching of Rovibrationally Excited Molecular Oxygen at Ultracold Temperatures, J. Phys. Chem. A. 105, 2348, 2001.

V. Kharchenko and A. Dalgarno, Refractive Index for Matter Waves in Ultracold Gases, Phys. Rev. A. 63, 023615, 2001.

A. Derevianko, J.F. Babb and A. Dalgarno, High-precision Calculations of van der Waals Coefficients for Heteronuclear Alkali-metal Dimers, Phys. Rev. A. 63, 052704, 2001.

B. Zygelman, A. Saenz, P. Froelich, S. Jonsell and A. Dalgarno, Radiative Association of Atomic Hydrogen with Antihydrogen at Subkelvin Temperatures, Phys. Rev. A. 63, 052722, 2001.

A. Derevianko, R. Côté, A. Dalgarno and G.-H. Jeung, Enhanced Cooling of Hydrogen by a Buffer Gas of Alkali-Metal Atoms, Phys. Rev. A 64, 011404(R), 2001.

N. Balakrishnan and A. Dalgarno, Chemistry at Ultracold Temperatures, Chem. Phys. Lett. 341, 652, 2001.

R.C. Forrey, N. Balakrishnan, A. Dalgarno, M.R. Haggerty and E.J. Heller, Effect of Quasi-Resonant Dynamics on the Predissociation of van der Waals Molecules, Phys. Rev. A. 64, 022706-1, 2001.

C. Zhu, N. Balakrishnan and A. Dalgarno, Vibrational Relaxation of CO in Ultracold ^{3}He Collisions, J. Chem. Phys. 115, 1335, 2001.

N. Geum, G.-H. Jeung, A. Derevianko, R. Cote and A. Dalgarno, Interaction Potentials of LiH, NaH, KH, RbH and CsH, J. Chem. Phys. 115, 13, 2001.

A. Dalgarno, P. Froelich, S. Jonsell, A. Saenz and B. Zygelman, Collisions of H and $\overline{\text{H}}$, in New Directions in Antimatter Chemistry and Physics, Eds. C.M. Surko and F. A. Gianturco (Kluwer, The Netherlands) 2001.

M. Bouledroua, A. Dalgarno and R. Côté, Diffusion and Excitation Transfer of Excited Alkali Metal Atoms Phys. Rev. A. 65, 012701, 2001.

S. Jonsell, A. Saenz, P. Froelich, B. Zygelman and A. Dalgarno, Stability of Hydrogen-antihydrogen Mixtures at Low Energies, Phys. Rev. A. 64, 052712, 2001.

S. Jonsell, A. Saenz, P. Forelich, R.C. Forrey, R. C. Forrey, R. Côté and A. Dalgarno, Long-range Interactions between Two 2*S* Excited Hydrogen Atoms, Phys. Rev. A. 65, 042501, 2002.

A. Belyaev, A. Dalgarno and R. McCarroll, The Dependence of Nonadiabatic Couplings on the Origin of Electron Coordinates, J. Chem. Phys. 116, 5395, 2002.

E. Bodo, F. A. Gianturco and A. Dalgarno, Quenching of Vibrationally Excited CO(v=2) Molecules by Ultra-cold Collisions with ^{4}He Atoms, Chem Phys. Lett. 353, 127, 2002.

C. Zhu, A. Dalgarno and A. Derevianko, van der Waals Interactions between Molecular Hydrogen and Alkali-metal Atoms, Phys. Rev. A. 65, 034708, 2002.

E. Bodo, F. A. Gianturco and A. Dalgarno, The reaction of F + D_2 at Ultra-Cold Temperatures: The Effect of Rotational Excitation, J. Phys. B 35, 2391, 2002.

R. Krems and A. Dalgarno, Electronic and Rotational Energy Transfer in F($^2P_{1/2}$) + H_2 Collisions at Ultracold Temperatures J. Chem. Phys. 117, 118, 2002.

X. Chu and A. Dalgarno, Molecular Transition Moments at Large Internuclear Distances, Phys. Rev. A 66, 024701 (2002).

R.C. Forrey, V. Kharchenko and A. Dalgarno, On the Statistical Averaging Procedure for the Refractive Index of Matter Waves, J. Phys. B 35. L261, (2002).

A.M. Covington et al., Photoionization of Ne^+ Using Synchrotron Radiation, Phys. Rev. A. 66, 062710, 2002.

B. Zygelman, A. Dalgarno, M. J. Jamieson, and P.C. Stancil, Multichannel Study of Spin-Exchange and Hyperfine-Induced Frequency Shift and Line Broadening in Cold Collisions of Hydrogen Atoms, Phys. Rev. A 67,042715, 2003.

R.C. Forrey, S. Jonsell, P. Froelich and A. Dalgarno, Cold Collisions of Spin-Polarized Metastable Hydrogen Atoms, Phys. Rev. A 67 040701(R), 2003.

R. Krems and A. Dalgarno, Threshold Laws for Collisional Reorientation of Electronic Angular Momentum, Phys. Rev. A. 67, 050704-1, 2003.

N. Balakrishnan, G.C. Groenenboom, R.V. Krems and A. Dalgarno, The He-CaH($^2\Sigma^+$) Interaction: II. Collisions at Cold and Ultracold Temperatures, J. Chem. Phys. 118, 7386, 2003.

R. V. Krems, A. Dalgarno, N. Balakrishnan, and G. C. Groenenboom, Spin-flipping Transitions in $^2\Sigma$ Molecules Induced by Collisions with Structureless Atoms, Phys. Rev. A 67,060703 (R) (2003).

N. Balakrishnan and A. Dalgarno, On The Isotope Effect in F+HD Reaction at Ultracold Temperatures, J. Phys. Chem. in press.

R. V. Krems and A. Dalgarno, Disalignment Transitions in Cold Collisions of ^{3}P Atoms with Structureless Targets in a Magnetic Field, Phys. Rev. A in press.

Coherent Control with Four-Wave Mixing and Shaped Laser Pulses

DOE Grant No. DE-FG02-01ER15143

Marcos Dantus
Department of Chemistry and Department of Physics, Michigan State University, East Lansing MI 48824
dantus@msu.edu

1. Program Scope

Our DOE supported project is aimed at exploring the coherent manipulation of multiple quantum mechanical states. This work has proceeded in two different directions. We have carried out a number of gas phase three-pulse four wave mixing (FWM) measurements to improve our ability to load information using shaped laser pulses and to read the information stored in the quantum mechanical wave packets coherently. The second line of experiments deals with the coherent control in condensed phases. We have made a breakthrough in the understanding of the underlying requirements for coherent control of nonlinear optical processes in condensed phases and have shown control of two- and three-photon excitation in large molecules including proteins. Applications of these findings are beginning to emerge.

2. Manipulation of multiple quantum mechanical states in small isolated molecules

The goal of these experiments is to explore controlled excitation and manipulation of electronic and vibrational wave packets by coherent nonlinear optical methods. The research has focused on gas phase iodine where four-wave mixing (FWM) methods have been used to coherently prepare vibrational wave packets in the ground and excited states.[1] That work, together with a thorough theoretical analysis, was published in collaboration with Mukamel.[2] One of the motivating aspects was the possibility for storing and manipulating information in a quantum mechanical system. The project called for accurate measurements of the electronic decoherence rate (the time over which one can manipulate quantum states coherently without loss of information). We have measured the cross section for the long-range elastic collisions responsible for decoherence in neat iodine and for iodine in the presence of a number of buffer gases.[3] These fundamental measurements provide a foundation for understanding the dephasing interactions between molecules at distances that are up to ten times their van der Waals radii. Based on very encouraging results, we proposed a method for the coherent storage and manipulation of information that maintained coherence for nanoseconds. The setup combined a three-pulse photon echo arrangement and a pulse shaper. With this system, we showed that the spectrum of the signal beam provided a reliable output, reporting on the different transitions induced by the shaped second pulse.[4] This work has some similarities to the work on quantum computing using multiple pulse NMR. However, we have pointed out a number of advantages for using an optically based method. In the optical domain, quantum transitions are significantly more energetic than kT. NMR transitions are about eight orders of magnitude less energetic. This difference eliminates thermally induced errors in an optically based system even at room temperature. The train of optical pulses takes a couple of picoseconds instead of several seconds for the RF pulses needed in NMR, making an optical based system much faster.[4] The next step in our research project is to determine experimentally the accuracy with which one can encode two arrays of numbers and read out their product. These measurements will determine the scalability limits of the setup. This research project will be continued during the next granting period.

We carried out a research project on the molecular dynamics and interconversion between NO_2 and N_2O_4.[5] The study was carried out using the transient grating method. We observed rotational and vibrational wave packet dynamics that allowed us to determine the rotational constants of the molecules. We also observed the symmetric stretch of the unusually long N-N bond in N_2O_4. Our most significant finding was the absence of half revivals in the rotational wave packet dynamics of N_2O_4. This absence implies that the molecule is not perfectly planar as currently thought. Half revivals are only observed in molecules where symmetry imposes different population of even and odd rotational levels based on nuclear spin statistics. We observed that a large number of the N_2O_4 molecules dissociated into two NO_2 molecules in the presence of the far off-resonance laser fields. This implies that the barrier to dissociation is very small or not existent for certain geometrical configurations. We plan to follow up this study with additional measurements and collaboration with Professor Piotr Piecuch, who will calculate an even more accurate

ground state potential energy surface for this molecule using the method of moments. This project will be completed before the end of the present granting period.

3. Coherent control of large molecules in condensed phase

Instead of following the approach based on pulse shapers and learning algorithms suggested by Rabitz and implemented by Wilson, Gerber, Levis, Bucksbaum, and others, our approach towards coherent control of large molecules in the condensed phase has followed a completely different strategy. We have paid attention to changes in the power spectrum that are the direct result from pulse shaping. For a particular electric field E(t) inducing an n^{th} order optical transition, one can calculate the n^{th} order power spectrum. For example, the second order power spectrum contains frequencies proportional to $2\omega_0$, which are responsible to for two-photon excitation. The power spectrum depends on the spectral phase of the femtosecond pulses. This dependence can be calculated, therefore, the phase required to optimize a specific transition can be calculated and implemented using a pulse shaper. We have used this principle to demonstrate experimentally coherent control of two-, three- and higher order multiphoton excitation of large molecules including laser dyes and proteins.[6,7] We have expanded on this technology to demonstrate selective excitation of probe molecules in different micro-chemical environments.[8] We have, more recently, demonstrated selective two-photon microscopy (see Figure 1) [9] and have a number of additional applications to demonstrate in the future.

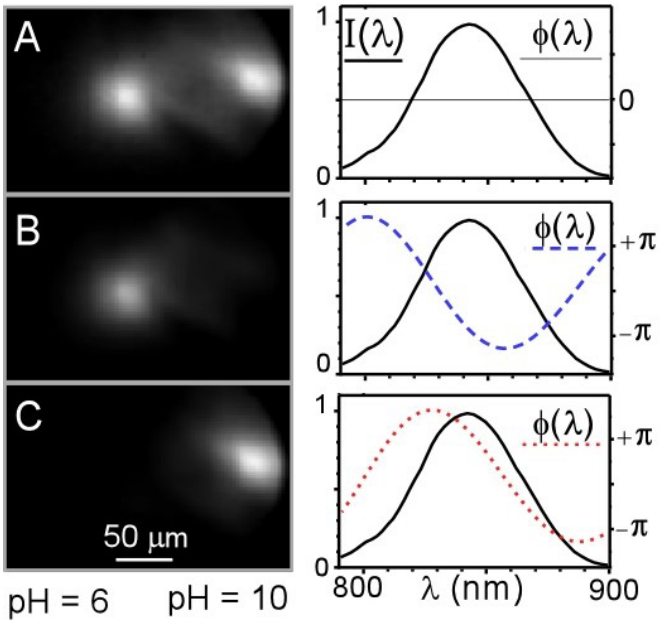

Figure 1, Experimental demonstration of pH-sensitive selective two-photon microscopy. The sample imaged has an acidic (left side of the frame at pH 6) and a basic (right side of the frame at pH 10) region, both labeled with HPTS. **A** Image of the sample obtained with transform-limited pulses. The diagrams on the right show the spectrum of the 21-fs laser pulses, centered at 842 nm, and the spectral phase of the pulse (blue dashed line or red dotted line, that maximize pH 6 or pH 10 fluorescence, respectively). **B** Image of the same sample and location obtained with pulses that have been optimized for selective excitation of HPTS in an acidic micro-environment. For this image $\alpha=1.5\pi$, $\gamma=20$ fs, and $\delta=0.75\pi$. **C** Image of the same sample and location obtained with pulses that have been optimized for selective excitation of HPTS in a basic micro-environment. For this image $\alpha=1.5\pi$, $\gamma=20$ fs, and $\delta=0.25\pi$.

The work described above would not have been possible without a significant amount of effort being invested on the development of pulse characterization and pulse shaping technology in our group during the present granting period. Our present setup is capable of taking in ultrashort femtosecond pulses, characterizing the phase distortions, compensating for the distortions and rendering transform limited pulses shorter than 15 fs in duration. These steps are now done automatically using a method developed by our group, that we have called multiphoton intrapulse interference phase scan (MIIPS).[8,10,11]

4. Future Work

A. Coherent control in the gas phase:

We are very encouraged by our first experiment using FWM for writing storing and reading information for a number of reasons. Most importantly, the signal level is relatively strong and can be separated easily from background scattered light. We are planning experiments that will establish how robust is this method with respect to thermal populations and noise. These results will also tell us realistic guidelines regarding scalability.

From a mathematical point of view, the proposed strategies based on photon echo pulse sequences can be used to perform the following functions: write, store in memory, read, sum, scalar product, direct products, matrix product between matrices and vectors. The large Hilbert space and the freedom to construct complex quantum gates give us the possibility to perform operations with quantum information within a single three-pulse sequence.

B. Coherent control in condensed phases:

The ability of controlling nonlinear optical processes in condensed phases opens up a number of applications in a variety of fields such as medicine and communications. The first application we have explored is selective multiphoton microscopy. We are planning experiments that can take advantage of the capabilities afforded by our method. We have identified single molecule/nanoparticle microscopy as one of the most important areas for exploration. We hope to pursue this application in the near future. We will continue to further the theory of multiphoton intrapulse interference for controlling nonlinear optics. We plan to demonstrate a number of additional applications, in the near future.

Publications Resulting from this Grant 2001-2003:

1 V. V. Lozovoy and M. Dantus, "Four-Wave Mixing and Coherent Control," in *Laser Control and Manipulation of Molecules*, A.D. Bandrauk, Y. Fujimura, R.J. Gordon Editors, ACS Publishing, Washington, p. 61 (2002).

2 I. Grimberg, V. V. Lozovoy, M. Dantus and S. Mukamel, "Femtosecond three pulse spectroscopies in the gas phase: density matrix representation," *J. Phys. Chem.* A, Feature 106, 5, 697 (2002). Our results featured in the cover.

3 M. Comstock, V. V. Lozovoy and M. Dantus, "Femtosecond photon echo measurements of electronic coherence relaxation between the $X(^1\Sigma_{g+})$ and $B(^3\Pi_{0u+})$ states of I_2 in the presence of He, Ar, N_2, O_2, C_3H_8," J. Chem. Phys. In press (2003)

4 V. V. Lozovoy and M. Dantus, "Photon echo pulse sequences with femtosecond shaped laser pulses as a vehicle for molecule-based quantum computation," *Chem. Phys. Letters*, 351, 213 (2002).

5 I. Pastirk, M. Comstock, and M. Dantus, "Femtosecond ground state dynamics of N_2O_4 and NO_2 investigated by degenerate four-wave mixing," *Chem. Phys. Letters*, 349, 71 (2001).

6 K. A. Walowicz, I. Pastirk, V. V. Lozovoy and M. Dantus, Multiphoton intrapulse interference. 1. Control of multiphoton processes in condensed phases, *J. Phys. Chem. A* 106, 9369 (2002). Our results were featured in the cover.

7 V. V. Lozovoy, I. Pastirk, K. A. Walowicz and M. Dantus, Multiphoton intrapulse interference. II. Control of two- and three-photon laser induced fluorescence with shaped pulses, *J. Chem. Phys.* 118, 3187 (2003).

8 J. Dela Cruz, I. Pastirk, V. V. Lozovoy, K. A. Walowicz and M. Dantus, Multiphoton Intrapulse Interference 3. Probing microscopic chemical environments, *J. Phys. Chem. A* in press, (2003)

9 I. Pastirk, J. Dela Cruz, K. A. Walowicz, V. V. Lozovoy and M. Dantus, Coherent control of two-photon microscopy with shaped femtosecond laser pulses, *Optics Express* 11, 1695 (2003)

10 M. Dantus, V. V. Lozovoy and I. Pastirk, Femtosecond spectral phase characterization, compensation and application to selective multiphoton spectroscopy, *OE magazine*, September, Feature Article (2003)

11 V. V. Lozovoy, I. Pastirk M. Dantus, "Multiphoton intrapulse interference 4; Characterization and compensation of the spectral phase of ultrashort laser pulses", Submitted, Optics Letters (2003)

High Intensity Laser Interactions with Atomic Clusters

Progress report (Fall 2003)

Principal Investigator:

Todd Ditmire
Department of Physics
University of Texas at Austin, MS C1600, Austin, TX 78712
Phone: 512-471-3296
e-mail: tditmire@physics.utexas.edu

Program Scope:

The nature of the interactions between high intensity, ultrafast laser pulses and atomic clusters of a few hundred to a few thousand atoms has come under study by a number of groups world wide. Such studies have found some rather unexpected results, including the striking finding that these interactions appear to be more energetic than interactions with either single atoms or solid density plasmas. Recent experiments have shown that the explosion of such clusters upon intense irradiation can expel ions from the cluster with energies from a few keV to nearly 1 MeV. This phenomenon has been exploited to produce DD fusion neutrons in a gas of exploding deuterium clusters. Under this project, we have undertaken a general study of the intense femtosecond laser cluster interaction. Our goal is to understand the macroscopic and microscopic coupling between the laser and the clusters with the aim of optimizing high flux fusion neutron production from the exploding deuterium clusters or the x-ray yield in the hot plasmas that are produced in this interaction. In particular, we are studying the physics governing the cluster explosions. The interplay between a traditional Coulomb explosion description of the cluster disassembly and a plasma-like hydrodynamic explosion is not entirely understood, particularly for small to medium sized clusters (<1000 atoms) and clusters composed of low-Z atoms. We are focusing on experimental studies of the ion and electron energies resulting from such explosions through various experimental techniques. Furthermore we are studying the effects that the explosions have in deuterated clusters and the fusion that is produced when these clusters expand.

Recent Progress

Much of the research undertaken previously under this project has been focused on the interaction of a intense 30 fs pulses with deuterium clusters. Since we are interested in the transition from a Coulomb explosion picture of the cluster (where it is assumed that the laser rapidly strips all the electrons from a cluster before it can explode) to a hydrodynamic picture (where the cluster explodes under the influence of the hot electron gas confined to the positively charged ion core), we have conducted cluster explosion studies that compare the explosion dynamics of low Z (hydrogen and deuterium) with those of clusters composed of higher Z constituents. The fusion experiments were conducted using the LLNL JanUSP laser which delivers 10 J. 100 fs pulses. The exploding cluster experiments were conducted using the THOR laser in Austin which delivers 0.75 J, 35 fs pulses.

1) Interactions with deuterated methane clusters

During this year, we concluded our campaign of fusion studies on the LLNL JanUSP laser. Following the studies of ion energies from CD_4 cluster reported last year, we measured fusion yields from CD_4 clusters and compared these data with our previous measurement of fusion yield in neat deuterium clusters. We conducted studies on clusters produced from a supersonic gas jet and varied the condition so that the CD_4

clusters were approximately the same size as the deuterium clusters in our previous experiments. Heteronuclear clusters like deuterated methane are very interesting since these mixed ion clusters may exhibit enhancements in ion energy through a dynamical effect in the Coulomb explosion. The Coulomb explosion of a single species cluster, like D_2 clusters, will eject deuterons with an energy given directly by the potential energy of the ion as it is initially in the fully stripped cluster. In exploding mixed ion clusters like CD_4 the light deuterons will outrun the heavier ions, explode in an outer shell with a higher average energy than would be expected from the naïve estimate of ion energy based on initial potential energy. This implies that the fusion yield could be substantially increased in plasmas formed from explosions of heteronclear clusters over that of neat D_2 clusters of the same size because of this kinematic enhancement of ion energies in the mixed ion case.

We examined the explosion of CD_4 clusters irradiated by the JanSUP laser at intensity up to 10^{20} W/cm^2. These clusters were produced by the same jet used in the D_2 experiments. The measured fusion yield as a function of laser energy is shown in figure 1 for a CD_4 cluster plasma. These data are compared to fusion yield in D_2 cluster plasmas. Initial measurements of the ion energy suggested some enhancement of the explosion in CD_4 clusters. This ion energy enhancement leads to a fusion yield enhancement at lower energy but the fusion yield is lower in CD_4 at higher laser energy. This fall off can be explained by the details of the energy balance in the plasma (explained in detail in ref. 7).

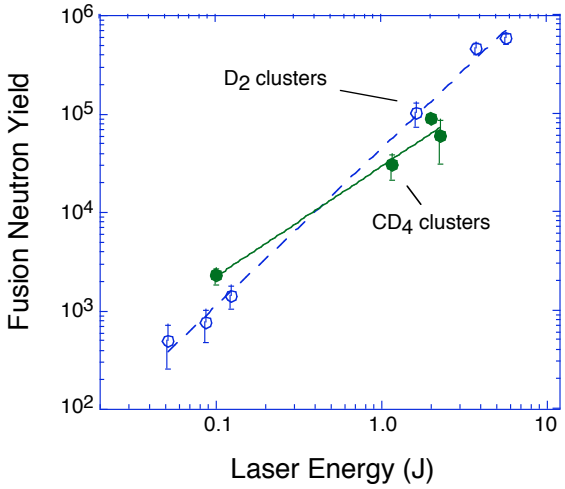

Figure 1: Measured fusion yield per laser shot vs energy for plasmas composed of neat deuterium clusters and plasmas composed of exploding CD_4 clusters of roughly the same size.

2) Ion angular distribution studies in exploding H_2 and Ar clusters.

Central to this project is the desire to understand the regimes in which the Coulomb explosion description is appropriate to describe the cluster explosion and when the electron fluid affects the explosion and the clusters explode in a hydrodynamic manner. Simple estimates indicate that, at intensity around 10^{17} W/cm^2 – 10^{18} W/cm^2, hydrogen clusters of a few thousand atoms expand by Coulomb explosion while similarly sized argon clusters (and higher Z) will explode hydrodynamically. One signature of this transition is in the angular distribution of the cluster ions with respect to the laser polarization.

Using the UT THOR laser and an ion time-of-flight spectrometer fitted with a low density cluster beam producing jet, we have studied the angular distributions of H_2 and Ar clusters. Figure 2 shows the measured average ion energies from Ar cluster with average size of ~ 10 nm diameter as a function of angle with respect to the laser polarization. We observe a slight enhancement of ion energies in the direction along the

polarization. This likely results from a hydrodynamic explosion which has an anisotropic electron temperature. More surprising are the distributions that we measure from the exploding hydrogen clusters. Three such distributions are illustrated in figure 3 While we expect a nearly isotropic distribution from the Coulomb exploding H_2 clusters, we, in fact, observe a slight hardening of the ion spectrum for ions ejected along the polarization axis. We are presently beginning simulations to understand this but this increase in the ion yield at the highest energies could result from fields set up by the outgoing electrons in the hydrogen cluster ionization.

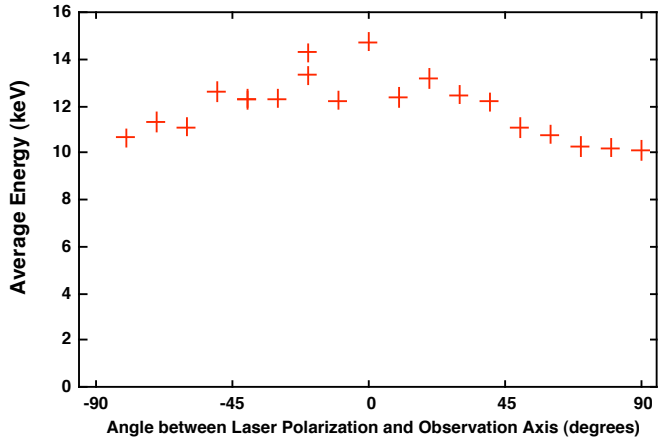

Figure 3: Measured average Ar ion energies from exploding Ar clusters irradiated by 37 gs pulses at inetsnity of ~ 1 x 10^{17} W/cm^2.

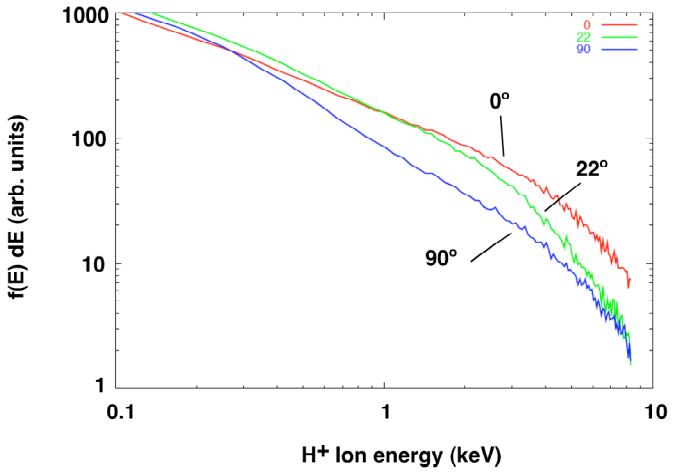

Figure 3: Measured average H^+ ion spectra from exploding H_2 as a function of the angle between the laser polarization. 0° is the spectrum emitted along the laser electric field direction and 90° are ions emitted perpendicular to the polarization.

Future Research Plans

Our future research plans are aimed at an understanding this transition in explosion dynamics expected from low to high Z clusters. We will concentrate on the ion and electron spectroscopy using the THOR laser.

1) Our next set of experiments at UT will be to examine the temporal dynamics of the ion energy distributions from hydrogen clusters (ie in the Coulomb explosion regime). We plan to carefully study pulse rise time effects, as well as the consequences of chirp. We will study both electrons and ions.

2) These experiments will be followed by greater attention to heteronuclear clusters. Note only will we examine the electron and ion energies from CD_4 clusters but we will examine other mixed species clusters, like HI.

3) Additional experiments will follow up on the two color pump-probe experiments. We have constructed a two pulse experiment. First we will study the explosions of high Z clusters in the hydrodynamic regime (ie Ar, Kr and Xe) with the two color experiment. This will let us look at the effects of the giant dipole resonance. We will also look at the angular distribution properties of these clusters which have been excited at resonance and compare with clusters driven with very short pulses (ie before the cluster can expand far enough to come into the resonance with the laser).

4) Finally, we plan to use the two pulse set-up to implement a "pump-pump" style experiment. These experiments with use two time delayed pulses of near equal intensity to learn about the extent of the cluster ionization as a function of time. This kind of experiment will give us information on how many electrons are confined in the cluster after the first ionizing pulse has passed.

Papers published or to appear on work supported by this grant (2001-2003):

1) T. D. Donnelly, M. Rust, I. Weiner, M. Allen, R. A. Smith, C. A. Steinke, S. Wilks, J. Zweiback, T. E. Cowan, and T. Ditmire, "Hard X-ray Production from Intense Laser Irradiation of Wavelength-Scale Particles" *J. Phys. B: At. Mol. Opt. Phys.* **34**, L313 (2001).

2) J. Zweiback, T. Ditmire, "Femtosecond Laser Energy Deposition in Strongly Absorbing Cluster Gases Diagnosed with Blast Wave Trajectory Analysis," *Phys. Plas.*, **8**, 4545 (2001).

3) J. Zweiback, T.E. Cowan, R. A. Smith, J. H. Hartley, R. Howell, G. Hays, K. B. Wharton, J. K. Crane, V. P. Yanovsky and T. Ditmire "Detailed Study of Nuclear Fusion From Femtosecond Laser-Driven Explosions of Deuterium Clusters" *Phys. Plas.* **9**, 3108 (2002).

4) K. W. Madison, P. K. Patel, M. Allen, D. Price, T. Ditmire, "An investigation of fusion yield from exploding deuterium cluster plasmas produced by 100 TW laser pulses" *J. Opt. Soc. Am. B* **20**, 113 (2003).

5) J. W. G. Tisch, N. Hay, K. J. Mendham, E. Springate, D. R. Symes, A. J. Comley, M. B. Mason, E. T. Gumbrell, T. Ditmire, R. A. Smith, J. P. Marangos, M. H. R. Hutchinson, "Interaction of intense laser pulses with atomic clusters: Measurements of ion emission, simulations and applications" *Nuc. Inst. Meth. B – Beam Interactins with Materials and Atoms* **205**, 310 (2003).

6) K. W. Madison, R. Fitzpatrick, P. K. Patel, D. Price, T. Ditmire, "The character of Coulomb explosions in deuterium cluster plasmas produced by 100 TW laser pulses" *Phys. Rev. A* to be published.

7) K. W. Madison, P. K. Patel, D. Price, A. Edens, M. Allen, T. E. Cowan, J. Zweiback, and T. Ditmire, "Fusion neutron and ion emission from laser induced explosions of deuterium and deuterated methane clusters" *Phys. Plas.* submitted

Ultracold Molecules: Physics in the Quantum Regime

John Doyle
Harvard University
17 Oxford Street
Cambridge MA 02138
doyle@physics.harvard.edu

1. Program Scope

Our research encompasses a unified approach to the trapping of both atoms and molecules. Our goal is to extend our very successful work with CaH to NH and approach the ultracold regime. We plan to trap and cool more than 10^{11} NH molecules loaded directly from a molecular beam. We have switched to the NH molecule due to its higher magnetic moment, 2 Bohr magneton versus 1 Bohr magneton for CaH. Elastic and inelastic collisional cross sections will be measured and cooling to the ultracold regime will be attempted. To date, no collisional cross sections have been measured for ultracold heteronuclear molecules and theory offers no accurate predictions. This work will be done with a cryogenic approach that does not require a dilution refrigerator, a considerable savings in time and complexity. We note that this proposal inherently contains the continued development of an important trapping technique, buffer-gas loading. This method was invented in our lab and its significant advantages (large numbers of trapped atoms and molecules as well as general applicability) indicate that further development is warranted.

2. Recent Progress

The milestones for this project are:

x–spectroscopic detection of ground-state NH molecules via LIF
x–production of NH in a pulsed beam
x–spectroscopic detection of ground-state NH molecules via absorption
x–injection of NH beam into cryogenic buffer gas (including LIF and absorption detection)
x–realization of 4 T deep trap run in vacuum
o–loading of NH molecules into cryogenic buffer gas with 4 T deep trap
o–measurement of spin-relaxation rate with He
o–trapping of NH
o–removal of buffer gas after trapping of NH
o–measurement of elastic and inelastic cross sections
o–attempt evaporative cooling

The project started 15 August 2002 and to date we have achieved the first 5 milestones (with "x's" in front). NH, like many of the diatomic hydrides, has several advantages for molecular trapping including large rotational constant and relatively simple energy level structure. There were several key questions before us when this project began. Could we produce enough NH using a pulsed beam? Is it possible to introduce a large number of NH molecules into a buffer gas? Would the light collection efficiency be enough for us to adequately detect fluorescence from NH? Could we get absorption spectroscopy to work so that absolute number measurements could be performed? We have now answered these questions, all to the positive.

There are key questions left. Will the spin relaxation rates with helium be low enough for us to buffer-gas load a magnetic trap? Will the NH-NH collision rates be adequate for evaporative cooling or will another method (like sympathetic or laser cooling) be necessary to cool NH into the ultracold regime. There is strong indication that the answer to the first is "yes." Recent theoretical

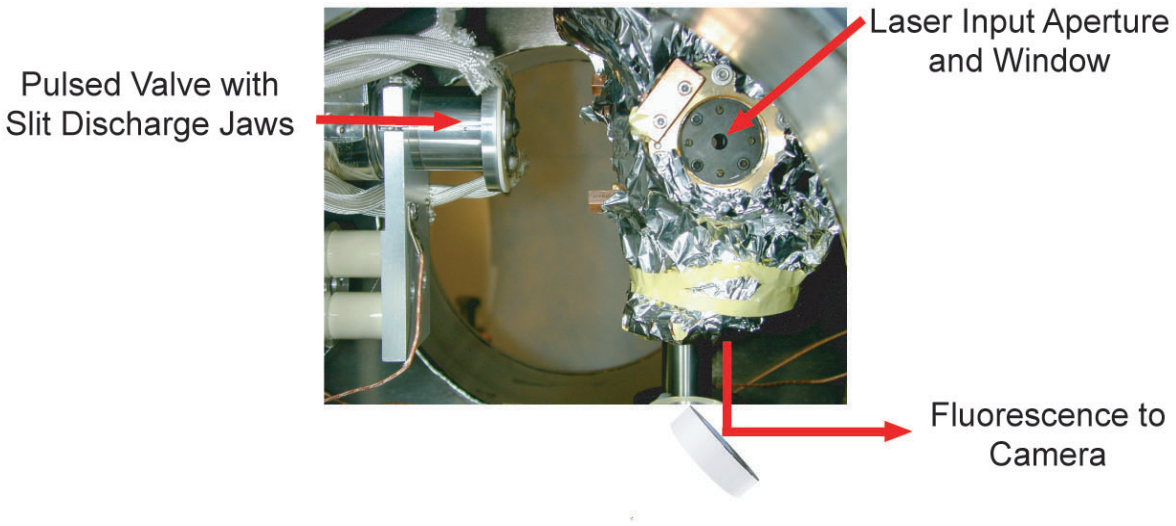

Figure 1: A photograph of our buffer-gas loading cell and NH discharge source. The discharge source (on the left) has been shown to deliver more than 10^{11} ground-state NH molecules into the cell. The cell is attached to the bottom of a liquid helium cryostat. Helium buffer gas flows out of a small hole that faces the discharge source while NH from the source flows in the other direction through the hole. An excitation laser enters through the aperture shown and fluorescence light from the cold molecules is collected with the aid of the mirror shown at the bottom. Both fluorescence and absorption spectroscopy was performed on the cold NH molecules.

calculations by Krems and coworkers (motivated by our experiment) indicate that NH will survive in the low-field-seeking state for several hundred thermalization times before it spin relaxes. The final question is still open and, indeed, answering this question is the key stated goal of this work.

Apparatus Development

We have constructed major apparatus and made several measurements. The measurements will be described in the subsequent section. Here we describe the apparatus only.

The heart of the apparatus is a beam machine that we use to produce pulsed NH in a supersonic beam. (We are in the supersonic regime only to maximize NH flux; 3 dimensional translational cooling and rotational cooling are provide by the buffer gas.) The design of the pulsed source is based on the production of OH via DC discharge as executed by Nesbitt. In short, we have a pulsed valve and a slit plate with a layer of BN in between. A voltage between the plates and the nozzle of the pulsed valve produces a discharge whenever we allow gas into the nozzle. This is done by opening the pulsed valve, with a solenoid, for times about 1 ms.

This beam is directed toward a cryogenic buffer-gas cell. This buffer-gas cell, see figure 1, was constructed with a small entrance orifice to allow the beam of NH to enter, thus buffer-gas cooling the NH. The cell is constructed of copper and the orifice is facing the pulsed beam. Several windows exist for the the introduction and collection of light. The window at the bottom of the cell is used to collect fluorescence emanating from the NH inside the cell. Windows on the side of the cell allow the introduction of laser excitation light. This cell is bolted onto the cold plate of a small liquid helium dewar. The cell, and, therefore, the helium buffer gas can be kept at temperatures as low as around 10 K.

All of these items are in a stainless steel "beam machine" box approximately 1 m X 50 cm

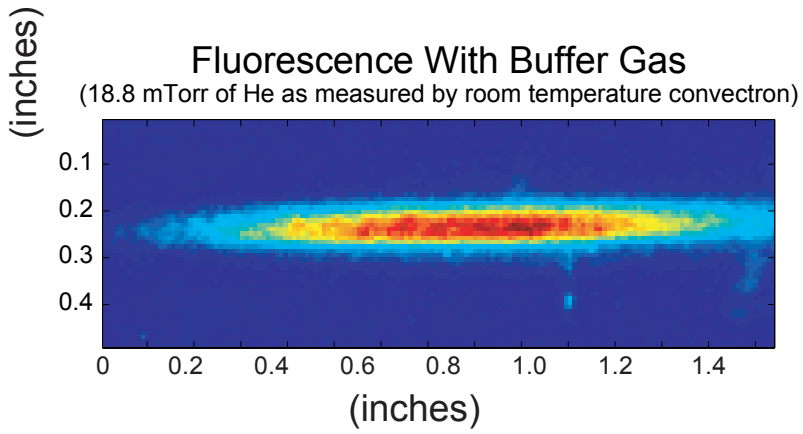

Figure 2: False-color image of cold NH molecules in the buffer-gas cell. These molecules were loaded into the cell in a single pulse from the discharge source and cooled to the temperature of the cell.

X 50 cm, pumped on by two large diffusion pumps. Windows on several faces of the beam machine allow introduction and collection of light. Fluorescence light is collected by an intensified CCD camera and read out via computer. Excitation light is produced by a coherent 699-21 ring dye laser doubled in an external build-up cavity. A doubled Sirah pulsed dye laser also produces excitation light. A balanced two-photodiode noise canceling absorption spectroscopy instrument is used for calibration of our fluorescence system. All of the lasers, the CCD camera, mass spectrometer and gas handling system are under computer control.

Measurements

In a series of experiments with a mass spectrometer we were able to detect the production of NH from the pulsed valve and optimize this production. The optimization parameters included voltage, current, valve opening time and gas content. For example, we studied backing gases of pure NH3, NH3 with nobel gases and NH_3 with N_2. These measurements indicated that we were converting approximately 1/10 of the NH_3 in the beam into NH.

In another series of experiments we were able to detect, using fluorescence spectroscopy, the successful introduction of NH from the pulsed beam into our cell. This was done both with the buffer-gas present and with no buffer-gas. Within an order of magnitude, the amount of NH making it into the cell was the same regardless of the presence of the buffer gas. This confirmed our model that the back streaming of helium out of the orifice (and toward the pulsed discharge source) would have little effect on the efficiency of buffer-gas capture. Typical fluorescence images are shown in figure 2. By employing absorption spectroscopy it was possible to make absolute measurements of the number of NH molecules in the buffer-gas. Greater than 10^{11} NH molecules were introduced and cooled into the buffer-gas cell in a single pulse from the discharge. We were able to determine the rotational and translational temperature of the NH in the buffer-gas and it was found to be, as expected, close to the cell temperature of 10 K.

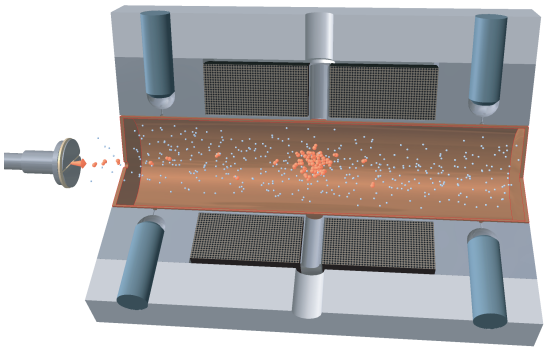

Figure 3: A schematic of the 4 T deep anti-Helmholtz magnetic trap. Such a superconducting trap, operating in vacuum, was recently demonstrated in our laboratory to reach full depth. this trap will be used in the next stages of the our experimental program to trap NH.

Latest Apparatus Development

Very recently we were able to finish the construction and testing of a novel in-vacuum superconducting magnetic trap. This magnet has an inner diameter of 7.5 cm and depth of greater than 4 Tesla (5.6 K for NH). There are large forces (about 100,000 lb.) developed as the coils, in the "anti-Helmholtz" configuration, are energized. We designed a mechanical support for the trap and had it machined in the local Harvard shop. Coils were wound by a commercial vendor. We then assembled and tested the device. To our knowledge, this is the first magnet of this type. We have submitted a publication on this magnet.

3. Future Plans

We continue on our program of trapping of NH. The next step is to buffer-gas load NH into the buffer-gas cell while the cell is inside the energized trap. In this was we should be able to spectroscopically determine the helium-NH spin relaxation rates. In order to aid this measurement, we are building a "lambda tip" refrigerator. This will allow us to cool our system down to close to 2 K, and enhance our ability to detect spin-relaxation. Immediately after that, we will cool our cell down to 0.4 K, and attempt trapping of the NH. This will require a He3 refrigerator. We are currently in the process of procuring this device.

Few-Body Reaction Imaging

Department of Energy 2003–2004

James M Feagin
Department of Physics
California State University–Fullerton
Fullerton CA 92834
jfeagin@fullerton.edu

Much of the progress with quantum information has relied heavily on quantum optics and manipulating photons. There is nevertheless fundamental interest in demonstrating analogous control with massive charged particles, for example correlated electrons and ions for which the DOE Office of Basic Energy Sciences has a long and distinguished history. With *few-body reaction imaging* we are working to develop tools for quantum control from the highly-evolved AMO industry of collision and few-body phenomena. Our research remains nevertheless part of a general effort in the AMO community to advance the basic understanding of collective few-body excitations. We are thus investigating the physics of nanoscale science, engineering, and technology (NSET) based on a long-time experience in AMO collision physics. We find there exists opportunity to contribute to at least two goals of the NSET initiative of the DOE: (i) Attain a fundamental understanding of nanoscale phenomena, and (ii) develop experimental characterization tools and theory to understand, predict, and control nanoscale phenomena.

We consider few-body reaction and fragmentation detection from the more general perspective of reaction imaging. We accordingly distinguish two parallel efforts with (i) new emphasis on *detection with interferometers* while (ii) pursuing ongoing work on *collective Coulomb excitations*.

Detection with Interferometers

Advances in coincidence detection technology for collisions involving charged particle or photon impact have evolved into a new field of few-body fragmentation spectroscopy.[1] Full kinematic information can now be extracted systematically on all collision fragments of few-body states from measurements of the momentum vectors of each fragment. With supersonically cooled targets, momentum detection to 1 au is now routinely achieved. With confined and cooled targets in magneto-optical traps, this precision is likely to improve in the near future by an order of magnitude. For example, B. DePaola and coworkers at Kansas State and independently N. Andersen and coworkers in Copenhagen have recently used trapped targets to resolve diffraction patterns in differential charge-transfer cross sections.[2] Parallel to this remarkable progress have been the developments in the field of atom optics concerned with manipulating with microstructures and light fields the motion of atoms and molecules and Bose-Einstein condensates to observe their interference and diffraction just like waves of light. For example, A. Zeilinger and coworkers in Vienna demonstrated recently the diffraction of fullerene molecules by standing light waves.[3] And in a remarkable tour de force, H. Batelaan and coworkers at Nebraska have demonstrated diffraction of electrons by standing light waves, thus establishing the Kapitza-Dirac effect 68 years after its prediction.[4]

[1] R. Dörner et al., Phys. Rep. **330**, 95 (2000).

[2] X. Flechard et al., Phys. Rev. Lett. **87**, 123203 (2001); M. van der Poel et al., Phys. Rev. Lett. **87**, 123201 (2001).

[3] O. Nairz et al., Phys. Rev. Lett. **87**, 160401-1 (2001).

[4] D. L. Freimund, K. Aflatooni, H. Batelaan, Nature **413**, 142 (13 Sep 2001). See also P. H. Bucksbaum, Nature **413**, 117 (13 Sep 2001).

In pioneering work on quantum correlation, Wootters and Zurek[5] analyzed how two-slit interference with photons changes when the recoil of a distant collimator slit is monitored. Motivated by the experimental interests of L. Cocke (Kansas State) and R. Dörner (Frankfurt), we have extended the description of Wootters and Zurek to particle impact ionization involving projectile interferometry and target-fragment recoil detection. Our intention is to combine few-body fragmentation spectroscopy with tools from atom optics to extract addtional amplitude and phase information from the reaction dynamics. This effort is thus much in the spirit of recent work by Forrey and coworkers to determine electron scattering amplitude information with electron interferometry.[6]

Our projectile wavefunction is just one component of an entangled 'projectile + target' state required by momentum conservation and generated when a projectile m_1 is scattered with momentum components $\mathbf{k}_1 \rightarrow \mathbf{k}_{f\pm} = \mathbf{k}_f \pm \mathbf{k}_0$ towards the entrance of a two-slit interferometer, as in the Wootters and Zurek analysis of photon diffraction.[7] Here, $\mathbf{k}_0$ is the momentum difference between the two slits. The fuzziness of the recoil momentum $\mathbf{K} = \mathbf{k}_2 + \mathbf{k}_3$ of the target-atom center of mass (CM) derives from that of the scattered projectile, viz. $\mathbf{K}_{f\pm} = \mathbf{K}_c - \mathbf{k}_{f\pm}$, since the system CM momentum $\mathbf{K}_c$ is conserved. Thus, for a given $\mathbf{K}_c$ component the system is described just outside the entrance of the interferometer by

$$|\chi_{nP\&T}\rangle = P_n^{-1/2}\left[f_{n+}|\mathbf{k}_{f+}\rangle|\mathbf{K}_{f+}\rangle + f_{n-}|\mathbf{k}_{f-}\rangle|\mathbf{K}_{f-}\rangle\right], \tag{1}$$

where $f_{n\pm} \equiv f_n(\mathbf{k}_{f\pm})$ are the amplitudes for projectile scattering towards the two slits with excitation of the target atom to the state n. Here, $P_n = |f_{n+}|^2 + |f_{n-}|^2$ is the probability that the scattered projectile enters the interferometer through one or the other slit.

Projectile interference is described by the probability of finding the superposition $|S_P\rangle = e^{ik_0\xi}|\mathbf{k}_{f+}\rangle + e^{-ik_0\xi}|\mathbf{k}_{f-}\rangle$, so that projectile detection inside the interferometer introduces the reduction of the state vector, $|\chi_{nP\&T}\rangle \rightarrow |\chi_{nT}\rangle = \langle S_P|\chi_{nP\&T}\rangle$. (Here ξ gives the distance from the axis of the interferometer of the detected projectile hitting the detector plate.) However, to maintain good fringe visibility, the whereabouts of the target CM *position* $\mathbf{r}_T = (m_2\mathbf{r}_2 + m_3\mathbf{r}_3)/(m_2 + m_3)$ has to be well defined. In the Wootters and Zurek analysis, this quantity is essentially fixed by the position $\mathbf{r}_3$ of the rigid support m_3 to which a spring and collimator slit m_2 are attached. In a scattering experiment with a massive recoil ion m_3, $\mathbf{r}_T \simeq \mathbf{r}_3$ could be a nearly fixed point inside a sufficiently compact reaction volume, say a magneto-optical trap, or the anchor point of a target atom to a surface. The CM position measurement introduces an additional reduction of the state vector, $|\chi_{nT}\rangle \rightarrow \chi_n(\xi) = \langle \mathbf{r}_T|\chi_{nT}\rangle$, where

$$\chi_n(\xi) \quad = \quad P_n^{-1/2}[f_{n+}\, e^{-ik_0\xi + i\mathbf{K}_{f+}\cdot\mathbf{r}_T} + f_{n-}\, e^{ik_0\xi + i\mathbf{K}_{f-}\cdot\mathbf{r}_T}], \tag{2}$$

and thus the interference pattern

$$I_n(\xi) = 1 + \frac{2\,|f_{n+}|\,|f_{n-}|}{P_n}\,\cos(2\,k_0\,\xi + 2k_0x_T - \Delta_n) \tag{3}$$

with $x_T \equiv \hat{\mathbf{k}}_0 \cdot \mathbf{r}_T$, since $\mathbf{K}_{f-} - \mathbf{K}_{f+} = \mathbf{k}_{f+} - \mathbf{k}_{f-} = 2\mathbf{k}_0$.[8] As a rule of thumb, the lateral width Δx_T of the reaction volume must be on the order of the slit separation s to ensure enough transverse coherence for good fringe visibility. In the Fraunhofer limit which defines $|S_P\rangle$, the fringe spacing $\Delta\xi$ is large compared to s, and so taking $\Delta x_T \ll \Delta\xi$, i.e. setting $x_T = 0$, is an ideal but appropriate limit.

The state n describes target internal excitation and an additional degree of freedom for sorting alternative subensembles of projectile-target entanglement. It was the essential element of our analysis, which follows closely that of Wootters and Zurek.

---

[5] W. K. Wootters and W. H. Zurek, Phys. Rev. D**19**, 473 (1979).

[6] R. C. Forrey, A. Dalgarno and J. Schmiedmayer, Phys. Rev. A**59**, R942 (1999), and references therein.

[7] J. M. Feagin and Si-ping Han, Phys. Rev. Lett. **86**, 5039 (2001).

[8] J. M. Feagin and Si-ping Han, Phys. Rev. Lett. **89**, 109302 (2002).

Along these lines, we have thus also had in mind the introduction of a second interferometer to probe the target recoil and alternative entanglements equivalent to Eq. (1).[9] One could in effect replace the recoil states $|\mathbf{K}_{f\pm}\rangle$ with for example the *marker* basis $|\tilde{\mathbf{K}}_{\pm}\rangle = |\mathbf{K}_{f+}\rangle \pm |\mathbf{K}_{f-}\rangle$ and reexpress Eq. (1) as

$$|\chi_{nP\&T}\rangle = |\chi^{+}_{nP}\rangle|\tilde{\mathbf{K}}_{+}\rangle + |\chi^{-}_{nP}\rangle|\tilde{\mathbf{K}}_{-}\rangle \tag{4}$$

with $|\chi^{\pm}_{nP}\rangle = P_n^{-1/2}\left[f_{n+}\,|\mathbf{k}_{f+}\rangle \pm f_{n-}\,|\mathbf{k}_{f-}\rangle\right]$. If one now considers a target-recoil measurement of say $|\tilde{\mathbf{K}}_{+}\rangle$ correlated to the projectile measurement $|S_P\rangle$, one obtains Eq. (2) with $\mathbf{r}_T = 0$ but now describing a *joint* projectile-target-recoil interference amplitude, i.e. $\langle S_P\tilde{\mathbf{K}}_{+}|\chi_{nP\&T}\rangle = \chi_n(\xi)$ with $\mathbf{r}_T = 0$.

In analyzing experiments of this sort, we have found for example that we can simplify and extend Hardy's remarkable "proof of nonlocality"[10] to any pair of reaction fragments. By performing a set of measurements in which varying degrees of information are revealed about the paths the fragments take through their respective interferometers and assuming locality (uncorrelated fragments) and hidden variables (realism), a contradiction can be obtained.[11]

We are also working to extend detection interferometry to include n-slit diffraction and other *quantum tomographic* techniques to image in addition the extremely fragile few-body states generated near fragmentation thresholds[12] and fundamental to the few-body Coulomb problem.

Single-Electron Circular Dichroism

Parallel to advances in recent years in photo double ionization has been a renewed interest in photo *single* ionization and the resulting photoelectron angular distributions for departures from the dipole approximation. Thus, Krässig and coworkers have reported measurements of nondipolar asymmetries in single photoelectron angular distributions using x rays from the National Synchrotron Light Source.[13]

Detection with interferometers could provide new probes of these angular distributions. Even in photo single ionization of unoriented atoms, it appears possible[14] to generate a circular dichroism analogous to the well established effect seen in photo *double* ionization.[15] Thus, circular dichroism is observed in the angular distributions of photoionized electron pairs and has been used to extract phase information unavailable with linearly polarized light. (We have also considered the generalization of this effect to molecular photo double ionization.[16]) In the case of photo single ionization, the idea is this: Introduce a two-port detector and let the pair of momentum vectors $\mathbf{k}_{f\pm}$ of the ionized electron entering each port take on the chiral role of the electron-pair momentum vectors $\mathbf{k}_1$ and $\mathbf{k}_2$ in photo double ionization. In effect, the handedness of the incident photons would be used to distinguish right and left ports. One thus obtains a one-electron circular dichroism of the form $\Delta \sim (\mathbf{k}_{f+} \times \mathbf{k}_{f-}) \cdot \mathbf{k}_{\gamma}$ as well as nondipolar phase information unavailable with linearly polarized photons. A new generation of experiments with atoms and molecules to study nondipolar effects is underway in a number of laboratories.

---

[9] We especially enjoy the review of such alternative "as-if realities" in the context of two-way interferometry by B.-G. Englert in Z. Naturforsch. C **54a**, 11 (1999). See also B.-G. Englert, M. O. Scully, and H. Walther, Am. J. Phys. **67**, 325 (1999).

[10] L. Hardy, Phys. Rev. Lett. **68**, 2981 (1992); Phys. Rev. Lett. **71**, 1665 (1993).

[11] J. M. Feagin, Phys. Rev. A, *in preparation* August (2003).

[12] J. M. Feagin, J. Phys. B: At. Mol. Phys. **28**, 1495 (1995).

[13] B. Krässig et al., Phys. Rev. Lett. **75**, 4736 (1995); M. Jung et al., Phys. Rev. A**54**, 2127 (1996).

[14] J. M. Feagin, Phys. Rev. Lett., **88**, 043001-1 (2002).

[15] V. Mergel et al., Phys. Rev. Lett. **80**, 5301 (1998) and references therein. (*Feagin is a coauthor on this paper.*)

[16] T. J. Reddish and J. M. Feagin, J. Phys. B: At. Mol. Opt. Phys. **32**, 2473 (1999).

A related dichroism and nondipolar probe is expected for excitation and fluorescence in which the fluorescence photon takes the role of the photoionized electron and could thus be analyzed with two-port interferometry. Such an experiment is currently underway by T. Gay and coworkers at the University of Nebraska. Nondipolar effects which can be probed in this way are being calculated for various systems.[17]

Collective Coulomb Excitations

The conventional detection of two electrons following photo-double ionization or electron-impact single ionization of simple atoms and molecules is already a highly-advanced technology, and one which has contributed enormously to our understanding of the correlated motion of electrons in the field of a positive ion. Thus, the study of the photo double ionization of the helium atom near threshold has played a key role. Not only does the final state involve three unbounded particles interacting via pure Coulomb forces, but the intrinsic dipole symmetry of the photoexcitation is simple and well defined. This system has thus served as a benchmark for both experimental[18] and theoretical[19] work.

The coincident measurement of two continuum electrons has been extended to the photo double ionization of molecular hydrogen in the isotopic form D_2,[20] and recently including coincident detection of the deuterons.[21] We have thus developed a basic description of the photo double ionization cross section for diatomic molecules[22] based closely on the cross section for helium. We derive a dependence of molecular excitation amplitudes on electron energy sharing and dynamical quantum numbers labeling internal modes of excitation of the escaping electron pair. We consider both linear and circular polarizations. The model is being compared to new and detailed D_2 fragmentation data taken by T. Weber and coworkers, as part of a follow-up to his PhD work in Frankfurt.[23] (Dr. Weber is currently a Humboldt Fellow working at LBNL with M. Prior and L. Cocke.)

Publications

Fully Differential Cross Sections for Photo Double Ionization of Fixed-in-Space D_2, Th. Weber et al, Phys. Rev. Lett., submitted August (2003). (*Feagin is a coauthor on this paper.*)

Comment on Reaction Imaging with Interferometry, J. M. Feagin and Si-ping Han, Phys. Rev. Lett. **89**, 109302 (2002).

Energy Sharing and Asymmetry Parameters for Photo Double Ionization of Helium 100 eV Above Threshold, A. Knapp et al, J. Phys. B: At. Mol. Opt. Phys. **35**, L521 (2002).

Circular Dichroism in Photo Single Ionization of Unoriented Atoms, J. M. Feagin, Phys. Rev. Lett., **88**, 043001-1 (2002).

Reaction Imaging with Interferometry, J. M. Feagin and Si-ping Han, Phys. Rev. Lett. **86**, 5039 (2001).

[17] J. M. Feagin, Phys. Rev. A, *in preparation* August (2003).

[18] R. Dörner et al, Phys. Rev. A**57**, 1074 (1998). (*Feagin is a coauthor on this paper.*)

[19] M. Walter, J. S. Briggs and J. M. Feagin, J. Phys. B: At. Mol. Opt. Phys. **33**, 2907 (2000).

[20] T. J. Reddish et al., Phys. Rev. Lett. **79**, 2438 (1997); N. Scherer et al., J. Phys. B: At. Mol. Opt. Phys. **31**, L817 (1998); J. P. Wightman et al., J. Phys. B: At. Mol. Opt. Phys. **31**, 1753 (1998).

[21] R. Dörner et al., Phys. Rev. Lett. **81**, 5776 (1998). (*Feagin is a coauthor on this paper.*)

[22] J. M. Feagin, J. Phys. B: At. Mol. Opt. Phys. **31**, L729 (1998).

[23] T. Weber et al., Phys. Rev. Lett., submitted August (2003). (*Feagin is a coauthor on this paper.*)

Theoretical Studies of Atomic Transitions

Charlotte Froese Fischer
Department of Electrical Engineering and Computer Science, Box 1679B
Vanderbilt University. Nashville, TN 37235
Email: Charlotte.F.Fischer@Vanderbilt.edu

Program Scope and Definition

The atomic structure project is concerned with the accurate determination of wave functions from which atomic properties can be predicted. Of particular importance are properties associated with energy transfer mechanisms such as transition probabilities, where relativistic effects are essential. Light elements have been investigated primarily in the Breit-Pauli approximation, but for heavier elements our methodology relies on variational Dirac-Hartree-Fock methods that include correlation, the Breit correction, and the effect of a finite nucleus.

Recent Progress

1. Breit-Pauli Studies

We have continued to refine and improve our "spectrum" calculations where all the energy levels up to a certain excitation level are computed along with all transitions between these levels, thus making it possible to determine lifetimes for excited states as well as branching ratios, Zeeman factors, and isotope shift parameters. Codes have been ported to the most advance parallel computer at NERSC, namely the IBM SP "seaborg" computer.

By employing systematic methods and including correlation and relativistic effects, wave functions for all levels in portions of the Li- through Si-like spectra have been determined, generally for ions up to Z=26. From these wave functions, some forbidden (E2, M1, M2) transitions and all possible E1 transitions have been computed. The results have been collected into a database with more than 150,000 LSJ transitions, accessible at: `http://atoms.vuse.vanderbilt.edu`. The database can be accessed either through a search function or direct access to the HTML files. In the search mode, the error in the transition energy along with the discrepancy in the length and velocity gauges (when appropriate) are also displayed so that the *ab initio* data can be evaluated. This web site is part of a GENeral Internet search Engine for Atomic Data (GENIE). All results from Be-like to Ne-like have been submitted to Atomic Data and Nuclear Data Tables for publication.

The database was launched on April 2002. Since that time, more than 10,000 different IPs have accessed the database. The total number of accesses to HTML data is close to 250,000, which is approximately 515 hits per day. The total number of searches approaches 22,000, or approximate 45 per day. The number of searches by sequence (where the number of electrons N is constant) and by atomic number A is as follows:

Sequence (N)	Searches	Atomic Number (Z)	Searches
3	163	3	667
4	438	4	2333
5	434	5	832
6	823	6	1579
7	567	7	1478
8	732	8	961
9	634	9	1866
10	1081	10	2156
11	916	11	1315
12	1136	12	416
13	780	13	1851
14	881	14	219
18	1408	18	867

In the case of the $2p^3\ {}^4S^o_{3/2}\ - 2p^3\ {}^2D^o_{5/2,3/2}$ forbidden transitions, the ratio of the transition rates was confirmed by Sharpee, Huestis, and Cosby (BAPS, DAMOP 2003, N3.001). They measured the line intensity ratio from night sky line spectra obtained with the Keck II ESI Instrument. The measured ratio of 1.80 ± 0.04 agrees well with the ratio of 1.78 derived from our data.

Transitions among excited states of Ne II has been a benchmark case where theory and experiment learned how to refine their techniques. Early publications(experiment, CIV3, MCHF, MCDHF) reported results that often differed dramatically from each other. Since then, labeling problems have been identified. In many cases, the latest Breit-Pauli results agree extremely well with the earlier multiconfiguration Dirac-Hartree-Fock (MCDHF) calculations though major differences with experiment remain. del Val *et al.* (J. Phys. B: **34** 2513 (2001)) have reported an extensive set of new experimental results which statistically are in better agreement with earlier MCDHF results. Though our latest MCHF results appear to be in somewhat better agreement with the most recent data by Djeniže *et al* (A & A **382** 359 (2002)), our results fall within both expermental uncertainties and *between* experimental values.

Transitions in the rare gases have been a subject of some interest recently, confirmed by our web statistics. Avgoustoglou and Beck (Phys. Rev. A **57**, 4286 (1998) applied relativistic many-body perturbation theory for a particle-hole state to neon. This work was later improved upon by Savukov *et al.* (Phys. Rev. A **66**,052501 (2002)) through the introduction of a combined configuration interaction (CI) and many-body-perturbation method (MBPT). Again, the model was for a particle-hole state which would not be as suitable for the ground state. The following table contains a comparison of the present transition energies and oscillator strengths for $2p^6\ {}^1S - 2p^5 3s\ {}^{1,3}P^o_1$ with observed and those from these theories. Our *ab initio* transition energies differ from observed by only a few cm^{-1}, whereas those based on the particle-hole model differ by a considerably greater amount. The CI-MBPT and present results are in excellent agreement with the experimental values obtained by Gibson and Risley (Phys. Rev. A **52** 4451 (1995)) whose error bars appear

Comparison of several theoretical transition data for $2p^6\ {}^1S - 2p^5 3s\ {}^{1,3}P$ transitions with experiment.

Source	$^3P_1^o$	$^1P_1^o$	f($^3P_1^o$)	f($^1P_1^o$	ratio
Exp. (NiST, Gibson & Risley)	134459	135885	0.01095(32)	0.1432(38)	13.1
Present Breit-Pauli	134452	135887	0.01095	0.1514	13.8
CI-MBPT (Savukov)	132738	134230	0.0102	0.1459	14.3
RMBPT (Avgoustoglou & Beck)	133770	135196	0.0163	0.161	9.9

to be realistic.

From a theoretical point of view, the accurate determination of energy levels and transition probabilities for Ca I is much more difficult than for Mg I. Energy levels, transition probabilities, and lifetimes have been determined for all levels of the Ca I spectrum up to $3d4p\ {}^1F_3^o$ using the multi-configuration Hartree-Fock method with lowest-order relativistic effects included through the Breit-Pauli Hamiltonian. The near degeneracy of the non-relativistic $3d4p\ {}^3F^o$ and $^1D^o$ term energies, differing by only 39.59 cm^{-1}, resulted in highly mixed Breit-Pauli levels for $3d4p\ {}^3F_2^o$ and $^1D_2^o$. Some intercombination transitions from these levels have transition probabilities of magnitude similar to weaker spin-allowed transitions. The "fine-tuned" transition probability for the $4s4p\ {}^3P_1^o$ – $4s4d\ {}^1D2$ transition was found to be 1.53 $\times 10^3$ s^{-1}, in agreement with a quenching rate observed in a doppler cooling experiment [Binnewies *et al* Phys. Rev. Lett. **87**, 123002 (2001)].

2. Relativistic Multiconfiguration Dirac-Hartree-Fock Calculations

The structure of negative ions is intrinsically different from that of positive ions in that the binding of the electrons arises from short-range interactions with a shallow potential well. At the ion storage ring CRYRING at the Manne Siegbahn Laboratory in Stockholm, S. Mannervik, D. Hanstorp, D. Pegg and others, have developed a Laser Probing Technique (LTP) for studies or metastable levels in singly charged ions. These techniques are now being applied to negative ions. In collaboration with this group, calculations have been performed for the lifetime of $5p^5\ {}^2P_{1/2}^o$ This level decays primarily through an M1 transition to the ground state, but E2 transitions are also present. Our graspVU code was used for this purpose which is an implementation of the multiconfiguration Dirac-Hartree-Fock (MCDHF) theory. Single- and double-excitations were applied in the generation of the wave function and also those configuration states that represent the polarization of the $4d^{10}$ core. The final predicted lifetime was 454 ms in excellent agreement with the experimental value of 430 ms.

Future Plans

Our spectrum codes perform well for lower members of a spectrum and we plan to extend our collection to include most of the spectra up to argon-like. As accuracy in measurement increases, isotope effects have become important. We plan investigate the calculation of the isotope shift parameter in the LSJ approximation which at present is only determined at the LS level. From such a parameter, isotope effects on energies can readily be determined for

the different isotopes.

Heavy atoms continue to be of interest as well as negative ions.

Recent Publications from DOE supported research)

1. *Landé g factors for* $2p^4(^3P)3p$ *and* $2p^4(^3P)3d$ *states of Ne II*, Charlotte Froese Fischerand P. Jönsson, J. Mol. Struct. (THEOCHEM) **537**, 55-62 (2001).

2. *Measurements and prediction of the* $6s6p\ ^{1,3}P_1$ *lifetimes in the Hg isoelectronic sequence* , L. J. Curtis, R. E. Irving, M. Henderson, R. Matulioniene, C. Froese Fischer, and E. H. Pinnington, Phys. Rev. A **63** 042502 (2001).

3. *Multiconfiguration Dirac-Hartree-Fock calculations of forbidden transitions between* $3s^2\ ^1S_0$, $3s3p\ ^3P_{0,1,2}$, $^1P_1$ *states for Mg-like ions.*, Yu Zou and Charlotte Froese Fischer, J. Phys. B: Atom. Molec. Phys. **34**, 915-931 (2001).

4. *Non-relativistic variational calculations opf atomic properties in Li-like ions: Li I to O VI*, M. Godefroid, Charlotte Froese Fischer and P. Jönsson, J. Phys. B: Atom. Molec. Phys. **34** 1079-1104 (2001).

5. *Breit-Pauli energy levels, lifetimes, and transition data: carbon-like spectra*, G. Tachiev and Charlotte Froese Fischer, Can. J. Phys. **79** 955-976 (2001).

6. *Magnetic dipole transitions between the lowest* $3d^4$ *J=2-3 transitions in highly charged Titanium-like ions*, Charlotte Froese Fischer and S. Fritzsche, J. Phys. B: Atom. Molec. Phys. **34** L767-L722 (2001).

7. *Breit-Pauli energy levels, lifetimes, and transition data: nitrogen-like and oxygen-like sequences*, G. Tachiev and Charlotte Froese Fischer, A & A **385** 716-723 (2002).

8. *Resonance transition energies and oscillator strengths in Lutetium and Lawrencium*, Y. Zou and Charlotte Froese Fischer, Phys. Rev. Lett. **88** 183001 (2002).

9. *Hyperfine-structure calculations of excited levels in neutral scandium* , J. Bierón, Charlotte Froese Fischer, and M. Godefroid, J. Phys. B: Atom. Molec. Phys. **35** 3337 (2002).

10. *Photodetachment of the* He^- $1s2s2p\ ^4P^o$ *in the region of the* $1s$ *threshold*, O. Zatsarinny, T. W. Gorczyca, and Charlotte Froese Fischer, J. Phys. B: Atom. Molec. Phys. **35** 4161-4178 (2002).

11. *Oscillator strengths for transitions ot high-lying excited state of carbon*, O. Zatsarinny and Charlotte Froese Fischer, J. Phys. B: Atom. Molec. Phys. **35** 4669-4683 (2002) .

12. *Allowed and spin-forbidden electric dipole transitions in Ca I* , Charlotte Froese Fischer and G. Tachiev, Phys. Rev. A **68** 012507 (2003).

13. *Breit-Pauli energy levels, lifetimes, and transition probabilities for the beryllium-like to neon-like sequences* , Charlotte Froese Fischer and G. Tachiev, Atomic Data and Nuclear Data Tables (submitted).

EXPERIMENTS IN MOLECULAR OPTICS

Robert J. Gordon,[a,b] Langchi Zhu,[a] and W. Andreas Schroeder[c]

[a]Department of Chemistry (m/c 111), University of Illinois at Chicago,
845 West Taylor Street, Chicago, IL 60607-7061, [b] email address: rjgordon@uic.edu

[c]Department of Physics (m/c 273), University of Illinois at Chicago,
845 West Taylor Street, Chicago, IL 60607-7061

1. Program Scope

The broad objective of this research program is to use the dipole force of an electromagnetic field to control the motion of neutral atoms and molecules. In these studies, the intensity gradient of a focused laser beam serves as a "molecular lens" that can be used to deflect, focus, and align a beam of particles.

The potential energy induced by a far off-resonant field is given by

$$U(r,q) = -\frac{1}{4}e^2(r)\left(\Delta a \cos^2 q + a_\perp\right),$$

where $\vec{e}(r)$ is the electric field, $\Delta\alpha = \alpha_{//} - \alpha_\perp$ is the polarizability anisotropy, $\alpha_{//}$ and $\alpha_\perp$ are the parallel and perpendicular components of the polarizability tensor, and θ is the angle between the principle axis of the molecule and the $\vec{e}$ vector. If the atom or molecule is in its ground electronic state, the polarizability is positive and the potential energy is negative. In this case the particle experiences an attractive force that draws it into the field. The radial gradient of $e^2(r)$ acts as a lens, which bends the trajectories of the particles. If in addition the polarizability is anisotropic, the $\Delta a \cos^2 q$ term induces a torque that aligns the molecules.

The ability to focus and align molecules has many potential applications. For example, a focused beam of molecules could be used to create nanostructures with novel electrical and optical properties. Aligned molecules could be used for stereospecific chemical reactions, for enhanced high harmonic generation, and for isotope separation.

2. Recent Progress

A. Deflection and separation of molecules in different rotational states. The force felt by a rotating anisotropic molecule depends on its spatial alignment. For simplicity, consider the rotation of a linear molecule. If $\vec{e}$ is perpendicular to the plane of rotation (i.e., if $|M_J| = J$), then the potential is determined by $a_\perp$, whereas if $\vec{e}$ lies in the plane of rotation (i.e., for $M_J = 0$), both components of the polarizability come into play. This effect could be used to separate molecules in different M_J states. Such an experiment is analogous to the Stern-Gerlach effect, where an inhomogeneous magnetic field is used to

separate M_S states. We calculate that the difference between the deflections of $|J=1, M_J=\pm 1\rangle$ and $|J=1, M_J=0\rangle$ is approximately 10% of their average deflection. In laboratory measurements we observed the deflection of an unresolved beam of CS_2 molecules, using a focused Nd:YAG laser (10 ns pulse width) to deflect the molecules and a dye laser to ionize them. The deflection was observed by imaging the parent ions onto a phosphor screen. We calculate that an order of magnitude improvement in resolution is necessary to observe the differential deflection of the M_J states of molecules such as HI and acetylene. A detailed analysis of the ion trajectories showed that a properly designed Einzel lens placed in the flight tube could provide the required enhancement in resolution while maintaining velocity-mapping conditions. This lens has been constructed and is currently being tested.

B. Alignment of molecules with ultrashort laser pulses. Molecules irradiated with an intense ultrashort laser pulse undergo a series of Raman transitions that produce rotational wave packets aligned along the direction of the e vector. These wave packets have a long-term coherence and display a recurrence of their alignment, with a revival time of $(2Bc)^{-1}$, where B is the rotational constant and c is the speed of light. Such revivals are valuable because they allow one to produce aligned molecules under field-free conditions.

The amount of alignment achievable with a single laser pulse has a saturation value of $\langle \cos^2 q \rangle \approx 0.9$. Recently, Averbukh and coworkers predicted that even greater alignment may be achieved with a sequence of properly timed pulses, with no saturation limit. In particular, two pulses with optimally selected kicks (proportional to $\int e^2(t)dt$) and delay times can produce a much greater alignment that a single pulse imparting the same total kick.

We have nearly completed setting up an experiment to demonstrate this effect with two pulses. Preliminary experiments with a single laser pulse demonstrated recurring alignment of I_2 and ICl. A more powerful Ti:Sapphire laser capable of supporting the multipulse experiment (2 W, 45 fs @ 1 kHz) was delivered in November, 2002. An autocorrelator, a pulse stretcher, and delay line optics have been constructed. A new molecular beam imaging machine has been designed to allow both the deflection and alignment experiments to be run simultaneously. Construction of the apparatus is in progress.

C. Nanolithography with focused molecular beams. A potentially valuable application of molecular optics is the creation of nanostructues by focusing a molecular beam of neutral molecules onto a surface. This technique is very powerful because it could be applied in principle to deposit any atom or molecule on any substrate. We have performed a detailed theoretical study (in collaboration with Tamar Seideman) of the feasibility of creating nanowires by this approach. In the original conception of this method, the laser and molecular beams are perpendicular to each other, and the laser beam is pulsed to obtain the requisite intensity. Difficulties with this configuration are that the duty cycle of the laser is very low, and additional deflecting and collimating

fields are necessary to prevent the deposition of material while the laser is off. Here we show that both problems can be solved by employing a grazing angle of incidence between the laser and molecular beams. At a small incidence angle, the reduced component of the kinetic energy transverse to the laser beam allows a proportionate reduction in laser intensity while maintaining the same focal length of the molecular beam. This reduction in intensity allows one to use a continuous-wave laser to create very long nanostructures. A further order of magnitude reduction in requisite power may be achieved by intersecting the laser and molecular beams inside of the laser cavity. We further show that the focal coordinates, (x_f, z_f), of the molecular lens and the width, W, of the nanowire scale as

$$x_f, z_f \sim m w_0 T_0 / m_c a_{//} I_0$$

$$W \sim W_i / w_0^2,$$

where m and m_c are the masses of the deposited molecule and the carrier gas, respectively, T_0 and W_i are the stagnation temperature and initial width of the molecular beam, and w_0 and I_0 are the 1/e radius of the field and peak intensity of the laser beam. A representative calculation shows that nanowires 50 nm wide and 100 *mm* long may be deposited with a 100 W Yb:YAG thin-disk laser.

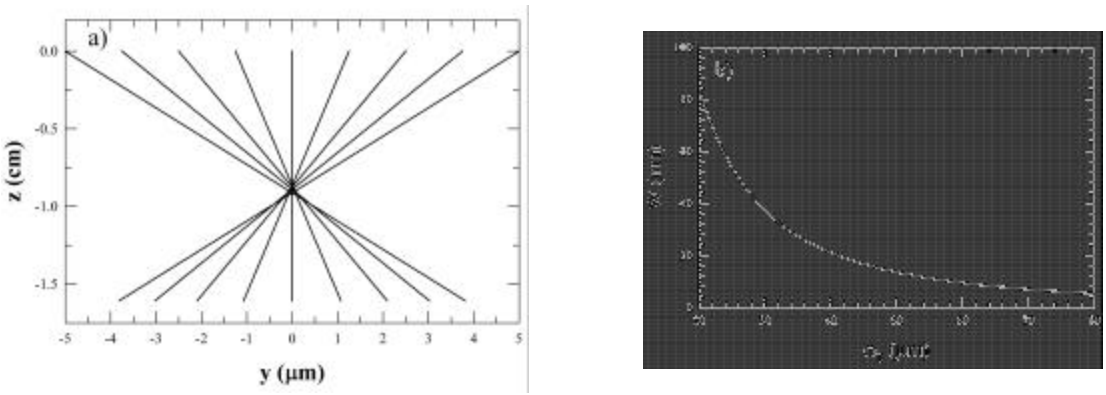

Figure 1. The effect of spherical aberration on the focal width of the molecular beam. (a) Trajectories for a molecular beam of I_2 in Kr having an initial width $W_i = 10\,mm$ focused by a laser with $w_0 = 30\ mm$, at a peak intensity of 10^8 W/cm^2 and an intersection angle of 5^0. Both the translational and rotational temperatures are zero. (b) Variation of the focal width with the radius of a circular Gaussian focus.

3. Future Plans

During the coming year we plan to continue working on the deflection and alignment experiments. Once the Einzel lens has been optimized, we will use the deflection apparatus to separate hydrogen halide molecules in different M_J states. We will then apply this technique to measure the hydrodynamic alignment of molecules in supersonic expansions. In the rotational wave packet experiment, we plan to implement

Averbukh's scheme for aligning molecules, initially with two kicks and later with a train of kicks. The latter will be accomplished using a spatial light modulator to split the second pulse into a programmed series of kicks. An immediate application of this technique is to separate molecular isotopomers, taking advantage of the enhanced ionization efficiency of aligned molecules and the property that the recurrence period of the rotational wave packet is proportional to the moment of inertia.

4. Publications in 2001-2003

S. Unny, Y. Du, L. Zhu, K. Truhins, R. J. Gordon, A. Sugita, M. Kawasaki, Y. Matsumi, R. Delmdahl, D. H. Parker, and A. Berces, "Above-Threshold Effects in the Photodissociation and Photoionization of Iodobenzene," J. Phys. Chem. A **105**, 2270 (2001).

S. Unny, Y. Du, L. Zhu, R. J. Gordon, A. Sugita, M. Kawasaki, Y. Matsumi, and T. Seideman, "Above-Threshold Dissociative Ionization in the Intermediate Intensity Regime," Phys. Rev. Lett. **86**, 2245 (2001).

H. Yamada, N. Taniguchi, M. Kawasaki, Y. Matsumi, and R. J. Gordon," Dissociative Ionization of ICl Studied by Ion Imaging Spectroscopy," J. Chem. Phys. **117**, 1130 (2002).

R. J. Gordon, L. Zhu, W. A. Schroeder, and T. Seideman, "Nanolithography Using Molecular Optics," J. Appl. Phys. **94**, 669 (2003).

Resonant Interactions in Quantum Degenerate Bose and Fermi Gases

Murray Holland

JILA, 440 UCB, University of Colorado, Boulder, CO 80309-0440
murray.holland@colorado.edu

I. Program scope

Feshbach resonances allow the interactions in a quantum degenerate gas to be controlled at a microscopic level. In general terms this manifests as an ability to tune the scattering length from large to small values and from positive (repulsive interactions) to negative (attractive interactions). However, near the resonance, the magnitude of the scattering length may become so large that it results in a break-down of the simple mean-field theories used to describe dilute gases. This is a very interesting problem requiring the development of a full quantum field theory of the resonance superfluid. The main goal of this research program has been the development of this resonance superfluid theory and its application to describe a wide range of phenomena with a focus on experimental verification.

II. Recent results

The resonance field theory we have formulated [6] has been quantitatively compared [3] with a recent experiment [Donley *et al.* Nature 2002] involving a Feshbach resonance in bosonic ^{85}Rb. In direct analogy with a Ramsey fringe experiment in atomic physics, a time-dependent magnetic field was used to create two intervals of strong coupling (i.e. near resonance) separated by a waiting interval $t_{\rm evolve}$ which could be varied in duration. In the strong coupling regions the scattering length was positive and many thousands of Bohr radii in magnitude (the highest values of the dimensionless parameter na^3, where n is the density and a is the scattering length, approach unity). This nonperturbative regime is typically considered to be a very challenging regime to explore theoretically. After applying the pulse sequence the experimenters observed three components: a residual condensate, a burst of atoms at higher energy with distinct spatial profile, and a missing fraction. As the time interval $t_{\rm evolve}$ was varied they observed oscillations in the proportion of atoms in each component.

Since the microscopic parameters are known to high precision for ^{85}Rb, we were able to model the dynamic experiment completely with no adjustable parameters. We calculated evolution trajectories for each value of $t_{\rm evolve}$ by solving the time-dependent Hartree-Fock-Bogoliubov equations appropriately renormalized to remove the ultraviolet divergences which would otherwise arise. We thereby predicted occupations in the atomic condensate, molecular condensate, and noncondensate components (Fig. 1). The agreement with the experimental observation is striking allowing the observed components to be unambiguously identified. Some of the properties which are correctly accounted for include the fringe frequency at the one percent level (which is a direct measure of the binding energy of the molecule in the 100 kHz scale) and the visibility and position of the fringes for each component. A phase offset in the oscillations is noted in the experimental data and reproduced in the theory.

The similarity between these observations at large positive scattering length and the observations in the earlier collapse experiment [Donley *et al.* Nature 2001] carried out in the same group at negative scattering length motivated us to consider the possibility of applying the resonance field theory to that situation as well [1]. This 'Bosenova' experiment explored the mechanical collapse instability arising from an attractive interaction. This collapse resulted in an unanticipated burst of atoms, the nature of which is a subject of current debate. We suggested a possible mechanism

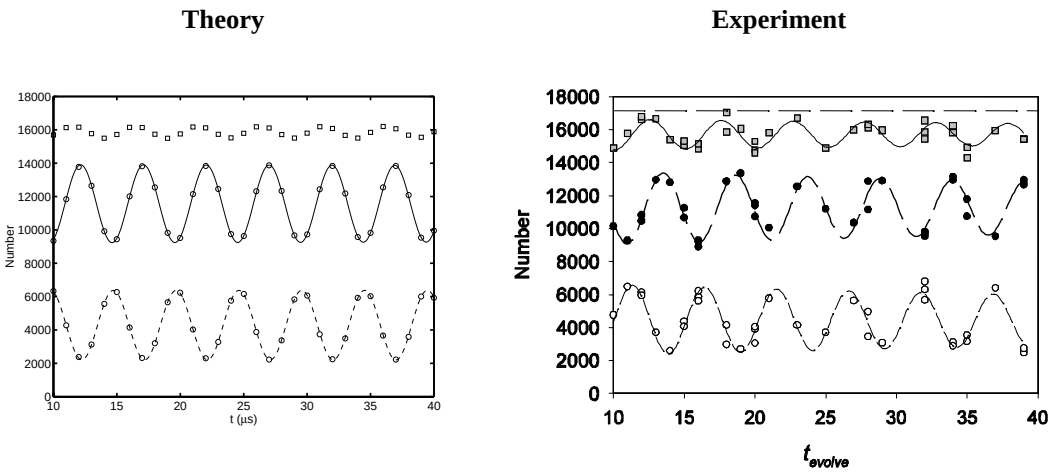

Figure 1: Ramsey fringe oscillations between the atomic condensate (theory-solid line) and the atomic noncondensate (theory-dashed line). These two components sum to the total number of recovered atoms (theory-squares) which excludes the molecular component. The experimental plot illustrates the analogous quantities for comparison.

for the formation of these bursts by application of the effective quantum field theory which includes explicitly the resonance scattering physics. Indeed, when applied to this inhomogeneous situation, which was technically very demanding in the three-dimensional geometry, the qualitative features of the experiment were well described.

On another front, there is currently a significant experimental effort to achieve superfluidity in a dilute Fermi gas by utilizing a Feshbach resonance to greatly increase the interactions. The direct application of the Bardeen-Cooper-Schrieffer (BCS) theory of superconductivity to a dilute Fermi alkali gas in this situation is incomplete because it quantifies the interatomic interactions by only the scattering length a. The requirement of having a high critical temperature in close proximity to the Fermi temperature in order to observe the superfluid transition experimentally means that the theory cannot involve just the scattering length and must account for the resonance state explicitly.

We developed a theory of the critical temperature for the formation of the fermion superfluid state which takes this into account [4]. We studied the behavior of the critical temperature in the crossover region in a path integral formulation and were able to consider the lowest order role of pair fluctuations in the resonance regime utilizing the same renormalization procedure described above for the Ramsey fringe studies. We have recently upgraded this proceedure to include mode coupling effects on the paired states lending strong credibility to the physical nature of the predicted high transition temperatures (shown in Fig. 2). Note that these calculations interpolate between the BEC limit at large negative detuning, and the BCS superfluidity limit at large positive detuning.

III. Future plans

An important aspect of the theory of the Ramsey fringes is the anomalous density which plays a major role in the calculated trajectories. In the case of fermions, the Hartree-Fock-Bogoliubov dynamics are straightforward to calculate in an analogous way. However, in that case there is no atomic condensate, and the generation of an anomalous pairing field is usually referred to as the formation of Cooper pairs. This is a topic we are currently investigating and is of timely experimental importance as a number of laboratories are investigating dynamic molecule formation in the quantum degenerate fermion gas.

The equilibrium studies are also being pursued further. One of the reasons the superfluid fermion gas, if realized,

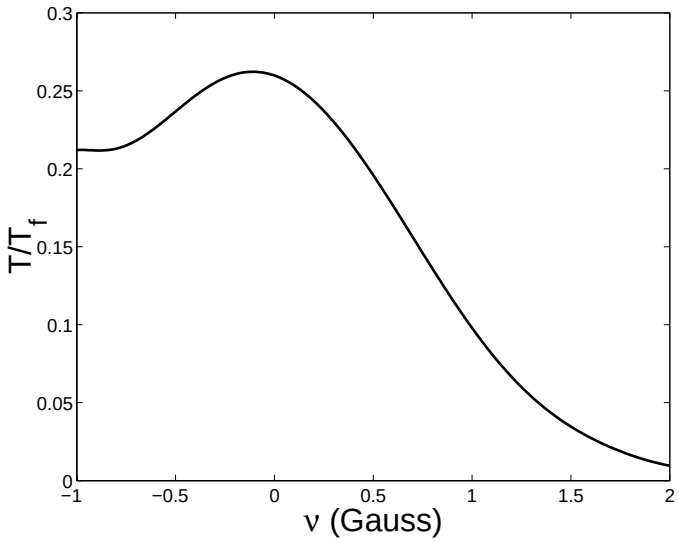

Figure 2: Ratio of the critical temperature T_c to the Fermi temperature T_F as a function of the magnetic field detuning ν across a Feshbach resonance for ^{40}K. At large negative detuning the transition is characterized by strongly bound composite pairs which Bose condense. At large positive detuning the prediction of the Bardeen-Cooper-Schrieffer theory emerges. The calculation shown here includes the complete pseudogap physics.

would be interesting is the connection with preformed Cooper pairing and the formation of a pseudogap. A major effort has been put into understanding the normal phase of high-Tc cuprate superconductors due to a growing belief that it this phase that holds the key to understanding the exotic behavior of these materials. One reason for this belief is the formation of a 'pseudogap', which is a strong suppression of weak excitations (as opposed to a 'gap' which causes a complete suppression), at temperatures far above T_c. One possible explanation for this pseudogap phase requires the onset of local paired correlations at a temperature T^*, which only become coherent when the temperature drops below T_c. Our Feshbach resonance model is an ideal system in which to study the pseudogap phase since it allows us to move well within this regime by varying the strength of the resonant interactions, an easily controlled experimental parameter.

For many reasons atomic gases appear to offer an ideal system in which to study the pseudogap phase since they potentially may allow a much simpler description to be developed than their condensed matter analogs. They are not encumbered by a number of complicating mechanisms, such as strong Coulomb interactions, d-wave pairing, interlayer tunneling, and so on. In addition the microscopic physics behind the interparticle interactions are well understood and parametrized at an extremely precise level.

Finally, we are currently investigating the connections between the highly rotating dilute Bose gas and the fractional quantum Hall effect system. This well known formal equivalence requires unfeasibly low temperatures to experimentally access these states for dilute gases. However, since the associated energy gap is directly related to the interaction strength, we are considering an alternative approach to increasing the temperature by tuning the interactions via a Feshbach resonance. The Feshbach resonance results in the generation of molecules and strongly correlated pairs giving a modification of the ground state nature.

IV. References to peer-reviewed DOE sponsored research 2001–2003

[Preprint] S. G. Bhongale, J. N. Milstein, M. J. Holland *Resonant formation of strongly correlated paired states in rotating Bose gases*, submitted to Phys. Rev. Lett. (2003).

[Preprint] J. Wachter, R. Walser, J. Cooper, M. Holland *Gapless kinetic theory beyond the Popov approximation*, submitted to Phys. Rev. A, (2003).

[1] J. N. Milstein, C. Menotti, M. J. Holland *Feshbach resonances and collapsing Bose-Einstein condensates*, New Journal of Physics, Focus Issue on Quantum Gases **5**, 52 (2003).

[2] S. G. Bhongale, R. Walser, and M. J. Holland, *Memory effects and conservation laws in the quantum kinetic evolution of a dilute Bose gas*, Phys. Rev. A 66, 043618 (2002).

[3] S. J. J. M. F. Kokkelmans and M. J. Holland, *Ramsey fringes in a Bose-Einstein condensate between atoms and molecules*, Phys. Rev. Lett. **89**, 180401 (2002).

[4] J. Milstein, S. J. J. M. F. Kokkelmans, and M. J. Holland, *A resonance theory of the crossover from Bardeen-Cooper-Schrieffer superfluidity to Bose-Einstein condensation in a dilute Fermi gas*, Phys. Rev. A **66**, 043604 (2002).

[5] M. L. Chiofalo, S. J. J. M. F. Kokkelmans, J. N. Milstein, and M. J. Holland, *Signatures of Resonance Superfluidity in a Quantum Fermi Gas*, Phys. Rev. Lett. **88**, 090402 (2002).

[6] S. J. J. M. F. Kokkelmans, J. N. Milstein, M. L. Chiofalo, R. Walser, and M. J. Holland, *Resonance Superfluidity: Renormalization of Resonance Scattering Theory*, Phys. Rev. A **65**, 053617 (2002).

[7] M. Holland, S. J. J. M. F. Kokkelmans, M. L. Chiofalo, and R. Walser, *Resonance Superfluidity in a Quantum Degenerate Fermi Gas*, Phys. Rev. Lett. **87**, 120406 (2001).

[8] M. Holland, J. Park, and R. Walser, *Formation of pairing fields in resonantly coupled atomic and molecular Bose-Einstein condensates*, Phys. Rev. Lett. **86**, 1915 (2001).

[9] J. Wachter, R. Walser, J. Cooper, and M. Holland, *Equivalence of kinetic theories of Bose-Einstein condensation*, Phys. Rev. A **64**, 053612 (2001); *Erratum* Phys. Rev. A **64**, 053612 (2001).

[10] R. Walser, J. Cooper, and M. Holland, *Reversible and irreversible evolution of a condensed bosonic gas*, Phys. Rev. A **63**, 013607 (2001).

Using Intense Short Laser Pulses to Manipulate and View Molecular Dynamics

Robert R. Jones, Physics Department, University of Virginia,
382 McCormick Road, P.O. Box 400714, Charlottesville, VA 22904-4714
rrj3c@virginia.edu

Program Scope

Our experiments utilize intense, short laser pulses to investigate strong field ionization and/or fragmentation processes in gas phase molecules. Our goal is to further illuminate the fundamental physical processes governing non-perturbative laser/molecule interactions. As a significant part of this, we intend to develop and demonstrate new or improved techniques for optical manipulation and probing of molecular structure, orientation, and/or alignment. For example, in one line of experiments, intense short electromagnetic pulses are being used to create rotational wavepackets whose dynamical evolution results in transient, field-free alignment of the molecules [1]. These molecules can then be used to study the role of alignment in strong-field molecular ionization [2]. In related work we will attempt to demonstrate transient, field free orientation of polar molecules by subjecting them to sub-picosecond half-cycle electric field pulses (a.k.a. HCPs)[3]. Due to the unipolar nature of the HCP field, the rotational wavepackets excited by a HCP have a "handedness" resulting in periodic orientation of the molecular dipole [4].

Another set of experiments will focus on "recollision" processes where photoelectrons, produced via multiphoton or tunneling ionization, are driven back into their parent molecules by the intense laser field [5]. The returning electron may rescatter, resulting in the production of very high energy Above Threshold Ionization (ATI) electrons, or may emit a VUV photon via High Harmonic Generation (HHG). Our goal is to investigate the extent to which these processes are modified in molecules, as compared to atoms, since the recolliding electrons coherently scatter from multiple, rather than single, nuclei. We are using intense 30 fsec laser pulses in conjunction with a Cold Target Recoil Ion Momentum Spectrometer (COLTRIMS) to determine if, and under what circumstances, the diffracted electrons or ions might serve as accurate time-resolved probes of molecular dynamics. Such probes might find application in direct viewing of strong field dissociation processes or intra-molecular energy transfer.

Recent Results and Progress

i) Feedback Control of Intense-Laser Fragmentation of Clusters

For the last two years we have investigated intense laser fragmentation of S_8 cluster rings. Our goal has been to examine the importance of pulse-shape in non-resonant strong field dissociative ionization and to determine the most effective strategy for optimizing specific fragment yields. Sulfur clusters provide interesting targets since they are atomically homogeneous and the ionization potential of the species, S_n ($1 \le n \le 8$), are approximately identical, 9.5 ± 1 eV [54]. With low intensity (10^{11} W/cm^2) unshaped 100 fsec pulses, essentially all singly-charged fragments S_n^+ are seen, but the parent molecular ion, S_8^+ dominates the spectrum. However, with increasing intensity or increasing pulse duration, smaller fragments are produced with higher efficiency. In general, this behavior is similar to that of other molecules, and appears to be relatively insensitive to wavelength.

In an attempt to alter the manner in which the clusters fragment, we enabled feedback control [6] of the laser parameters using a genetic algorithm [7] and liquid-crystal-based pulse-shaper [8].

Most of our efforts focused on optimizing simple yield ratios, S_N^+:S_M^+, with $8 \geq (N,M) \geq 1$. In nearly every case, use of the algorithm results in a significant improvement (as great as 4x or more) in the desired yield ratio, almost invariably through a large reduction of the denominator-ion yield with less or no reduction in numerator-ion signal.

In our initial experiments, the search algorithm was implemented using a standard frequency domain parameterization. Here the "genes" that determine the laser pulse shape are expressed directly as the phase (Type 1) or phase and amplitude (Type 2) of the laser field within a window in the spectral bandwidth. While easier to implement experimentally, this frequency domain parameterization did not utilize the full resolution of the pulse shaper, and the optimum pulse shapes obtained did not lend themselves to simple physical interpretation. More recently, we developed a time-domain control parameterization where individual genes are expressed as a specific property (i.e. amplitude, duration, phase, etc.) of one of several component pulses that are combined to produce the net temporal field. Again, two schemes, using phase-only (Type 3) or phase and amplitude (Type 4) shaping were implemented. The new parameterization takes advantage of the full resolution of the pulse-shaper, enabling the generation of pulses with significantly longer temporal structure and no temporal periodicity artifacts, while still limiting the search to 32 (or fewer) genes. On average, for a given yield ratio, we achieve similar gains with all 4 parameterizations. Using Type 3 or 4 shaping, however, it is very straightforward to quantify the importance of pulse complexity as the optimization can be run using 1, 2, 3… component pulses. In most cases, the 'best' pulse shape is not incredibly complex, yet the deviation from a single transform limited pulse is significant. Interestingly, the optimum pulses obtained using the different parameterizations have distinct differences. For example, quasi-periodic temporal structure that is evident in many of the Type 1 and Type 2 optimized pulse shapes does not appear using the other schemes. Apparently, and not surprisingly, there are many local maxima in the multidimensional surface that defines fragment ratio yield vs. laser characteristics. However, the use of multiple parameterizations is an effective tool for determining relative importance of various aspects of the optimized pulses in this, and other, closed-loop experiments. Ultimately, control over any highly non-linear optical process will be limited by intensity variation throughout the focal volume. The optimum pulse shape at one location in space will likely differ from that at other positions due to the difference in peak intensities. We believe that this is the primary factor limiting the gains achieved in the fragmentation experiments.

ii) Progress on Other Experiments

Much of the past year has been spent developing apparatus and techniques for the diffractive imaging and transient alignment/orientation efforts. These experiments require a source of rotationally and/or translationally cold, low-density molecules. We have implemented a liquid N_2 refrigerator to produce low-density beams of N_2 and D_2 with effective longitudinal and transverse temperatures of approximately 75K and 7K, respectively. The rotational temperatures are presumably ~75K as well. This or a similar source will be used for the transient alignment and diffraction measurements.

Additional progress on the transient alignment experiments includes the synchronization of the 1 kHz outputs of our 2 mJ, 100 fsec and 1 mJ, 30 fsec amplifiers to a precision of less than 100 fsec. This is accomplished by using a single 20 fsec mode-locked oscillator to seed both amplifiers. The amplified 100 fsec laser pulses have now been employed to transiently align N_2, and that

alignment has been probed by Coulomb exploding the molecules with circularly polarized, 30 fsec laser pulses. Also, we have modified the data collection software for the wire grid anodes to enable real time determination of the average molecular alignment prior to their explosion. This analysis will provide crucial real-time feed back for future experiments investigating optimal alignment using shaped laser pulses in a closed control loop.

Progress is also being made on the transient orientation front. LiCl will be the initial target in the HCP induced, field-free orientation experiments. Since Coulomb explosion will eventually be used to probe the orientation, a thermal molecular beam apparatus is being used to characterize LiCl dissociative ionization by 100 fsec laser pulses, and a new TOF spectrometer is being constructed to improve fragment energy resolution.

Future Plans

In the immediate future we will begin experiments exploring the use of laser pulse-shaping to optimize molecular alignment [9]. Once, we perfect the technique, we hope to first align and then ionize molecules in a systematic investigation of the role of alignment in the apparent suppression of ionization that was previously observed for some diatomic molecules but not others. Similar measurements are now underway in other laboratories [10].

Following the installation of the new ion spectrometer, the next step in the orientation experiments will be the addition of a pulsed gas nozzle to rotationally cool the LiCl prior to its exposure to a HCP. Low rotational temperatures will be crucial for producing a coherent wavepacket with a pronounced, temporally recurring dipole orientation. Later this Fall, we will test new hardware that should increase the magnitude of currently available HCP fields by over an order of magnitude [3]. This field increase will be necessary to excite the broad range of rotational states that is required to achieve strong orientation, particularly in molecules with smaller dipole moments. We hope to measure HCP-induced or combined HCP/intense-laser-induced transient orientation soon afterward.

References

1. T. Seideman, Phys. Rev. Lett. 83, 4971 (1999); F. Rosca-Pruna and M.J.J. Vrakking, Phys. Rev. Lett. 87, 163601 (2001).
2. A. Talebpour, S. Larochelle, and S.L. Chin, J. Phys. B 29, L677 (1996); M.J. DeWitt and R.J. Levis, Phys. Rev. Lett. 81, 5101 (1998); M. Lezius, B. Blanchet, D.M. Raymer, D.M. Villeneuve, A. Stowlow, and M. Yu. Ivanov, Phys. Rev. Lett. 86, 51 (2001); S.M. Hankin, D.M. Villeneuve, P.B. Corkum, and D.M. Raymer, Phys. Rev. A 64, 013405 (2001).
3. D. You, R.R. Jones, P.H. Bucksbaum, and D.R. Dykaar, Opt. Lett. 18 290 (1993).
4. M. Macholm and N.E. Henriksen, Phys. Rev. Lett. 87, 193001 (2001).
5. H. Nikura, F. Legare, R. Hasbani, A.D. Bandrauk, M.Yu. Ivanov, D.M.Villeneuve, and P.B. Corkum, Nature 417, 917 (2002).
6. R.S. Judson and H. Rabitz, Phys. Rev. Lett. **68**, 1500 (1992).
7. B. Pearson, J.L. White, T.C. Weinacht, and P.H. Bucksbaum, Phys. Rev. A **63**, 063412 (2001).
8. A.M. Weiner, D.E. Leaird, J.S. Patel, and J.R. Wullert, Opt. Lett. 15, 326 (1990); M.M. Wefers and K.A. Nelson, Opt. Lett. 18, 2032 (1993).
9. I.Sh. Averbukh and R. Arvieu, Phys. Rev. Lett. 87, 163601 (2001).
10. I.V. Litvinyuk, K.F. Lee, P.W. Dooley, D.M. Raymer, D.M. Villeneuve, and P.B. Corkum, Phys. Rev. Lett. 90, 233003 (2003).

Publications from DOE Sponsored Research (2001-2003)

1. E. Wells, M.J. DeWitt, and R.R. Jones, "Comparison of Intense Field Ionization of Diatomic Molecules and Rare Gas Atoms," Physical Review A **66**, 013409 (2002).

2. S.N. Pisharody and R.R. Jones, "Phase-Controlled Stair-Step Decay of Autoionizing Radial Wavepackets," Physical Review A **65**, 033418 (2002).

3. R.R. Jones, S. Pisharody, and R. van Leeuwen, "Laser Manipulation of Differential Autoionization Yields: Pump-Dump Control Through Coupled Channels," *Laser Control and Manipulation of Molecules*, ACS Symposium Series **826**, A. Bandrauk, R.J. Gordon, and Y. Fujimura, Eds. (2002).

4. M.J. DeWitt, E. Wells, and R.R. Jones, "Ratiometric Comparison of Intense Field Ionization of Atoms and Diatomic Molecules," Physical Review Letters **87**, 153001 (2001).

5. R. van Leeuwen, K. Vijayalakshmi, and R.R. Jones, Phys. Rev. A **63**, 033403 (2001).

Spectroscopy of Nanoparticles Produced by Laser Ablation of Microparticles

John W. Keto
Physics Department, The University of Texas at Austin, Austin,TX 78712
keto@physics.utexas.edu

1.0 Introduction

Our goal is to develop techniques for the synthesis of nanocomposite and nano-heterogeneous materials and devices that combine the functional advantages obtained from the "size-tunable" properties of nanocomposite materials with the fabrication and direct-write advantages available from nanoparticles (NPs) manufactured by Laser Ablation of Microparticles (LAM) from an aerosol source. These materials are often found to have size tuneable optical properties and very large nonlinear susceptibilities. The fabrication of functional devices based on these materials requires the ability to assemble individual nanoparticles in micrometer patterns in a way compatible with current planar semiconductor technology.

In the production of Stransky-Krastonov (SK) quantum dots, small islands of a dis-similar semiconductor are grown on an underlying substrate with lattice parameters chosen so as to minimize strain between the materials. These islands are then encapsulated in the same material as the substrate by depositing additional atoms epitaxially about the islands. If the growth rate is sufficiently smaller than the diffusion rates for the atoms on the surface then defects at the interface are minimized and the dots have a high efficiency for fluorescence. We are attempting a similar material synthesis by depositing nanoparticles on a substrate material with higher bandgap but selected for a good lattice match. We have then attempted to encapsulate the nanoparticles by near epitaxial growth of the substrate material about the nanoparticle. To date we have produced both Si NP in SiO_2, Si in AlO_3 and GaN NP in AlN. Unlike in S-K quantum dots, however, the nanoparticle lattice is not necessarily indexed to the lattice of the substrate and the defect density at the particle interface may be high. These defects may quench exciton fluorescence at the interfaces. Of course we are experimenting with a broad spectrum of process parameters to minimize such defects in the growth of the composites and only preliminary spectroscopic studies have been completed.

One solution to the problem of interface defects, first achieved by Bawendi for CdSe nanoparticles is to shell the core particle during the growth phase.[1] He successfully shelled CdSe NP with ZnS and ZnSe materials. If the interface within the shell can be grown defect free and prevents the exciton from reaching the surface of the NP the exciton is protected from the environment outside of the NP. Another approach would be to trap the exciton within the NP on an impurity site. Hole donors such as boron would trap the hole within the bulk of the nanoparticle. Since the excitation energy for the impurity is below the bandgap the excition should trap at the impurity site and not on surface defect states, which have been shown not to be within the gap. If this site is sufficiently distant from the surface the exciton would be protected from defects at the surface. Naturally this may prevent tuning of the exciton energy by confinement since the size of the electron wavefunction would have to smaller than the NP, but other benefits of the NP such as low temperature scintering and low scattering cross section are retained. The latter enables the composite, nanostructured material to have a high optical

---

[1] M. Danek, K. F. Jensen, C. B. Murray, and M. G. Bawendi, Chem. Mater. **8,** 173(1996).

quality. If surface defect states are hole traps, hole donor impurities would trap the hole within the NP and an excited electron correlated to the trapped hole on the impurity would be confined and shifted in energy much like the band gap of the particle. Impurity states with large transition rates could then be used for high QE efficient PL devices, or states with long radiative lifetimes for stable light amplification could be selected (such as Ti or Er).

2.0 Brief Review of LAM

We previously have shown that it is possible to produce nanoparticles (NP) by laser ablation of microparticles (LAM).[2,3] Since these initial studies, we have significantly increased production rates of NP by developing a continuous flowing aerosol process in which the microparticles (MP) are introduced in an aerosol and NP are produced in an aerosol. We have successfully used this process to fabricate useful quantities of unagglomerated glass, metal, and semiconductor NP.[4] We have also demonstrated that under certain ablation conditions, it was possible to preserve the composition of alloy MP in the NP so that alloy NP with a controlled composition could be produced.[5]

The production of NP using the aerosol LAM process has been previously described in detail. In summary, a KrF excimer laser (λ = 248 nm) with a 12 ns pulse width at 200 Hz is focused onto a MP aerosol stream contained within a coaxial buffer gas. The laser initiates breakdown and shock-wave formation in each MP resulting in compression and heating.[6] NP are formed behind the shockwave as the pressure drops. The NP are both photoionized and thermally ionized during their formation resulting in a significant charge on the NP. This is advantageous because the NP produced using LAM remain unagglomerated for the period of time that they are charged and can be collected electrostatically during this time.

Mass production of nanoparticles with a narrow size distribution is important to the emerging field of nano-photonics. Synthesis technique for particles to be used in these applications must produce high quality, individual, nanoparticles with narrow size distributions. When using metal target microparticles, NPs are formed within both a surface plume and shock heated material, resulting in a width of the size distribution of about 35% of the mean size;[7] for semiconductor and nanoparticles we do not observe such a bimodal distribution, and the size spread is about 25% of the mean size.[8] We have also demonstrated that the size distribution can be filtered institu during electrostatic collection.[3] Mean size can be controlled from 2-20 nm with the aersol gas type and pressure.[9]

We have also demonstrated that it is possible to directly write films, micron-scale lines, and other structures onto substrates using supersonic jet deposition of nanoparticle

---

3. C.-B. Juang, H. Cai, M. F. Becker, J. W. Keto, and J. W. Brock, Appl. Phys. Lett. **64,** 40-42 (1994).

3. M. F. Becker, J. R. Brock, and J. W. Keto, US Patent #5,585,020 1996).

4. W. T. Nichols, J. W. Keto, D. E. Henneke, J. R. Brock, G. Malyavanatham, M. F. Becker, and H. D. Glicksman, Appl. Phys. Lett. **78,** 1128-1130 (2001).

5. W. T. Nichols, G. Malyavanatham, M. P. Beam, D. E. Henneke, J. R. Brock, M. F. Becker, and J. W. Keto, in *Mat. Res. Soc. Symp. Proc., Nanophase and Nanocomposite Materials III*; *Vol. 581*, edited by S. Komarneni, J. C. Parker, and H. Hahn (MRS, Warrendale, PA, 2000), p. 193-198.

6. J. Lee, M. F. Becker, and J. W. Keto, J. Appl. Phys. **89,** 8146-8152 (2001).

7. W. T. Nichols, G. Malyavanatham, D. E. Henneke, J. R. Brock, M. F. Becker, and J. W. Keto, *"Bimodal nanoparticle size distributions produced by laser ablation of microparticles in aerosols"*, J. of Nanoparticle Res. 4(5), 423-432(2002).

8 J. W. Keto, W. Nichols, D. O'Brian,[2] M. F. Becker,[2]and D. Kovar, "Nanoparticles: Building Blocks for Nanostructured Materials," to be published AIP Conf. Proc "Atoms to Nanostructures"

9 W. T. Nichols, G. Malyavanatham, D.E. Henneke, J.R. Brock, M.F. Becker, J.W. Keto & H.D. Glicksman, "Gas and pressure dependence for the mean size of nanoparticles produced by laser ablation of flowing aerosols," J. Nanoparticle Res. **2**, 141-145(2000).

aerosols generated by LAM. The advantages of aerosol processing using nanomaterials manufactured in a laser ablation process over existing technologies are higher deposition rates (~μm/sec), films can be fabricated at low deposition temperatures that do not require subsequent high temperature heat treatment, the overall purity of the original feedstock powders are preserved, lines and other two-dimensional structures and arrays can be written directly onto substrates without subsequent post-processing, and the nanoparticles are used immediately after fabrication so that no surfactant stabilization step is needed.

3.0 Impurity doped nanoparticles

Doped nanoparticles should in principle be possible using LAM by beginning with the appropriately doped micron sized powders. Possible impurities include B, Er, Ti, and Cr impurities in both Si and GaN nanoparticles. We have recently used ball milling to produce PZT micropowders with varying compositions as the starting material for LAM. Metal impurities might be added to semiconductor powders by diffusion or with the appropriate collaboration, low energy ion implantation can be used to deposite metal ions in a semiconductor powder. For experiments reported here, we have used Er doped Phosphate glass powders as a source of microparticles for nanoparticle generation. The Er concentration in this powder was near saturation of the bulk material (5.7 ± 1.4 at. %). This concentration is sufficiently large that at least a few impurity atoms should be left within the nanoparticle.

The microparticles were captured in the aerosol gas using a fluidized-bed powder feeder. The starting powder consisted of irregularly shaped pieces with dimensions on the order of 1-10 μm. Er doped fiber lasers normally emitt at 1535 nm and confinement would push the transition toward 1000 nm. For applications involving the communication industry it would be an advantage to produce NPs which are not shifted relative to the bulk, so the microparticles were entrained in an argon aerosol at one atm pressure in order to produce a mean size of the particles on the order of 20 nm.[10] Following ablation the produced nanoparticles were collected by supersonically impaction onto carbon TEM grids for size and structure analysis or onto quartz substrates for optical studies.

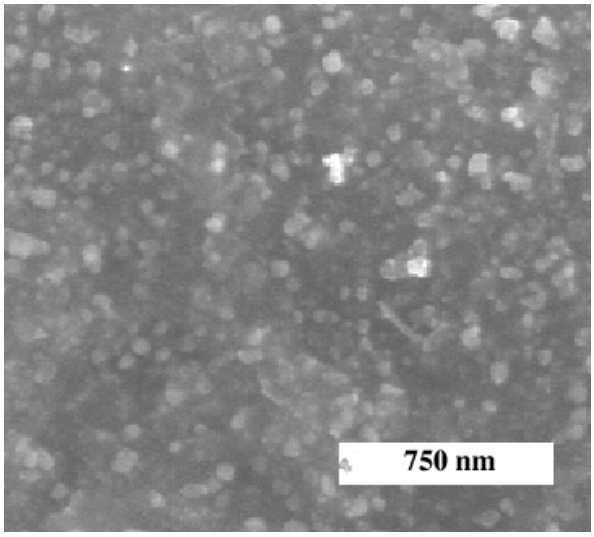

Fig. 1. SEM image of a dense deposition of Er doped phosphate glass NPs.

Threshold in laser fluence for laser ablation was found to be on the order of 1 J cm^{-2}. Like for experiments with PZT[11] the breakdown threshold was not sharp as it is for metals and semiconductors. We attribute this both to the irregular shape of the particles and to their poor optical absorption which makes shock production within the particle difficult. The produc-tion efficiency of NPs using LAM with this material would be greatly improved by coating the microparticles with Er metal.

---

[10] W. T. Nichols, G. Malyavanatham, D.E. Henneke, J.R. Brock, M.F. Becker, J.W. Keto & H.D. Glicksman, "Gas and pressure dependence for the mean size of nanoparticles produced by laser ablation of flowing aerosols," J. Nanoparticle Res. **2**, 141-145(2000).

[11] Gokul Malyavanatham, Daniel T. O'Brien, Michael F. Becker, William T. Nichols, John W. Keto, Desiderio Kovar, Sebastien Euphrasie, Thomas Loue, and Philippe Pernod, "Thick films fabricated by laser ablation of PZT microparticles," submitted to J. of Mat. Res.

Shown in Fig. 2 is a SEM of a region where the nanoparticles were collected with sufficient density on the quartz substrate to form a nanostructured film. The particles lack sharpness because of charging of the glass and a lack of resolution SEM The composition of the particles, averaged over an area of many particles, was measured using energy dispersive spectroscopy (EDS) in the SEM. We found a 50% deficiency for Er(2.8±1.4 at. %), Ytt(5.±2 at. %) and La(4.8±3.4 at. %) and a 20% increase for P atoms in the NP relative the the starting powder. We also found evidence in High resolution TEM micrographs of NP of segregation. Small NP particles (~4 nm dia) of relatively high contrast was found within the nanostructured films. A similar behavior was found for the production of dense deposits of PZT NP and were attributed to the weak shocks formed in the microparticles. Uniformity in the quality of PZT and the current glass materials may benefit from thin metal coatings of the starting microparticles.

Microluminescence spectra were obtained from areas ~1 μm in diameter of the NPs shown in Fig. 1. The excitation laser, λ= 798 nm, was focused onto the sample and spectra obtained through a microscope equipped with a holographic notch filter to block the laser light. The light was dispersed in a spectrometer and measured with an InAs CCD array detector. An example spectrum is shown in Fig. 2 which is similar to spectra obtained for ion implanted glasses.[12] Similar spectra were obtained for samples at temperatures as low as 10 K. Radiative lifetimes were only 0.5 ms shorter than that of the starting microparticles, indicating that the nanostructured materials did not significantly increase the defect or impurity quenching of the Er ions.

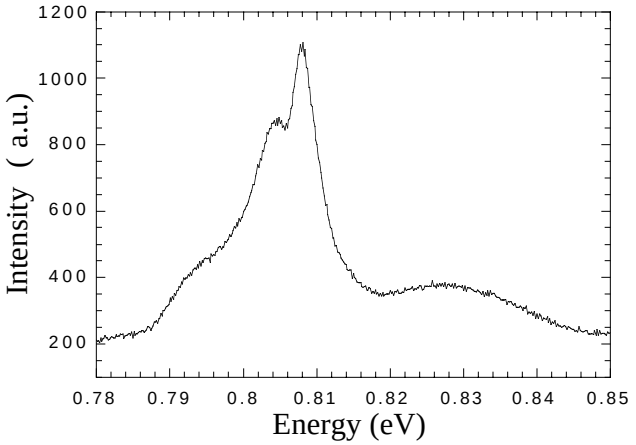

Fig. 2 Fluorescence of Er+ in glass NPs

5.0 DOE Supported Publications

1. W.T. Nichols, D.E. Henneke, G. Malyavanatham, M.F. Becker†, J.R. Brock, and J.W. Keto, and H. D. Glicksman, "Large scale production of nanocrystals by laser ablation of aerosols of microparticles," Appl. Phys. Lett. **78**, 1128-1130(2001).
2. W. T. Nichols, G. Malyavanatham, D. T. O'Brien, D. Kovar, M. F. Becker, and J. W. Keto, "Supersonic nanocrystal deposition for nanostructured materials," Mat. Res. Soc. Symp. Proc. **703**, (Material Research Soc., Pittsburg, 2002), p 5.51-5.56.
3. Dale E. Henneke, Gokul Malyavanatham, Desiderio Kovar, D. T. O'Brien, M. F. Becker and William T. Nichols, and J. W. Keto, "Stabilization of silver nanoparticles in nonanoic acid: a temperature activated conformation reaction observed with surface enhanced Raman spectroscopy," to be published, J. Chem. Phys.
4. Gokul Malyavanatham, Daniel T. O'Brien, Michael F. Becker, William T. Nichols, John W. Keto, Desiderio Kovar, Sebastien Euphrasie, Thomas Loue, and Philippe Pernod, "Thick films fabricated by laser ablation of PZT microparticles," submitted to J. of Mat. Res.
5. Gokul Malyavantham, Daniel T. O'Brien, Michael F. Becker, John W. Keto, and Desiderio Kovar, "Au-Cu nanoparticles produced by laser ablation of mixtures of Au and Cu microparticles," submitted Appl. Phys. Lett.
6. J.W. Keto, W. Nichols, D. O'Brian,[2] M. F. Becker,[2] and D. Kovar, "Nanoparticles: Building Blocks for Nanostructured Materials," to be published AIP Conf. Proc, "Atoms to Nanostructures"

[12] A. Polman, D. C. Jacobson, D. J. Ealesham, R. C. Kisler, and J. M. Poate, J. Appl. Phys 70, 3778(1991).

Theory of fragmentation and rearrangement processes in ion-atom collisions

J. H. Macek

Department of Physics and Astronomy,
University of Tennessee, Knoxville, Tennessee and
Oak Ridge National Laboratory, Oak Ridge, Tennessee
email:jmacek@utk.edu

1 Program scope

Atomic processes that produce three or more species in the final state continue to challenge the best theoretical techniques. Computer simulations of total cross sections have reached a level of reliability comparable to that for two-body channels, however, energy and angular distributions of particles in the final state have only recently been simulated. Even here, electron distributions in 1-5 keV proton-hydrogen atom collisions are difficult to extract owing to the need for high accuracy over large volumes. One aspect of our work is to supplement *ab inito* calculations with analytic treatments at large distances where numerical methods are impractical. A second aspect of our work is to examine processes that involve two or more electrons. Here we focus on processes involving the negative hydrogen ion since it is frequently used as a prototype for studies of the correlated motion of two electrons. Finally, we plan to use the hidden crossing theory to examine processes such as protonium formation in the interactions of slow antiprotons with atomic hydrogen that are difficult simulate numerically owing to their the large number of physical channels that are involved.

The projects listed in this abstract are sponsored by the Department of Energy, Division of Chemical Sciences, through a grant to the University of Tennessee. The research is is carried out in cooperation with Oak Ridge National Laboratory under the ORNL-UT Distinguished Scientist program.

2 Recent progress

Computer simulation of ionization in proton and antiproton collisions with hydrogen atoms by Schultz and co-workers have obtained electron distributions for 1-5 keV projectiles for a small selection of impact parameters. Our analytic treatment for top-of-barrier propagation of the slow electrons brings the computed electron distributions into good agreement with measurements on proton-Helium atom collisions. Unfortunately, our analytic treatment involves a critical step, namely the replacement of cartesian coordinates with prolate spheroidal coordinates typically used for stationary states of the hydrogen molecular ion, that was not justified on an *ab. initio* basis. We have recently shown that this replacement is correct when the relative velocity of the projectile and target are less than the mean velocity of the initially bound electron, thus placing our low energy modification of the top-of-barrier propagator on a sound footing. With this important justification established we can now employ the theory for a variety of low-energy collisions.

Results of our previous calculations with zero-range models for ionization of neutral hydrogen by impact on helium targets and for stripping of loosely bound electrons from negative hydrogen ions in similar collisions have been brought to bear on experimental measurements of electron distributions for these processes[1,2]. We find that slow electrons are well reproduced by our calculations for negative hydrogen ion projectiles, while fast electrons are distributed in accord with our computations for hydrogen atom atom projectiles. The cross section magnitudes, however, suggest an novel influence of the "spectator" electron that we model using the hidden crossing theory. This influence is unexpected, but may be a general feature of low-velocity collisions involving multielectron transitions.

The hidden crossing theory has been adapted to include processes where the relative motion of the target and projectile must be represented by the wave theory, rather than the classical trajectory representation. As an extreme case where the relative motion is clearly quantal, we consider protonium formation in antiproton-atomic hydrogen collisions. Here the projectile is actually bound in a stationary state while the atom electron is ejected, thus the relative motion of the antiproton and proton must be treated according to the quantum theory. We have shown how this can be done within the framework of the advanced adiabatic theory or the hydrogen molecular ion Sturmian representation [3]. In either case, we compute the distribution of

protonium over the n and ℓ quantum numbers even for states with principal quantum number of the order of 250. Our distributions agree, within statistical error, with classical trajectory Monte Carlo distributions.

3 Future plans

At present we have two forms for the top-of-barrier propagator, one valid at low velocity and one applicable at high velocity. The high velocity version has that virtue that it becomes equal to the free particle propagator when the relative velocity is much larger than the mean velocity of the initial electron, while the the low velocity version employs an approximate potential that is accurate over a larger region of electron coordinates. We will seek a representation of the propagator that combines these features in order to examine electron distributions that have been measured for relative velocities that are comparable to the mean velocity in the initial state.

Our exact calculations of zero range models for impact of negative hydrogen ions and neutral hydrogen atoms on helium will be extended to include other targets. Calculations will be compared with measurements of electron energy distributions to further examine the novel role of "spectator" electrons in multielectron processes.

The hidden crossing theory will be applied to the formation of bound proton-antiproton species in collisions of antiprotons with neutral species which have no bound negative ion. This work will explore the universality of our adaptation of the molecular Sturmian theory for processes where the projectile-target motion must be described in the wave picture rather than with classical trajectories.

4 References to DOE sponsored research that appeared in 2001-2003

1. Exact electron spectra in collisions of two zero-range potentials with non-zero impact parameters S.Yu. Ovchinnikov, D.B. Khrebtukov, and J.H. Macek, *Phys. Rev. A* **65**, 032722 (2002).

2. Electron Emission in $H^- - He, H_2$ Collisions, G. N. Ogurtsov, S. Yu.

Ovchinnikov, and V. M. Mikoushkin, in (23rd International Conference on Photonic Electronic and Atomic Collisions, invited talks, July 2003 Stockholm, Sweden).

3. Ionization of atoms by antiproton impact, J. H. Macek in *Electron Scattering From Atoms, Molecules, Nuclei and Bulk Matter*, Ed. by C.Whelan, (Kluwar Scientific 2002).

5 Publications from DOE sponsored Research that appeared in 2003

1. Electron Emission in $H^- - He, H_2$ Collisions, G. N. Ogurtsov, S. Yu. Ovchinnikov, and V. M. Mikoushkin, in (23rd International Conference on Photonic Electronic and Atomic Collisions, invited talks, July 2003 Stockholm, Sweden).

2. Annihilation of Low Energy Antiprotons in Hydrogen, S. Yu, Ovchinnikov and J.H. Macek, in (17th International Conference on the Application of Accelerators in Research and Industry, November 2002, Denton TX), *AIP Conference Proceedings*, **680**) (2003).

3. Ionization Dynamics in Atomic Collisions, S. Yu. Ovchinnikov, J. H. Macek, Yu. S. Gordeev, and G. N. Ogurtsov, in *Atomic Processes* Ed. by S. Shevel'ko, (Springer, 2003), Ch. 25.

6 Articles submitted in 2003 but not yet published

1. Dynamics of Ionization in Atomic Collisions, J. H. Macek, Yu. S. Gordeev, and G. N. Ogurtsov, *Physics Reports*.

Electron/Photon Interactions with Atoms/Ions

Alfred Z. Msezane
amsezane@ctsps.cau.edu

Department of Physics and Center for Theoretical Studies of Physical Systems
Clark Atlanta University, Atlanta, Georgia 30314

Program Scope and Definition

We investigate many-electron correlation, interchannel coupling and relativistic effects in electron impact excitation of atoms/ions and photoionization of atoms/ions. Specifically, we have studied the role of many-electron correlation effects in the generalized oscillator strengths (GOS's) of the noble gas atoms and the importance of multipolarity contribution to their GOS's. Also, correlations in the form of interchannel coupling (interchannel correlations) on dipole and nondipole photoelectron angular asymmetry parameters have been investigated in photoionization of atoms.

Recent Progress

A.1 Generalized Oscillator Strengths for Monopole and Quadrupole Excitation of the Noble Gas Atoms

The inelastic scattering cross section of a fast charged particle from an atom can be suitably investigated through the GOS [1], which is proportional to the cross section. The GOS, introduced by Bethe [1], manifests directly the atomic wave functions and the dynamics of the atomic electrons. The reasons for the great interest in the GOS's are numerous and include the probing of the intricate nature of the valence and inner-shell electronic excitations [2] and the determination of the positions of the characteristic extrema. The recent first time absolute measurement of the GOS's for the lowest nondipole discrete transition in Ar [2] and their subsequent reinterpretation [3] as well as the recent measurement of the GOS's in Kr [4] and the agreement obtained with the RPAE calculations [5] have motivated the present investigation.

Here we have investigated the GOS's for quadrupole and monopole (and their sums) excitation of the outer np $\rightarrow$ (n + 1)p, (n + 2)p levels of the noble gas atoms Ne, Ar, Kr and Xe over the broad range of momentum transfer q values, from q = 0 up to q = 8 a.u., the region of their accessibility. The purpose of this investigation is to understand and delineate the relative contributions to the GOS of the various discrete transition multipolarities to guide measurements. The calculations were performed using the one-electron Hartree-Fock (HF) approximation and with many-electron correlation effects taken into account within the RPAE for the quadrupole and monopole excitations. We found that the GOS's for the quadrupole np$\rightarrow$(n + 1)p transitions of Ne, Ar, Kr and Xe are characterized by two maxima, while the corresponding GOS's for the monopole excitations have a single maximum only [6]. In all the Ne, Ar, Kr and Xe transitions, the monopole GOS contributes the largest component to the sum, with the monopole GOS being

as large as a factor of about 2 of the quadrupole GOS in Xe. This further demonstrates that, contrary to the assertion in [2], the Ar 3p-4p is not exclusively a quadrupole transition.

A.2 Generalized Oscillator Strengths for Open-Shell and Closed-Shell Atoms

We have developed a methodology [7] to calculate the GOS's for discrete transitions in both open-shell and closed-shell atoms. Our resultant expression exhibits a simpler mathematical structure since it contains only a single summation over the orbital angular momentum ℓ instead of over two as in existing formulae. A new Coulomb matrix element and an improved computer code for the RPAE method for open-shell atoms have also been developed. We have used the new RPAE code to investigate the GOS's for the oxygen $2p^4$ (^{3}P) $\rightarrow$ $2p^2(^2P)3s(^2P)$ and $2p^4$ (^{3}P) $\rightarrow$ $2p^2(^4S)3s(^2S)$ transitions and compared our results with the experimental data [8] at the electron impact energies of 100eV, 150eV and 200eV. For the latter transition, a minimum in the GOS has been found at around the momentum transfer q = 1.26 a.u. This value compares reasonably well with that measured by Kanik *et. al* [8]. For the former transition the characteristic minimum has been found at q = 1.11 a.u.

B. Photoionization of Two Open-Shell Atoms or Ions

B.1 General

Studying the photoionization process is generally important for the understanding of correlation and dynamic effects as well as many-body systems. In photoionization of open-shell atoms the angular asymmetry parameter, b is in general both term and photon energy dependent. The slow progress in theoretical studies of the photoionization of the 3s subshell of Cl, for example, is partly due to the fact that the target and the residual ion are both open-shell. Also, the multiple open-shell nature of the inner-shell of excited highly charged ions, permits the investigation of correlation and relativistic effects readily [9]. Recently, it has been concluded that b for the 4s photoionization of atomic Sc is sensitive to interchannel coupling [10], causing it to become energy-dependent. Also, Whitfield *et al* [11] attributed the discrepancies between their measured b and the simple Hartree-Fock (HF) results for Cl 3s to the presence of strong interchannel interaction and CI, including ionization with excitation.

The reduced dipole matrix element, particularly designed to study the photoionization of atoms or ions having two open-subshells, has been evaluated in the LS coupling scheme [12]. The resultant expression has been employed to study the photoionization of chromium 4s and oxygen 2s as well as the asymmetry parameter, b for atoms with two open subshells.

B.2 Photoionization Cross Sections for Chromium Ground State

We have used our [12] reduced dipole matrix elements, Eqs. (5) and (6) to calculate the photoionization cross sections of chromium from its ground state. The photoionization process of interest is $3p^6\ 3d^5\ 4s(^7S) \rightarrow 3p^6\ 3d^5\ (^6S)\ \varepsilon p\ (^7P)$, where the ground state has two open-shells, which are half filled. Both our [12] length and velocity cross sections agree excellently with those calculated using the spin-polarized techniques.

B.4 Partial Photoionization Cross Sections for Oxygen 2s Inner-Shell

Although oxygen has only one open-shell, its 2s inner-shell photoionization cannot be evaluated using the reduced dipole matrix element for the single open-shell atom. However, it can be calculated using the expression for two open-shell atom. We have calculated the partial cross sections for the photoionization of oxygen 2s using our Eqs. (5) and (6) [12]:

(a) $1s^2\ 2s^2\ 2p^4\ (^3P) \rightarrow 1s^2\ 2s\ 2p^4\ (^4P)\, \varepsilon p\ (^3S, ^3P, ^3D)$

(b) $1s^2\ 2s^2\ 2p^4\ (^3P) \rightarrow 1s^2\ 2s\ 2p^4\ (^2P)\, \varepsilon p\ (^3S, ^3P, ^3D)$

We have compared our calculated photoionization cross sections for the reaction (a) with those from the measurement and calculation of Wilhelmi *et.al*. [13]. The R-Matrix cross sections, which agree reasonably well with ours are larger than those measured by the same authors by about a factor of two. This large discrepancy was explained [13] as due to a systematic error in the normalization of the measured data [13].

We have also calculated the cross sections for reaction (b) and determined the ratio of the cross sections of reaction (b) to (a). When the photon energy is larger than 100eV our results are in good agreement with the experimental data [14]. For $h\nu$ < 100eV our ratios are larger than the measured ones. This is due to the neglect of all correlation effects in our HF wave functions, which are known to be very important in the low energy region.

B.5 Photoelectron Angular Distribution Parameters for Cl

We have continued to generate sophisticated CI wave functions for many ions of importance in astrophysics and fusion plasmas and used some of them in photoionization and electron impact studies. In particular, our large CI calculation using Program CIV3 of Hibbert of the lowest 62 fine-structure levels of Cl^+ has resolved the controversy concerning the correct identification of the lowest $^1P^0$ level of Cl^+, viz. the $3s^23p^3\ (^2D^0)\ 3d\ ^1P^0$ [15], rather than the popular $3s3p^5\ ^1P^0$. The incorrectly identified lowest $^1P^0$ level of Cl^+ has been used in a recent measurement [11] and calculation [16] of the b's for $Cl^+\ 3s3p^{5\ 3,1}P^0$. The misidentification of the $^1P^0$ level permeates the published literature.

Recently, we have used the wave function for Cl^+ in the R-matrix method to investigate the b parameters for $Cl^+\ 3s3p^5\ ^3P^0$ and $Cl^+\ 3s^23p^3\ (^2D^0)\ 3d\ ^1P^0$ in the photoionization of the ground state of Cl [17] and contrasted our results with that of the measurement [11]. There is still more work required for the understanding of the measured b's.

Future Plan

- Continue to develop new methodologies for accurate Regge pole trajectories calculation for singular scattering potentials, important in chemical reactions.
- Generate sophisticated CI wave functions for ions/atoms for oscillator strengths and collision strengths calculations as well as for use in electron impact excitation and photoionization studies.

- Investigate correlation structures in dipole and nondipole photoionization as well as photoionization of inner-shell and open-shell atoms and ions.

References and Some Recent Publications from DoE Supported Research

[1] H.A. Bethe, Ann. Phys. **5**, 325 (1930); M. Inokuti, Rev. Mod. Phys. **43**, 297 (1971)
[2] X.Q. Fan and K.T. Leung, Phys. Rev. A**62**, 062703 (2000)
[3] A.Z. Msezane, Z. Felfli, M. Ya. Amusia, Z. Chen and L.V. Chernysheva, Phys. Rev. A**65**, 054701 (2002)
[4] Wen-bin Li, *et al.*, Phys. Rev. A**67**, 062708 (2003)
[5] Z. Chen and A.Z. Msezane, J. Phys. B**33**, 5397 (2000)
[6] M. Ya Amusia, L.V. Chernysheva, Z. Felfli and A.Z. Msezane, Phys. Rev. A**67**, 022703 (2003)
[7] Zhifan Chen, N. Cherepkov and A.Z. Msezane, Phys. Rev. A**67**, 0240701 (2003)
[8] I. Kanik, P.V. Johnson, M.B. Das, M.A. Khakoo and S.S. Tayal, J. Phys. B**34**, 2617 (2001)
[9] T.W. Gorczyca, Z. Felfli, N.C. Deb and A.Z. Msezane, Phys. Rev. A**63**, 010702 (R) (2000); T.W. Gorczyca, N.C. Deb and A.Z. Msezane, Phys. Rev. A**66**, 042716 (2002)
[10] Z. Altun and S.T. Manson, Phys. Rev. A**61**, 030702 (R) (2000)
[11] S.B. Whitfield, K. Kehoe, M.O. Krause and C.D. Caldwell, Phys. Rev. Lett. **84**, 4818 (2000)
[12] Zhifan Chen and A.Z. Msezane, Phys. Rev. A, In Press, (2003)
[13] O. Wilhelmi, G. Mentzel, B. Zimmermann and K.H. Schartner, Phys. Rev. A**60**, 3702 (1999)
[14] S.J. Schaphorst, M.O. Krause, C.D. Caldwell, H.P. Saha, M. Pahler and J. Jiménez-Mier, Phys. Rev. A**52**, 4656 (1994)
[15] N.C. Deb, D.S.F. Crothers, Z. Felfli and A.Z. Msezane, J. Phys. B**36**, L47 (2003)
[16] H.P. Saha, Phys. Rev. A**66**, 010702 (R) (2002)
[17] Z. Felfli, N.C. Deb, D.S.F. Crothers and A.Z. Msezane, J. Phys. B**35**, L419 (2002)

1. "Angle-Optimized Energy-Variable Method for Electron Differential Cross Section Measurement", A.Z. Msezane, Z. Felfli and D. Bessis, Phys. Rev. A, **65**, 050701(R) (2002)
2. "Trapped Dilute Atomic Fermi Gas", M. Ya. Amusia, A.Z. Msezane and V.R. Shaginyan, Physics Letters A**293**, 205 (2002)
3. "Cross Sections of Discrete Levels Excitation of Noble Gas Atoms in Compton Scattering", M. Ya. Amusia, L.V. Chernysheva, Z. Felfli and A.Z. Msezane, Phys. Rev. A**65**, 062705 (2002)
4. "New Semiclassical Approach for Calculating Regge Poles Trajectories for Singular Potentials", N.B. Avdonina, S. Belov, Z. Felfli, A.Z. Msezane and S.N. Naboko, Phys. Rev. A**66**, 022713 (2002)
5. "Correlation Structure in Nondipole Photoionization", M. Ya Amusia, A.S. Baltenkov, L.V. Chernysheva, Z. Felfli, S.T. Manson and A.Z. Msezane, Phys. Rev. A**67**, 060702 (R) (2003)
6. "High Precision Regge Poles and Residues for Singular Scattering Potentials", C.R. Handy, C.J. Tymczak and A.Z. Msezane, Phys. Rev. A, Rapid Commun., **66**, 050701 (R) (2002)
7. "Generation of Converging Regge-Pole Bounds for Arbitrary Rational Fraction Scattering Potentials", C.R. Handy, A.Z. Msezane and Z. Yan, J. Phys. A**35**, 6359 (2002)
8. "Electron Scattering by the SH Radical using the R-matrix Method" K.L. Baluja and A.Z. Msezane, J. Phys. B**35**, 437 (2002)
9. "Strong Electron Correlations in Photoionization of Spin-Orbit Doublets", M. Ya Amusia, L.V. Chernysheva, S.T. Manson, A.Z. Msezane and V. Radojevic, Phys. Rev. Lett. **88**, 093002 (2002)

Ultrafast Coherent Soft X-rays: A Novel Tool for Spectroscopy of Collective Behavior in Complex Materials

Keith A. Nelson
Department of Chemistry, Massachusetts Institute of Technology
Cambridge, MA 02139
Email: kanelson@mit.edu

Henry C. Kapteyn, Margaret M. Murnane
JILA, University of Colorado and National Institutes of Technology
Boulder, CO 80309-0440
E-mail: kapteyn@jila.colorado.edu

Program Scope

In this project, nonlinear time-resolved spectroscopy of condensed matter using coherent soft x-rays is being studied. The primary experimental objective is to obtain direct access to both femtosecond time resolution and mesoscopic length scale resolution. The length scale is defined through transient grating, or time-resolved four-wave mixing, measurements in which the grating spacing is on the order of the soft x-ray wavelength. The primary scientific objective is to measure both the correlation length scale and the correlation time scale, and to determine whether there is any direct association between them, for collective responses including structural relaxation in polymers, supercooled liquids, and other complex materials. A broader objective is to enable nonlinear time-resolved x-ray spectroscopy of condensed matter generally, including investigation of electronic and structural evolution on short length and time scales.

Femtosecond pulses at soft x-ray wavelengths can be produced through high harmonic generation. [1] It is now possible to reach nanojoule energies in such pulses, sufficient for nonlinear time-resolved spectroscopy of condensed matter. Given the high spatial coherence and focusability of the output, intensity levels comparable to those typically used in condensed-matter femtosecond spectroscopy with visible pulses can be reached. Thus there is strong reason to hope for successful extension of spectroscopic methods now widely used in visible and nearby wavelengths to the soft x-ray regime.

In current time-resolved measurements of condensed-matter collective dynamics, the relevant time scales may be measured but the relevant length scales are rarely determined and often are not well understood. For example, structural relaxation in simple molecular liquids occurs in femtosecond/picosecond time scales and is only weakly temperature-dependent. In supercooled liquids, the responses are often highly nonexponential, extending over a wide range (several decades) of time scales even at a simple temperature and changing enormously (i.e. by many decades) as the temperature is cooled and the viscosity increases. [2] A great many materials including synthetic polymers and biopolymers, molecular and ionic liquids, and some aqueous solutions show this behavior.

Current time-resolved measurements cannot resolve many of the most-fundamental physics issues, since essentially all the important correlation lengths are far smaller than any length scale that is currently experimentally accessible. In transient grating measurements, energy is deposited into sample material in a grating pattern, inducing a transient response as the sample relaxes. The grating fringe spacing defines the length scale over which correlated dynamics are measured. [3] In familiar cases, the fringe spacing is used to define an acoustic

wavelength or the length scale over which thermal or mass diffusion is measured. However, structural relaxation dynamics are associated with density or molecular orientational correlation lengths or polymer persistence lengths that generally extend over nanometers, not microns. Direct measurement of the length and time scales is still possible through transient grating experiments, but the light wavelength must be short enough to produce fringe spacings on the order of the correlation lengths can be produced. This requires soft x-ray wavelengths, i.e. wavelengths on the order of tens of nanometers or shorter.

Recent Progress

Recent progress toward demonstration of the coherent soft x-ray four-wave mixing and spectroscopy of high-wavevector acoustic phonons has been made on three fronts: development of a simple and practical test setup for detecting transient x-ray diffraction, detection of coherent soft x-ray transient diffraction, and development of optical methods for generation of high-wavevector acoustic waves.

A diagram of the test setup for ultrafast soft x-ray FWM is shown in figure 1 below. In this setup, we are using soft x-rays to probe a periodically structured sample that is transiently heated. We have made considerable progress in developing a simplified, hollow-waveguide geometry for generating high harmonics. Pulses from an ultrafast laser amplifier system are focused into a hollow argon-filled waveguide, generating light at 30-40 nm wavelength. In recent work, we showed that this geometry can produce flux of $>10^{12}$ photons/sec, with near-perfect spatial coherence [4]. This beam is refocused to a line <<25 micron in width using a grazing incidence curved mirror. This beam is reflected from a surface—in this case damascene, a pattern of alternating copper and silicon lines, manufactured for use in microelectronics. The soft x-rays diffract from this surface pattern, and we observe first and second-order diffracted light using a CCD. The signal level from this setup is measurable even in a single incident pulse, and modest averaging allows us to obtain diffracted signal intensities with better than 1% accuracy.

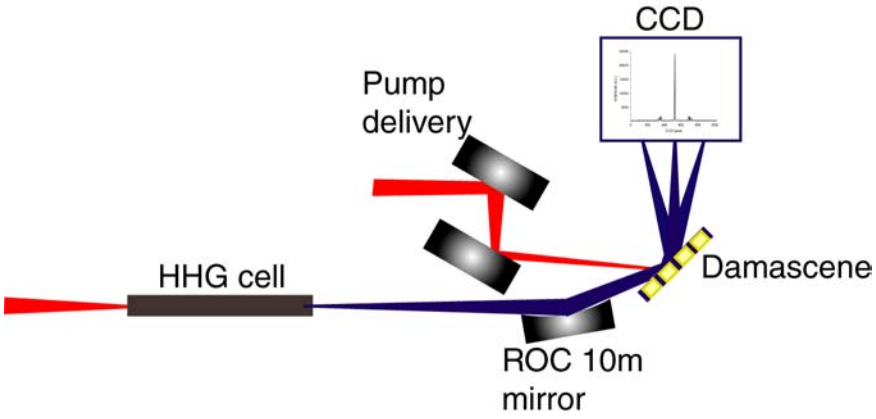

Figure 1: Transient soft x-ray diffraction setup.

We recently conducted the first measurements of time-resolved soft x-ray diffraction using this setup. In this experiment, a single excitation pulse heats the damascene, and differential absorption and thermal expansion of the different materials in the structure give rise to coherent acoustic wave generation upon irradiation by the excitation pulse.

Figure 2 shows data collected from the damascene sample following excitation at t = 0 with a single 800-nm excitation pulse. The signal corresponds to the intensity of the first-order diffraction. The figure shows data collected with the soft x-ray probe (blue curve) as well as with

an 800-nm probe pulse. Although the x-ray data are noisier due to the HHG intensity fluctuations, it is clear that for the available x-ray pulse delay, a similar time-dependence is observed. Following the diffraction out to longer time scales with the optical probe pulse at various diffraction orders reveals acoustic oscillations superimposed on the signal that arises from steady-state thermal expansion at the copper strips of the damascene structure. Although the data are preliminary, it is clear that time-resolved soft x-ray diffraction is observed.

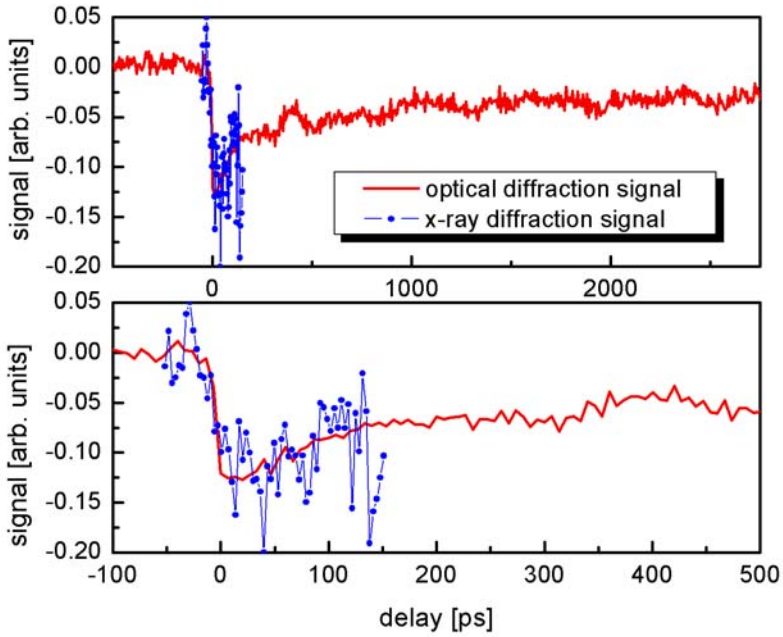

Figure 2: Transient soft x-ray diffraction signal.

In parallel work aimed at experimental access to high-wavevector acoustic phonons, a novel pulse shaping apparatus ("Deathstar") has been constructed, demonstrated, and used for acoustic wave generation. The pulse shaper consists of a recirculating partial reflectance loop into which the excitation pulse is injected. The pulse circulates up to seven times around the loop, each time partially coupling out to produce up to seven evenly spaced pulses. The unique feature of the pulse shaping approach is that it allows pulse repetition rates as low as a few GHz (a total waveform duration of several nanoseconds) and as high as THz. Conventional pulse shaping methods do not allow for generation of low-frequency, GHz, pulse trains. The pulse sequences are used to irradiate a thin metal film, giving rise to heating and thermal expansion and the launching of an acoustic wave into the film.

Figure 3 shows data recorded from a 15-nm aluminum film. An 800-nm pulse is transformed into six pulses with a 400-GHz repetition rate, and these are directed to the sample. The acoustically induced displacement is detected from the back side of the sample using time-resolved interferometry. This permits observation of the sequence of acoustic pulses. Differentiation of the signal with respect to time yields the time-dependent acoustic strain.

In similar measurements, acoustic waves have been generated in a metal film (the "transducer") on one side of a silica glass substrate and detected at the back of a second metal film (the "receiver") on the opposite side of the substrate. Thus high-wavevector acoustic wave propagation through the substrate has been measured. This is of interest in disordered solids where sufficiently short acoustic waves undergo localization and cannot propagate. With this

method, acoustic waves can be measured as long as they propagate entirely through the sample from the transducer to the receiver. With x-ray four-wave mixing, acoustic waves will be characterized all the way into the overdamped limit since they will be monitored immediately upon photogeneration.

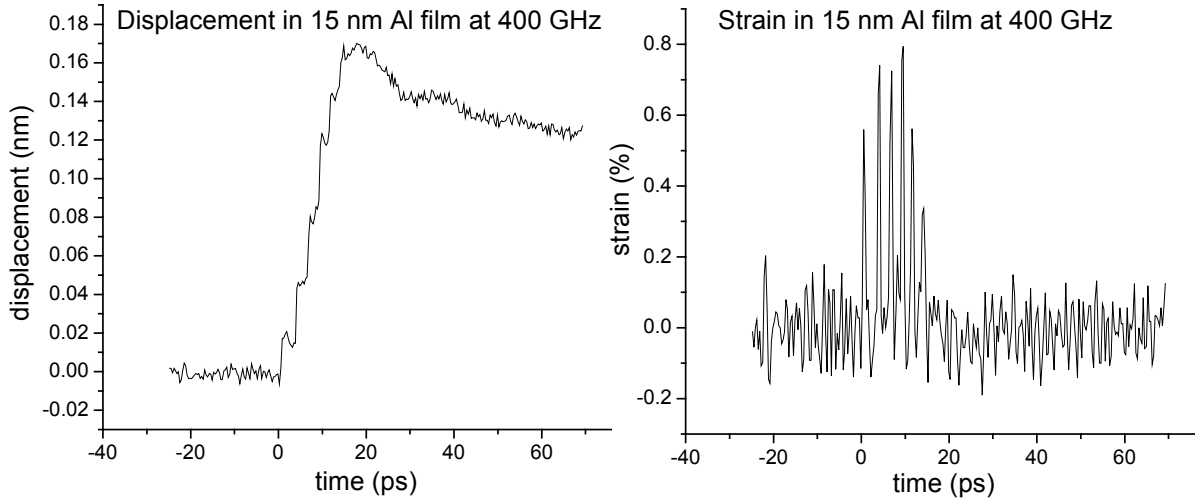

Figure 3: Acoustic response from Al film excited by periodic pulse train.

Future Plans

Experiments similar to those conducted on the damascene are under way with a variety of spatially periodic structures and with soft x-ray as well as optical excitation pulses. The results will be important in that they will demonstrate sufficient soft x-ray pulse energy for excitation as well as probing of the responses. Following this stage, four-wave mixing measurements will be attempted on unpatterned samples, using crossed soft x-ray excitation pulses to generate the acoustic and thermal responses. This will reach the objective of demonstrating experimental capabilities described in the first section of the report. Systematic study of disordered solid and liquid samples will follow, permitting comparison to the measurements conducted with optical pulse sequences and extension of them to higher frequencies and regimes of far higher acoustic attenuation rates.

References

1. "Phase-Matched Generation of Coherent Soft-X-Rays," A. Rundquist, C. Durfee, Z. Chang, S. Backus, C. Herne, M. M. Murnane and H. C. Kapteyn, Science **280**, 1412 – 1415 (1998).
2. See e.g. Supercooled liquids: Advances and novel applications, ACS Symp. Ser. **676**, J. T. Fourkas D. Kivelson, U. Mohanty and K. A. Nelson, eds. (Amer. Chem. Soc., Washington, D.C. 1997).
3. "Testing of Mode-coupling Theory Through Impulsive Stimulated Thermal Scattering", by I.C. Halalay, Y. Yang, and K.A. Nelson, Transport Theory and Stat. Phys. **24**, 1053-1073 (1995).
4. "Generation of spatially coherent light at extreme ultraviolet wavelengths," R. A. Bartels, A. Paul, H. Green, H. C. Kapteyn, M. M. Murnane, S. Backus, I. P. Christov, Y. W. Liu, D. Attwood, and C. Jacobsen, Science, vol. 297, pp. 376-378, 2002.

Theoretical Studies of Resonant Electron-Polyatomic Collisions

A. E. Orel
Department of Applied Science
University of California, Davis
Davis, CA 95616
aeorel@ucdavis.edu

Program Scope

This program is a broad first-principles attack on resonant electron-polyatomic collisions which removes the level of empiricism that characterizes most current theoretical efforts. Modern *ab initio* techniques, both for the electron scattering and the subsequent nuclear dynamics studies, are used to attack previously unreachable areas. Specifically, this work addresses vibrational excitation, dissociative attachment, and dissociative recombination problems in which a full multi-dimensional treatment of the nuclear dynamics is essential and where non-adiabatic effects are expected to be important.

Recent Progress

0.1 *Ab Initio*

Study of Low-Energy Electron Collision with Ethylene

In collaboration with T. N. Rescigno, LBL, we have carried out a study of low-energy electron collision with ethylene using the complex Kohn variational method. Electron scattering by hydrocarbons is particularly relevant to cold plasma technology. Although ethylene, C_2H_4, is one of the simpler hydrocarbon molecules, there have been only very limited studies on its interaction with low-energy electrons.

Ethylene is a closed-shell molecule which possesses a permanent quadrupole moment. There are two important features in its scattering, a Ramsauer-Townsend minimum at very low electron scattering energies and a low-lying shape resonance whose position and width are strongly affected by target-distortion effects. The resonance is of $^2B_{2g}$ symmetry and corresponds to the temporary capture of the incident electron into an empty, antibonding, valence orbital. Although extensive calculations on electron scattering from ethylene have been performed from threshold to around 50 eV in the fixed-nuclei approximation at the equilibrium geometry previous calculations found it difficult to describe experimental angular differential cross sections at electron-impact energies below 3 eV.

Calculations which included the effects of dynamic polarization were performed over a range of different geometries. The effects of nuclear motion were included by vibrationally averaging the T-matrices over the zero point C-C stretch mode vibrational motion. The inclusion of dynamic polarization and the effect of nuclear motion were equally critical in producing accurate results. The integrated elastic, momentum transfer and differential cross sections were found to be in excellent agreement with experiment.

The results of the calculation are described in a paper submitted to Physical review A.

0.2 Low Energy Positron Collisions with Molecular Targets

In collaboration with T. N. Rescigno, LBL, we have extended the Complex Kohn variational method to address positron-molecule scattering. The trial wave function was taken as a close-coupling expansion in molecular target states and is constructed as a sum of product terms involving discretized N-electron target

pseudostates, χ_γ, and channel functions, ϕ_γ, describing the scattered positron:

$$\Psi(r_1, ..r_N, r) = \sum_\gamma \chi_\gamma(r_1, ..r_N)\phi_\gamma(r). \quad (1)$$

The sum includes both energetically open and closed-channel terms, the latter being essential for the proper description of target polarization and distortion effects. The positron channel functions, $\phi_\gamma(r)$, were expanded in terms of square-integrable (Gaussian) functions and, for energetically open channels, numerical continuum functions as well. The various bound-bound, bound-free and free-free matrix elements that are needed in the construction of the Hamiltonian in this trial basis were easily calculated in terms of the one-particle transition densities between the various target states.

The method was used to calculate both elastic and electronic excitation cross sections for H_2 and N_2. The elastic cross sections, for both H_2 and N_2, are in excellent agreement with previous *ab initio* studies. The excitation cross sections for H_2 agree well with recent measurements, but show only qualitative agreement with experiment in the case of N_2.

A paper describing the method and its application is in preparation for submission to Physical Review A.

Future Plans

0.3 Dissociative Recombination of the Water Ion

We have begun a study on dissociative recombination of the water ion via collision with low energy electrons. A series of fixed nuclei calculations, as a function of symmetric stretch and bond angle, on electron scattering from the water ion have been carried out for the four symmetries and two spin couplings of the system. A number of resonances were discovered, however, the majority of them parallelled the highest B_2 ion curve. They represent members of a Rydberg series converging to this ionic state. Note that as they lie above the ground state of the ion, they appear as scattering resonances, the so-called 'core-excited' resonances, seen in OH^+ and CH^+ DR. Some, however, were dissociative. All the resonances were fit with a Breit-Wigner form and the resonance parameters were abstracted. We plan to continue these calculations to determine the three-dimensional potential energy surfaces for the resonances. These will be used as input into a full-dimensional treatment of the DR process in this system.

Preliminary electron scattering calculations have begun on H_3O^+. We plan to study the resonances in this system and eventually carry out studies on dissociative recombination.

0.4 *Ab Initio* Study of Low-Energy Electron Collision with Fluoroethylene

We plan to extend, in collaboration with T. N. Rescigno, LBL, our recent calculations of low-energy electron collision with ethylene using the complex Kohn variational method to the study of substituted ethylene, in particular fluoroethylene. This system was recently studied by Buckman, and there is much experimental data available, including differential cross sections at low energy and vibrational excitation cross sections.

"Low-Energy Electron Interactions with Complex Targets"

Thomas M. Orlando, *School of Chemistry and Biochemistry and School of Physics, Georgia Institute of Technology, Atlanta, GA 30332-0400*
thomas.orlando@chemistry.gatech.edu

Objectives: The primary objectives of this program are to investigate the fundamental physics and chemistry involved in low-energy (1-100 eV) electron scattering with molecular solids, surfaces and interfaces. The program is primarily experimental and concentrates on the important questions concerning how gas-phase concepts have to be modified when trying to understand electron collisions with complex condensed-phase targets.

Progress: The program began in July 2002 and has focused on three main tasks that are being carried out in the newly established Electron- and Photon-Induced Chemistry on Surfaces (EPICS) Laboratory at the Georgia Institute of Technology (GIT).

Task 1. Quantum-resolved electron-stimulated processes on water ice films.

1. A. Electron-stimulated production of O_2 from condensed nanoscale water films.

We have completed a study of the electron energy threshold, fluence, and temperature dependence for O_2 production during low-energy (5-100 eV) electron bombardment of thin (~ 40 bilayer) amorphous and crystalline D_2O ice films deposited on a Pt(111) substrate in vacuum. The electron energy threshold (referenced to the vacuum level) for O_2 formation is approximately 10 ± 2 eV.

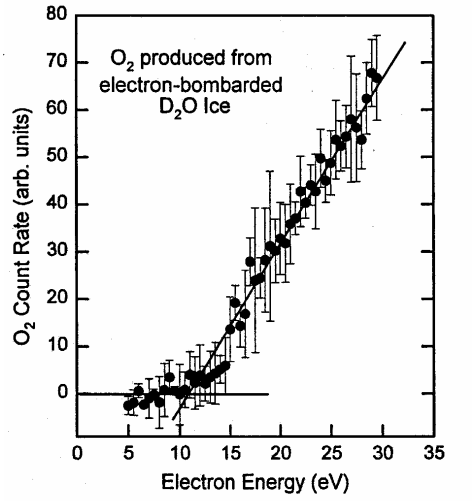

Figure 1. The yield of molecular oxygen as a function of the incident electron energy. The threshold value is ~10 ± 2 eV and is related to valence level electronic excitations and direct ionization.

This threshold is due to valence level electronic excitations or ionization of condensed water molecules. Comparison of the fluence dependence with kinetic models shows that the formation of O_2 is dominated by direct excitation and dissociation of a stable precursor molecule, and not by diffusion and recombination of oxygen atoms. The O_2 yield is also strongly dependent upon the temperature of ice, is different for crystalline and amorphous ice films, and is indicative of surface and bulk structural transitions.

1. B. Electron-Stimulated Desorption of H^+, H_2^+ and $H^+(H_2O)_n$ from nanoscale water thin-films. Electron beam induced production and desorption of H^+, H_2^+, OH^+ and $H^+(H_2O)_n$ has been studied from nanoscale water films. The high proton kinetic energy distributions and the linear yield vs. dose are indicative of proton formation and desorption by two-hole and two-hole, 1-electron final states. These localized states are produced either directly or via Auger decay

pathways and desorption occurs from the vacuum surface interface as a result of a Coulomb explosion. The proton yield increases from 80 to 150 K and then drops dramatically as the temperature exceeds 150 K. The increased yield is associated with structural and physical changes in the adsorbed water that include disordering and longer excited state lifetimes. The decreased yield is correlated with water desorption. H_2^+ is also formed from adsorbed water and primarily involves direct dissociative ionization channels. Both the H^+ and H_2^+ yields depend upon the water coverage in a manner well described by the energy deposition probability. Some reactive scattering of energetic protons and two-hole Coulomb interactions produce H_3O^+ and other higher mass clusters such as $H^+(H_2O)_n$, where n=2-6.

Task 2. Simulated desorption/ dissociation of adsorbates.
2. A. Probing the uptake and autoionization of HCl on low-temperature water ice. We have completed a study of the interaction of HCl on low-temperature (80- 140 K) water ice surfaces using low-energy (5 –500 eV) electron-stimulated desorption (ESD) and temperature programmed desorption (TPD). This experiment relies upon the results of the previous task which examined the ESD of protons and protonated clusters $(H^+)(H_2O)_n$, where n=1-6. As discussed above, these cation desorption channels involve localized two-hole states and the yields are very sensitive to the local disorder in the terminal layer of the ice. We have observed an enormous reduction of the proton signal and a concomitant increase in the protonated cluster signals due to the presence of sub-monolayer quantities of HCl. This occurs at temperatures as low as 80 K and indicates rapid uptake and non-activated autoionization of HCl. This forms ion-pairs that lead to disorder, reduced numbers of dangling bonds and increased hole-localization. The latter results in cluster formation due to the increased lifetimes of two-hole final states which produce fast protons. The uptake and facile auto ionization of HCl is further supported by TPD studies which show that desorption of HCl is commensurate with desorption and removal of the multilayer ice. Adsorption of molecular HCl occurs only at temperatures below 120 K and for HCl doses > 1 ML. These results clearly demonstrate the utility of ESD to probe the interactions of molecules with low-temperature ice surfaces.

Task 3. Desorption enhancements due to interference/diffraction effects. We have continued calculations to explore spatial pattering of substrates by using interference and diffraction during electron scattering. The two frames on the left illustrate the interference pattern expected from an ordered array of scattering centers whereas the frame on the right is the full hemisphere mapping of the probability density distribution for electron excitation of a Cl terminated Si(111)-(1x1) surface. It is clear from Figure 2 that the excitation exhibits spatially localized maxima (yellow and red regions) and minima (blue regions). Whether a particlar site or domain on a surface experiences a maximum or a minimum depends on i) the electron energy (wavelength), ii) the electron direction of incidence and iii) the arrangement of nearest-neighbor atoms.

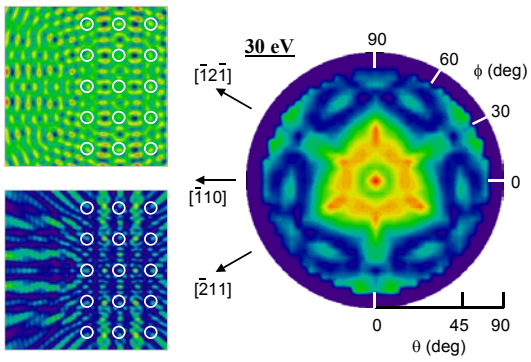

Figure 2. The top left frame indicates the interference pattern of a plane wave interacting with an array of scattering centers. The bottom left frame is a plot of Ψ*Ψ, the probability of finding an electron. The frame on the right is a plot of the probability density distribution or electron excitation probability for a Si(111):Cl surface. The calculation was carried out using spherical wave scattering, incident electron energy of 30 eV, and for excitation localized on the Si atom.

Since the probability of desorption is proportional to the incident electron density at the site of the "absorbers", the total desorption yield depends upon the local atomic structure and the k-vector of the incident wave.

Future Plans:

We are continuing our work on all three tasks.

Task 1. Vacuum ultraviolet photo-induced processes in water films: The competition between ionization and dissociation. -In order to investigate the relative importance of ionization vs. direct dissociative excitation, we have constructed and tested a vacuum ultraviolet photon source based on the non-linear third harmonic generation in rare-gas (Xe and Ar) mixtures. This has been coupled to an ultrahigh vacuum system that has been equipped to perform neutral particle detection using resonance enhanced multiphoton ionization (REMPI). Future efforts will allow us to compare the quantum-state and velocity distributions of the atomic and molecular hydrogen and oxygen produced by VUV photon bombardment. This will allow us to determine the relative importance of the energy-loss channels involving triplet states and resonance scattering.

Task 2. State-resolved measurements of DEA and electron-stimulated dissociation of O_2 and Cl_2 co-adsorbed with water. Competition between autoionization and dissociative and electron attachment occurs during the decay of transient negative-ion "reonances" produced during low-energy electron scattering with co-adsorbed molecules. Particularly interesting examples are physisorbed O_2 or is Cl_2 on multi-layer ices. When are examining the neutral atomic product yields using REMPI and the negative ion yields using TOF techniques to investigate the nature of the substrate (water) induced coupling/perturbations on the states which normally support DEA resonances.

Task 3. Improved Theory and Experimental Investigations of DESD

We have continued the theoretical treatment of DESD and have added Debye-Waller terms to account temperature effects. However, the description should be improved by the incorporation of more realistic scattering potentials rather than the muffin-tin approximation. We are upgrading the code/theory to include these changes. In addition, we will complete the construction of a new system which will allow us to perform DESD with full angular resolution. Initial work is focusing on Si patterning using Si(111):Cl and $SiCl_4$(g) is underway.

Publications:

1.) T. M. Orlando and M. T. Sieger, "The Role of Electron-stimluated production of O_2 from water ice and the radiation processing outer solar system surfaces" *Surf. Sci.* **528**, 1-7 (2003).

2.) J. Herring, T. M. Orlando and A. Alexandrov, "Electron-stimulated desorption of H^+, H_2^+ and $H^+(H_2O)_n$ from nanoscale water thin-films", submitted, *Phys. Rev. B.*

3.) J. Herring, A. Alexandrov, and T. M. Orlando "Probing the interaction of hydrogen chloride on low-temperature water ice surfaces using electron stimulated desorption", J. Herring, A. Alexandrov, and T. M. Orlando, submitted, *J. Chem. Phys*.

4.) T. M. Orlando, M. T. Sieger, D. Oh and C. Lane, "Electron Collisions with Complex Targets: Diffraction Effects in Stimulated Desorption", submitted, *Physica Scripta.*

Mode-specific polyatomic photoionization far from threshold: Molecular physics at third generation light sources

Erwin D. Poliakoff, Chemistry Department, Louisiana State University, Baton Rouge, LA 70803, epoliak@lsu.edu

Our research focuses on photoelectron scattering in the anisotropic fields characteristic of polyatomic molecules. Using vibrationally resolved photoelectron spectroscopy, we study the influence of mode-selected geometry changes on continuum resonances. In order to interpret the results, we also perform studies to elucidate the mechanism responsible for excitation of nontotally symmetric vibrations, which are ubiquitous, even though they are nominally forbidden. In studies related to the VUV work, x-ray absorption and excitation spectroscopy is used on systems where geometry changes can be locked in, either by surface adsorption or by steric effects. This research permits us to generate previously inaccessible data on continuum spectroscopy for molecular systems, and yields unanticipated correlations between electronic and vibrational degrees of freedom in molecular physics.

Recent progress

Using high resolution photoelectron spectroscopy, we have studied how vibrational and electronic motion are coupled for CO_2, CS_2, N_2O, BF_3, and Ar_2. This work concentrates on polyatomics because they allow us to interrogate how resonances respond to mode-specific geometry changes. As one example, we just completed an extensive study of the energy dependence of all of the vibrational branching ratios in CO_2 $4\sigma_g^{-1}$ photoionization, even the symmetry forbidden degrees of freedom.

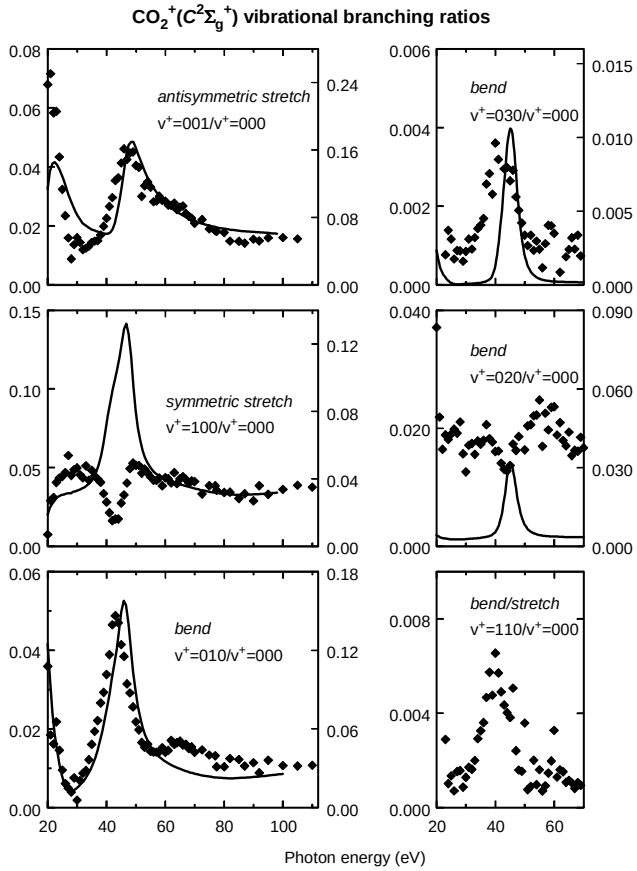

Figure 1. *Vibrational branching ratios following $4\sigma_g^{-1}$ photoionization of CO_2. Theoretical results are also shown. (The axis scales for theory are on right side of each frame; for experiment, on left.) The theoretical curves are generated in the independent particle approximation. The agreement between theory and experiment for the (010) and (001) vibrations demonstrate that these forbidden transitions do* ***not*** *result from interchannel effects. There is poor agreement between theory and experiment for the (100) or (020) levels, and it appears that this is the result of a Fermi resonance between these levels that is not addressed by theory.*

Data were acquired over the range 20-110 eV. This is the first study in which vibrationally resolved data have been acquired as a function of energy for *all* of the vibrational modes of a polyatomic system. As mentioned above, we devoted considerable effort to clarify the mechanism responsible for the single-quantum excitations of the nontotally

symmetric vibrations. While the existence of such forbidden transitions is well-established, all previous studies have attributed their existence to interchannel vibronic coupling effects that result from a breakdown of the Born-Oppenheimer approximation (e.g., Herzberg-Teller, Renner-Teller, and Jahn-Teller effects). By probing the energy dependence of such excitations and enlisting the theoretical support of Prof. Robert Lucchese of Texas A&M, we have demonstrated that there is a simpler and qualitatively different mechanism that is responsible, namely *photoelectron-mediated vibronic symmetry breaking*. This effect arises from the sensitivity of the photoelectron dipole amplitudes to adiabatic changes in molecular geometry, and our studies on several molecules have demonstrated that this phenomenon is widespread, and may in fact be responsible for many previous observations of nominally forbidden vibrations that have been cited in the literature. This effect is a direct but significant generalization of the effect leading to non-Franck-Condon behavior in diatomic systems observed by the NBS group many years ago. In any event, the current results demonstrate this *intrachannel* mechanism is responsible for all of the forbidden transitions observed in the systems that we have studied to date. We believe that we also understand why theory and experiment disagree for the single quantum symmetric stretch and two quanta bending motions (cf. Fig. 1); it is likely that the Fermi resonance between the $v^+ = (100)$ and (020) levels results in an interference effect, although this has not been verified.

New results have also been obtained for $5\sigma_u^{-1}$ photoionization of CS_2. While there are similarities with CO_2, there is also a significant difference. Specifically, Fig. 2 shows that the symmetric stretch branching ratio is relatively flat for CS_2, in striking contrast to the antisymmetric stretch branching ratio curve. This behavior implies that the localization of the quasibound continuum electron is qualitatively different for CS_2.

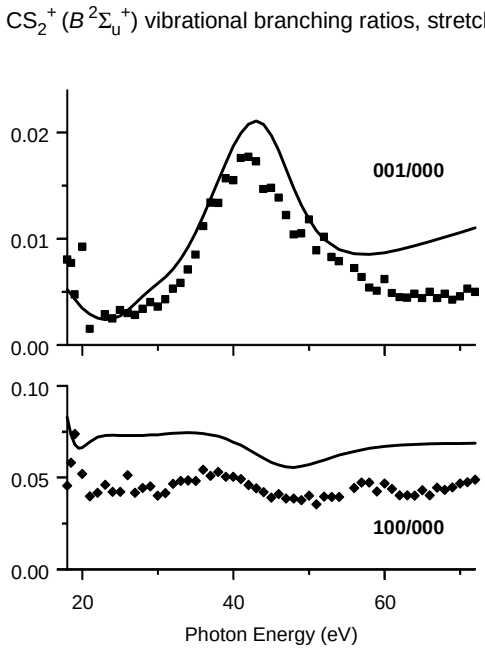

Figure 2. *The branching ratio curves for CS_2 exhibit an extreme example of mode specificity. There is a strong enhancement in the antisymmetric stretch branching ratio, while the symmetric stretch branching ratio is nearly constant. This comparison allows us to extract spatial information regarding the continuum electron localization.*

Specifically, these results indicate that the quasibound continuum photoelectron is localized in the regions between the atoms, and along the molecular axis. The antisymmetric stretch causes the nuclei to approach more closely than the symmetric stretch (by approximately a factor of $\sqrt{2}$), so the resonance seen in Fig. 2 has greater sensitivity to the antisymmetric stretch. This is corroborated by theory, which exhibits excellent agreement with experiment. The excursion in the branching ratio is the result of a $5\sigma_u \rightarrow k\sigma_u$ shape resonance. One might suppose that this transition is forbidden, but the $u \rightarrow u$ transition is occurring because of the symmetry breaking induced by the photoelectron. There are many resonant channels predicted by theory, but most of them do not carry significant oscillator strength. The contour maps for all of the resonant wavefunctions are mapped out in Fig. 3, and theory shows that the one responsible for the energy dependence of the antisymmetric stretching branching ratio is the $5\sigma_u \rightarrow k\sigma_u$ shape resonance in the bottom frame. As expected from the qualitative argument mentioned above, the amplitude for this channel is indeed highly localized in the spatial region between the atoms and along the axis.

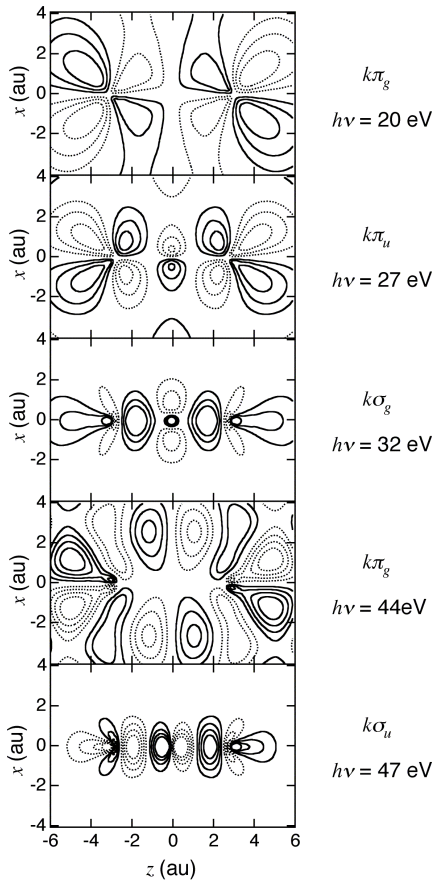

Figure 3. *CS_2 shape resonant contour maps. While theory predicts that there are several shape resonant channels present in this molecule – as shown in this figure – only the $k\sigma_u$ resonance (bottom frame) carries appreciable oscillator strength. The sensitivity of the CS_2 resonance to the antisymmetric stretching vibration is consistent with the quasibound photoelectron being localized in the region between the atoms for the molecule.*

There are a few notable points highlighted by these results. First, the bottom frame of Fig. 3 shows that the resonant wavefunction has an unprecedented nodal pattern. Such a multinode pattern (7 nodes along the internuclear axis) has never been observed previously. Secondly, the type of localization – between the atoms and along the bonds – is unique. There have been continuum $k\sigma$ resonances localized over entire triatomic peripheries, and there have been $k\pi$ resonances that have been shown to point away from the molecular axis, but there has never been a direct verification of the bond-localized behavior shown in the bottom frame of Fig. 3. This demonstrates that there is considerable diversity in the types of localization which are realized in molecular scattering processes, even far from threshold. This underscores the point that comprehensive vibrationally resolved studies on polyatomic systems uncover qualitatively new phenomena in molecular physics.

In our N_2O investigation, there are two points worth emphasizing. First, the branching ratio curves display a high degree of mode-specificity, as was the case for both CO_2 and CS_2. However, the excursions are occurring in an energy range where no pronounced continuum resonances have been predicted in previous theoretical work, so calculations are ongoing for that system.

For BF_3, our new branching ratio results contradict the interchannel coupling mechanism invoked in earlier BF_3 studies to explain excitation of the $v^+ = (0010)$ level – the in-plane asymmetric stretch. Theoretical work is ongoing for this molecule as well. Note that this system is the first nonlinear molecule studied, and the effects observed for simple linear triatomic systems persist. However, the types of localization possible for larger molecular systems become more varied, and the BF_3 results show that larger molecular systems are amenable to study.

We have also started a new line of research at the ALS, and it is based on a straightforward instrumental modification. The experimental apparatus housing the Scienta SES-200 photoelectron energy analyzer has been modified to include a supersonic beam source. This development was a collaboration with Dr. John Bozek at the ALS, as were all of the VUV studies mentioned above. This supersonic source was used in a study of Ar_2, where

individual electronic states of the ion were resolved in the photoelectron spectrum, and such spectra were acquired as a function of energy. This type of study can be used to generate partial photoionization cross section curves for atomic and molecular clusters over a wide range of energies; such data have never been accessible previously. Moreover, the supersonic source will also reduce the rotational and Doppler broadening and enable vibrationally resolved studies of larger molecular systems (e.g., aromatic hydrocarbons, alkenes, dienes, and related targets).

There was one other diatomic study we completed in 2003. We studied vibrationally resolved CO $4\sigma^{-1}$ photoionization from 20 to 185 eV at the LSU synchrotron facility using the dispersed fluorescence method developed by my group. Comparison with results for the $2\sigma_u^{-1}$ channel of the isoelectronic N_2 molecule shows the branching ratio curves for these two systems to be qualitatively different due to the underlying scattering dynamics: CO has a shape resonance at low energy but lacks a Cooper minimum at higher energies whereas the situation is reversed for N_2. The contrasting behavior of these isoelectronic systems is surprising.

Finally, we have used inner-shell spectroscopy on geometrically constrained molecular systems. These studies are currently in press, and they provide an alternative experimental strategy for understanding connections between continuum spectroscopy and molecular structure. Two classes of systems were studied, ring compounds with heteroatoms and self-assembled monolayers on metallic surfaces. These studies corroborated the main conclusions from the VUV work at the ALS, namely that shape resonances are highly sensitive to bond angle. These studies also emphasize the implication that XANES spectra are affected by the sensitivity of continuum resonances to changes in bond angles in more complex polyatomic systems.

Future plans

Most of the near-term future work will focus on VUV photoelectron spectroscopy, and we plan to extend our current studies in two ways. First, more complex molecular systems with additional degrees of freedom will be investigated, as alluded to above. Secondly, we will study additional cluster systems (both atomic and molecular) using the supersonic beam source. This will focus primarily on dimers. Both types of future studies rely on the supersonic beam source. The cooling capability of the supersonic source accesses vibrationally resolved studies of larger molecular systems, and it also generates the clusters desired as targets for partial photoionization cross section studies.

Publications:

E.D. Poliakoff, *Studies of Molecular Photoionization Dynamics Using Ionic Fluorescence, in Chemical Applications of Synchrotron Radiation* (World Scientific, Singapore, 2002) ed. T.K. Sham

G. Farquar, S.A. Alderman, E.D. Poliakoff, and B. Dellinger, *X-ray Spectroscopic Studies of the High Temperature Reduction of Cu(II)O by 2-Chlorophenol on a Simulated Fly-Ash Surface*, Environ. Sci. Technol. **37**, 931-935 (2003)

E.E. Doomes, P.N. Floriano, R.W. Tittsworth, R.L. McCarley, and E.D. Poliakoff, *Anomalous XANES spectra of octadecanethiol adsorbed on Ag(111)*, J. Phys. Chem. B (in press, 2003)

E.E. Doomes, R.L. McCarley, E.D. Poliakoff, *Correlations between heterocycle ring size and X-ray spectra*, J. Chem. Phys. (in press, 2003)

The following manuscripts have been completed and will be submitted by the time of the 2003 contractors meeting.

G.J. Rathbone, E.D. Poliakoff, J.D. Bozek, R.R. Lucchese, P. Lin, *Mode-specific photoelectron scattering effects on $CO_2^+(C^2\Sigma_g^+)$ vibrations*, J. Chem. Phys. (in preparation)

G.J. Rathbone, E.D. Poliakoff, J.D. Bozek, R.R. Lucchese, *Evidence for a $d\sigma$ localized continuum wavefunction: $5\sigma_u^{-1}$ photoionization of CS_2*, Phys. Rev. Lett. (in preparation)

G.J. Rathbone, R.M. Rao, E. D. Poliakoff , K. Wang, V. McKoy, *Vibrational branching ratios in photoionization of CO and N_2*, J. Chem. Phys. (in preparation)

"Isotopically Enriched Thin Films and Nanostructures by Ultrafast Pulsed Laser Deposition"

Peter P. Pronko
University of Michigan
Center for Ultrafast Optical Science
Department of Electrical Engineering and Computer Science
6109 IST Bldg., 2200 Bonisteel Boulevard
Ann Arbor, MI 48109
pronko@eecs.umich.edu

Program Scope and Definition

This project involves the study of spontaneous isotopic enrichment of lighter isotopes along the central axis of ultrafast laser ablation plasmas. It is proposed that spontaneous magnetic fields, both toroidal and longitudinal, act to confine the emitted ionic component of the plume and induce centrifuge like rotation that produces the observed enrichments. Our early work at 780 nm, 120 fs, 2 x 10^{14} W/cm^2 demonstrated the generality of the phenomena for isotopic elements in the periodic table up to mass 73 [1,2]. Continued research under this program has demonstrated similar separation effects for chemical species of ablated binary compounds such as the Ni/Cu alloy at 5 x 10^{15} W/cm^2. Comparison of these results with those obtained by conventional plasma centrifuges shows strong similarities and reinforces the proposed model [2]. In our recent work [3] it has been shown that, in addition to isotope enrichment in the ablation plumes, one also observes dense concentrations of sub-micron clusters being formed for metallic and semiconductor materials

Recent Results

These clusters are being studied experimentally and models are being tested in relation to their mechanism of formation. Recent experiments, using time delayed secondary pulses in the 10^{16} W/cm^2 range, show that at 5 to 10 picoseconds, after the initial pulse, a resonant absorption of energy into the preformed plasma occurs. Figure 1 shows that characteristic resonant behavior [4] associated with secondary pulse absorption in our experiments. Examination of the change in detailed charge states associated with the results of Fig. 1 imply that the second pulse is absorbed in the leading edge of the expanding plasma [5,6]. The way in which this occurs and the effect it has on the clusters provides useful insights into their possible formation mechanism. Theoretical publications, based on molecular dynamics (MD) and heat dissipation models [7,8] have suggested explosive boiling from a superheated liquid as a possible mechanism for the cluster formation process. However, our double pulse experiments do not support such a process.

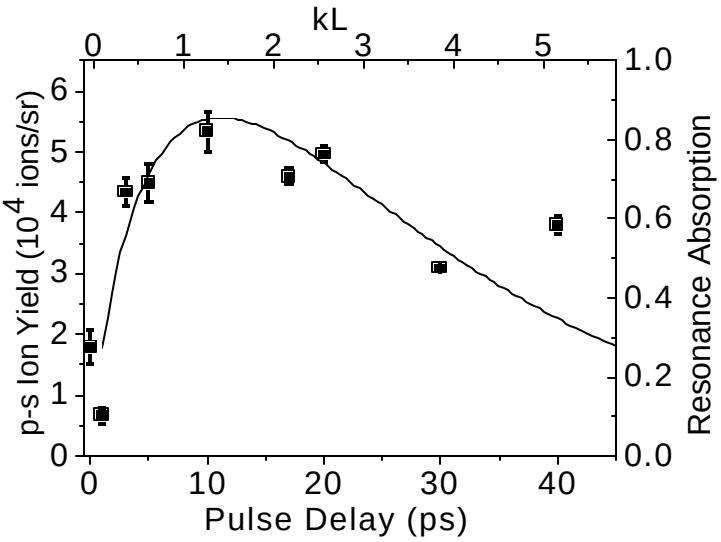

Fig. 1 Measured P polarized resonant absorption characteristics from ion yields in pre-formed silicon ablation plasma [5].

Although the experimental cluster size distributions show, in some cases, a bi-modal distribution as suggested by molecular dynamics, the time sequence of appearance for the clusters versus ions and neutrals is not the same as in the MD case. The phase explosion model predicts a simultaneous appearance of ions, neutrals, and clusters in the ablation plume. Experimentally one observes significant time delays (microseconds) between these entities. This suggests that plasma phenomena are playing an important role in the process and our work has been aimed at understanding what these effects might be. In that regard, a magnetic pinch jet-nozzle mechanism has been investigated, the results of which were recently published [3]. Additionally, the observed effect of a secondary pulse on cluster size distributions is contrary to that expected from phase explosion of a superheated liquid. It is observed in our experiments that the large clusters are preferentially eliminated after the secondary pulse with the size distribution showing smaller mean sizes and narrower rms variation within the distribution. The results of MD suggest that the smaller clusters should be eliminated by absorption of energy in the leading edge of the ablation plume leaving the larger clusters that occur in the later stages. The results we observe are more generally supported by expansion and condensation out of a supersonic nozzle (magnetic or otherwise) as suggested by the following equation describing cluster formation in such systems [9]:

$$\Gamma = k \frac{(d / \tan a)^{0.85} p_0}{T_0^{2.29}}$$

where d is the jet throat diameter in μm, α is the jet expansion half angle, p_0 is the backing pressure, T_0 is the initial gas temperature, and k is an experimental scaling constant. Cluster size is based on the average atoms per cluster being $N_c \sim \Gamma^2$. Using anticipated values from our plasma experiments, this equation predicts cluster sizes close to those observed (100-200 nm). Multi-pulse experiments would cause an increase in pressure and temperature such that, on balance, smaller clusters would result.

In addition to the double pulse work, we have done preliminary experiments on the effects of triple and quadruple pulses at various time delays. The parameter space in such experiments becomes significantly broader, however the results suggest that multiple pulses can provide a certain amount of sequential compression and re-expansion during the very early stages of the ablation process. This kind of control over the plasma plume dynamics is intriguing and provides a possible approach to manipulating both the isotope enrichment process and the cluster size distributions. Figures 2 show the effect of single and multiple secondary pulses on the absorption of energy by the plasma as a function of picosecond time delay. The vertical axis represents average ion concentration as observed in the far field of the plume. Similar effects are observed for average ion energy as well. These tertiary and quaternary pulses are expected to also have an effect on the isotope enrichment and cluster sizes.

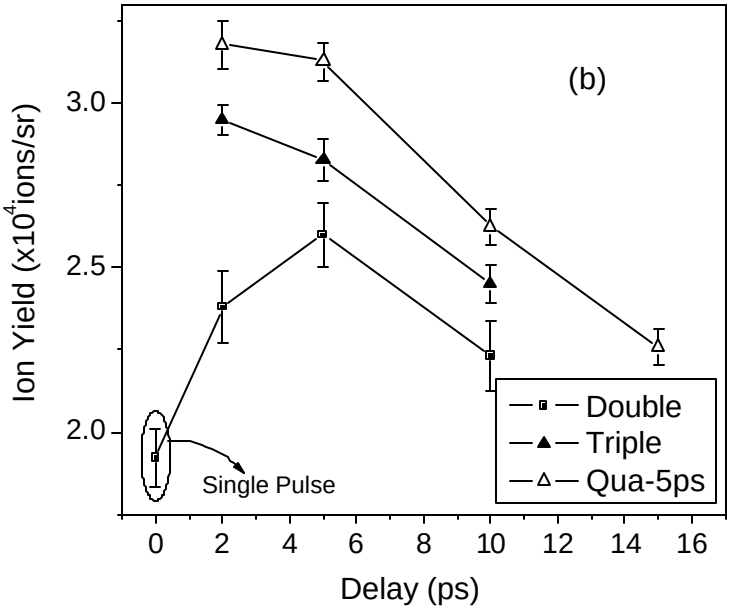

Fig. 2 Average ion yield produced by single and multi-pulse for silicon ablation. The intensity of the ablation laser pulse is 25% of the maximum ($2x10^{16}W/cm^2$), or 5×10^{15} W/cm^2 for single-pulse and it is equally distributed to each pulse in a multi-pulse sequence. Time-delay of double-pulse and equally separated triple-pulse is represented by the x-axis. For quadruple-pulse, t_1 and t_3 are fixed at 5-ps, and t_2 is represented by the x-axis.

Future Plans:

Experiments are planned, using multi-pulse techniques, to determine the mechanisms of formation for the sub-micron clusters. Attempts will be made to distinguish plasma phenomena versus explosive boiling mechanisms. Alternative mechanisms will also be considered. Variation and control of mean cluster size will be examined relative to multi-pulse processes. Optical methods will be considered to measure cluster sizes, in flight, as a function of time delay. The consequences of these pulse control methods on isotope enrichment will also be examined. The crystal structure of the deposited clusters will be examined, as well as their defect properties. The effects of high velocity impact upon deposition will be investigated in terms of residual crystal structure and dislocation density of the clusters. The dissolution of the clusters, by surface diffusion, on hot substrates will be investigated. Continued attempts to optimize and achieve isotopically enriched deposited material will be pursued. This work will be performed on elemental metal and semiconductor materials.

References:

[1] P. A. VanRompay, Z. Zhang, J. A. Nees, and P. P. Pronko, "Isotope Separation and Enrichment by Ultrafast Laser Ablation," Proc. SPIE **3934**(43)(2000).

[2] P. A. VanRompay, "Mass Separation for Ions in Ultrafast Ablation Plumes," (PhD Thesis, University of Michigan, Ann Arbor, 2003).

[3] P.P. Pronko, Z. Zhang, and P.A. VanRompay, “Critical Density Effects in Femtosecond Ablation Plasmas and Consequences for High Intensity Pulsed Laser Deposition”, Appl. Surf. Sc. **208-209**, 492 (2003).

[4] W. L. Kruer, *The physics of laser plasma interactions* (Addison-Wesley, Redwood City, Calif., 1988), pp. xviii, 182 ill.

[5] Z. Zhang, P.A. VanRompay, and P.P. Pronko, “Ion Characteristics of Laser-Produced Plasma using a Pair of Collinear Femtosecond Laser Pulses”, Appl. Phys. Lett. **83**, 431 (2003).

[6] Z. Zhang, P. A. VonRompay, and P. P. Pronko, "Multi-Diagnostic Comparison of Femtosecond and Nanosecond Pulsed Laser Plasmas," J. Appl. Phys **92**, 2867 (2002).

[7] L. V. Zhigilei, "Dynamics of the Plume Formation and Parameters of the Ejected Clusters in Short-Pulse Laser Ablation," Appl. Phys. A **76**, 339 (2003).

[8] J. K. Chen and J. E. Beraun, "Modeling of Ultrashort Laser Ablation of Gold Films in Vacuum," J. Opt A **5**, 168 (2003).

[9] O. F. Hagena and W. Obert, “Cluster Formation in Expanding Supersonic Jets: Effects of Pressure, Temperature, Nozzle Size, and Test Gas”, J. Chem. Phys. **56**, 1793 (1972).

CONTROL OF MOLECULAR DYNAMICS:
ALGORITHMS FOR DESIGN AND IMPLEMENTATION

Herschel Rabitz
Department of Chemistry
Princeton University
Princeton, NJ 08544
hrabitz@princeton.edu

Program Scope

During the past year, research was done in the following three areas: (A) molecular control feasibility analysis on ozone isomerization, (B) controlled dynamics mechanism identification, and (C) robustness of quantum control processes. In category (A), the creation of metastable triangular ozone from its normal form has been a challenge for many years. Traditional photochemical preparation methods have not succeeded due to the severe atomic rearrangements involved. This is a situation that appears ideal for shaped laser pulse quantum control. Thus, as a forerunner to an experiment, a feasibility study for controlling ozone isomerization dynamics to form the ring compound has been conducted. In category (B), the number of quantum control simulations and experiments is rising rapidly, but the mechanisms of the controlled dynamics has generally remained a mystery. This aspect of the research concerns the development of algorithms to reveal the control mechanisms in simulation studies and ultimately in the laboratory. In category (C), a good understanding of how the control field occurs with inherent noise in the laser pulse and the inevitable coupling to the environment is of paramount importance for improving the quality of the quantum control processes.

Recent Progress

In category (A), we have formulated a simple rigid-bender model for a preliminary quantum control analysis of ozone isomerization. Moreover, in collaboration with Reinhard Schinke (Germany), we have performed high quality *ab initio* calculations, in conjunction with a recently developed multidimensional interpolation technique, the reproducing Kernel Hilbert space method. This effort has produced a global potential energy surface and the corresponding dipole moment function of the X^1A_1 state of ozone, covering the open minimum, the ring minimum, and the ring-opening reaction path (including the ring-opening transition state). Based on the newly developed potential energy surface and dipole moment function, we

are currently undertaking the control feasibility studies of the ozone isomerization process along the minimum energy reaction path, within the framework of adiabatically constrained Hamiltonian methods.

In category (B), we have formulated a general Hamiltonian encoding (HE) technique in arbitrary representations for revealing quantum control mechanisms. Specifically, we have studied two physically motivated cases (1) a generalized interaction representation and (2) the interaction adiabatic representation. The former allows for isolating the effects of the dynamics of interest in the evolution driven by a reference Hamiltonian and the latter makes possible the study of nonadiabatic transitions. The capability of this encoding technique was demonstrated in an analysis of the dynamics of stimulated Raman adiabatic passage in a three-level Hamiltonian, with special attention given to isolating nonadiabatic effects.

In category (C), we have demonstrated, via simulated closed-loop population transfer experiments, that the optimal control cost functional can be properly tailored (by incorporating the measurement variance due to random field noise) to find robust fields that effect a stable outcome despite the temporal fluctuation in the pulse, as well as the interaction of the quantum system with the environment. We have also shown that the influence of control field fluctuations on the optimal manipulation of quantum dynamics phenomena is connected to a serendipitous situation that the expectation value of quantum observables are bilinear in the evolution operator and its adjoint. It is found that robustness occurs because of the optimization process (including signal averaging of the observables over an ensemble of noise-contaminated fields) reduces sensitivity to noise-driven quantum system fluctuations.

Future Plans

In the coming year, we will continue to conduct our research in the three general areas just described. In Category (A), in collaboration with Gabriel Balint-Kurti (England), we plan to perform the control feasibility study of ozone isomerization in full dimensionality (i.e. in two and three dimensions) using time-dependent wave packet propagation approaches. In addition, we plan to expand the feasibility studies to other molecular systems, including acetylene–vinylidene isomerization control, which is important for understanding intramolecular rearrangement processes including gas-phase combustion of hydrocarbons and the formation and decomposition of carbenes. In category (B), we plan to explore various procedures aiming at directly applying the HE technique in the laboratory by modulating the control field. In category (C), we plan to carefully assess the nature of shaped laser-pulse

field noise, through varying the noise in specific ways to observe its impact on the optimal control process. We also plan to apply explicit techniques, for example the HE method in (B), to identify the actual quantum pathways linking the initial and final states in the presence of control noise.

Publications of DOE Sponsored Research(2002 - Present)

1. Revealing quantum-control mechanisms through Hamiltonian encoding in different representations, A. Mitra, I. R. Solá, and H. Rabitz, Phys. Rev. A, **67**, 043409 (2003).

2. Tying the loop tighter around quantum systems, H. Rabitz, J. Mod. Opt., in press.

3. Quantum physics under control, I. Walmsley and H. Rabitz, Physics Today, in press.

4. Development of solution algorithms for quantum optimal control equations in product spaces, Y. Ohtsuki and H. Rabitz, Proceedings of CRM, in press.

5. Reproducing kernel Hilbert space interpolation methods as a paradigm of high dimensional model representations: application to multidimensional potential energy surface construction, T.-S. Ho and H. Rabitz, J. Chem. Phys., in press.

6. Quantum system optimal control landscapes, H. Rabitz, M. Hsieh, and C. Rosenthal, Science, submitted.

7. Quantum optimal control of ozone isomerization, M. Artamonov, T.-S. Ho, and H. Rabitz, in preparation.

2003 BES-AMOS Research Meeting

PI: Mark Raizen and Manfred Fink

Physics Department, The University of Texas at Austin

RLM 10.316

Austin Texas 78712

E-mail address: Raizen@Physics.utexas.edu

and Fink@Physics.utexas.edu

I Program Scope

Our research program focuses on the development of a method to cool atoms and molecules of any choice as long as they have a stable gaseous phase. Our approach starts with a very cold supersonic beam, whose internal temperature is 1 milliKelvin or less. The high velocity of the particles forming the beam will be reduced by elastically scattering the atoms/molecules from a very cold single crystal surface (20-40K), which moves in the beam direction. This will enable the continuous control of the mean velocity over a large range, after scattering, down to a few tens of m/s or even below as the crystal surface's velocity approaches v/2 of the impacting particles[1,2]. We will use decelerating optical lattices to bring the slow particles to rest and they will be trapped in optical far-off resonant traps (FORTs).

As the long term goal, we propose two major applications of the cold-beam technology. The first is the controlled deposition of unique patterns on surfaces to create nanostructures of different shapes and materials, an important development in nano-scale science. Toward this goal we will combine the new beam source with a novel technique to atomic and molecular lithography that utilizes spatially dependent interactions to generate squeezed motional states. This approach will enable background-free deposition of parallel periodic structures on a scale of 10-30 nm, which could find applications in the development of magnetic storage devices as well as new catalytic materials based on nano-particles.

The second application is to use slowed, but not necessarily ultra cold, atoms and molecules as unique probes for surfaces. Looking at the angular distributions, the scattered particles' Bragg diffraction will reveal the structure of the very same nanostructures which have been produced before. The intensity in specular direction of the scattered particles will reveal the interaction potential through the resonances of the incident projectiles with the eigenstates of the interaction potential. [3]

II Recent Progress

Figure 1 shows schematically the apparatus we are building to prove the feasibility of the ideas outlined above, i.e., to produce intense cold atomic and/or molecular beams without restrictions. There are two elements which are essential for our experiment. The first is the reproduction of the ultra cold supersonic jet which has been reported twice [4,5]. The authors achieved 1000m/s with a velocity spread of 1m/s for helium. This corresponds to an internal energy of 1 milliKelvin. The second issue is the proof that the particles in the jet scatter truly elastically from the moving surfaces. Note that in the center of mass system the incoming and outgoing velocity will be 500m/s. Only in the laboratory frame will the exit velocity be close to zero. We know from two previously published results [6,7] that at very low temperatures the energy loss processes at the single crystal surface decrease and become irrelevant to us. In the language of the surface scientist; the Debye-Waller factor, which is the ratio of the elastic to total scattering, will approach unity. This limit will be reached at higher temperatures when the Debye temperature of the surface is high. Therefore we will try LiF ($?_D$ = 735K) and MgO ($?_D$ = 925K) to see if the asymptotic limit is already satisfied at liquid nitrogen temperature. We base our expectation on the data of ref 5 and 6. The authors reported the limit at 40K for Cu ($?_D$ = 315K) and Ag ($?_D$ = 215K).

There is also a technical challenge we have to solve. The rotor seen in figure 1 has to spin at 1.3 kHz at the low crystal temperature and in ultra high vacuum. There has been an arrangement reported [8] where a similar turret has been successfully rotated at 3.5 kHz at 77K. The critical issue is the balancing of the rotating crystal holder.

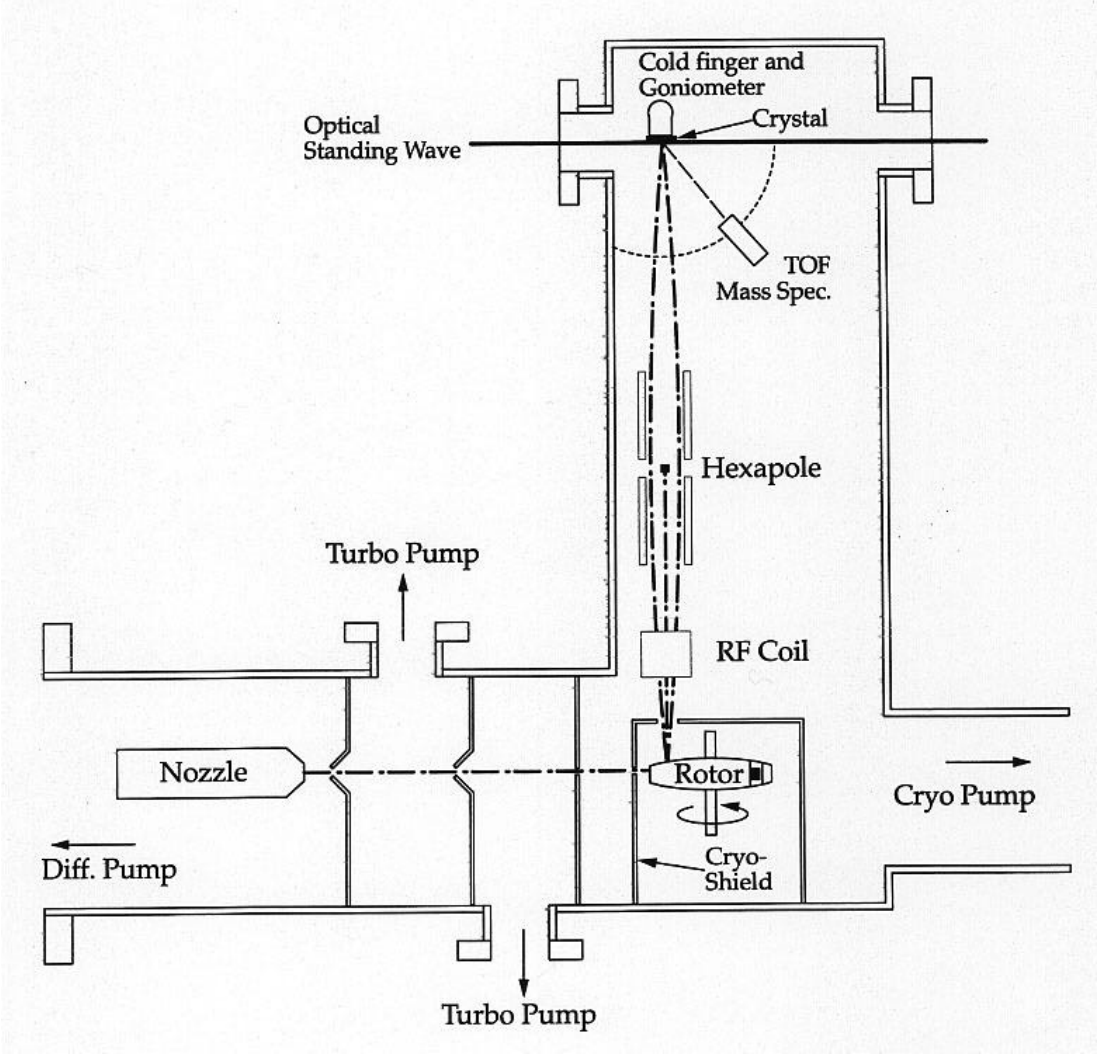

Figure 1

Currently we have the following components running: the supersonic jet with a very large diffusion pump to ensure a high pd value where p is the backing pressure behind the nozzle and d the nozzle diameter. The larger pd the lower the internal temperature in the jet. In order to maintain UHV at the rotor two differential pumping stations have been built. The rotor and its cryoshield have been assembled. Behind the rotor are two quadrupole mass spectrometers to derive the velocity of the particles from the position of the spectral lines and from the broadening the velocity spread. The spectrometers are currently 5 meters apart. All measurements have been done with helium only. In order to keep the crystal surfaces clean we have a CO_2 laser which will ablate all impurities. This technique was successful as

described in Ref 6. The LiF surface will maintain its cleaved purity by coating the freshly cut crystals with camphor. It will vaporize in the vacuum and we have shown with our quadrupole mass spectrometer that there is no thermal desorption when the crystal is heated up to 400C.

III Future Plans

All efforts are currently focused on the production of slow helium atoms. Since we can control the velocities of the scattered He atoms with the rotor speed we also control the de Broglie wavelengths. We will use a SiN-grating to diffract the helium beam and evaluate qualitatively the properties of the slowed particles. We chose this technique since it is the first step toward the determination of the real and imaginary part of the scattering factors of He from single crystal surfaces. This will be done by recombining the first order beam with the specularly diffracted beam. The scattered intensity is expected to vary dramatically at discrete energies due to bound state resonances. These features have already been found previously by Boato [3]. The first step toward unknown targets will be reached by using more interesting surfaces than pyrolytic graphite. The first molecules of choice are H_2, D_2, HD. Now we can see the influence of rotational and vibrational states on the bound states of the crystal surface. These states will be populated by resonance Raman pumping.

IV References

1 B. Doak, K. Kevern, A. Chizmeshya, R. David and G. Comsa, SPIE. **2995**, 146 (1997)

2 A. Speyerl and M. M. Malik, Nucl. Instr. Meth., **A284**, 2000 (1989).

3 G. Boato, "Atomic and Molecular Beam Methods" Vol 2, Chapter 12, 1992) Editor G. Scoles.

4 J. Wang V. A. Shamanian, B. R. Thomas, J. M. Wilkerson, J. Riley, C. F. Giese and W. R. Gentry, Phys. Rev. Lettt. **60**, 696, (1988).

5 K. Winkelmann, 11th Rarified Gas Dynamics **2**, 899 (1979)

6 F. Althoff, T. Andersson and S. Andersson, Phys. Rev. Lett. **79**, 4420 (1997).

7 T. Andersson, F. Althoff, P. Linde, M. Hassel, M. Persson, and S. Andersson, J. Chem. Phys., **113**, 9262 (2000).

8 E. Radeschutz and H. Langhoff, Z. Physik, **B25**, 37 (1976)

"Quantum/Classical Atomic Interactions"

F. Robicheaux
Auburn University, Department of Physics, 206 Allison Lab, Auburn AL 36849
(robicfj@auburn.edu)

Project Scope

The main effort of this project has evolved into a study of the atomic processes that occur in ultra-cold plasmas. Typically, the plasmas we study have electron temperatures between 1 and 100 K, sizes of a few 100 μm, and evolve over time scales of several 10 μs. The main interest is the non-linear interplay between atomic and plasma processes. For example, two free electrons can scatter near an ion so that one becomes captured by the ion and the other gains energy. Thus, a Rydberg atom is formed and energy is released to the free electrons. The Rydberg atom can serve as a heat source for the plasma because other electrons can scatter from the Rydberg atom and drive the atom to more deeply bound states. We find that the huge role played by the Rydberg atoms in the plasma is analogous to that played by dust in dusty plasmas: the evolution of the properties of the Rydberg atoms and the plasma are strongly linked. Our goal with this project was to understand some of the basic and peculiar properties of ultra-cold plasmas and demonstrate how they arise from the non-perturbative coupling of atomic and plasma physics.

In our previous studies, the ultra-cold plasmas were not in a magnetic field. We have begun studies of ultra-cold plasmas in strong magnetic fields. The motivation for this study is the interplay between the atomic and plasma physics in strong magnetic fields. A further motivation is that recent experiments have claimed the formation of anti-Hydrogen by causing anti-protons to traverse ultra-cold positron plasmas; unfortunately, very little is known about the processes that lead to the anti-Hydrogen formation or about the properties of the anti-Hydrogen atoms. We are in the process of developing ideas and computer programs to understand the basic atomic processes in strong magnetic fields. The processes that will need to be understood include: three body recombination, electron-Rydberg atom scattering, photon emission from Rydberg atoms, motion of Rydberg atoms, and electron-proton scattering. Even crude estimates of some of these processes will greatly improve our understanding about the formation and evolution of Rydberg atoms in strong magnetic fields.

Recent Progress

Interest in the interaction of cold electrons with cold positive ions led us to investigate the phenomena discovered in ultra-cold, neutral plasmas. Experiments performed in S. Rolston's group (NIST), T. Gallagher's group (U of Virginia)/ P. Pillet's group (Orsay), and G. Raithel's group (U of Michigan) showed many puzzling features; these features were fundamental and showed that often the basic processes were not well understood. Although these experiments did not use a strong magnetic field (like those in the anti-Hydrogen experiments), we felt this would be a good starting problem. Our theoretical studies of this problem resulted in 2 publications [3,4].

Our calculations were able to explain most of the puzzling features in the experiments through a proper understanding of the role played by the formation of Rydberg atoms and their subsequent interaction with electrons in the plasma. We were able to show that the anomalously fast expansion of the plasma at later times could be fully explained by three body recombination with subsequent scattering from the Rydberg atoms. We were able to explain the strange time evolution of the Rydberg atom binding energy in terms of a measurement effect and a rapid heating of the electron part of the plasma at early times. We predicted that the Coulomb coupling parameter (essentially the ratio of potential energy to kinetic energy) should not be high even for the plasmas that start very cold due to the heating from atom formation; this is important because if the Coulomb coupling parameter is large then highly correlated behavior is expected. We were able to make detailed comparisons with several measurements: time dependence of the flux of electrons escaping the plasma, the distribution of binding energies for Rydberg atoms as a function of temperature, the time dependence of the number of Rydberg atoms. We predicted several other effects: ion acoustic waves should be frozen into the plasma at later times; there should be a correlation between the speed of the Rydberg atom and its binding energy; and the center of the plasma should be initially hotter than the edges and the time scale for equilibration is longer than would be expected.

We also attempted to simulate the conversion of a Rydberg gas into an ultra-cold plasma in order to understand experiments by Gallagher and Pillet. Our simulations did show a conversion on roughly the time scale seen in the experiments. However, the evolution of our Rydberg gas did not resemble that in the experiments. The Rydberg gas passed through a phase of mostly high angular momentum states that was not seen in the experiments. Thus, this is still an open problem.

We have recently started simulations of atomic processes in strong magnetic fields. We are beginning with the simulation of three body recombination in a strong magnetic field. We have completed the first stage of this study and have submitted it for publication in Phys. Rev. A. Glinsky and O'Neil computed the rate for this process in the limit that the magnetic field strength goes to infinity. In this limit, the electrons can only move along the field and the positive ion is fixed in space. They obtained a rate that was roughly a factor of 10 smaller than the B=0 rate. We noted that in the recent experiments to make anti-Hydrogen the magnetic fields are very large (3 or 5.4 T) but are not in the limit of Glinsky and O'Neil. We performed classical Monte Carlo simulations of the three body recombination rate including next order effects in 1/B. Our simulations allowed the proton to have its full motion while the electron motion was found using the guiding center approximation since the cyclotron orbit of the electron was by far the fastest time scale and smallest length scale. We found that the recombination rate was roughly 60% higher than in the B=infinity limit for a proton moving slowly through an electron gas.

An important aspect of this project is to provide guidance and understanding for the anti-Hydrogen experiments. We investigated the properties of the atoms formed by three body recombination. Unfortunately, we found that the speed of the anti-atom across the magnetic field line was roughly the transverse speed of the anti-

proton before the recombination (this means that the anti-atoms will have a tendency to fly out perpendicular to the trap) and we found that the anti-atoms did not have large dipole moments (this means that the ability to guide the motion of the anti-atoms will be reduced). We did find a feature that may aid the anti-hydrogen experiments: the recombination for an anti-proton moving with a substantial speed along the field becomes substantially reduced when the anti-proton speed becomes comparable to the positron thermal speed. Since the speed of the anti-proton perpendicular to the magnetic field is roughly 1/40 the positron speed, this may allow for a directionality of the recombined anti-Hydrogen.

Future Plans

We plan to continue studies of ultra-cold plasmas with no magnetic field. It would be interesting to understand three body recombination just after creation of the plasma. How does the recombination occur and how do the Rydberg states evolve if the plasma initially has a large Coulomb coupling constant? We also plan to continue investigating basic unexplained phenomena. For example, the experiment on the conversion of a Rydberg gas into an ultra-cold plasma has not been understood: the source of the energy to convert the Rydberg atoms into free electrons plus ions is not known. Also, there are new experiments that are being planned so simple ideas that arise from the simulations can have an impact.

The main effort will be in understanding atomic and plasma processes in strong magnetic fields. There are several open atomic physics questions that we will address. (1) Electron-proton scattering is one of the main processes for the thermalization and slowing of the heavy ion. The zero field result is not applicable for the magnetic fields and temperatures in the anti-Hydrogen experiments. (2) In both experiments, the anti-protons traverse the positron cloud on a time scale short compared to the recombination time. Thus, we need to compute how many atoms have recombined after a fixed (short) time. Most important will be the distribution of energies of these atoms. (3) We will need to simulate the electrostatic fields in the experiments and the motion of the anti-Hydrogen atoms to find out whether they can reach different regions of the trap.

The goal for this project is to obtain some immediate results that can aid in the interpretation and understanding of atomic processes in strong magnetic fields. The source of anti-protons will be interrupted soon. There are several other projects for which we have long term plans.

DOE Supported Publications (2001-2003)

[1] C. Wesdorp, F. Robicheaux, and L.D. Noordam, Phys. Rev. A **64**, 033414 (2001).
[2] M. Ferrero and F. Robicheaux, Chem. Phys. **267**, 93 (2001).
[3] F. Robicheaux and J.D. Hanson, Phys. Rev. Lett. **88**, 055002 (2002).
[4] F. Robicheaux and J.D. Hanson, Phys. Plasmas **10**, 2217 (2003).

D.O.E. grant DE-FG 03-00ER15084

Development and utilization of bright tabletop sources of coherent soft x-ray radiation

Principal Investigators:
Jorge J. Rocca,
Electrical and Computer Engineering Department, Colorado State University, Fort Collins, CO 80523-1373
Telephone: (970)-491- 8514/8371, Fax: 970 (491) – 8671, e-mail: rocca@engr.colostate.edu
Henry C. Kapteyn
JILA/Physics Department, University of Colorado, Boulder, CO 80309-0440
Telephone (303) 492-8198, Fax:(303) 492-5235 , e-mail: kapteyn@jila.colorado.edu
Carmen S. Menoni
Electrical and Computer Engineering Department, Colorado State University, Fort Collins, CO 80523-1373
Telephone: (970)-491- 8659, Fax: 970 (491) – 8671, e-mail: carmen@engr.colostate.edu

Program Description

This project investigates aspects of the development and utilization of compact XUV sources based on fast capillary discharges and high order harmonic up conversion [1,2]. These sources are very compact, yet can generate soft x-ray radiation with peak spectral brightness several orders of magnitude larger than a synchrotron beam lines. The work includes the characterization of some of the important parameters that enable the use of these sources in unique applications, such as the degree of spatial coherence and the wavefront characteristics that affect their focusing capabilities. In relation to source development, we are investigating the amplification of high order harmonic pulses in a discharge pumped soft x-ray amplifier. This work in motivated by the possibility of obtaining pulses that combine some of the advantages of these two types of sources in terms of pulse energy and duration, and also with the opportunity to investigate aspects of seeded amplification in the soft x-ray regime. Results to date include the demonstration of an ultra-compact discharge pumped 46.9 nm amplifier that can be operated either in the seeded or unseeded modes. In term of source characterization, we have completed measurements that show that the output of these sources can reach essentially full spatial coherence [3,4] and have fully characterized the beam of a discharge-pumped tabletop soft x-ray laser in term of amplitude and phase using a novel Shack-Hartmann soft x-ray wavefront sensor [5]. Recent application results include the first study of the damage threshold and damage mechanism of XUV mirrors exposed to intense focalized 46.9 nm laser radiation, and the observation of laser-induced-periodic surface nano-structures induced by XUV laser light.

Study of damage threshold and damage mechanism of XUV multilayer mirrors exposed to intense 46.9 nm laser pulses

High reflectivity XUV mirrors with high damage threshold mirrors are key elements for enabling numerous applications of the rapidly advancing high power coherent sources at these wavelengths, which include new table-top soft x-ray laser sources], high order harmonics, and free-electron lasers. This is particularly important as the peak power and fluence of XUV and soft x-ray sources have reached unprecedented values. For example the XUV radiation fluence at the exit of the plasma column in capillary discharge Ne-like Ar lasers operating at 46.9 nm can exceed 1 J/cm^2 [6]. Significant progress has been made in the developing of high reflectivity Sc/Si mirrors for the 35-50 nm range [6] with reflectance values as high as 43 percent in the vicinity of 47 nm [7]. However, the damage threshold of these mirrors when exposed to high peak powers of XUV light has not been studied. We have studied the optical damage mechanisms and damage threshold of Sc/Si EUV (35-50 nm range) mirrors exposed to high power XUV laser radiation. The study was conducted by focusing the output of a tabletop capillary-discharge Ne-like Ar laser emitting nanosecond duration pulses of ~ 0.13 mJ at a wavelength of 46.9 nm. The resulting damage of the coatings exposed to fluences ranging from 0.01 to 10 J/cm^2 was analyzed with optical microscopy, scanning electron microscopy (SEM), transmission electron microscopy (TEM), and with small-angle X-ray diffraction (λ=0.154 nm) techniques. Our results show similar values of damage threshold of ~ 0.1 J/cm^2 for Sc/Si multilayer coatings on Si and SiO_2 substrates, compared to 0.7

J/cm^2 found necessary to damage a bare Si substrate. The Sc/Si multilayers were deposited by dc-magnetron sputtering at 3 mTorr of Argon pressure on superpolished borosilicate glass. The multilayers on borosilicate glass consisted of 10 periods of Sc/Si layers, each with a thickness of ~ 26.7 nm, and a ratio of layer thickness H(Sc)/H(Si) ~ 0.7. The multilayer coatings deposited on Si consisted of 33 periods of Sc/Si pairs with the same parameters as the borosilicate glass ones.

Figure 1 shows optical microscope images of damaged areas of coatings deposited on a Si wafer resulting from average XUV fluences of 0.15 J/cm^2 (a), 0.5 J/cm^2 (b) and 5 J/cm^2 (c). At 0.15 J/cm^2 At the lower fluences large areas with discoloration and undulations of the coating are observed. These areas are most likely produced by heat-triggered interdiffusion in the upper layers of the coatings. This surface modification, which already appears at fluences of ~ 0.08 J/cm^2, establishes the damage threshold for the Sc/Si multilayers defined in this work. In comparison, the onset of damage in bare Si substrates measured in this work appears at significantly larger irradiation fluence of 0.7 J/cm^2. The areas with larger local fluences (Fig. 1b) are covered with cracks resulting from significant mechanical tensile stress generated

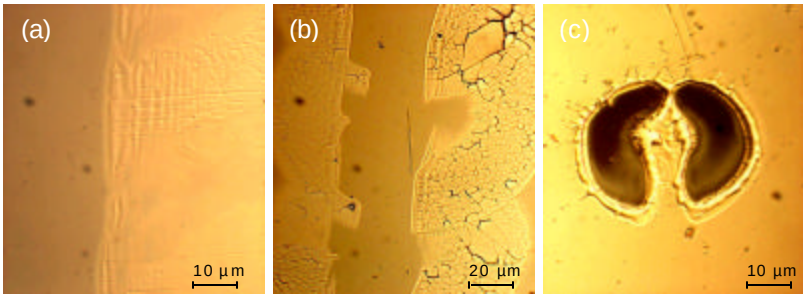

Fig.1. SEM micrographs of the damaged areas of Sc/Si multilayer mirror coatings exposed to 46.9 nm laser beam fluences of 0.15 J/cm^2 (a), 0.5 J/cm^2 (b), and 5 J/cm^2 (c).

by thermal expansion and the following cooling down process [8]. At even larger fluences of ~ 5 J/cm^2 the coating is fully evaporated from the center of the irradiated spot and the Si substrate is also damaged (Fig. 1c). Electron microanalysis data reveals that Sc is absent in the center part of the damaged region. Small-angle X-ray diffraction analysis of samples irradiated with ≥ 0.1 J/cm^2 emission fluence shows a noticeable drop in the intensity of the diffraction peaks with respect to the unexposed areas.(Fig 2 a).

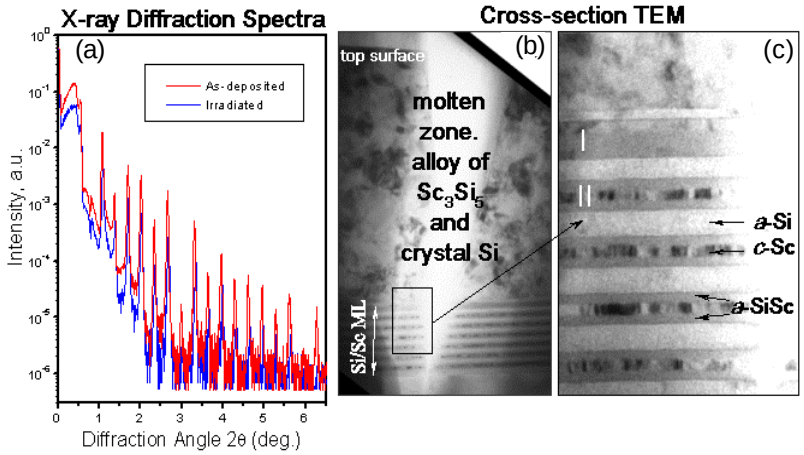

Fig.2. a) Small-angle X-ray diffraction patterns in the as-deposited and XUV-irradiated coatings. Laser fluence: 0.21 J/cm^2. b) Cross-sectional TEM image of the molten zone, and c) survived layers (magnified) of a sample irradiated with 0.21 J/cm^2 pulses of 46.9 nm radiation.

However, the peak's position remains approximately the same, indicating that the coating is only partially destroyed. This evidence suggests that while at these fluences the top layers of the coating are melted, the layers adjacent to the substrate remained unchanged. This interpretation of the X-ray diffraction data was

confirmed by cross-section TEM imaging of the sample exposed at 0.21 J/cm^2. The TEM image of Fig.2b shows that the top 700 nm of the coating are molten, while ~180 nm (7 periods) adjacent to the substrate are not destroyed. The molten layer constitutes an alloy of Sc_3Si_5 and crystal Si as determined from electron diffraction data. Analysis of the surviving multilayer coating beneath the molten layer indicates that changes in layer thickness have occurred within a distance of less than 2 periods from the molten region (Fig.2c), thus the heat affected zone (HAZ) did not exceed ~50 nm. Comparison of the layer structure in the HAZ with that of isothermally annealed samples indicates that the various stages of structural and phase transformations observed within a few periods of the coating under laser irradiation are the same as in samples annealed at different temperatures. The changes taking place in the Sc-containing layer nearest to the molten region (indicated by I in Fig. 2(b)) correspond to a stage of formation and crystallization of Sc_3Si_5 silicide that have been previously observed in isothermally annealed coatings at 430 °C after 1 hour. In the next Sc-containing layer (indicated by II in Fig. 2(b)) only minor expansion of the ScSi silicide interface layers is observed, which is a result of solid state amorphization. Similar effects have been observed at annealing temperatures of less than 200 °C.

Laser-induced periodic surface nano-structures generated by a 46.9 nm laser.

The formation of periodic surface structures on surfaces by laser light with wavelengths ranging from the visible to the mid-infrared has been extensively studied [9]. In accordance with theory in those cases the scale of the patterns, which is proportional to the wavelength of the light, is in the micrometer scale. We have used a 46.9 nm tabletop capillary discharge laser to generate laser-induced periodic surface structures with nanoscale dimensions. Figure 3 shows linear structures broken into a pearl chain obtained in PMMA. The distance between the neighboring lines is 60 nm. The results illustrates the potential of XUV radiation for nanoscale processing materials.

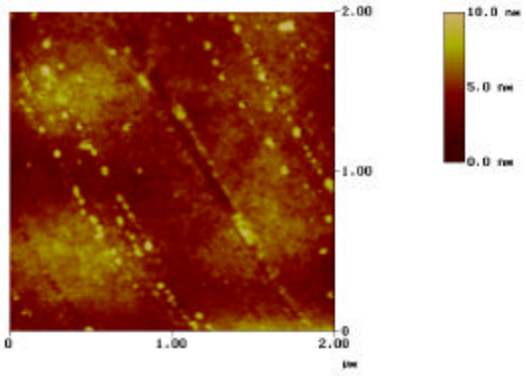

Fig. 3. AFM topographic image of PMMA surface irradiated with a 46.9 nm capillary discharge laser. Linear structures broken into a pearl chain can be seen on the surface. The distance between the neighboring lines is ~ 60 nm.

Progress towards the amplification of high order harmonic pulses in a discharge pumped soft x-ray amplifier

Progress has been made toward the demonstration high order harmonic amplification in a discharge pumped amplifier. The scheme could produce soft x-ray pulses with energy several orders of magnitude larger than the HH seed pulse, and with pulse width more than two orders of magnitude shorter than those of the unseeded discharge-pumped amplifier. To conduct this experiment we have successfully development the compact discharge-pumped amplifier that has an open-end structure to allow the injection and extraction of the HH pulses, and have optimized the generation of HH pulses at 46.9 nm utilizing phase-matching and pulse-shaping techniques. Figure 4 shows the harmonic amplification experimental setup. The high order harmonic pulse is generated using phase-matched frequency conversion in a Xe capillary waveguide. The pulse is subsequently injected into the compact discharge pumped amplifier that produces gain at 46.9nm by electron impact excitation of the 3p $^1S_0$- 3s $^1P_1$ transition of Ne-like Ar. Applications of high order harmonic pulses requires a precise synchronization of events. For this purpose we have successfully developed a laser triggered spark gap that can control the firing of the discharge with sub-nanoscond jitter Initial harmonic amplification experiments pointed out

the need of streaked detection. A home-developed streak camera was implemented and tested monitoring the output of the capillary discharge XUV amplifier (insert in Fig. 4).

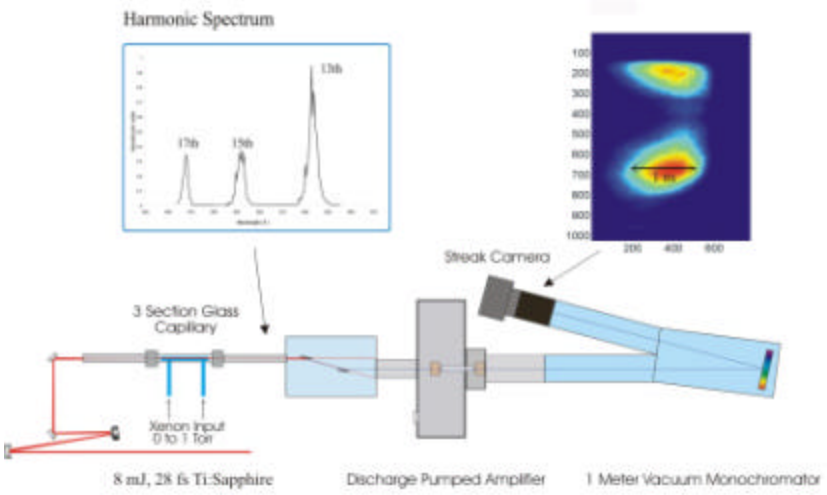

Figure 4. Schematic representation of set up developed to study the amplification of the 15th harmonic of a Ti:sapphire laser in a Ne-like Ar plasma column generated by a fast capillary discharge. A streak of the XUV amplifier output and a spectra of the harmonic seed are also shown.

Future plans include the diagnostics of the amplified high harmonic pulses utilizing the recently developed streak-camera based detection system. The measurements will be utilized to diagnose and optimize the amplification process.

References

1. B. R. Benware, C. D. Macchietto, C. H. Moreno, and J. J. Rocca, Phys. Rev. Lett. **81**, 5804 (1998).
2. Rundquist, C. Durfee, S. Backus, C. Herne, Z. Chang, M. Murnane, H. Kapteyn, Science **280,** 1412 (1998).
3. Y. Liu, M. Seminario, F.Tomasel, C.Chang, J.J Rocca and D.TA. ttwood, Phys. Rev. A**, 63** 033802, (2001).
4. R.A. Bartels, A. Paul, H. Green, H.C. Kapteyn, M.M. Murnane, S. Backus, I.P. Chistov, Y.W. Liu, D. Attwood and C. Jacobsen, Science,.**297**, 376,(2002).
5. S. Le Pape, Ph. Zeitoun, M. Idir, P. Dhez, J.J. Rocca**,** and M. François, Phys. Rev. Lett. **88**, 183901 (2002)
6. Yu. A. Uspenskii, et. al Opt. Lett. **23**, 771 (1998).
7. J. J. Rocca, M. Frati, B. Benware, M. Seminario, J. Filevich, M. Marconi, K. Kanizay, A. Ozols, I. A. Artiukov, A. Vinogradov, and Y. A. Uspenskii, C. R. Acad. Sci. IV-Phys. **1**, 1065 (2000).
8. A. I. Fedorenko, et. al, J. X-ray Sci. Technol. **9**, 35 (2001).
9. "Pulsed Laser Deposition of Thin Films", Eds. D.B. Chrisey and G.K. Hubler, John Wiley & Sons, pp. 90.

Publications

1. S. Le Pape, Ph. Zeitoun, M. Idir, P. Dhez, J.J. Rocca**,** and M. François, "Electromagnetic field distribution measurements in the soft x-ray range: full characterization of a soft x-ray laser beam", Phys. Rev. Lett. **88**, 183901 (2002)
2. Y. Liu, M. Seminario, F. G. Tomasel, C. Chang, J. J. Rocca and D. T. Attwood, "Achievement of Essentially Full Spatial Coherence in a High Average Power Soft X-Ray Laser," Phys. Rev. A, **63,** 033802, (2001).
3. B. Luther, L. Furfaro, A. Klix and J.J. Rocca, "Femtosecond laser triggering of a sub-100 picosecond jitter high voltage spark gap", Appl. Phys. Lett., **79**, 3248-3250 (2001).
4. Y. Liu, D.T. Attwood, J.J. Rocca, H. Kapteyn, and M. Murnane, " Spatial Coherence of Currently Available EUV/Soft X-Ray Sources", 8th International Conference on X-Ray Lasers, AIP Conf. Proc., Vol 641, pp 607-612, (2002).
5. J.J. Rocca, J.L. Chilla, S. Sakadzic, A. Rahman, J. Filevich, E. Jankowska, E. Hammersten, B.M. Luther, H. Kapteyn, M.M. Murnane, and V. Shyaptsev, "Advances in capillary discharge soft x-ray laser research", SPIE Procc. Vol. 4505, pp. 1-6, 2001.

DE-FG02-98ER14877

Measurement of Electron Impact Excitation Cross Sections of Highly Ionized Ions:ArXVII, AlXII, and NeIX

A. J. Smith and D. R. Robbins

Morehouse College, 830 WestView Dr SW, Atlanta, GA 30314

email: asmith@morehouse.edu

Unfunded Liaison/Collaborator: P. Beiersdorfer

Lawrence Livermore National Laboratory, Livermore, California USA

Scope of work: We use the Lawrence Livermore National Laboratory electron beam ion trap, EBIT-I, to investigate electron-ion interactions by carrying out measurements on x-ray emissions from these interactions. Most atoms in the periodic table can be ionized to any desired degree in EBIT-I by a highly compressed electron beam which is nearly monoenergetic. The ions can then be trapped and excited by the same electron beam. The electron beam energy may be tuned to select various processes of interest for study. We use a variety of high-resolution Bragg Crystal spectrometers, in curved or flat geometry and a series of low-resolution solid state detectors to measure line positions and line intensities. Our measurements yield accurate wavelengths, cross sections, and resonance strengths for various transitions. Our data is useful for understanding the atomic physics of highly ionized atomic species, for the development of spectral modeling codes, and for the development of density and temperature diagnostics for laboratory as well as for astrophysical plasmas. In this presentation we discuss our on-going measurements and analyses of data.

1 Electron Impact Excitation cross sections for He-like Ar^{16+}

In an earlier experiment we measured the ratio of the intensity of the intercombination line, 1s3p $^3P_1$- 1s^2 $^1S_0$ to that of the resonance line , 1s3p $^1P_1$ - 1s^2 $^1S_0$, for various heliumlike ions and found that two different codes based on the distorted wave approximation (DWA) significantly underestimated our observed values. The measurements were done at excitation energies near the threshold value for exciting the resonance line, where we do not expect contributions to line strengths from cascades. We concluded then that part of the discrepancy between experiment and theory was due to difficulties in calculating cross sections in DWA, as well as to the transverse motion of electrons in the beam. The latter phenomenon essentially leads to a depolarization of emitted x-ray photons. To determine how much of the discrepancy is due to the cross sections, we have made detailed measurements of the cross sections for EIE of n = 3 - 1 transitions in heliumlike Ar^{16+} at various energies using EBIT-I.

We have used a high-resolution crystal spectrometer in von Hámos geometry, and normalized our measurements to theoretical radiative recombination cross sections, which can be calculated to a high degree of accuracy. We have calculated the cross sections using the code of Zang, Sampson, and Clark, which is based on the distorted wave approximation. We have also used the Flexible Atomic Code (FAC) of M. F. Gu. Our results are shown in Figure 1.

We have integrated the measured cross sections over a Maxwellian distribution of electron energies and thus calculated collisional excitation rate coefficients at various electron temperatures. Our rate coefficients can be compared with those measured in tokamak plasma measurements. The results have been submitted for publication and an abstract submitted for presentation at the forth coming Southeastern Section of the APS meeting in Wrightsville, NC, November 6-8, 3003. The initial comparison of our data with theory shows general agreement with both theories. We have also obtained excitation rate coefficients similar values we find in tkamak literature.

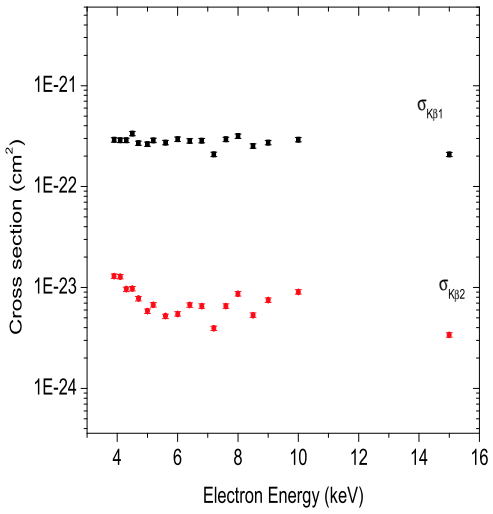

Figure 1. Cross sections for electron impact excitation (EIE) of the intercombination line (Kβ2, lower curve) and the resonance line (Kβ1, upper curve) of heliumlike Ar^{16+}, excited in EBIT-I. These cross sections have been normalized to theoretical radiative recombination cross sections.

2 Dielectronic recombination in heliumlike Ti^{20+} and Cr^{22+}

We have measured resonance strengths for dielectronic recombination (DR) in heliumlike Cr^{22+} and Ti^{20+} using a low-resolution germanium detector. We sweep the electron beam energy through the DR resonances and we observe x-ray photons emitted during the stabilization phase of the two stage DR process. These measurements are essentially extensions of our argon measurements, which was published earlier (see Fig 2) to ions with higher values of Z. We also observe x-ray photons from radiative recombination (RR) into n=2, and we use the cross sections for RR to normalize the observations. RR cross sections, like cross sections for photoionization (the inverse process to RR), can be calculated to an accuracy of 1-3%. Our measurements are in good agreement with calculations using the MCDF code and carried out for these measurements.

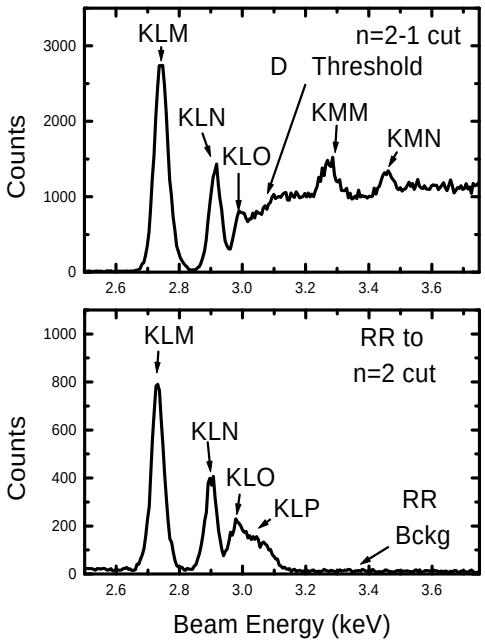

Figure 2. Dielectronic recombination in heliumlike argon. The plot shows low-resolution data taken with a solid state detector. The upper curve represents transitions of the type 1s2lnl' - $1s^2$nl' + γ while the lower curve represents transitions of the type 1s2lnl' - $1s^2$2l + γ', for n=3, 4, 5, and $\geq$6 etc.

3 Measurements of the Polarization of the Kβ2 line of heliumlike V^{21+}

Plasma polarization spectroscopy has become an important diagnostic tool for determining anisotropic electron velocity distributions in plasma. Electron beam ion trap x-rays are polarized and the crystals used in the high-resolution measurement have reflectivities which depend on the polarization of the incident x-ray. We have carried out some polarization measurements using EBIT-1, including the polarization of the Kβ2 line of heliumlike V^{21+} [7]. We use a standard two-crystal technique for these measurements. The polarization of the line(s) of interest are derived from the ratio(s) of intensities the line(s) in the two crystals.

4 Level specific DR resonance strengths in He-like Ti^{20+} and Cr^{22+}

We have measured the dielectronic satellite spectra for heliumlike Ti^{20+} and Cr^{22+}, using the LLNL EBIT-I and the EBIT high resolution Bragg crystal spectrometers. We sweep the electron beam energy across individual DR resonances, and measure resonance strengths for the strongest DR resonances in doubly excited lithiumlike Ti^{19+} and Cr^{21+} . We have used calculations based on the MCDF code to predict the excitation energies as well as the x-ray energies of these transitions. We use various heliumlike or hydrogenlike lines excited directly by electron impact excitation and published theoretical atomic data to calibrate the spectrometers for wavelength measurements. Our measurements include the 1s2l2l', 1s2l3l' and 1s2l4l' series of resonances. We show a typical observed KLL spectrum and its comparison with theory in Fig. 3.

5 Future Work

We plan to continue to look more closely at the discrepancy between theory and experiment in connection with the ratio of the intercombination line to the resonance line in heliumlike systems. Since heliumlike systems are rather simple, it should be possible to make measurements that determine which models predict the best values for excitation cross sections and branching ratios. We expect to make measurements of EIE cross sections for heliumlike Ne^{8+} soon.

6 Acknowledgments

We gratefully acknowledge support by the Office of Basic Energy Science, Chemical Sciences Division. This work was performed under the auspices of the Department of Energy by Lawrence Livermore National Laboratory under contract No. W-7405-ENG-48 and by Morehouse College under contract No. DE-FG02-98ER14877.

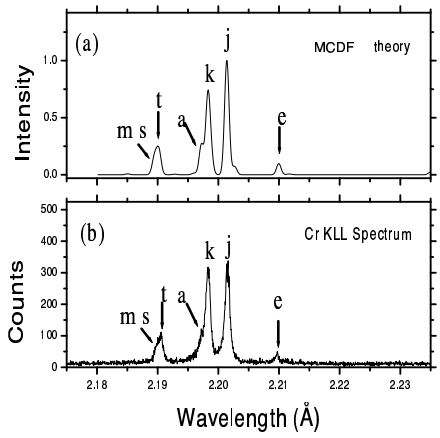

Figure 3. Dielectronic satellite spectra of heliumlike Cr^{22+} showing individual KLL resonances. The observed spectrum (b) was excited in EBIT and recorded with a high resolution Bragg crystal spectrometer using a LiF(200) crystal. The theoretical (a) spectrum was calculated with the MCDF code. Similar results have been obtained KLM, KLN and KLO resonances, and for Heliumlike Ti^{20+}.

Publications List

[1] "Ratios of n = 3 - 1 Intercombination to Resonance Line Intensities for Heliumlike ions with Intermediate Z-values," A. J. Smith, P. Beiersdorfer, K. J. Reed, A. L. Osterheld, V. Decaux, K. Widmann, and M. Chen, Phys. Rev. **A** 62 012704 (2000).

[2] "Measurement of Polarization of the Kβ2 line of heliumlike V^{21+}," A. J. Smith, P. Beiersdorfer, K. L. Wong and K. J. Reed, In Proceedings of 3rd US-Japan Workshop on Plasma Polarization Spectroscopy, Livermore, CA June 18-21, 2001, P. Beiersdorfer and T. Fujimoto, editors, University of CA, LLNL Report No UCRL-ID-146907 (UC-LLNL, Livermore, 2002) p299-306.

[3] "Recent Livermore Excitation and Dielectronic Recombination Measurements for Laboratory and Astrophysical Spectral Modeling," P. Beiersdorfer, G. V. Brown, M.-F. Gu, C. L. Harris, S. M. Kahn, S.-H. Kim, P. A. Neill, D. W. Savin, A. J. Smith, S. B. Utter, and K. L. Wong, Proceedings of the International Seminar on Atomic Processes in Plasmas, NIFS Proceedings Series No. NIFS-PROC-44 (National Institute for Fusion Studies, Nagoya, Japan 2000) ed. T. Kato and I. Murakami, p. 25-28.

[4] "Current Research with Highly Charged Ions in EBIT-II and SuperEBIT" P. Beiersdorfer, J. A. Britten, G. Brown, H. Chen, E. J. Clothiaux, J. Cottam, E. Förster, M.-F. Gu, C. L. Harris, S. M. Kahn, J. K. Lepson, P. A. Neill, D. W. Savin, H. Schulte-Schrepping, L. Schweikhard, A. J. Smith, E. Träbert, J. Tschischgale, S. B. Utter, and K. L. Wong, Physica Scripta T92, 268(2001).

[5] "Photometric calibration of an EUV flat field spectrometer at the advanced light source," M. may, J. Lepson, P. Beiersdorfer, D. Thorn, H. Chen, D. Hey, and A. J. Smith, Rev. Sci. Instrum. 74, 2011(2003).

[6] "Improved electron-beam ion-trap lifetime measurement of Ne^{8+} 1s2s $^3S_1$ level," E. Träbert, P. Beiersdorfer, G. V. Brown, A. J. Smith, S. B. Utter, M. F. Gu and D. W. Savin, Phys. Rev. A **60**, 2034 (1999).

[7] "Experimental M1 transition rates of coronal lines from Ar X, Ar XIV, and Ar XV" E. Träbert, P. Beiersdorfer, S. B. Utter, G. V. Brown, H. Chen, C. L. Harris, P. A. Neill, D. W. Savin, A. J. Smith, Astrophys. J **541**, 506 (2000).

[8] "Measurement of the Polarization of the Kβ2 line of V^{21+}", A. J. Smith, P. Beiersdorfer, E. Träbert, K. J. Reed, presented at the 3rd US-Japan Plasma Polarization Spectroscopy workshop, June 18-21, 2000, at the Lawrence Livermore National Laboratory, Livermore, CA, to be published in proceedings.

DYNAMICS OF FEW-BODY ATOMIC PROCESSES

Anthony F. Starace

The University of Nebraska
Department of Physics and Astronomy
116 Brace Laboratory
Lincoln, NE 68588-0111
Email: astarace1@unl.edu

PROGRAM SCOPE

The major goal of this project is to understand the physics underlying the interaction of real atomic systems with strong external fields. Nearly all the atomic systems considered for study are many-electron systems. We treat their interactions, i.e., electron correlations, as accurately as possible. The strong external fields considered are mainly intense laser fields. In some cases our studies are supportive of and/or have been stimulated by experimental work carried out by other investigators funded by the DOE AMO physics program.

RECENT PROGRESS

A. **Role of Rescattering in Intense Field Double Ionization Processes**

As described in Refs. [1], [2], and [5], we have developed a two-active-electron (TAE) approach for solving the time-dependent Schrödinger equation (TDSE) for the interaction of a multi-electron system with an ultrashort, intense, and linearly polarized laser pulse. A technique for obtaining angular distributions for double ionization by such pulses has also been developed. The approach for solving the TDSE in the TAE approximation is full dimensional and accounts for correlations between the two electrons, as well as the polarization of the core. It is based on a configuration-interaction expansion of the time-dependent wave function in terms of one-electron atomic orbitals. Applying the method to the lithium negative ion (Li^-), we display the time-dependent dynamics of the intense field double detachment process. In all cases, angular distributions for double ionization exhibit the influence of electron-electron correlations. In the case of intense fields, both electrons may be ejected perpendicularly to the laser polarization axis; this does not occur for the single photon, weak field case. In recent work [7], we have shown that very general symmetry and angular momentum selection rules for a two-electron wave function having initially $L = 0$ permits this perpendicular ejection only for the case in which an even number of photons is absorbed.

More recently, we have carried out numerical experiments on single and double ionization by a single cycle pulse (SCP) and by a double half-cycle pulse (DHP) that show that single and double ionization are larger for the SCP than for the DHP. Since rescattering only occurs for the SCP case, these results suggest that the rescattering mechanism enhances both single and double

ionization. On the other hand, angular distributions for double ionization by a half-cycle pulse, for which rescattering does not apply, show the existence of a significant shakeoff contribution to double ionization, in which one electron is ejected in the direction opposite to that of the laser field force direction. A manuscript on this work has been submitted for publication.

B. **Photo Double Ionization (PDI) of He**

Single-photon, two electron ionization of He has been analyzed, taking into account electron correlation using lowest-order perturbation theory (LOPT) and including all individual electron angular momenta in the final two-electron continuum [6]. Perturbative account of electron correlation in the final state, which describes the so-called TS-1 mechanism of double photoionization, combined with a variational account of electron screening, is found to provide results for the triply differential cross section (TDCS) at an excess energy of 20 eV that are in excellent agreement with both absolute experimental data and results of non-perturbative calculations, for all kinematics of the process in which the TS-1 mechanism is expected to dominate.

More recently, we have used a LOPT approach (in the interelectron interaction) to evaluate the TDCS for PDI of He over a wide range of excess energies and, for the case of circularly polarized photons, to analyze the circular dichroism effect. We have found that for an excess energy of the order of tens of eV, the PDI process is dominated by the "virtual" (off-shell) knock-out mechanism, while the "direct" (on-shell) knock-out mechanism is rather small for the large mutual angles at which the CD effect is maximum. As a result of these findings, we can deduce that the CD effect in PDI at intermediate energies originates from the non-zero electron Coulomb phase shifts. A manuscript on this work is being prepared for submission.

C. **GeV Electrons from Ultra Intense Laser Interactions with Highly Charged Ions**

As described in Ref. [3], we have investigated laser interactions with highly charged hydrogenic ions using a three-dimensional Monte Carlo simulation. We first demonstrated that free electrons cannot be accelerated to GeV energies by the highest intensity lasers because they are quickly expelled from the laser pulse before it reaches peak intensity. We have shown that highly charged ions exist that (1) have deep enough potential wells that tunneling ionization is insignificant over the duration of an intense, short laser pulse, and (2) have potentials that are not too deep, so that the laser pulse is still able to ionize the bound electron when the laser field reaches its peak intensity. We have shown that when the ionized electron experiences the peak intensity of the laser field, then it is accelerated to relativistic velocity along the laser propagation direction (by the Lorentz force) within a tiny fraction of a laser cycle. Within its rest frame it then "rides" on the peak laser amplitude and is accelerated to GeV energies before being expelled from the laser pulse.

More recently, we have carried out an extensive set of calculations to examine the dependence of the ionized electron energy spectrum on the experimentally controllable parameters. These include the target ion and the laser intensity, frequency, duration, and focal properties. An analysis of these results is currently being done; a manuscript is simultaneously being prepared for submission.

D. **Static and Dynamic Polarizabilities for He**

In Ref. [8] we have presented a new approach for the calculation of the static dipole polarizability of the helium ground state that includes logarithmic terms in both ground and intermediate states within a variationally stable, coupled-channel adiabatic hyperspherical approach. We have shown that for any fixed number of coupled channels this approach is capable of obtaining a value for the static polarizability that is comparable to the results obtained with optimized parameters. The two methods appear comparable in their use of computer resources.

Results for the dynamic polarizability have also been presented whose accuracy is comparable to that of the best results of other authors, especially in the photon frequency range corresponding to the one-photon transitions. In fact, one of the advantages of the present approach is the ability to furnish reliable and converged results even in the resonance region due to the nonexistence of poles in the transition matrix element. These accurate predictions for the dynamical polarizability imply that our approach is capable of predicting highly accurate values for multiphoton cross sections of helium (as well as other two-electron systems).

D. **Control of Entanglement of Two Interacting Spin 1/2 (Heisenberg) Systems**

In Ref. [4], we have shown that for the case of two interacting spin 1/2 qubits whose interaction is anisotropic (i.e., different in different directions), the critical temperature (above which entanglement no longer exists) is dependent on the magnitude of the magnetic field, which is chosen to be constant along the z axis. More recently, we have analyzed the entanglement of a two qubit XY chain in thermal equilibrium at temperature T in the presence of an external magnetic field B in arbitrary directions: $\mathrm{B} = \mathrm{B}_x \hat{\mathrm{x}} + \mathrm{B}_y \hat{\mathrm{y}} + \mathrm{B}_z \hat{\mathrm{z}}$. We find that for a B field having a component along the $\hat{\mathrm{x}}$ or the $\hat{\mathrm{y}}$ direction, ferromagnetic (FM) and antiferromagnetic (AFM) chains lead to different forms of entanglement, and that even for the isotropic XX chain the two qubits can be entangled at any finite T by adjusting the field strength. It is found that quantum phase transitions occur for AFM chains but not for FM chains, except for the Heisenberg-Ising case, for which the entanglement is the same for AFM and FM chains. A manuscript on this work is in preparation.

FUTURE PLANS

Our group is currently carrying out research on the following projects: (1) Search for non-dipole effects on photo-double-ionization of He using LOPT; (2) Calculation of benchmark, two-photon ionization cross sections of He using a variationally-stable, coupled hyperspherical-channel approach; (3) Calculation of the triply differential cross section for two-photon double ionization of He using a LOPT approach (in anticipation of future experimental measurements), including examination of circular dichroism effects; (4) Analysis of laser focal effects and two-electron effects on production of GeV electrons with intense lasers from highly charged ions; (5) Analysis of the time-dependence and decoherence of the entanglement of interacting spin 1/2 (Heisenberg) systems.

2001-2003 PUBLICATIONS STEMMING FROM DOE-SPONSORED RESEARCH

[1] G. Lagmago Kamta and A.F. Starace, "Angular Distributions for Double Ionization of Li^- by an Ultrashort, Intense Laser Pulse," Phys. Rev. Lett. **86**, 5687 (2001).

[2] G. Lagmago Kamta and A.F. Starace, "Angular Distributions for Double Ionization by an Ultrashort, Intense Laser Pulse: The Case of Li^-," in *Super-Intense Laser-Atom Physics*, edited by B. Piraux (Kluwer, Dordrecht, The Netherlands, 2001), pp 143-152.

[3] S.X. Hu and A.F. Starace, "GeV Electrons from Ultra-Intense Laser Interaction with Highly-Charged Ions," Phys. Rev. Lett. **88**, 245003 (2002).

[4] G. Lagmago Kamta and A.F. Starace, "Anisotropy and Magnetic Field Effects on the Entanglement of a Two Qubit Heisenberg XY Chain," Phys. Rev. Lett. **88**, 107901 (2002).

[5] G. Lagmago Kamta and A.F. Starace, "Multielectron System in an Ultrashort, Intense Laser Field: A Nonperturbative, Time-Dependent Two-Active Electron Approach," Phys. Rev. A **65**, 053418 (2002).

[6] A.Y. Istomin, N.L. Manakov, and A.F. Starace, "Perturbative Calculation of the Triply Differential Cross Section for Photo-Double-Ionization of He," J. Phys. B **35**, L543 (2002).

[7] G. Lagmago Kamta and A.F. Starace, "Two-Active Electron Approach to Multielectron Systems in Intense Ultrashort Laser Pulses: Application to Li^-," J. Mod. Optics **50**, 597 (2003).

[8] M. Masili and A.F. Starace, "Static and Dynamic Dipole Polarizability of the He Atom Using Wave Functions Involving Logarithmic Terms," Phys. Rev. A **68**, 012508 (2003).

FEMTOSECOND AND ATTOSECOND LASER-PULSE ENERGY TRANSFORMATION AND CONCENTRATION IN NANOSTRUCTURED SYSTEMS

DOE Grant No. DE-FG02-01ER15213

Mark I. Stockman, Pi

Department of Physics and Astronomy, Georgia State University, Atlanta, GA 30303

1 Program Scope

The program is aimed at theoretical investigations of a wide range of phenomena induced by ultrafast laser-light excitation of nanostructured or nanosize systems, in particular, metal/semiconductor/dielectric nanocomposites and nanoclusters. Among the primary phenomena are processes of energy transformation, transfer, and localization on the nanoscale and coherent control of such phenomena.

2 Recent Progress

2.1 Surface-Plasmon Eigenmodes of Nanosystems

Interaction of light with nanosystems occurs via elementary polar excitations (eigenmodes) of these systems called surface plasmons. These eigenmodes are of both fundamental and applied points of view. We have developed theory of surface plasmons of complex nanosystems.[1,2] We have established that, in contrast to the known properties of Anderson localization of electrons, there always are surface plasmons both delocalized and localized, co-existing at the same frequencies. There can exist no system all surface plasmon modes of which are Anderson-localized, which is rigorously proven as a theorem. This work constitutes a basis for understanding of nanooptics of disordered nanosystems.

2.2 Coherent Control of Ultrafast Energy Localization on Nanoscale

Our research has significantly focused on problem of controlling localization of the energy of ultrafast (femtosecond) optical excitation on the nanoscale. This is a formidable problem since it is impossible to achieve such concentration by optical focusing due to the nanosize of the system, or by near-field excitation, because the energy of such excitation is transferred across the entire nanosystem during ultrashort periods on order of the light-wave oscillation. We have proposed and theoretically developed a distinct approach to solving this fundamental problem. [2-5] This approach, based on the using the relative phase of the light pulse as a functional degree of freedom, allows one to control the spatial-temporal distribution of the excitation energy on the nanometer-femtosecond scale. We have shown that using even the simplest phase modulation, the linear chirp, it is possible to shift in time and spatially concentrate the linear local optical fields, but the integral local energy does not depend on the phase modulation. In contrast, for nonlinear responses, the integral local energy cam efficiently be coherently controlled. It is difficult to overestimate possible applications of this effect, including nano-chip computing, nanomodification (nanolithography), and ultrafast nano-sensing.

2.3 Microscopic Theory of Interacting Electrons in Semiconductor Nanosystems

We have contributed to the microscopic, many-body theory of the electronic and optical properties of interacting electrons in semiconductor nanostructures based on the self-consistent Random Phase Approximation also known as *GW*-approximation.[6] The technique used in this research is based on the non-equilibrium Green's function method by Baym and Kadanoff. This theory allows us to calculate the intersubband absorption, effective electron masses, and Fermi-edge discontinuity for electrons with Coulomb interaction in quantum wells without any adjustable parameters.

2.4 Theory of Coherent Near-Field Optical Microscopy

We have developed theory of phase-sensitive near-field scanning optical microscopy (in collaboration with the group of Dr. Victor Klimov, LANL).[7] Near-field spectroscopic studies of metal nanoparticles with broad-band white-continuum femtosecond pulses have found that the near field extinction of metal nanoparticles in

the blue region of the spectrum changes to the enhanced transmission in the red region. The developed theory shows that this effect is due to the interference of secondary electromagnetic waves emitted by the metal nanoparticles and the radiation of the near-field optical microscope (NSOM) tip. The latter radiation contains both magnetic-dipole and electric dipole parts. The interference of these radiations of the tip and the metal nanosystem in the far zone depends on their relative phase that in turn is determined by the detuning from the surface plasmon resonance in the metal nanosystem. Owing to this interference, it is possible to determine the spectral phase of the surface plasmon resonances in metal nanoparticles. In turn, this allows us to determine the positions of these resonances with unprecedented resolution.

2.5 SPASER: New Idea, Effect, and Prospective Devices

The above-discussed and other known effects and applications in nanooptics are passive, i.e., based on the excitation of the nanosystem by external laser radiation. This mode of excitation has obvious drawbacks: most of the radiation is lost and only a small fraction of photons interact with the nanosystem; it is difficult or impossible to concentrate the excitation in space and time on nanometer-femtosecond scale; the exciting radiation creates a significant background to the relatively weak emissions by the nanosystem. We have introduced a principally different concept of SPASER (Surface Plasmon Amplification by Stimulated Emission of Radiation).[8]

The spaser radiation consists of surface plasmons that are bosons just like photons and undergo stimulated emission, but in contrast to photons can be localized on the nanoscale. Spaser as a system will incorporate an active medium formed by two-level emitters, excited in the same way as a laser active medium: optically, or electrically, or chemically, etc. One promising type of such emitters are quantum dots (QDs). These emitters transfer their excitation energy by radiationless transitions to a resonant nanosystem that plays the role of a laser cavity. These transitions are stimulated by the surface plasmons already in the nanosystem, causing buildup of a macroscopic number of the surface plasmons in a single mode. Spaser is predicted to generate ultrashort (10-100 fs) ultraintense (optical electric field ~10^8 V/cm or greater) pulses of local optical fields at nanoscale. When realized experimentally spaser may completely change the nanooptics.

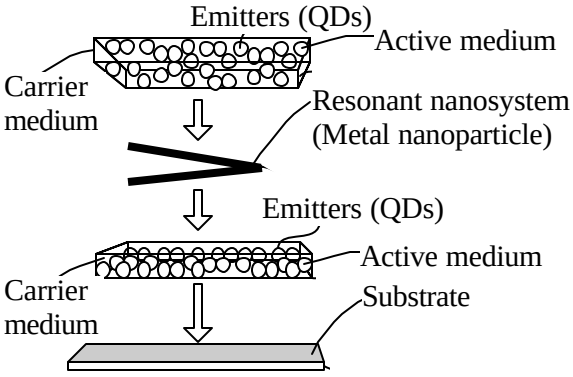

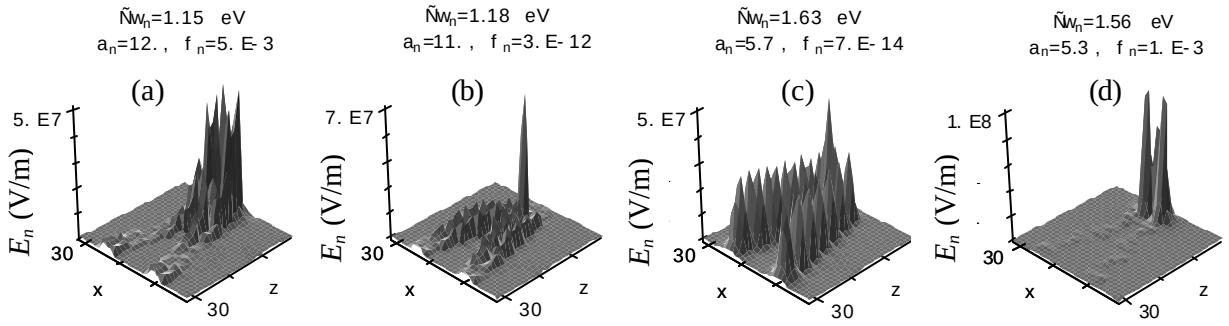

Fig. 2. Eigenmodes (surface plasmons) with highest gains for the frequencies w_n, gains a_n, and oscillator strength f_n shown. The local electric field amplitude is $E_n\sqrt{N_n+1/2}$, where N_n is the number of the surface plasmons in an *n*th mode.

2.6 Short Papers and Abstracts in Conference Proceedings

Apart from the above-cited papers, there is a series of short papers and abstracts published in Proceedings of various Conferences.[9-20]

3 Future Plans

We will develop both the theory in the directions specified above and the collaborations with experimental group. Among the projects in works, we will consider effects of nonlocality of the dielectric response of nanosystems; this nonlocality is expected to dominate electromagnetic interaction in nanocomposites of metal nanoparticles and semiconductor quantum dots. Another project will be nanoplasmonic imaging, including the spaser-amplified nanolenses. We will also consider different types of spasers. Yet another project in the works is the study of second harmonic generation in nanosystems.

Publications Resulting from the Grant

[1] M. I. Stockman, S. V. Faleev, and D. J. Bergman, *Localization vs. Delocalization of Surface Plasmons in Nanosystems: Can One State Have Both Characteristics?*, Phys. Rev. Lett. **87**, 167401-1-4 (2001).

[2] M. I. Stockman, *Ultrafast Processes in Metal-Insulator and Metal-Semiconductor Nanocomposites* (Invited talk), In: Ultrafast Phenomena in Semiconductors VII, Proceedings of SPIE (K. F. Tsen, J. Song, and H. Jiang, eds.), Vol. **4992**, 60-74 (2003).

[3] M. I. Stockman, S. V. Faleev, and D. J. Bergman, *Coherent Control of Femtosecond Energy Localization on Nanoscale*, Phys. Rev. Lett. **88,** 067402-1-4 (2002).

[4] M. I. Stockman, S. V. Faleev, and D. J. Bergman, *Coherently-Controlled Femtosecond Energy Localization on Nanoscale,* Appl. Phys. B **74**(9), 63-67 (2002).

[5] M. I. Stockman, S. V. Faleev, and D. J. Bergman, *Coherently-Controlled Femtosecond Energy Localization on Nanoscale*, In: Ultrafast Phenomena XIII (Springer Series in Chemical Physics), pp. 496-498 (Springer, Berlin, Heidelberg, New York, 2003).

[6] S. V. Faleev and M. I. Stockman, *Self-Consistent Random-Phase Approximation and Intersubband Absorption for Interacting Electrons in Quantum Well*, Phys. Rev. B **66**, 085318-1-11 (2002).

[7] A. A. Mikhailovsky, M. A. Petruska, M. I. Stockman, and V. I. Klimov, *Broadband, Near-Field, Interference Spectroscopy of Metal Nanoparticles Using Femtosecond White-Light Continuum,* Optics Lett. (2003). [In print: Accepted for publication.]

[8] D. J. Bergman and M. I. Stockman, *Surface Plasmon Amplification by Stimulated Emission of Radiation: Quantum Generation of Coherent Surface Plasmons in Nanosystems*, Phys. Rev. Lett. **90**, 027402-1-4 (2003).

Short Papers and Abstracts in Conference Proceedings

[9] D. J. Bergman, M. I. Stockman, and S. V. Faleev, *Anderson Localization vs. Delocalization of Surface Plasmons in Nanosystems*, QELS 2002 (Long Beach, CA, May 19-24, 2002), QELS 2002 Technical Digest, pp. 259-260 (OSA, 2002).

[10] M. I. Stockman, S. V. Faleev, and D. J. Bergman, *Femtosecond Energy Concentration in Nanosystems Coherently Controlled by Excitation Phase*, The Thirteenth International Conference on Ultrafast Phenomena (Vancouver, BC, Canada, May 12-17, 2002), Technical Digest, pp. 135-136 (OSA, 2002).

[11] D. J. Bergman, M. I. Stockman, and S. V. Faleev, *Anderson Localization vs. Delocalization of Surface Plasmons in Nanosystems*, APS March 2002 Meeting (Indianapolis, Indiana, March 18-22, 2002), Bulletin of American Physical Soc. 47, 1265 (2002).

[12] S. V. Faleev and M. I. Stockman, *Self-Consistent Random-Phase Approximation for Interacting Electrons in Quantum Wells and Intersubband Absorption*, APS March 2002 Meeting (Indianapolis, Indiana, March 18-22, 2002), Bulletin of American Physical Soc. 47, 1189 (2002).

[13] M. I. Stockman, S. V. Faleev, and D. J. Bergman, *Femtosecond Energy Localization on Nanoscale Controlled by Pulse Phase*, APS March 2002 Meeting (Indianapolis, Indiana, March 18-22, 2002), Bulletin of American Physical Soc. 47, 734 (2002).

[14] M. I. Stockman, S. V. Faleev, S. G. Matsik, A. G. U. Perera, and H. C. Liu, *Experimental and Many-Body Theoretical Investigations of Intersubband Far Infrared Absorption in Quantum Well Photodetectors*, APS March 2002 Meeting (Indianapolis, Indiana, March 18-22, 2002), Bulletin of American Physical Soc. 47, 59 (2002).

[15] M. I. Stockman and D. J. Bergman, *Quantum Nanoplasmonics: Surface Plasmon Amplification by Stimulated Emission of Radiation (SPASER)*, QELS 2003 (Baltimore, Maryland June 1-6, 2003), Postdeadline Papers Book, Talk #QThPDA10, OSA (2003).

[16] A. Mikhailovsky, M. Petruska, M. I. Stockman, A. Bartko, M. Achermann, M. I. Stockman, and V. I. Klimov, *Near-Field Phase-Sensitive Spectroscopy of Metal Nanoassemblies*, QELS 2003 (Baltimore, Maryland June 1-6, 2003), Technical Digest, Talk #QtuA2, OSA (2003).

[17] M. I. Stockman, D. J. Bergman, and Takayoshi Kobayashi, *Coherent Control of Nanoscale Localization of Ultrafast Optical Excitation in Nanostructures*, QELS 2003 (Baltimore, Maryland June 1-6, 2003), Technical Digest, Talk #QMJ4, OSA (2003).

[18] D. J. Bergman, Takayoshi Kobayashi, and M. I. Stockman, *Coherent Control of Linear and Nonlinear Ultrafast Optical Excitation of Nanosystems* APS March 2003 Meeting (Austin, Texas, March 3-7, 2003), Bulletin of American Physical Soc. **48**, 976 (2003).

[19] M. I. Stockman and D. J. Bergman, *Quantum Nanoplasmonics: Surface Plasmon Amplification through Stimulated Emission of Radiation (Spaser)*, APS March 2003 Meeting (Austin, Texas, March 3-7, 2003), Bulletin of American Physical Soc. **48**, 976 (2003).

[20] A. Mikhailovsky, M. Petruska, A. Bartko, M. Achermann, M. I. Stockman, and V. I. Klimov, *Near-Field Interference Spectroscopy of Individual Metal Nanostructures* APS March 2003 Meeting (Austin, Texas, March 3-7, 2003), Bulletin of American Physical Soc. **48**, 852 (2003).

Laser-Produced Coherent X-Ray Sources

Donald Umstadter (dpu@umich.edu)
1006 ERB/Gerstaker Bldg., University of Michigan, Ann Arbor 49109-2099

I. PROGRAM SCOPE

We experimentally and theoretically explore the physics of ultra-high-intensity laser-plasma interactions with the goal of developing a novel and practical source of x-rays, one which has keV-energy, femtosecond-duration, and is small enough to fit in a university laboratory [1–4]. One promising approach involves the scattering of intense laser light off of a laser-accelerated electron beam. The resulting Doppler-shifted high-order harmonic generation can reach keV energy using current laser technology, but the accelerator and wiggler regions are only one millimeter in length. Like existing x-ray synchrotrons and harmonic generation from atomic media, these sources have applications to ultrafast chemistry and biology, inner-shell electronic processes and phase transitions.

II. RECENT PROGRESS

When laser light intensity approaches 10^{18} W/cm^2, the relativistic regime is reached, in which electrons quiver nonlinearly and radiate harmonic light, with each harmonic having its own unique angular distribution. This is referred to as nonlinear Thomson scattering or relativistic Thomson scattering and has been previously demonstrated by us from free electrons that are either in quasi-neutral plasma or laser-accelerated electron beams [5, 6]. In the latter case, the characteristic signatures are found to be (1) emission of even order harmonics (extending to at least the 30^{th}, the range limit of the spectrometer that was used), (2) a linear dependence on the electron density, (3) a significant amount of harmonics even with circular polarization and (4) a much smaller spatial region over which these harmonics are produced as compared to harmonics from atomic media. Imaging of the harmonic beam shows that it is emitted in a narrow cone with a divergence of only 2-3 degrees.

While this work demonstrated the basic principle that a collimated beam of XUV radiation could be generated via nonlinear Thomson scattering, the degree of control over the scattering process in such single-beam experiments is limited. Furthermore, the interpretation of the results is complicated by the presence of plasma effects. Another drawback is that, because the laser and electron beams are co-propagating in the single-laser–beam case, the scattered harmonics are Doppler down-shifted. Consequently, we have begun investigating scattering from the collision of a laser-generated electron beam with a high-intensity counter-propagating laser pulse (as shown in Fig. 1). In this geometry, the scattered light is Doppler up-shifted, scaling as γ^2 (where γ is the relativistic factor associated with the electron beam energy). X-rays can thus be generated with electron beams of energy of only a few MeV. Recently, we have successfully implemented this geometry to generate a low-divergence beam of high-brightness polychromatic soft x-rays with subpicosecond duration.

The experiments involve the precise spatiotemporal overlap of two high intensity, subpicosecond pulses from a hybrid Titanium:Sapphire-Neodymium:YAG laser system, which has an output power of 10 TW, at a wavelength of 1.053 μm and pulse duration of 400 fs. The output of the laser was split into two unequal components. The stronger of the two beams was tightly focused onto a high-density, photo-ionized gas target to generate a relativistic electron beam by means of a laser wakefield. In order to obtain XUV radiation, the electron beam was collided with the second tightly focused laser pulse, which was incident at an angle of 135 degrees with respect to the first laser beam (shown in Fig. 1). Fig. 2 shows a top-view image of the linear Thomson scattered light, which arose from the self channelling of each pulse in the plasma. The interaction point is chosen to lie outside the gas jet so that plasma effects are negligible. The top-view imaging serves as a diagnostic of the spatial overlap at full laser power.

Another diagnostic, which ensures overlap in both space and time of the two ultrashort tightly focused laser pulses, is the deflection of the laser-generated electron beam by the second high power pulse. Such deflection is predicted to occur by the process of direct laser acceleration of electrons in vacuum and is observed in our experiments, as shown in Fig. 3. The electron beam spatial profile is recorded when it impinges on a fluorescent screen that is then imaged by a CCD camera. This

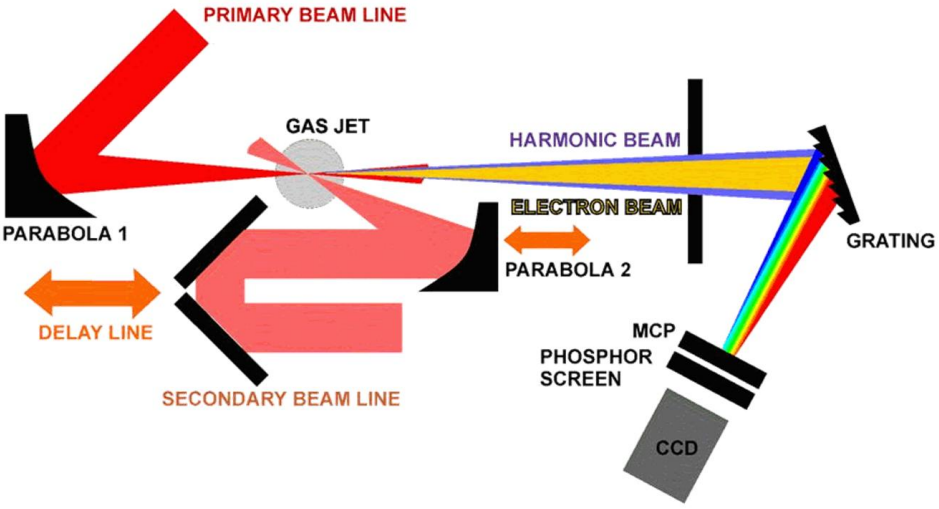

FIG. 1: Schematic of the experimental setup used to measure the scattered spectrum.

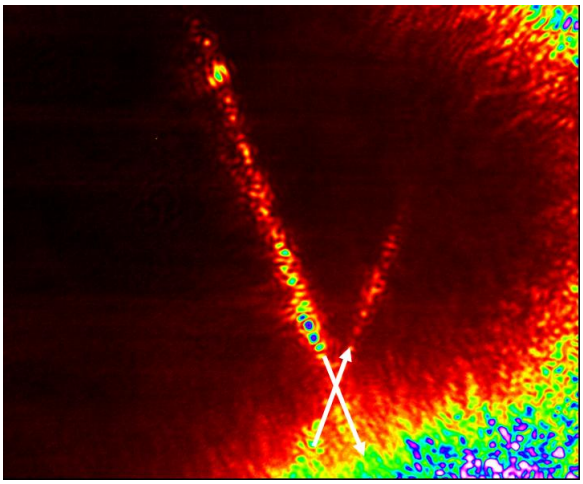

FIG. 2: Image of linear Thomson scattering obtained by looking down the gas jet in Fig. 1. The scattering was produced by propagation of the colliding laser pulses though the gas jet plasma. The collision takes place in the vacuum region near where the electron beam exits the gas jet. The distance from top of the figure to the bottom is ~ 1 mm.

diagnostic also provides a means to measure the duration of the laser-generated electron beam (~ 1 ps) and thus sets an upper limit on the temporal duration of the XUV beam of 1 ps.

Nonlinear Thomson scattering is complementary to the deflection of the electron beam in vacuum. The experimental parameters were chosen such that the mean energy of the electrons was 1 MeV, for which the Doppler shift ($2\gamma^2 \sim 18$ eV) lies within the spectrometer's spectral range. Fig. 4 shows the results with this experimental geometry (shown schematically in Fig. 1). As can be seen from Fig. 4, the signal amplitude with two beams is twice as much as that with a single beam. The typical shape of the spectrum is consistent with what is expected theoretically. Since linearly polarized light is used, there is a contribution to the odd harmonics from the bound electrons, and thus the signal at the odd harmonics is greater than at the even harmonics. The results here are depicted only for the harmonic orders, but similar enhancement is observed over the entire spectral range, consistent with the expectation that the emission should be a blue-shifted continuum. The

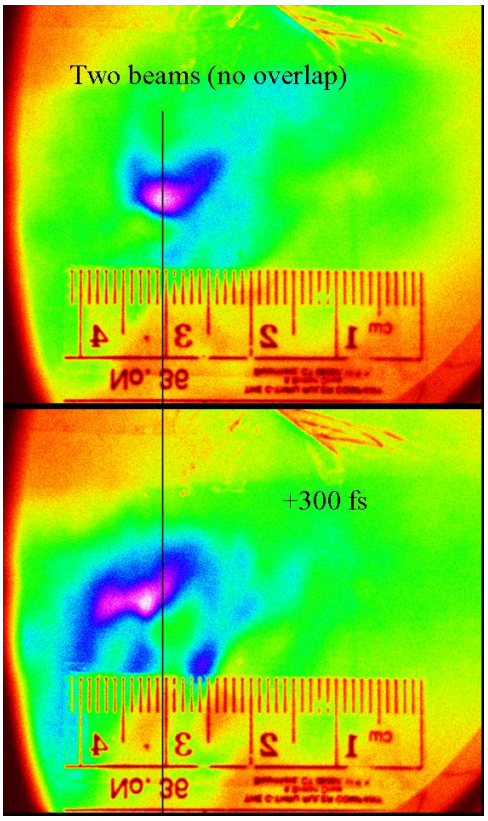

FIG. 3: Spatial profile of an electron beam accelerated by an intense laser pulse. Top: when the two laser beams do not overlap, the electron beam accelerated by one of the beams is not deflected. Bottom: when the two laser beams do overlap, the electron beam accelerated by one of the beams is deflected by the ponderomotive force of a colliding high-intensity laser pulse.

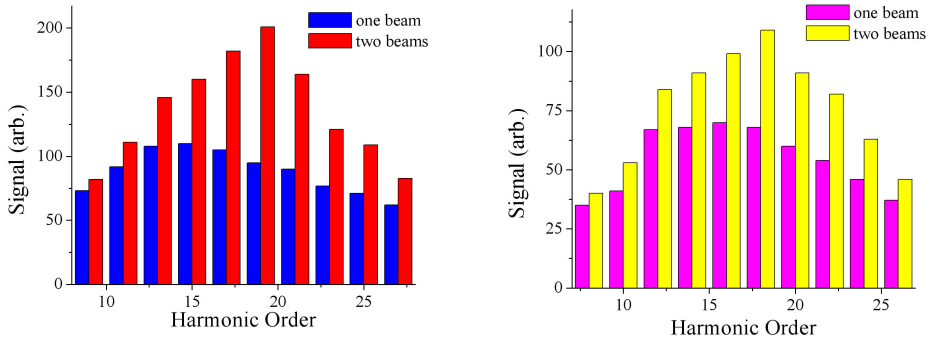

FIG. 4: Comparison between the scattered light spectra at odd (left) and even (right) harmonics for the one- and two-beam cases. A two-fold enhancement is seen when the laser and electron beam are overlapped. The signal at odd orders is larger due to contribution from the bound electrons.

total photon number is found to be 10^9 for the entire measured spectral range. There are 10^7 photons in a 1% bandwidth about the harmonics.

We have been studying the nonlinear scattering problem theoretically [7–9]. The dependence of free electron orbits on the phase of an ultra-intense light field was solved, which is critical for a thorough understanding of the basic scattering phenomenon [9]. The optimal laser and electron beam parameters and geometry for the generation of x-rays were also determined [7, 8]. It was found that a normalized vector potential of $a_0 \sim 2$ (corresponding to a laser intensity of $I \sim 6 \times 10^{18}$

W/cm^2) should not be exceeded by the scattering beam, but that the electron beam should have the highest value of γ possible, with the scattering amplitude scaling as γ^6.

III. FUTURE PLANS

In the next year, we will use a spectrometer capable of measuring harder x-rays in order to characterize the source in this important spectral range. We also plan to study short-wavelength generation with much shorter duration laser pulses and much higher laser intensities. The theoretical predictions for this highly relativistic regime [7–9] can then be tested. Access to this novel regime will be obtained with a laser system at Michigan that has reached 30-TW peak power and has a 30-fs pulse duration. We have also begun collaborating with the Laboratoire d'Optique Appliquee in Palaiseau, France, on similar experiments with their 100-TW laser system. Current efforts are also being made in parallel to improve the energy, monochromaticity and emittance of laser-produced electron beams by means of optical injection of electrons [3].

While the scattering from a single electron is precisely predicted by our analytical models [7–9], in order to theoretically investigate the many-body problem of the interaction of intense laser light with an electron beam or a quasi-neutral plasma, we have begun to employ a particle-in-cell (PIC) code, coupled to a scattering solver. This solves Maxwell's equations, the fully relativistic equations of electron motion in the field of an intense laser pulse, and the Thomson scattering formula. It has been massively parallelized to run on the Michigan computer cluster (> 100 machines) and thus can model the laser and electron parameters over the entire interaction region. The code predictions will then be compared with the experimental results.

IV. PUBLICATIONS SUPPORTED BY THE GRANT DURING 2001–2003

Reprints of these papers are available at http://www.eecs.umich.edu/USL-HFS/pubs.html.

---

[1] D. Umstadter, "Physics and Applications of Relativistic Plasmas Driven by Ultra-intense Lasers," *Phys. of Plasmas* **8**, 1774—1785 (2001) [invited].

[2] D. Umstadter, S. Banerjee, S. Chen, E. Dodd, K. Flippo, A. Maksimchuk, N. Saleh, A. Valenzuela, and P. Zhang, "Developments in relativistic nonlinear optics," *AIP Conf. Proc.* **611**, 95 (2002) [invited].

[3] D. Umstadter, "Laser-driven x-ray sources," *2003 Yearbook in Science and Technology* (McGraw-Hill, New York, 2003), p. 215. [invited].

[4] D. Umstadter, "Relativistic Laser-Plasma Interactions," *Journal of Physics D: Applied Physics* **36**, R151-R165 (2003) [invited].

[5] S. Banerjee, A. R. Valenzuela, R.C. Shah, A. Maksimchuk and D. Umstadter, "High Harmonic Generation in Relativistic Laser Plasma Interaction," *Phys. Plasmas* **9**, 2393 (2002) [invited].

[6] S. Banerjee, A. R. Valenzuela, R. C. Shah, A. Maksimchuk, and D. Umstadter, "High-harmonic generation in plasmas from relativistic laser-electron scattering," *J. Opt. Soc. Am. B* **20**, 182 (2003).

[7] Y. Y. Lau, Fe He, Donald P. Umstadter, and Richard Kowalczyk, "Nonlinear Thompson scattering: A Tutorial," *Phys. Plasma* **10**, 2155 (2003).

[8] F. He, Y. Y. Lau, D. P. Umstadter, and R. Kowalczyk, "Backscattering of an Intense Laser Beam by an Electron," *Phys. Rev. Lett.* **90**, 055002 (2003).

[9] F. He, Y. Y. Lau, D. Umstadter and T. Strickler, "Phase dependence of Thomson scattering in an ultraintense laser field," *Phys. Plasma*, **9**, 4325 (2002).

[10] K. Nemoto, A. Maksimchuk, S. Banerjee, K. Flippo, G. Mourou, and D. Umstadter and V. Yu. Bychenkov, "Laser-triggered Ion Acceleration and Table Top Isotope Production," *Appl. Phys. Lett.* **78**, 595 (2001).